STICK INSECT RESEARCH IN THE ERA OF GENOMICS: EXPLORING THE EVOLUTION OF A MESODIVERSE INSECT ORDER

EDITED BY: Sven Bradler and Thomas Robert Buckley
PUBLISHED IN: Frontiers in Ecology and Evolution

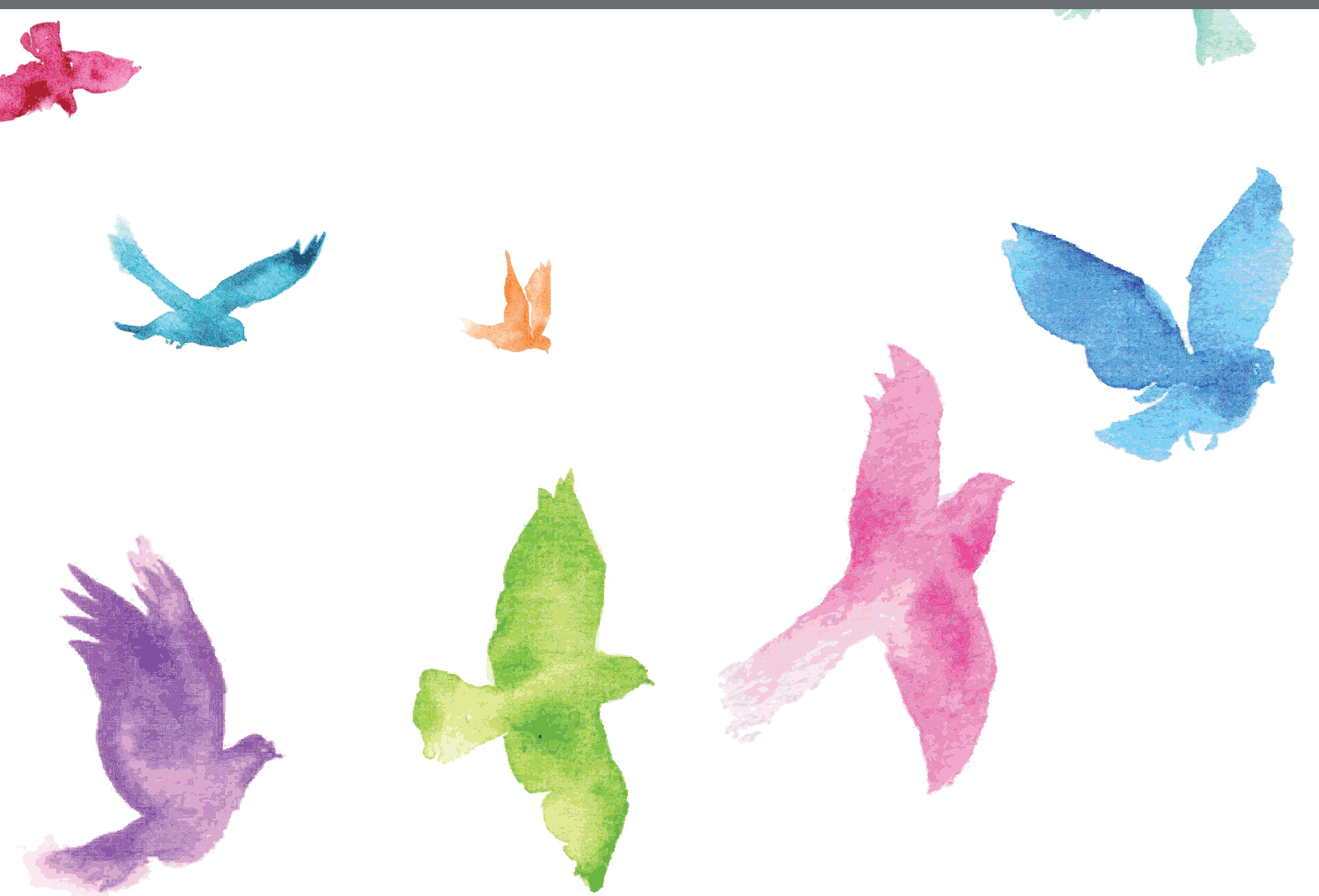

frontiers Research Topics

frontiers

ISSN 1664-8714
ISBN 978-2-88966-371-2
DOI 10.3389/978-2-88966-371-2

About Frontiers

Frontiers is more than just an open-access publisher of scholarly articles: it is a pioneering approach to the world of academia, radically improving the way scholarly research is managed. The grand vision of Frontiers is a world where all people have an equal opportunity to seek, share and generate knowledge. Frontiers provides immediate and permanent online open access to all its publications, but this alone is not enough to realize our grand goals.

Frontiers Journal Series

The Frontiers Journal Series is a multi-tier and interdisciplinary set of open-access, online journals, promising a paradigm shift from the current review, selection and dissemination processes in academic publishing. All Frontiers journals are driven by researchers for researchers; therefore, they constitute a service to the scholarly community. At the same time, the Frontiers Journal Series operates on a revolutionary invention, the tiered publishing system, initially addressing specific communities of scholars, and gradually climbing up to broader public understanding, thus serving the interests of the lay society, too.

Dedication to Quality

Each Frontiers article is a landmark of the highest quality, thanks to genuinely collaborative interactions between authors and review editors, who include some of the world's best academicians. Research must be certified by peers before entering a stream of knowledge that may eventually reach the public - and shape society; therefore, Frontiers only applies the most rigorous and unbiased reviews.
Frontiers revolutionizes research publishing by freely delivering the most outstanding research, evaluated with no bias from both the academic and social point of view. By applying the most advanced information technologies, Frontiers is catapulting scholarly publishing into a new generation.

What are Frontiers Research Topics?

Frontiers Research Topics are very popular trademarks of the Frontiers Journals Series: they are collections of at least ten articles, all centered on a particular subject. With their unique mix of varied contributions from Original Research to Review Articles, Frontiers Research Topics unify the most influential researchers, the latest key findings and historical advances in a hot research area! Find out more on how to host your own Frontiers Research Topic or contribute to one as an author by contacting the Frontiers Editorial Office: researchtopics@frontiersin.org

STICK INSECT RESEARCH IN THE ERA OF GENOMICS: EXPLORING THE EVOLUTION OF A MESODIVERSE INSECT ORDER

Topic Editors:
Sven Bradler, University of Göttingen, Germany
Thomas Robert Buckley, Manaaki Whenua Landcare Research, New Zealand

Citation: Bradler, S., Buckley, T. R., eds. (2021). Stick Insect Research in the Era of Genomics: Exploring the Evolution of a Mesodiverse Insect Order. Lausanne: Frontiers Media SA. doi: 10.3389/978-2-88966-371-2

Table of Contents

frontiers in Ecology and Evolution

EDITORIAL
published: 25 November 2020
doi: 10.3389/fevo.2020.619418

Editorial: Stick Insect Research in the Era of Genomics: Exploring the Evolution of a Mesodiverse Insect Order

Sven Bradler[1]* *and Thomas R. Buckley*[2,3]

[1] Department of Animal Evolution and Biodiversity, Johann-Friedrich-Blumenbach Institute for Zoology and Anthropology, University of Göttingen, Göttingen, Germany, [2] School of Biological Sciences, Faculty of Science, University of Auckland, Auckland, New Zealand, [3] Manaaki Whenua - Landcare Research, Auckland, New Zealand

Keywords: Phasmatodea, evolution, phylogeny, biogeography, neuroanaomy, transcriptomes

Editorial on the Research Topic

Stick Insect Research in the Era of Genomics: Exploring the Evolution of a Mesodiverse Insect Order

Stick and leaf insects are an emerging model system for exploring evolutionary biology, with a vibrant and increasing community of scientists dedicated to using these insects as research tools. In 2016, part of this community met in Orlando, Florida (USA) during the 25th International Congress of Entomology (ICE) and participated at a symposium held on September 26th that gave rise to the present Research Topic. Most of the papers were inspired by this symposium of the same title, but further authors felt encouraged to contribute their studies to this collection of articles that now covers a wide range of issues in phasmatodean biology and evolution. The scientific themes investigated in this Research Topic include speciation and evolution of reproductive strategies, such as asexual reproduction, for which the species-poor and phylogenetically relictual Californian *Timema* serves as model taxon and provides significant insights (e.g., Schwander et al., 2011). In this context, Parker et al. infer the role of olfactory proteins by comparing their differential expression in juveniles and both sexual and asexual *Timema* species. Unexpectedly, the authors could not find evidence that olfactory proteins with a putative role in sexual communication are under relaxed selection in the asexual species. Hopefully, the list of olfactory genes provided in this study will trigger future studies on olfaction in stick insects within and beyond the *Timema* model system and further functional studies that will shed more light on the molecular evolutionary patterns observed. Another aspect of phasmatodean reproductive strategies is reflected by the highly diverse egg-laying modes that Robertson et al. investigate within a phylogenetic framework across the whole diversity of Phasmatodea. The team reveals numerous independent origins of various oviposition techniques that can be expected to play an important role in ecological niche diversification. Besides egg-laying techniques, the properties of the diversely shaped and structured seed-like eggs themselves (as most recently reviewed by O'Hanlon et al., 2020) need to be taken into account in future studies. Büscher et al. unveil an equally high diversity among phasmatodean tarsal attachment structures, again with an impressive degree of convergent evolution. The variety of tarsal adhesive structures and egg-laying strategies might be best explained in the context of

Edited and reviewed by:
Mark A. Elgar,
The University of Melbourne, Australia

***Correspondence:**
Sven Bradler
sbradle@gwdg.de

Specialty section:
This article was submitted to Phylogenetics, Phylogenomics, and Systematics, a section of the journal Frontiers in Ecology and Evolution

Received: *20 October 2020*
Accepted: *02 November 2020*
Published: *25 November 2020*

Citation:
Bradler S and Buckley TR (2020) Editorial: Stick Insect Research in the Era of Genomics: Exploring the Evolution of a Mesodiverse Insect Order. Front. Ecol. Evol. 8:619418. doi: 10.3389/fevo.2020.619418

adaptive radiations in geographic isolation that regularly shaped the diversity in this group (Bradler et al., 2015). A further trait of major significance for these insects' radiation is their flight ability or lack thereof, which regularly varies between closely related taxa and even between sexes of the same species (Whiting et al., 2003). The scenario by Whiting et al. (2003) according to which wings were lost in the ancestral stick insect and regained after a radiation of wingless taxa led to an extremely controversial discussion as being a violation of Dollo's law, the assumption of irreversible evolution (Stone and French, 2003; Goldberg and Igic, 2008). This problem is tackled here by Zeng et al. who investigate wing morphology across a representative taxon sampling and suggest relatively rapid evolutionary transitions between wingless and volant forms in both directions.

Although molecular analyses account for most of the progress in understanding the phylogeny and evolution of phasmatodeans, reconstructions based on traditional Sanger sequencing data (including above studies) still suffer from a poorly resolved phylogenetic backbone. This has now dramatically changed with the transcriptomic data set presented by Simon et al. which resolves even the deepest branching events in the phasmid-tree-of-life with high support. Surprisingly, even for the earliest lineages, biogeographic distribution played a major role as has been demonstrated many times for younger clades (Bradler et al., 2015).

These transcriptomic data do not only contribute to the previously difficult-to-resolve phasmatodean relationships but also facilitate a plethora of further comparative studies such as the investigation of phasmatodean pectinase enzymes, which apparently stem from gut bacteria via ancient horizontal gene transfer (Shelomi et al., 2016), or neuropeptide precursors (Bläser and Predel, 2020).

It is noteworthy that the study by Robertson et al., which is the most comprehensive global phylogeny of stick and leaf insects published (covering nearly 300 species), largely converges to the topology of the transcriptomic tree even for some deep nodes. Given the restricted resolution provided by traditional molecular markers at early evolutionary nodes or by mitogenomes that appear incapable of recovering even repeatedly corroborated and undisputed clades like Heteropterygidae, Lonchodidae, or Lanceocercata (as most recently shown by Forni et al., in press), expansion of the phylogenomic approach by Simon et al. via DNA enrichment is the method of choice to tackle the persisting taxonomic problems in the future.

Based on these highly resolved trees, it will be now possible to reconstruct the evolution of crucial traits more reliably. One being body size, a fundamental and easily observable attribute of organisms, which has been largely neglected in the past but is inferred here for European stick insects by Shelomi and Zeuss. The authors do not find evidence for the validity of Bergmann's rule, the assumption of organisms being larger at higher latitudes, and rightfully state that the largest stick insects are in fact known from the tropics, such as the two spectacular new *Achrioptera* species from Madagascar (Glaw et al.). Another rule that awaits investigation is Cope's rule which describes the tendency of organisms to evolve toward larger body size over time (phyletic size increase). While the advantages associated with larger size appear obvious, such as enhanced success in defense and predation (Hone and Benton, 2005), this influential concept came under criticism as being merely a psychological artifact (Gould, 1997). However, recent large-scale analyses across metazoan fossils revitalized the validity of Cope's concept (Heim et al., 2015), for which the regularly giant-sized stick insects might serve as an ideal study system.

Finally, the various defensive systems exhibited by phasmatodeans have never been studied in an evolutionary context. This includes their impressive forms of masquerade crypsis also involving behavioral aspects such as motion camouflage (Bian et al., 2016) that enable phasmatodeans to deceive visually hunting predators, but also the lesser known defensive glands that are ubiquitous among stick insects and described here by Strauß et al. as consisting of conserved and novel elements. Hopefully, broader comparative studies will follow for all the fascinating aspects covered in this compilation of articles.

AUTHOR CONTRIBUTIONS

Both authors listed have made a substantial, direct and intellectual contribution to the work, and approved it for publication.

ACKNOWLEDGMENTS

Sincere thanks to the authors, reviewers, and editors for their valuable contributions to this Research Topic.

REFERENCES

Bian, X., Elgar, M. A., and Peters, R. (2016). The swaying behavior of *Extatosoma tiaratum*: motion camouflage in a stick insect? *Behav. Ecol.* 27, 83–92. doi: 10.1093/beheco/arv125

Bläser, M., and Predel, R. (2020). Evolution of neuropeptide precursors in Polyneoptera. *Front. Endocrinol.* 11:197. doi: 10.3389/fendo.2020.00197

Bradler, S., Cliquennois, N., and Buckley, T. R. (2015). Single origin of Mascarene stick insects: ancient radiation on sunken islands? *BMC Evol. Biol.* 15:196. doi: 10.1186/s12862-015-0478-y

Forni, G., Plazzi, F., Cussigh, A., Conle, O., Hennemann, F., Luchetti, A., et al. (in press). Phylomitogenomics provide new perspectives on the Euphasmatodea radiation (Insecta: Phasmatodea). *Mol. Phylogenet. Evol.* doi: 10.1016/j.ympev.2020.106983

Goldberg, E. E., and Igic, B. (2008). On phylogenetic tests of irreversible evolution. *Evolution* 62, 2727–2741. doi: 10.1111/j.1558-5646.2008.00505.x

Gould, S. J. (1997). Cope's rule as psychological artefact. *Nature* 386, 199–200. doi: 10.1038/385199a0

Heim, N. A., Knope, M. L., Schall, E. K., Wang, S. C., and Payne, J. L. (2015). Cope's rule in the evolution of marine animals. *Science* 347:867–870. doi: 10.1126/science.1260065

Hone, D. W. E., and Benton, M. J. (2005). The evolution of large size: how does Cope's Rule work? *Trends Ecol. Evol.* 20, 1–6. doi: 10.1016/j.tree.2004.10.012

O'Hanlon, J. C., Jones, B. R., and Bulbert, M. W. (2020). The dynamic eggs of the Phasmatodea and their apparent convergence with plants. *Sci. Nat.* 107:34. doi: 10.1007/s00114-020-01690-1

Schwander, T., Henry, L., and Crespi, B. J. (2011). Molecular evidence for ancient asexuality in *Timema* stick insects. *Curr. Biol.* 21, 1129–1134. doi: 10.1016/j.cub.2011.05.026

Shelomi, M., Danchin, E. G. J., Heckel, D., Wipfler, B., Bradler, S., Zhou, X., et al. (2016). Horizontal gene transfer of pectinases from bacteria preceded the diversification of stick and leaf insects. *Sci. Rep.* 6:26388. doi: 10.1038/srep 26388

Stone, G., and French, V. (2003). Evolution: have wings come, gone and come again? *Curr. Biol.* 13, R436–R438. doi: 10.1016/S0960-9822(03)0 0364-6

Whiting, M. F., Bradler, S., and Maxwell, T. (2003). Loss and recovery of wings in stick insects. *Nature* 421, 264–267. doi: 10.1038/nature01313

Conflict of Interest: The authors declare that the research was conducted in the absence of any commercial or financial relationships that could be construed as a potential conflict of interest.

frontiers in Ecology and Evolution

ORIGINAL RESEARCH
published: 05 April 2017
doi: 10.3389/fevo.2017.00025

Bergmann's and Allen's Rules in Native European and Mediterranean Phasmatodea

Matan Shelomi[1,2]* *and Dirk Zeuss*[3]

[1] Department of Entomology, National Taiwan University, Taipei, Taiwan, [2] Department of Entomology, Max Planck Institute for Chemical Ecology, Jena, Germany, [3] Department of Ecology—Animal Ecology, Faculty of Biology, Phillips-Universität Marburg, Marburg, Germany

Bergmann's rule states that organisms at higher latitudes should be larger and thicker than those closer to the equator to better conserve heat, and Allen's rule states that they will have shorter and thicker limbs at higher latitudes. Alternative explanations for latitudinal size clines include plant productivity and seasonality. The rules generally hold in endotherms, but in insects different species within the same genus can respond to latitude in unpredictable ways. We present the first biogeographical analysis of these rules in stick insects (order Phasmatodea), using four European species. Their long and thin bauplan makes the Phasmatodea ideal for ecomorphological studies of body length, which could identify the evolutionary drivers of their remarkable size range (including the world's longest insects). Using preserved specimens from collections across Europe; body segment and limb measurements were taken for both genders of the species *Bacillus rossius, Clonopsis gallica, Leptynia attenuata*, and *Pijnackeria hispanica*. Lengths and volumetric features were compared to latitude as well as annual mean temperature, net primary productivity, and annual growing degree days, using weighted linear regressions and ANOVA analyses. At lower latitudes/higher temperatures, *B. rossius* and *L. attenuata* had longer limbs [Allen clines] and were larger bodied and/or longer [converse-Bergmann clines], while the other species did not show latitudinal clines *per se*. This matches what was predicted based on closely related insects and the presence of large Phasmatodea in the tropics, but violates the temperature-size rule. Most variation in size could be attributed to temperature, but untested factors could also play a role Whether these ecogeographic rules hold true for tropical Phasmatodea and whether genetics or environment play are more important in determining adult length are topics for future research.

Keywords: phasmatodea, Bergmann's rule, Allen's rule, latitudinal cline, insect ecology, morphometrics

OPEN ACCESS

Edited by:
Thomas Buckley,
Landcare Research, New Zealand

Reviewed by:
Alberto G. Sáez,
University of Zurich, Switzerland
Dmitry Yurievich Sherbakov,
Limnological Institute (RAS), Russia
Marco Gottardo,
University of Siena, Italy

***Correspondence:**
Matan Shelomi
mshelomi@ntu.edu.tw

Specialty section:
This article was submitted to Phylogenetics, Phylogenomics, and Systematics, a section of the journal Frontiers in Ecology and Evolution

Received: *28 November 2016*
Accepted: *21 March 2017*
Published: *05 April 2017*

Citation:
Shelomi M and Zeuss D (2017) Bergmann's and Allen's Rules in Native European and Mediterranean Phasmatodea. Front. Ecol. Evol. 5:25. doi: 10.3389/fevo.2017.00025

INTRODUCTION

The most highly studied ecogeographical rule is Bergmann's (1847) rule. According to the most recent and most thorough critical translation of the original German manuscript (Salewski and Watt, 2017), the rule states that, all else equal, "within species and amongst closely related species of homeothermic animals [those that maintain a constant internal body temperature] a larger size is often achieved in colder climates than in warmer ones, which is linked to the temperature budget

of these animals." Bergmann assumed that an animal's surface area determines its rate of heat dissipation, and its volume determines its heat production, meaning the surface-area-to-volume ratio (SA:V) represents its thermoregulatory ability. Because volume increases faster than surface area due to the square-cube-law, the SA:V of an organism decreases as it gets larger, also implying less heat loss per heat generated, or less heat production needed to maintain body temperatures. Thus, Bergmann's rule can be summarized as saying homeothermic animals will have a lower SA:V at higher latitudes and/or altitudes. A similar rule is Allen's (1877) rule, which states that, within endothermic [generating their own body heat] species, extremity length decreases as latitude increases, for similar thermoregulatory reasons.

Many have debated considerably about the exact definitions and nuances of these rules: Do they apply to ectotherms [animals that predominantly gain heat from the environment]? Can they be tested in intraspecific studies? Must they inherently imply a causative mechanism, and must that always be temperature regulation? (Mayr, 1956; Ray, 1960; Watt et al., 2010; Meiri, 2011; Olalla-Tárraga, 2011) The nuances of Bergmann's rule are particularly highly debated due to the lack of complete English translations of Bergmann's original manuscript (Salewski and Watt, 2017). In addition to thermoregulation, other explanations for Bergmann-type clines include differential dispersal rates, starvation resistances, resource availability, precipitation, primary plant productivity, habitat diversity, seasonality, genetics, and chance (Geist, 1987; Partridge and Coyne, 1997; Blackburn et al., 1999; Meiri et al., 2007). For simplicity, we will use the terms "Bergmann's rule" to cover body size clines and "Allen's rule" to cover extremity size clines over latitude or altitude regardless of taxon-level, thermal regulation, or proposed mechanism driving the cline.

Both rules hold well in mammals and birds and can be considered valid ecological generalizations in these endothermic groups (Meiri and Dayan, 2003; Purvis and Orme, 2005; Salewski and Watt, 2017). In ectotherms, however, heat is not generated but absorbed from the external environment (Ray, 1960). Animals with larger surface areas lose and gain heat faster, and larger volumes mean more heat can be stored but more heat is needed to affect a change in body temperature. Thus, selection for faster heat transfer should lead to larger SA:V ratios, while selection for more stable internal temperatures should lead to smaller SA:V ratios, and either can be preferable for hot or cold climates (Ashton and Feldman, 2003). While some ectotherms try to maintain a constant internal body temperature (homeothermy, such as basking reptiles), others are fully poikilothermic [body temperature varies according to the environment], and many are on a spectrum between the two. These temperature effects will interact with other proposed mechanisms, such as with food availability to affect energy efficiency and demand (Reim et al., 2006). The matter is further complicated by the temperature-size rule, which states that ectotherms will grow slower at cold temperatures but will reach larger adult sizes (van Voorhies, 1996). If this growth rate is standardized across time, then the adult body length may be dependent on season length. Whether the temperature-size rule holds or not is debated (Ray, 1960; Mousseau, 1997), and the mechanisms behind this rule (such as the relative effects of increased cell size or cell number, or of genetics and plasticity) are also contested and unclear (Partridge and Coyne, 1997; Angilletta and Dunham, 2003; Angilletta et al., 2004; Blanckenhorn and Llaurens, 2005; Karl and Fischer, 2008). We stress here that all these "rules" are descriptions of patterns for which multiple exceptions are allowed, and not "laws" in the sense that they are obeyed in all cases.

Among terrestrial ectothermic vertebrates, Bergmann and Allen's rule generally hold for amphibians and turtles (Alho et al., 2011), while snakes and lizards follow the opposite (Ashton and Feldman, 2003), with exceptions in each group. Species showing these "converse-Bergmann" clines are larger in warmer climates, meaning lower latitudes and altitudes. These results held regardless of sample size and other experimental values, suggesting that they are biologically significant for these taxa (Ashton, 2004). By contrast, data on insects shows highly unpredictable variation in size clines, with different species within the same genus often showing contrasting relationships to latitude (Shelomi, 2012). In addition to Bergmann and converse-Bergmann clines, there are non-linear clines: Cases where, for example, organisms are largest at the middle (Vamosi et al., 2007) or the extremes (Johansson, 2003) of their latitudinal range, or where an increasing cline stops or resets periodically [stepwise or sawtooth cline], usually due to changes in voltinism and seasonality (Masaki, 1972; Nylin and Svärd, 1991). Many species showed no clines at all (Nylin and Svärd, 1991; Shelomi, 2012). Experimental design elements such as the body parts measured, inter/intraspecific variability, geographical range size, and contiguousness (whether the samples come from one continuous range or several, unconnected sites) all had effects on the results (Shelomi, 2012). However, some general patterns seemed to appear at the taxonomic level of orders. For example: Coleoptera are more likely to show converse-Bergmann clines, Diptera Bergmann, and Plecoptera no cline (Shelomi, 2012).

Notably absent from the literature is ecogeographical data on the stick and leaf insects (order Phasmatodea). Though this order is generally poorly studied, the lack of morphometrical data is particularly surprising due to the evolutionary importance of size on this order. Phasmatodea range from the small Timematodea of 2–3 cm in length to the world's longest insect, a record presently held by the Bornean *Phobaeticus chani* Bragg 2008 (Phasmatidae), at 567 mm from foretarsi to hindtarsi, and 357 mm for the body alone (Whitman, 2008). Phasmatodea are often sexually dimorphic, with females being considerably larger than males. They usually follow the reverse of Rensch's (1943) rule, which states that sexual size dimorphism decreases with size in species where females are larger, meaning the dimorphism in phasmids increases with size (Abouheif and Fairbairn, 1997). With their long but thin bauplan, nearly cylindrical in all but the leaf insects (Phylliidae, which have a cylindrical body cavity but broad, leaf-mimicking projections), Phasmatodea are easy to measure for morphometrical assays, and are hence ideally suited for testing Bergmann's and Allen's rules.

Whether Phasmatodea follow these rules is not predictable, but the existence of the record-breakers in the tropics suggests

converse-Bergmann clines. Based on taxonomic proximity, converse-Bergmann clines or no clines are predicted because those are the most common results for Bergmann's rule assays in the closely related Orthoptera (Shelomi, 2012). The only intraspecific data on the subject is a comparison of two specimens of *Dares murudensis* Bragg 1998 (Heteropterygidae), including the holotype, which suggested that this species may be larger at low altitudes [converse-Bergmann cline] (Büscher, 2014). It is also unclear if temperature is the determining force in Phasmatodea size, not only due to the aforementioned alternative mechanisms for size clines, but also because Phasmatodea body dimensions likely influence the effect and success of their mimesis: The ratio of length to thickness and the location of the six limbs can increase or decrease their resemblance to the plants on which they live and feed, and therefore their camouflage ability (Robinson, 1966). Experiments on cultured specimens of the Indian stick insect *Carausius morosus* Sinety 1901 in Germany suggested that they grow slightly longer at lower temperatures, suggesting Bergmann's and the temperature-size rule hold in this species (Kann, 1937, as cited by Ray, 1960), however these effects could be overshadowed in the field by a number of other processes.

In this study, we performed the first ever test of Bergmann's and Allen's rule in the Phasmatodea, using four species with native habitats across Europe and the southern Mediterranean coast (Brock, 1991). Our hope is to open the field of Phasmatodea morphometrics, whose ultimate end is to answer the question of how and why the order evolved its incredible range of lengths and body sizes.

MATERIALS AND METHODS

Species and Measurements

The species chosen are four species endemic to Europe: *Bacillus rossius* Rossi 1788 (Bacillidae), *Clonopsis gallica* Charpentier 1825 (Bacillidae), *Leptynia attenuata* Pantel 1890 (Heteronemiidae), and *Pijnackeria hispanica* Bolívar 1878 (Heteronemiidae). For information on the recent generic revision of the latter two, see Scali (2009). The geographical ranges of these species cover a broad enough latitudinal range to capture possible non-linear clines and seasonality effects, but are not so broad as to be unlikely to show any cline at all, as has been a complication of studies crossing several continents (Shelomi, 2012). When available we included subspecies (ex: *B. rossius rossius, B. rossius redtenbacheri*), but not other species in the same genus (ex: *B. grandii*, *B. atticus, B. whitei*). Data was also collected for *C. morosus* Sinety 1901 (Phasmatidae), an Indian stick insect known as an invasive species in the UK and Azores as well as South Africa and California (Headrick and Wilen, 2011; Borges et al., 2013), however too few ($n = 22$) such wild-caught specimens were found for further analysis.

Measurements were done on pinned and dry-mounted specimens in entomological and natural history museum collections (**Table S1**). Only adult male and female individuals were measured, as determined based on their known minimum lengths (Brock, 1991). Specimens without legible locality data were omitted. Specimens labeled as reared or cultivated were not included in the analysis unless they were captured in adulthood and died shortly thereafter. The geographical localities of these specimens are presented in **Figure 1**.

Measurements were made in mm using Maxwell brand digital calipers with an error of ±0.1 mm, on the following body parts [abbreviations used in data tables] (**Figure 2**): The length of the head [HL], thorax [TL], abdomen (all 10 segments combined) [AL], forelimb from the distal end of the trochanter to the tip of the arolium [FLL], hind femur [HFL]; and the width of the head [HW], middle thorax (where the middle pair of legs originate) [MT], and the waist (where the hind legs originate) [WT]. Because Phasmatodea can regenerate limbs, and the regenerated limbs will never become as long as the originals (Maginnis, 2008), we ignored limbs noticeably much smaller than the paired limbs on the same individual or other specimens. We generally used the left forelimb and right hind femur, except in cases where said appendage was missing, damaged, or regenerated. For incomplete or damaged specimens, we recorded only what was suitable for measurements.

We defined "body length" [BL] as the sum of HL+TL+AL. We also created a metric "fully extended length" [L] as FLL+TL+AL that represents the length of the insect when it holds its forelimbs alongside its head in line with the rest of its body, as they do when attempting to maximize their mimesis toward a branch (Robinson, 1966). This measurement may be a better indicator of selection due to factors affecting camouflage. We estimated surface area (SA, square mm), volume (V, cubic mm), and thoracic circumference (ThC, mm) using BL and the mean of MT and WT with the formulae for these metrics for a cylinder (see also Zeuss et al., 2017). While most Bergmann assays historically only use linear measurements, the use of SA and V allows for the most direct testing of Bergmann's rule via the SA:V ratio's cline over latitude (Salewski and Watt, 2017).

Locality and Independent Variables

Location data and collection date was obtained from specimen labels. From the locations, approximate GPS coordinates were extracted, using center-points of cities or the nearest large park/forests as likely collection areas if no further details were given on the data labels. Specimens with localities that were too generic [Ex: "France"] were omitted. Altitude/Elevation data was also collected, however too few samples (<20%) had this information for further analysis.

From the GPS data we calculated latitude and longitude. The independent, environmental variables for our analyses each test a possible mechanism that could drive a Bergmann-type cline: Annual Mean Temperature [AMT, °C], representing Bergmann's original thermoregulatory hypothesis (Hijmans et al., 2005; http://www.worldclim.org/current); Net Primary Productivity [NPP, grams dry matter per sq. m per year], representing plant resource availability (data from the FAO GeoNetwork, http://www.fao.org/geonetwork/srv/en/metadata.show?id=36915, period 1976–2000); and total annual Growing Degree Days [GDD, a measure in heat units calculated for each day by subtracting a base temperature, in our case 5°C, from the day's mean temperature], representing the length of the year's growing season as the annual amount of

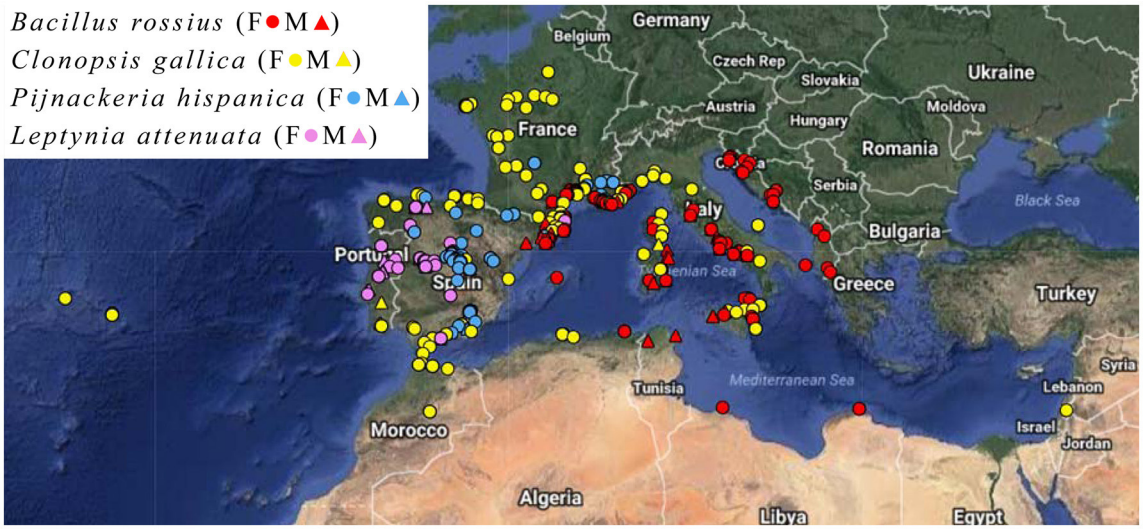

FIGURE 1 | Locality map of the Phasmatodea specimens. Key: Female (circle), male (triangle), *Bacillus rossius* (red), *Clonopsis gallica* (yellow), *Pijnackeria hispanica* (blue), *Leptynia attenuata* (violet). Map made using HamsterMap.com and satellite imagery from Google Earth.

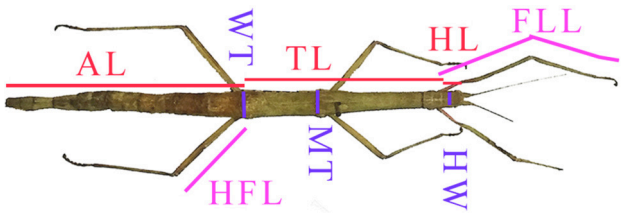

FIGURE 2 | Morphometrical measurements and abbreviations used in this study. Based on a figure of a female *Clonopsis gallica* from Brock (1991), which is representative of the morphology of all species examined here. AL, abdomen length; FLL, forelimb length; HFL, hind femur length; HL, head length; HW, head width; MT, middle thorax width; TL, thorax length; WT, waist width.

thermal energy available for plant and insect growth (New et al., 1999; https://nelson.wisc.edu/sage/data-and-models/atlas/maps.php?datasetid=31&includerelatedlinks=1&dataset=31). In our study area, AMT and GDD were negatively correlated with latitude, while NPP was positively correlated with latitude due to increased aridity around the Mediterranean Sea relative to central Europe (Zeuss et al., 2017).

Statistical Analysis

We analyzed each species and gender combination separately. We did not find enough *C. gallica* males or *P. hispanica* males for meaningful statistical analysis ($n = 7$ and 17 respectively), and so did not analyze them further. Statistics were weighted based on latitude and longitude locality to control for pseudoreplication caused by unequal numbers of specimens per location. We used R to perform weighted single linear regressions for the effects of latitude, longitude, year of collection, and each of the three environmental variables, plus a multiple linear regression for a model of the three environmental variables' effects on each body size measurement, using ANOVA for the significance testing (R Development Core Team, 2008). Because the environmental variables are intercorrelated to some extent, we used the R package *hier.part* to determine the independent linear contributions of each variable via hierarchical partitioning (Walsh and Mac Nally, 2013) with R-squared as the goodness of fit measure. We also performed canonical correspondence analysis (CCA) using *rcorr* (Harrell, 2016) on unweighted data. Log transformations of the data did not affect the results of the statistical assays, so we present the results with the untransformed data here.

RESULTS

Basic Statistics

A total of 1,437 individual insects were measured from 18 museums (**Table S1**) across eight nations, representing localities from 23 European and North African nations under modern borders. Of these individuals, 869 had usable locality data for inclusion in this assay. The locations of each specimen are shown in **Figure 1**. Further data on the status of the museum collections is available in Shelomi (2016).

The results of the statistical analysis are summarized in **Tables 1, 2** and fully provided in **Data Sheet S1**. The raw data is available in **Table S2**. Of all the measurements, head length and width were likely the least accurate due to their low ranges and the uneven head shape of Phasmatodea, so these variables may not be trustworthy. All other metrics were reliably measured, with thorax length and hind femur length both the easiest and most accurate to measure. **Figure 3** shows the effect of latitude on each species/sex combinations' fully extended length (L), with the linear regression equation given if a significant effect was detected. **Figure 4** shows the same for SA:V. **Figure 5** shows

TABLE 1 | Summary of weighted single and multiple linear regression assay and hierarchical partitioning results of ecogeographical body size variation in European Phasmatodea.

Assemblage (Total *n*)	Metric	Single variables (slope, $R^{\wedge}2$, *p*)					Full Model ($R^{\wedge}2$, *p*)	Full model variables (slope,%I, *p*)		
		Latitude	Longitude	AMT	NPP	GDD		AMT	NPP	GDD
B.rossius female (173)	TL	−0.049*	ns	+0.09**	ns	ns	0.097*	+88.0**	ns	ns
	AL	−0.091**	ns	+0.12**	ns	+0.025•	0.18**	+87.8**	ns	ns
	HFL	−0.10**	ns	+0.057*	ns	ns	0.058•	+87.6*	ns	ns
	SA	−0.145***	ns	+0.099**	−0.060*	+0.070*	0.100*	+21.7**	ns	ns
	V	−0.169***	ns	+0.11**	−0.068*	+0.097**	0.11*	+13.7**	ns	ns
B.rossius male (103)	TL	ns	ns	ns	−0.057•	ns	ns	ns	ns	ns
	AL	ns	ns	ns	ns	ns	ns	ns	ns	ns
	HFL	ns	ns	ns	ns	ns	ns	ns	ns	ns
	SA	−0.099*	ns	+0.052•	ns	ns	ns	ns	ns	ns
	V	−0.103*	ns	+0.051•	ns	ns	ns	ns	ns	ns
C.gallica female (315)	TL	ns	ns	ns	+0.0015•	ns	ns	ns	ns	ns
	AL	+0.033*	ns	ns	ns	ns	ns	ns	ns	ns
	HFL	ns	−0.023*	ns	ns	ns	ns	ns	ns	ns
	SA	+0.042*	+2.04*	ns	ns	ns	ns	ns	ns	ns
	V	+0.024•	+11.6**	ns	ns	ns	ns	ns	ns	ns
L.attenuata female (60)	TL	−0.24*	ns	+0.52***	ns	+0.49***	0.54**	+43.6***	ns	ns
	AL	ns	ns	+0.39**	ns	+0.28**	0.46**	+43.5**	+31.6•	ns
	HFL	−0.38**	ns	+0.63***	ns	+0.41**	0.67***	+66.9***	+14.3***	ns
	SA	ns	ns	ns	ns	+0.18*	ns	ns	ns	ns
	V	ns	ns	ns	ns	+0.14•	ns	ns	ns	ns
L.attenuata male (66)	TL	−0.27**	+0.49*	+0.33**	ns	+0.11•	0.44**	+63.3**	ns	ns
	AL	−0.14•	ns	+0.44***	ns	ns	0.52**	+76.7***	ns	−22.2*
	HFL	−0.22*	+0.50*	+0.26*	ns	ns	0.38*	+66.2**	ns	ns
	SA	ns	ns	ns	ns	ns	ns	ns	ns	ns
	V	ns	ns	ns	ns	ns	ns	ns	ns	ns
P.hispanica female (128)	TL	ns	ns	ns	+0.073*	−0.13**	0.11•	ns	ns	−15.5•
	AL	ns	ns	−0.10*	+0.12*	−0.22***	0.20**	+70.2*	+1.5•	−28.3•
	HFL	ns	ns	−0.35***	+0.17**	−0.30***	0.37***	−57.3***	+14.2•	ns
	SA	ns	ns	−0.108*	ns	−0.18**	0.140*	+7.6*	ns	−40.4•
	V	ns	ns	−0.062•	ns	−0.097*	ns	ns	ns	ns

*The number of specimens for each species/gender pair is given in parenthesis, although the number of specimens for each metric may be smaller due to damaged specimens (see the complete data in **Table S2**). Data for B. rossius and C. gallica includes the geographic outliers. Dependent variables/Body size metrics are thorax length (TL), abdomen length (AL), hind femur length (HFL), surface area (SA), and volume (V). Statistics were calculated with linear regression models weighted by the number of specimens per latitude-longitude location, using single regression for five variables [latitude, longitude, annual mean temperature (AMT), net primary productivity (NPP), and growing degree days (GDD)] and a multiple regression model for AMT+NPP+GDD. For single regressions, the amount of explained variance is given as the adjusted R^2 value, with +/− indicating the direction of the relationship. The R^2 for the full model is also provided. For the variables within the full model that had a significant effect, the amount of explained variance is given as a percentage of independence (%I) based on hierarchical partitioning. Significance statistics are based on an F-test of the regression model for the single regression variables and for the full multiple model, and based on an ANOVA of the model for the environmental variables within the multiple model. ns, not significant, $p > 0.1$, •, not significant, $p > 0.05$, *$p < 0.05$, **$p < 0.01$, ***$p < 0.001$.*

schematic illustrations of the mean, minimum, and maximum sizes of these insects.

Correlation Analyses: Effects on Insect Size

In the single regressions, decreasing lengths and widths with higher latitude and lower AMT was observed in *B. rossius* females. Similar effects were noted in the multiple regression assays, with ANOVA suggesting that AMT, which is negatively correlated with latitude, had the strongest and often only significant effect on these species' metrics. Hierarchical partitioning attributed the majority (>50%) of the independent effects of the multiple model on AMT for lengths, but GDD for thickness. Among the tested parameters here, therefore, AMT is the strongest statistical contributor to latitudinal clines in body segment and limb lengths, and GDD to

TABLE 2 | Summary of unweighted single correspondence analysis results of ecogeographical body size variation in European Phasmatodea.

Assemblage (Total *n*)	Metric	Correspondance analysis (*r* or rho, *p*)					
		Latitude	Longitude	AMT	NPP	GDD	Year
B. rossius female (173)	TL	−0.2**	ns	0.28***	ns	ns	ns
	AL	−0.26***	ns	0.31***	ns	0.16*	ns
	HFL	−0.24**	ns	0.28***	ns	ns	ns
	SA	−0.31***	ns	0.33***	−0.15•	0.23**	ns
	V	−0.33***	ns	0.33***	−0.16*	0.26***	ns
B .rossius male (103)	TL	ns	ns	ns	−0.2*	ns	ns
	AL	ns	ns	ns	ns	ns	ns
	HFL	ns	ns	ns	ns	ns	ns
	SA	−0.25*	0.29**	0.2*	ns	ns	ns
	V	−0.27**	0.32**	0.21*	ns	ns	0.19•
C. gallica female (315)	TL	0.12*	−0.1•	0.1•	0.16**	ns	−0.14*
	AL	0.15**	ns	ns	ns	ns	ns
	HFL	ns	−0.27***	0.11•	ns	ns	ns
	SA	0.12*	0.15**	ns	ns	ns	ns
	V	0.11•	0.19***	ns	ns	ns	ns
L. attenuata female (60)	TL	−0.49***	ns	0.49***	0.49***	0.49***	0.52***
	AL	−0.27*	ns	0.27*	0.27*	0.27*	0.32*
	HFL	−0.57***	ns	0.31*	0.31*	0.31*	0.32*
	SA	ns	ns	0.3*	0.3*	0.3*	0.47***
	V	ns	0.22•	0.28*	0.28*	0.28*	0.43**
L. attenuata male (66)	TL	−0.48***	0.38**	0.53***	ns	0.34**	ns
	AL	−0.37**	ns	0.59***	ns	0.31*	ns
	HFL	−0.42***	0.4**	0.44***	ns	0.3*	ns
	SA	−0.22•	0.3*	0.29*	ns	ns	ns
	V	ns	0.28*	ns	ns	ns	ns
P. hispanica female (128)	TL	ns	ns	−0.19*	0.21*	−0.29***	0.38***
	AL	ns	ns	−0.25**	0.26**	−0.35***	0.42***
	HFL	ns	0.17•	−0.51***	0.38***	−0.48***	0.38***
	SA	ns	ns	ns	ns	−0.23*	0.29*
	V	ns	ns	ns	ns	−0.18•	0.23*

*See caption for **Table 1**. Statistics were calculated with correspondence analysis for all measured metrics (**Data Sheet S1**), of which five are presented here. The Pearson's r or Spearman's rho rank correlation coefficient with slope is given with a symbol for the statistical significance as calculated with the rcorr program. ns, not significant, $p > 0.1$, •, not significant, $p > 0.05$, *$p < 0.05$, **$p < 0.01$, ***$p < 0.001$.*

widths and SA:V (**Table 1**). In the CCA, all non-head size metrics significantly decreased with increasing latitude ($p < 0.01$) and correspondingly decreasing AMT ($p < 0.01$), with width-based metrics (widths, surface area, volume, SA:V, and circumfrerence) only increasing with decreasing GDD ($p < 0.01$), and increasing NPP ($p < 0.05$). Longitude and year had no effect.

Three apparent outliers in the *B. rossius* females existed: These specimens were from two locations on the northern coast of Libya (**Figure 1**), having low latitudes but also small sizes (easily noticed in **Figures 3**, **4**). Excluding these outliers produced stronger single and multiple variable effects, with appearance of an effect of NPP (positive correlation, $p < 0.05$) in the multiple regression model not present with the outliers (**Data Sheet S1**).

B. rossius males showed no length clines except in the aforementionedly unreliable head size dimensions. In single regression models, *B. rossius* males were significantly thinner at larger latitudes ($p < 0.05$) with an overall increase in SA:V ($p < 0.05$), but this effect vanished in the multiple model ($p > 0.1$). The CCA showed negative effects on width based metrics alone for increasing latitude and decreasing AMT, as well as strong ($p < 0.01$) positive effects of increasing longitude.

In the single regression analyses for *C. gallica* females, the abdomen was slightly significantly ($p < 0.05$) larger in higher latitudes, the limbs were shorter ($p < 0.05$) in higher longitudes

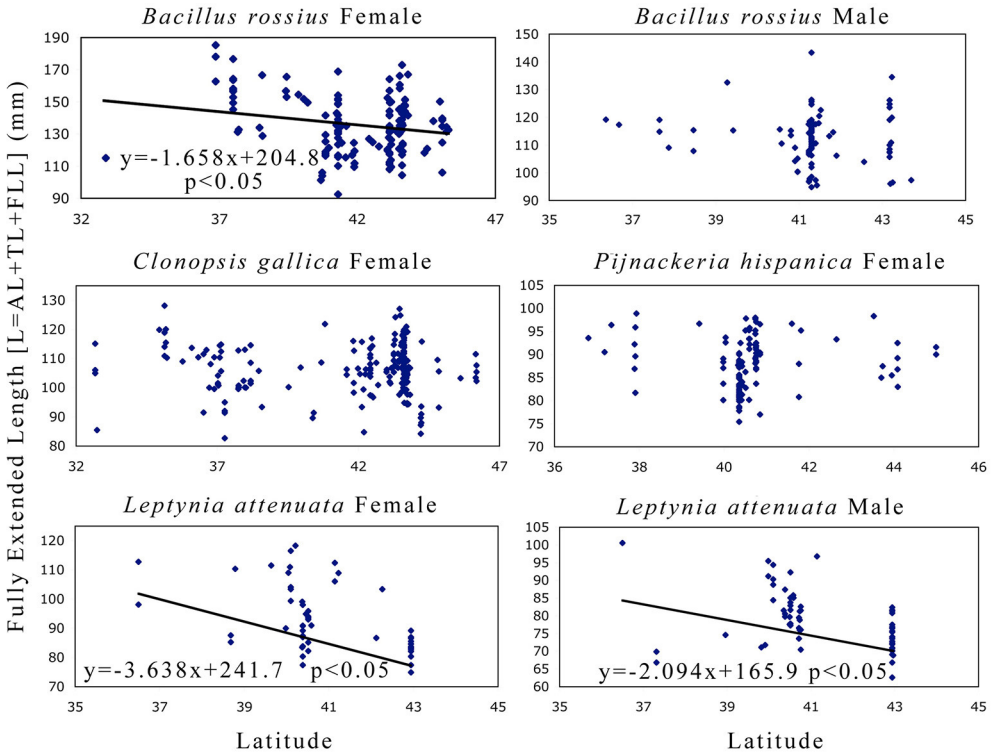

FIGURE 3 | Fully extended length as a function of latitude in Phasmatodea. This variable (L) is the sum of both body [abdomen and thorax] and extremity [forelimb] lengths, so these metrics address Allen's rule [limb length] directly and have historically been used to measure Bergmann's rule [body size]. This metric also has the most direct implication in mimesis, as the extended pose is used by these species to maximize branch-mimicking camouflage. The results suggest that female *B. rossius* and both gender *L. attenuata* are shorter at higher latitudes (Allen cline, converse-Bergmann cline). Each point represents an individual specimen. Latitude values are in decimal degrees, L in mm. If the single linear regression weighted by the number of specimens per latitude-longitude location was significant, then the regression line, its equation, and its significance level are provided.

[eastward], and no significant effects of environmental variables were noted. *C. gallica* had a significantly larger surface area ($p < 0.05$) and, to a lesser extent, volume ($p < 0.1$) at higher latitudes and longitudes, resulting in a barely insignificant ($p < 0.1$) decrease in SA:V ratio with latitude alone but a strongly significant decrease for longitude alone ($p < 0.001$). Hierarchical partitioning suggested NPP affects lengths while AMT and GDD affect width, but the multiple regression models were not significant for this species. CCA suggested increased body segment length with increasing latitude ($p < 0.05$), plus reduced limb length ($p < 0.001$) but increased width, and overall size ($p < 0.01$) with increasing longitude [moving eastward].

Eleven longitudinal outliers in *C. gallica* existed (**Figure 1**), 10 from three locations in the Azores [−28.6 to −25.6° longitude] and one from Israel [35.0° longtidue]. Nearly 20° of longitude existed between these specimens groups and their next closest specimens [Iberia and Sicily respectively], meaning they greatly reduced the contiguousness of the dataset and nearly tripled the total longitudinal range. Removing these samples had slight changes in the significance of the observed correlations, with the most noticable effect of removing the latitudinal cline for abdomen length. CCA revealed significantly shorter limbs and larger bodies with increased longitude, with increasing AMT, NPP, and collection year all positively affecting length, but reduced effect of latitude. GDD was never significant in *C. gallica* CCA.

Single regressions for both genders of *L. attenuata* reported decreasing lengths with higher latitude and lower AMT, and increased width with higher GDD for females only. In *L. attenuata* males only, longitude also had a positive effect on limb and thorax lengths. In the mixed model, AMT had the strongest and often only significant effect on these species' metrics. For females, hierarchical partitioning attributed the majority (∼65%) of the independent effects of the multiple model on AMT for limb length, but GDD took a larger share of the independent effects for body segment lengths. CCA on females found significant negative effects of increased latitude on body and limb length, but significantly positive and, notably, equal sized effects of AMT, NPP, and GDD ($p < 0.05$). Year had significant positive effects on all metrics (older specimens were smaller). Note that *L. attenuata* specimens had the smallest range for all environmental factors and that this was our smallest dataset. For males, hierarchical partitioning suggested AMT is the strongest statistical contributor for most metrics, and CCA found significant negative effects of latitude but positive effects for longitude ($p < 0.05$), AMT ($p < 0.001$),

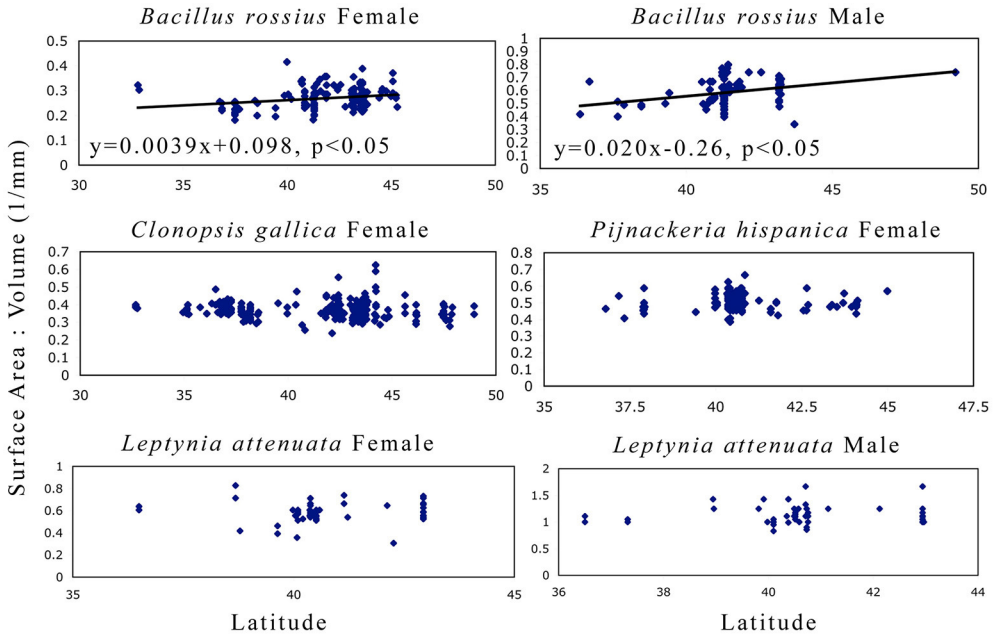

FIGURE 4 | Surface area to volume ratio as a function of latitude in Phasmatodea. These results address Bergmann's rule of whether or not the SA:V ratio correlates with latitude. Larger bodies have a smaller SA:V ratio. Only *B. rossius* shows a cline, present in both genders, where individuals in higher latitudes are smaller bodied than those in lower latitudes (converse-Bergmann cline). Each point represents an individual specimen. Latitude values are in decimal degrees, SA:V in mm^{-1}. If the single linear regression weighted by the number of specimens per latitude-longitude location was significant, then the regression line, its equation, and its significance level are provided.

and GDD ($p < 0.05$) only for lengths only. Year had no effect.

In *P. hispanica* females, single regression suggested a negative effect of GDD ($p < 0.01$) and AMT ($p < 0.05$) on limb and body lengths, and a positive effect of NPP on lengths ($p < 0.05$). CCA suggested the same, as well as a positive effect of year ($p < 0.01$). This was the only time AMT and GDD were found to have negative effects on specimen size. In the multiple-variable model, limb and body lengths showed different clinal directions: Abdomen length was now positively correlated to AMT ($p < 0.05$), while limb length was still strongly negatively correlated to AMT (FLL: $p < 0.01$, HFL: $p < 0.001$). *P. hispanica* widths did not differ significantly with any independent variable, and neither did SA:V, although surface area was significantly ($p < 0.05$) positively correlated with AMT in the single and multiple regression models. Hierarchical partitioning suggested AMT is usually the strongest contributor to among the environmental factors. Overall these idiosyncratic responses produced no latitudinal (**Figure 3**) or longitudinal clines for lengths in *P. hispanica* females using any statistical model.

Correlation Analyses: Environment to Geography

Table 3 shows, for each data set, whether the environmental factors correlate to latitude or longitude. We include these data because of samples where the environmental clines and geographic clines do not align. In general, AMT and GDD should decrease and NPP increase with increasing latitude. For AMT this pattern held strongly ($p < 0.001$) for all except the female *L. attenuata* ($p < 0.01$) and *P. hispanica* ($p < 0.05$) datasets. The same correlations existed for GDD, very strong ($p < 0.001$) in all but these two ($p < 0.01$). NPP correlated positively and strongly ($p < 0.001$) with latitude for all except the male *B. rossius* set, where the correlation was weaker ($p < 0.05$), and the two *L. attenuata* sets, where it did not correlate at all ($p > 0.1$). Environmental factors responded to longitude differently, especially NPP, whose correlation to longitude could be positive, negative, or not significant depending on species, sex, and presence or absence of outliers within the dataset.

DISCUSSION

Bergmann's, Allen's, and Temperature-Size Rules in European Phasmatodea

As in all ecogeographical studies, the possibility exists that the sampling did not cover a sufficient range to account for true clines, linear or otherwise. Due to the limitations of museum collection efforts, which are not random in location or timing of collecting (Shelomi, 2016), as well as climate and environmental change over time, we may have missed changes over the decades. Other potential biases are whether the original collectors preferentially kept or noticed larger specimens, whether smaller adults were erroneously discarded as nymphs by the original collectors or in this analysis, or whether smaller adult legs were mistakenly identified as regenerations and excluded. These

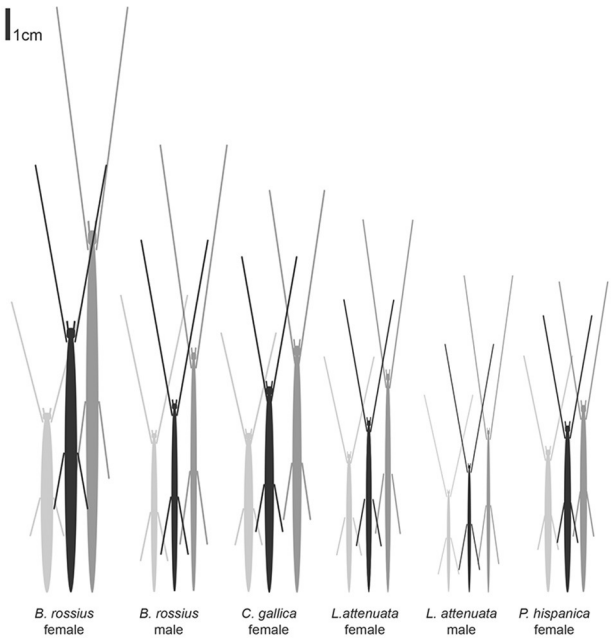

FIGURE 5 | Schematic of the mean, minimum, and maximum sizes of Phasmatodea in this study. Images were made to a scale of 10 pixels per mm first using ellipses with a height of the mean body length [BL] and width of the mean waist thickness [WT], with forelimbs drawn with the length of the mean forelimb length [FLL], and hind femurs drawn with the length of the mean hind femur length [HFL] connected to the insect at the proper location [thorax-abdomen junction] based on the mean abdomen length [AL]. These were scaled up or down according to the largest and smallest recorded insect [L]. Image Credit: Shelomi.

TABLE 3 | Summary of correspondence analysis results between geographic location and climate factor.

Species + Sex	Correspondance analysis (slope and significance)					
	AMT/Lat	NPP/Lat	GDD/Lat	AMT/Lon	NPP/Lon	GDD/Lon
B. rossius female	−0.49***	0.61***	−0.84***	ns	0.24*	ns
B. rossius female†	−0.43***	0.51***	−0.82***	ns	0.36**	ns
B. rossius male	−0.68***	0.38*	−0.7***	0.5**	ns	0.6***
C. gallica female	−0.58***	0.49***	−0.77***	ns	−0.15•	ns
C. gallica female†	−0.55***	0.5***	−0.75***	ns	ns	ns
L. attenuata female	−0.59**	ns	−0.67**	ns	−0.51*	ns
L. attenuata male	−0.73***	ns	−0.81***	−0.47*	−0.63**	−0.63**
P. hispanica female	−0.35*	0.72***	−0.47**	−0.19	0.45**	−0.11

*For each species/sex dataset, the correlation of Lat(itude) and Lon(gitude) to the three environmental factors was calculated. The Pearson's r or Spearman's rho rank correlation coefficient with slope is given with a symbol for the statistical significance as calculated with the rcorr program. ns, not significant, $p > 0.1$, •, not significant, $p > 0.05$, *$p < 0.05$, **$p < 0.01$, ***$p < 0.001$. †, without outliers as described in the text.*

would all bias the samples toward larger insects. Larger nymphs erroneously labeled as adults would have the opposite effect. While only dry specimens were used to avoid the shrinking effects of ethanol, different preservation methods of the different collectors, such as the substance used to kill the insects in the field and whether the insects dried straight or contorted, would also affect the final specimen dimensions. Adult phasmatodea live for several months, so one cannot tell from the date of collection of an adult whether they spent formative months of their development in colder or warmer seasons. Lastly, the data cannot account for effects of altitude, as most specimen labels did not include altitude data. These factors should all be kept in mind when interpreting the results.

The single-variable regression lines for latitude were better fits to the data than the full model [lower *p*-values on the *F*-test of the regression lines] for *B. rossius* and *C. gallica*, and were better fits for AMT and GDD in all species, so the frequent absence of an observed effect of GDD in the mixed regression models may be due to autocorrelation from AMTs effect on GDD. Overall and from our three environmental variables, much of the variation in body size of the specimens was attributed to AMT, with GDD also important for body width in particular but not limb length. Little was ever attributed to NPP, which also rarely had an effect in the models. This suggests that abundance of available plant matter has less of a role than the available heat energy in European Phasmatodea size. Alternatively this is because NPP was highly variable over longitude within the datasets, even if it correlated reliably with latitude.

B. rossius females showed unambiguous converse-Bergmann clines, being longer, thicker, and overall larger (smaller SA:V ratios, **Figure 4**) at lower latitudes and at warmer climates (higher AMTs). These results fit our hypothesis for converse-Bergmann clines in the Phasmatodea based on the presence of giant Phasmatodea species in the tropics and what was observed for the related Orthoptera, but contradict the temperature-size rule that was observed for *Carausius*. The species also followed Allen's rule (**Figure 3**), but likely not for thermoregulatory reasons. *B. rossius* males also showed converse-Bergmann clines in the single regression model (**Figure 4**) and the CCA (**Table 2**), but no clines for limb length.

C. gallica showed detectable but statistically insignificant ($0.05 < p < 0.1$) Bergmann clines for body size [higher surface areas and volumes plus lower SA:V at higher latitudes], due primarily to increased abdominal length. None of the measured environmental factors had significant effects. The results are thus borderline between Bergmann and no cline. One problem may be the species' large longitudinal distribution (**Figure 1**), as non-contiguousity can obscure the true nature of an ecogeographic cline (Shelomi, 2012), as was strongly the case for *B. rossius* with the Libyan specimens. Indeed, longitude had significant, positive effects on body size and negative effects on limb length in *C. gallica*, which were more noticable ($p < 0.01$) when the longitudinal outliers were removed, however removing these outliers also reduced the impact of latitude on abdomen

length (**Data Sheet S1**). Longitude normally does not figure into ecogeographic clines, however the impact of the Atlantic currents on weather and the large geographical spread of this species provide variables that could covary with longitude in Europe. Limb length was not correlated with latitude or environment, but was strongly negatively affected by increasing longitude. *C. gallica* also had the greatest total ranges in the environmental factors than the other species, even after removing the outliers, but there is no guarantee that these factors change linearly with latitude and longitude across Europe. We reserve judgment on whether *C. gallica* truly follows Bergmann's or Allen's rules pending more collecting of this widespread species, especially from the Balkans and Turkey where the species is known to occur (Brock, 1991), but from which region few collected specimens are available for a number of reasons (Shelomi, 2016).

L. attenuata of both genders had significantly longer bodies and limbs in lower latitudes and were possibly thicker at higher GDDs, but did not show trends for SA:V. Males of this species had slightly longer limbs at high longitudes, while older specimens from females were generally larger. Note that this species is the thinnest of the four (width range 1.1–3.3 mm for females, 0.6–1.3 mm for males), which might have affected our ability to accurately measure and detect clines in width or variables that depend on width. That would explain the lack of significant latitudinal clines for SA:V in this species (**Figure 4**) despite the significant cline in length alone. At the extreme aspect ratio of the Phasmatodea, where length is more than one or even two orders of magnitude longer than diameter, tests of Bergmann's rule for this order, or at least its skinniest species, may thus be best performed with length alone as a proxy for size. Precedent is ample, as a majority of Bergmann's rule assays over decades, most involving far less elongated species than *Leptynia,* have used length instead of SA:V (Shelomi, 2012). We thus state that *L. attenuata* shows converse-Bergmann clines as we defined them, follows Allen's rule, and does not obey the temperature-size rule. In addition, the R^2 values for the multiple model for lengths were higher for *L. attenuata* than for other species, suggesting the environmental variables chosen explain a larger percentage of the size variation, although the values for the other species are not unusual for this type of data set (Zeuss et al., 2017). Note also that, almost the opposite of *C. gallica*, this species covered the smallest geographic and environmental range, in which envrionment and geography were the least well correlated (**Table 3**), and had the smallest sample size, bordering being too low for sufficient power ($\alpha \geq 0.8$) for the CCA.

For *P. hispanica* females, no latitudinal clines for volumetric measurements were noted, though this species too has a small width (1.3–2.8 mm) that likely limited the reliability of surface area and volume estimates. However, no latitudinal clines for lengths were noted for this species either [except for head length, which we have stated is an unreliable metric]. Unique among the examined Phasmatodea, *P. hispanica* showed a negative correlation between lengths and AMT and GDD in most models, suggesting the temperature-size rule holds for this species and that longer seasons and/or more time available for growth correlate with smaller sizes. The factors that decrease with latitude (AMT, GDD) had negative effects while the factor that increased with latitude (NPP) had positive effects on size, which suggests a Bergmann cline despite no detectible latitudinal cline. The environmental factors also affected limb length in a way that suggests a converse-Allen cline without an latitudinal correlation. The lack of a direct latitudinal cline despite the strong effects of these environmental clines in the models may be due to the reduced correlation among these variables and latitude over the geographical range of *P. hispanica* (**Table 3**).

To summarize: *B. rossius* shows an unambiguous converse-Bergmann cline (increased SA:V with latitude) and Allen cline (reduced limb length with latitude). *L. atenuata* shows the same clines for lengths, but not SA:V, so it follows Allen's rule but would not fullfill Salewski and Watt's (2017) interpretation of Bergmann's rule. *C. gallica* showed weak but not significant Bergmann clines but no response to the environmental factors, while *P. hispanica* showed no geographic clines but strong enivronmental responses that would otherwise lead to a Bergmann cline.

Significance for Phasmatodea Globally

As in insects in general (Shelomi, 2012), whether Phasmatodea show latitudinal clines depends on species and sex. No generalizations for the order can be concluded from four species alone, two of which showed clear converse-Bergmann and Allen clines while the other two were ambiguously non-clinal tending toward Bergmann. The evidence tentatively suggests converse-Bergmann clines or absence of a cline will be more common for Phasmatodea than Bergmann clines, as was the case with the closely related order Orthoptera (Shelomi, 2012). Size in non-clinal species may be due to reduced climate/latitude correlations in their particular range (**Table 3**), or the species is affected by something other than climate or has a nonlinear relationship to latitude that was not evident in our analyses.

Among our enivronmental variables, Phasmatodea size changes were best explained with temperature (AMT and, to a lesser extent, GDD), but not plant productivity (NPP). The latter is noteworthy given the dependence of Phasmatodea on plant matter as a diet. We also see converse-Bergmann clines together with Allen clines that would otherwise be contradictory, suggesting that, for an organism as long and thin as the Phasmatodea, the body's allometry is more akin to that of the limbs. If we assume the thermoregulatory hypothesis is true, then the larger size of Phasmatodea evolved to increase heat transfer rates, perhaps to cool faster in the tropics or to better retain heat absorbed in the day for use during the Phasmatodea's nocturnal hours of activity. This could be tested with thermoregulatory experiments, as was done along altitudinal gradients for grasshoppers (Ashby, 1997) and bees (Stone, 1993).

More likely, however, is that Phasmatodea body and limb size do not have a significant thermoregulatory function, but refelect temperature dependent growth rates. Phasmatodea growth rate and/or final size may be positively dependent on heat (GDD) in nymphal or even egg stages. Except possibly *P. hispanica*, none of our species followed the temperature-size rule's prediction that ectotherms grow faster in warm temperatures but reach smaller sizes. Instead our species were generally larger at warmer

climates. Phasmatodea would not be the first organisms to show converse clines to the temperature-size rule, whose generality for ectotherms has already been called into question (Angilletta et al., 2004). Our data does not address the question how fast these insects mature to their final size, which may or may not violate that aspect of the temperature-size rule.

Other ecological values, which may or may not correlate with climate and geographic location, could play a role. Body and limb length affect the insects' crypsis, so the type of plant in a Phasmatodea species' envrionment and its preferred host may affect the evolution of limb and body segment lengths and proportions. Prior laboratory research shows the choice of food plant may or may not affect Phasmatodea size (Hsiung and Panagopoulos, 1998; Boucher and Varady-Szabo, 2005), however many species are polyphagous and are not expected to have co-evolved with a certain plant. Limb size may also have different selective pressures than the body. Phasmatodea lose legs often, both via autotomy to escape predators and, frequently, due to molting complications (Maginnis, 2008). These pressures could select for longer or shorter limbs. The links to latitudes for these hypotheses are possible clines in plant presence (as food or a mimesis target), predator diversity (with longer limbs differently suited to mimicry and/or more likely to be grabbed by a predator rather than the body), and humidity (which may decrease the chance of a molting complication and thus allows for longer legs to evolve). Species-specific importance of these factors could, for example, explain why *P. hispanica* shows converse-Allen clines while the other species do not.

Extending this analysis to other species is required before drawing conclusions for the entire order. Seeing if such patterns exist in species with stronger sexual dimorphisms, especially those with heavyset, non-flying females and slender, flying males, would be interesting given the different evolutionary constraints on body size for the different sexes in these species, as well as to formally test Rensch's rule. Comparing results in tropical climates to our temperate and semi-arid European and North African dataset could reveal other anomalies. The Libyan specimens suggest that, over a larger latitudinal range, non-linear clines would likely emerge due to negative effects of desert areas between the temperate zones and the equatorial rainforests. These and the *C. gallica* outliers (the Azores and Israel, **Figure 1**) show the impact large and non-contiguous samples can have obsfucating any underlying patterns.

One question particularly easily addressed with Phasmatodea is comparing the sizes of those in their native habitat with those reared outside of it: Is body size determined by genetics or by local climate? The large number of Phasmatodea enthusiasts breeding stick insects worldwide provides an ample data-source, especially in Europe where cross-border trade of non-native Phasmatodea is unregulated and private Phasmatodea ownership is not restricted. Tests on the invasive *C. morosus* comparing wild-caught populations in their native range in India with populations and cultures abroad would be another way to address this question. To that end, we are sharing data on 121 reared and wild-caught *C. morosus* specimens found in the museums visited for this study (**Table S3**).

In regard to Bergmann's rule, however, the many confounding variables between the field and the lab as well as founder effects of the likely inbred reared stock would make meaningful analysis difficult. Common-garden experiments are the gold standard method to formally test theories of, for example, temperature effects on size clines. Collections of *Carausius* specimens or eggs from India and from other regions where it has invaded, and rearing their descendents or hatching the collected eggs respectively in controlled environments in a lab could formally separate the effects of genetics and environmental variables. This can also be done with any other Phasmid species: Taking eggs or individuals from different ends of their size and latitudinal range, rearing groups of each under controlled environments, and seeing whether size responses differ between native and non-native groups.

While we cannot make general conclusions about climate-size relationships in Phasmatodea at this time, we have generated the first dataset in the field of Phasmatodea morphometrics to be used toward this aim. It is our hope that future analyses of Phasmatodea size clines in other parts of the world and common-garden experimental testing of hypothesized mechanims for these clines will eventually explain the existence and evolution of their extreme and record-setting sizes.

AUTHOR CONTRIBUTIONS

MS conceived of the project, acquired measurement data, contributed to statistical analysis, and drafted and approved of the final manuscript. DZ acquired the environmental data, contributed to statistical analysis, and revised and approved of the final manuscript. All agree to be accountable for the content of the work.

FUNDING

Travel for this research was supported by the Orthopterists' Society's Theodore J. Cohn research grant (2015).

ACKNOWLEDGMENTS

Special thanks to Pamm Mihm and Michel Lecoq (Orthopterists' Society). Thanks to the following people, listed in no particular order, for use of their museum collections: Peter J. Schwendinger (Geneva); Fabrizio Rigato (Milan); Maggie Reilly and Jeanne Robinson (Glasgow); Dmitri Logunov (Manchester); Sheila Wright and Andrew King (Nottingham); Amoret Spooner (Oxford); Judith Marshall, Ben Price, and George Beccaloni (London); Jerome Constant (Brussels); Tony Robillard, Simon Poulain, and Emmanuel Delfosse (Paris); Glòria Masó Ros and Berta Caballero (Barcelona); Mercedes París (Madrid); Eva Monteiro and Luis Filipe Lopes (Lisbon); Kai Schütte, Ilonka Rehmann, Thure Dalsgaard (Hamburg); Angelika Weirauch and Stephan Blank (Müncheberg); Michael Ohl (Berlin); Ralph S. Peters and Karin Ulmen (Bonn); Klaus Schönitzer, Bärbel Stock-Dietel, and Franz Schmolke (Munich); Christian Schmidt (Dresden). Thanks also to the following people, in no

particular order, who provided information about their museum collections, which were not visited due to lack of appropriate specimens at the time: Volker Lohrmann and Michael Stiller (Übersee-Museum, Bremen), Gellért Puskás and Dávid Murányi (Magyar Természettudományi Múzeum, Budapest), John Cooper (Booth Museum of Natural History, Brighton), Michael Wilson (National Museum of Wales, Cardiff), Elaine Charwat (Linnean Society of London), Hannah Allum (Weston Park Museum, Sheffield), Nigel T. Monaghan (National Museum of Ireland, Dublin), Olivier Gerriet (Muséum d'Histoire naturelle de Nice), Roy Danielsson (Lund University Museum of Zoology), Niklas Apelqvist (Naturhistoriska Riksmuseet, Stockholm), Henrik Enghoff (Natural History Museum of Denmark, Copenhagen), Hans Mejlon (Uppsala University Zoological Museum), Karla Schneider (Zentralmagazin Naturwissenschaftlicher Sammlungen der Martin-Luther-Universität, Halle an der Saale), Maria Dimaki (Goulandris Natural History Museum, Athens), Apostolos Trichas (Natural History Museum of Crete), Luca Bartolozzi (La Specola - Museo di Storia Naturale di Firenze [Florence]), Roberta Salmaso (Museo Civico di Storia Naturale, Verona), Marinella Garzena (Museo Regionale di Scienze Naturali, Turin).

SUPPLEMENTARY MATERIAL

The Supplementary Material for this article can be found online at: http://journal.frontiersin.org/article/10.3389/fevo.2017.00025/full#supplementary-material

Data Sheet S1 | Full results of the statistical analyses of the ecogeographical clines in European Phasmatodea. Note that *Bacillus rossius* and *Clonopsis gallica* female data is presented twice: Once including the outlier specimens and once without. Metrics (dependent variables) are in mm or factors thereof (sq. mm for surface area, etc). The full model is AMT+NPP+GDD. Significance statistics (*p*-values) are based on an *F*-test of the regression models for the R^2 values (also given for the slopes of the single linear regression), and based on an ANOVA of the results of the multiple linear regression (given with the slopes of the independent variables). For correspondence analysis, the Pearson's r or Spearman's rho rank correlation coefficient with slope is given with a symbol for the statistical significance as calculated with the *rcorr* program. Key: AL, abdominal length; AMT, annual mean temperature (°C); BL, body length [HL+TL+AL]; FLL, forelimb length; GDD, growing degree days (heat units based on 5°C threshhold); HFL, hind femur length; HL, head length; HW, head width; %I, percentage of variance in the full model explained by each variable; L, fully extended length [FLL+TL+AL]; MT, width of the middle thorax; *n*, number of specimens used for the analysis [values will differ due to incomplete specimens, such as one missing its rear limbs, etc.]; NPP, net primary productivity (grams dry matter per sq. m per year); SA, surface area; SA:V, surface area to volume ratio; ThC, thoracic circumference; TL, thorax length; V, volume; WT, width of the waist. Blank cells mean no significant effect ($p > 0.1$). •, not significant, $p > 0.05$, $*p < 0.05$, $**p < 0.01$, $***p < 0.001$.

Table S1 | Museum collection codes used in supplementary tables.

Table S2 | Raw data for endemic European and Mediterranean Phasmatodea in European museum collections. Museum collection codes in **Table S1**. Localities based on [translations of] the locality labels of each specimen. Date is the date of collection according to the label. Key: AL, abdominal length; BL, body length [calculated as HL+TL+AL]; F, female; FLL, forelimb length; HFL, hind femur length; HL, head length; HW, head width; L, fully extended length [calculated as FLL+TL+AL]; M,male; MT, width of the middle thorax; SA, surface area [calculated as BL*ThC]; SA:V, surface area to volume ratio; ThC, thoracic circumference [calculated as Pi (π) * the mean of Mt and WT]; TL, thorax length; V, volume [calculated as (the mean of MT and WT)^2* Pi (π) * BL]; WT, width of the waist.

Table S3 | Raw data for reared and wild-caught *Carausius morosus* in European museum collections. Museum collection codes in **Table S1**. Localities based on [translations of] the locality labels of each specimen. Those with "REARED" under "City, other" were likely raised in captivity. Date is the date of collection according to the label. Key: AL, abdominal length; BL, body length [calculated as HL+TL+AL]; F, female; FLL, forelimb length; HFL, hind femur length; HL, head length; HW, head width; L, fully extended length [calculated as FLL+TL+AL]; MT, width of the middle thorax; SA, surface area [calculated as BL*ThC]; SA:V, surface area to volume ratio; ThC, thoracic circumference [calculated as Pi (π) * the mean of Mt and WT]; TL, thorax length; V, volume [calculated as (the mean of MT and WT)^2* Pi (π) * BL]; WT, width of the waist.

REFERENCES

Abouheif, E., and Fairbairn, D. J. (1997). A comparative analysis of allometry for sexual size dimorphism: assessing Rensch's rule. *Am. Nat.* 149, 540–562. doi: 10.1086/286004

Alho, J. S., Herczeg, G., Laugen, A. T., Räsänen, K., Laurila, A., and Merilä, J. (2011). Allen's rule revisited: quantitative genetics of extremity length in the common frog along a latitudinal gradient *J. Evol. Biol.* 24, 59–70. doi: 10.1111/j.1420-9101.2010.02141.x

Allen, J. A. (1877). The influence of physical conditions in the genesis of species. *Radic. Rev.* 1, 108–140.

Angilletta, M. J. Jr., and Dunham, A. E. (2003). The temperature-size rule in ectotherms: simple evolutionary explanations may not be general. *Am. Nat.* 162, 332–342. doi: 10.1086/377187

Angilletta, M. J. Jr., Steury, T. D., and Sears, M. W. (2004). Temperature, growth rate, and body size in ectotherms: fitting pieces of a life-history puzzle. *Integr. Comp. Biol.* 44, 498–509. doi: 10.1093/icb/44.6.498

Ashby, P. D. (1997). Conservation of mass-specific metabolic rate among high- and low-elevation populations of the acridid grasshopper *Xanthippus corallipes*. *Physiol. Zool.* 70, 701–711. doi: 10.1086/515877

Ashton, K. G. (2004). Sensitivity of intraspecific latitudinal clines of body size for tetrapods to sampling, latitude and body size. *Integr. Comp. Biol.* 44, 403–412. doi: 10.1093/icb/44.6.403

Ashton, K. G., and Feldman, C. R. (2003). Bergmann's rule in nonavian reptiles: turtles follow it, lizards and snakes reverse it. *Evolution* 57, 1151–1163. doi: 10.1111/j.0014-3820.2003.tb00324.x

Bergmann, K. (1847). Ueber die verhältnisse der wärmeökonomie der thiere zu ihrer grösse. *Gottinger Stud.* 3, 595–708.

Blackburn, T. M., Gaston, K. J., and Loder, N. (1999). Geographic gradients in body size: a clarification of Bergmann's rule. *Divers. Distribut.* 5, 165–174.

Blanckenhorn, W. U., and Llaurens, V. (2005). Effects of temperature on cell size and number in the yellow dung fly *Scathophaga stercoraria*. *J. Therm. Biol.* 30, 213–219. doi: 10.1016/j.jtherbio.2004.11.004

Borges, P. A., Reut, M., Ponte, N. B., Quartau, J. A., Fletcher, M., Sousa, A. B., et al. (2013). New records of exotic spiders and insects to the Azores, and new data on recently introduced species. *Arquipélago. Life Mar. Sci.* 30, 57–70.

Boucher, S., and Varady-Szabo, H. (2005). Effects of different diets on the survival, longevity and growth rate of the Annam stick insect, *Medauroidea extradentata* (Phasmatodea: Phasmatidae). *J. Orthoptera Res.* 14, 115–118. doi: 10.1665/1082-6467(2005)14[115:EODDOT]2.0.CO;2

Brock, P. (1991). *Stick Insects of Britain, Europe, and the Mediterranean*. London: Fitzgerald Publishing.

Büscher, T. (2014). Identification of PSG 332 (Dares sp. "Crocker Range"). *Phasmid Study Group Newslett.* 133, 1–3. doi: 10.13140/RG.2.1.2325.8647

Geist, V. (1987). Bergmann's rule is invalid. *Can. J. Zool.* 65, 1035–1038. doi: 10.1139/z87-164

Harrell, Jr. F. E. (2016). *Hmisc: Harrell Miscellaneous. R Package Version 4.0-2*. Available online at: https://cran.r-project.org/package=Hmisc

Headrick, D., and Wilen, C. A. (2011). Indian Walking Stick. *Pest Notes* 74157, 1–3.

Hijmans, R. J., Cameron, S. E., Parra, J. L., Jones, P. G., and Jarvis, A. (2005). Very high resolution interpolated climate surfaces for global land areas. *Int. J. Climatol.* 25, 1965–1978. doi: 10.1002/joc.1276

Hsiung, C.-C., and Panagopoulos, D. (1998). Preliminary observations on the effects of food plant on the stick insect *Eurycantha calcarata* Lucas (Cheleutoptera: Phasmatidae). *J. Orthoptera Res.* 7, 93–98. doi: 10.2307/3503500

Johansson, F. (2003). Latitudinal shifts in body size of *Enallagma cyathigerum* (Odonata). *J. Biogeogr.* 30, 29–34. doi: 10.1046/j.1365-2699.2003.00796.x

Kann, F. (1937). Temperatureinflüsse auf die Wachstumsstadien von *Dixippus (Carausius) morosus*. *Biol. Gen.* 13, 25–66.

Karl, I., and Fischer, K. (2008). Why get big in the cold? Towards a solution of a life-history puzzle. *Oecologia* 155, 215–225. doi: 10.1007/s00442-007-0902-0

Maginnis, T. L. (2008). Autotomy in a stick insect (Insecta: Phasmida): predation versus molting. *Florida Entomol.* 91, 126–127. doi: 10.1653/0015-4040(2008)091[0126:AIASII]2.0.CO;2

Masaki, S. (1972). Climatic adaptation and photoperiodic response in the band-legged ground cricket. *Evolution* 26, 587–600. doi: 10.2307/2407055

Mayr, E. (1956). Geographical character gradients and climatic adaptation. *Evolution* 10, 105–108.

Meiri, S. (2011). Bergmann's Rule – what's in a name? *Glob. Ecol. Biogeogr.* 20, 203–207. doi: 10.1111/j.1466-8238.2010.00577.x

Meiri, S., and Dayan, T. (2003). On the validity of Bergmann's rule. *J. Biogeogr.* 30, 331–351. doi: 10.1046/j.1365-2699.2003.00837.x

Meiri, S., Yom-Tov, Y., and Geffen, E. (2007). What determines conformity to Bergmann's rule? *Glob. Ecol. Biogeogr.* 16, 788–794. doi: 10.1111/j.1466-8238.2007.00330.x

Mousseau, T. A. (1997). Ectotherms follow the converse to Bergmann's Rule. *Evolution* 51, 630–632. doi: 10.2307/2411138

New, M., Hulme, M., and Jones, P. (1999). Representing twentieth-century space-time climate variability. Part I: development of a 1961-90 mean monthly terrestrial climatology. *J. Clim.* 12, 829–856. doi: 10.1175/1520-0442(1999)012<0829:RTCSTC>2.0.CO;2

Nylin, S., and Svärd, L. (1991). Latitudinal patterns in the size of European butterflies. *Holarct. Ecol.* 14, 192–202. doi: 10.1111/j.1600-0587.1991.tb00652.x

Olalla-Tárraga, M. Á. (2011). "*Nullius in Bergmann*" or the pluralistic approach to ecogeographical rules: a reply to Watt et al. (2010). *Oikos* 120, 1441–1444. doi: 10.1111/j.1600-0706.2011.19319.x

Partridge, L., and Coyne, J. A. (1997). Bergmann's Rule in ectotherms: is it adaptive? *Evolution* 51, 632–635. doi: 10.2307/2411139

Purvis, A., and Orme, C. D. L. (2005). "Evolutionary Trends in Body Size," in *Deciphering Growth*, eds J. C. Carel, P. A. Kelly, and Y. Christen (Berlin: Springer-Verlag), 1–18.

R Development Core Team (2008). *R: A Language and Environment for Statistical Computing*. Vienna: R Foundation for Statistical Computing. Available online at: http://www.R-project.org

Ray, C. (1960). The application of Bergmann's and Allen's rules to the poikilotherms. *J. Morphol.* 106, 85–108. doi: 10.1002/jmor.1051060104

Reim, C., Teuschl, Y., and Blanckenhorn, W. U. (2006). Size-dependent effects of temperature and food stress on energy reserves and starvation resistance in yellow dung flies. *Evol. Ecol. Res.* 8, 1215–1234.

Rensch, B. (1943). Studien über Korrelation und klimatische Parallelität der rassenmerkmale von Carabus-Formen. *Zool. Jahrb.* 76, 103–170.

Robinson, M. H. (1966). *Anti-Predator Adaptations in Stick- and Leaf-Mimicking Insects*. Dissertation, University of Oxford.

Salewski, V., and Watt, C. (2017). Bergmann's rule: a biophysiological rule examined in birds. *Oikos* 126. doi: 10.1111/oik.03698

Scali, V. (2009). Revision of the Iberian stick insect genus *Leptynia* Pantel and description of the new genus *Pijnackeria*. *Ital. J. Zool.* 76, 381–391. doi: 10.1080/11250000802702062

Shelomi, M. (2012). Where are we now? Bergmann's rule sensu lato in insects. *Am. Nat.* 180, 511–519. doi: 10.1086/667595

Shelomi, M. (2016). Status of Europe's native & invasive phasmatodea collections. *Metaleptea* 36, 22–25.

Stone, G. N. (1993). Thermoregulation in four species of tropical solitary bees: the roles of size, sex and altitude. *J. Comp. Physiol. B* 163, 317–326. doi: 10.1007/BF00347782

Vamosi, S. M., Naydani, C. J., and Vamosi, J. C. (2007). Body size and species richness along geographical gradients in Albertan diving beetle (Coleoptera: Dytiscidae) communities. *Can. J. Zool.* 85, 443–449. doi: 10.1139/Z07-021

van Voorhies, W. A. (1996). Bergmann size clines: a simple explanation for their occurrence in ectotherms. *Evolution* 50, 1259–1264.

Walsh, C., and Mac Nally, R. (2013). *hier.part: Hierarchical Partitioning*. R package version 1.0-4. Available online at: http://CRAN.R-project.org/package=hier.part

Watt, C., Mitchell, S., and Salewski, V. (2010). Bergmann's rule; a concept cluster? *Oikos* 119, 89–100. doi: 10.1111/j.1600-0706.2009.17959.x

Whitman, D. W. (2008). The significance of body size in the Orthoptera: a review. *J. Orthoptera Res.* 17, 117–134. doi: 10.1665/1082-6467-17.2.117

Zeuss, D., Brunzel, S., and Brandl, R. (2017). Environmental drivers of voltinism and body size in insect assemblages across Europe. *Glob. Ecol. Biogeogr.* 26, 154–165. doi: 10.1111/geb.12525

Conflict of Interest Statement: The authors declare that the research was conducted in the absence of any commercial or financial relationships that could be construed as a potential conflict of interest.

frontiers in Ecology and Evolution

ERRATUM
published: 05 September 2017
doi: 10.3389/fevo.2017.00105

Erratum: Bergmann's and Allen's Rules in Native European and Mediterranean Phasmatodea

Frontiers Production Office *

Frontiers Media SA, Lausanne, Switzerland

Keywords: phasmatodea, Bergmann's rule, Allen's rule, latitudinal cline, insect ecology, morphometrics

OPEN ACCESS

Approved by:
Frontiers in Ecology and Evolution Editorial Office, Frontiers Media SA, Switzerland

***Correspondence:**
Frontiers Production Office production.office@frontiersin.org

Specialty section:
This article was submitted to Phylogenetics, Phylogenomics, and Systematics, a section of the journal Frontiers in Ecology and Evolution

Received: *23 August 2017*
Accepted: *23 August 2017*
Published: *05 September 2017*

Citation:
Frontiers Production Office (2017) Erratum: Bergmann's and Allen's Rules in Native European and Mediterranean Phasmatodea. Front. Ecol. Evol. 5:105. doi: 10.3389/fevo.2017.00105

An erratum on

Bergmann's and Allen's Rules in Native European and Mediterranean Phasmatodea
by Shelomi, M., and Zeuss, D. (2017). Front. Ecol. Evol. 5:25. doi: 10.3389/fevo.2017.00025

Due to a production error, Figure 2 legend was not updated during proof editing. The legend should read:

FIGURE 2 | Morphometrical measurements and abbreviations used in this study. Photograph is of *Carausius morosus*, which is representative of the morphology of all species examined here. AL, abdomen length; FLL, forelimb length; HFL, hind femur length; HL, head length; HW, head width; MT, middle thorax width; TL, thorax length; WT, waist width. Photo credit: M. Shelomi.

frontiers in Ecology and Evolution

ORIGINAL RESEARCH
published: 30 November 2017
doi: 10.3389/fevo.2017.00151

Multiple Identified Neurons and Peripheral Nerves Innervating the Prothoracic Defense Glands in Stick Insects Reveal Evolutionary Conserved and Novel Elements of a Chemical Defense System

Johannes Strauß[1], Christoph-Rüdiger von Bredow[2†], Yvette M. von Bredow[2†], Konrad Stolz[1], Tina E. Trenczek[2] and Reinhard Lakes-Harlan[1]**

[1] AG Integrative Sensory Physiology, Institute for Animal Physiology, Justus-Liebig-Universität Gießen, Gießen, Germany,
[2] Institute for General and Applied Zoology, Justus-Liebig-Universität Gießen, Gießen, Germany

The defense glands in the dorsal prothorax are an important autapomorphic trait of stick insects (Phasmatodea). Here, we study the functional anatomy and neuronal innervation of the defense glands in *Anisomorpha paromalus* (Westwood, 1859) (Pseudophasmatinae), a species which sprays its defense secretions when disturbed or attacked. We use a neuroanatomical approach to identify the nerves innervating the gland muscles and the motoneurons with axons in the different nerves. The defense gland is innervated by nerves originating from two segments, the subesophageal ganglion (SOG), and the prothoracic ganglion. Axonal tracing confirms the gland innervation via the anterior subesophageal nerve, and two intersegmental nerves, the posterior subesophageal nerve, and the anterior prothoracic nerve. Axonal tracing of individual nerves reveals eight identified neuron types in the subesophageal or prothoracic ganglion. The strongest innervating nerve of the gland is the anterior subesophageal nerve, which also supplies dorsal longitudinal thorax muscles (neck muscles) by separate nerve branches. Tracing of individual nerve branches reveals different sets of motoneurons innervating the defense gland (one ipsilateral and one contralateral subesophageal neuron) or the neck muscle (ventral median neurons). The ipsilateral and contralateral subesophageal neurons have no homologs in related taxa like locusts and crickets, and thus evolved within stick insects with the differentiation of the defense glands. The overall innervation pattern suggests that the longitudinal gland muscles derived from dorsal longitudinal neck muscles. In sum, the innervating nerves for dorsal longitudinal muscles are conserved in stick insects, while the neuronal control system was specialized with conserved motoneurons for the persisting neck muscles, and evolutionarily novel subesophageal and prothoracic motoneurons innervating the defense gland.

Keywords: stick insect, neuroanatomy, defense gland, innervation, motoneurons

OPEN ACCESS

Edited by:
Sven Bradler,
University of Göttingen, Germany

Reviewed by:
Fanny Leubner,
University of Göttingen, Germany
Thomas Van De Kamp,
Karlsruhe Institute of Technology, Germany

****Correspondence:***
Johannes Strauß
johannes.strauss@physzool.bio.uni-giessen.de
Reinhard Lakes-Harlan
reinhard.lakes-harlan@physzool.bio.uni-giessen.de

† These authors have contributed equally to this work.

Specialty section:
This article was submitted to Phylogenetics, Phylogenomics, and Systematics, a section of the journal Frontiers in Ecology and Evolution

Received: *30 September 2017*
Accepted: *14 November 2017*
Published: *30 November 2017*

Citation:
Strauß J, von Bredow C-R, von Bredow YM, Stolz K, Trenczek TE and Lakes-Harlan R (2017) Multiple Identified Neurons and Peripheral Nerves Innervating the Prothoracic Defense Glands in Stick Insects Reveal Evolutionary Conserved and Novel Elements of a Chemical Defense System. Front. Ecol. Evol. 5:151. doi: 10.3389/fevo.2017.00151

INTRODUCTION

In stick insects (Phasmatodea), paired exocrine defense glands are found in the prothorax (Bedford, 1978; Chow, 2008; Bradler, 2009). The gland opening is located at the anterio-dorsal pronotum. The defense glands are an autapomorphic character for the Phasmatodea (Grimaldi and Engel, 2005; Bradler, 2009). Even in the Indian walking stick *Carausius morosus* which apparently does not produce defensive secretions (Bässler, 1983; Carlberg, 1985a), the glands are found in the prothorax albeit in relatively small size (Marquardt, 1940; Stolz et al., 2015). In species displaying chemical defense, the paired defense glands produce the defense fluid from a secretory epithelium lining the inner gland muscle layers (Happ et al., 1966; Strong, 1975; Eisner et al., 1997). The defense secretions have been studied for the biochemical components in detail in different species of stick insects (e.g., Meinwald et al., 1962; Smith et al., 1979; Chow and Lin, 1986; Ho and Chow, 1993; Bouchard et al., 1997; Eisner et al., 1997; Dossey et al., 2006, 2008; Schmeda-Hirschmann, 2006; summarized in Dettner, 2015). In *Anisomorpha* species, the principle component of the defense spray is anisomorphal, a monoterpene dialdehyde (Meinwald et al., 1962) which occurs in three diastereomers in *Anisomorpha buprestoides* (Dossey et al., 2006).

In addition, the importance of chemical defense secretion for the survival of stick insects has been shown in behavioral assays as an effective mechanism against predators for several species (Eisner, 1965; Carlberg, 1981, 1985b,c, 1986a, 1987; Bouchard et al., 1997; Dossey et al., 2012; but see Nentwig, 1990). The defense glands can be employed in defense against predators like birds or rodents by secreting or spraying a repellent or irritating fluid, or by releasing an odor (Eisner, 1965; Bedford, 1978; Carlberg, 1986a; Eisner et al., 2005). Secretion release usually covers parts of the body surface with the fluid, while spraying release occurs over a distance at potential predators (Carlberg, 1986b; Eisner et al., 1997, 2005; van de Kamp et al., 2015).

Aimed spraying is arguably the most complex among these chemical defense behaviors. Behavioral experiments have shown that *A. buprestoides* can direct the spray from either both glands, or only a single gland, depending on the direction of contact (Eisner, 1965). Further, they can spray in an aimed direction at birds prior to any contact with the insect body (Eisner, 1965). In general, different sensory stimuli are integrated for fluid ejection including vision and touch. The chemical defense must thus be under a neuronal control which goes beyond local, reflex-like circuits in the prothorax. A previous comparative study has revealed a complex innervation pattern of the glands by three peripheral nerves from the subesophageal and prothoracic ganglion in four species including *C. morosus* (Stolz et al., 2015). The most prominent nerve supplying the defense glands, the Nervus anterior, originates in the subesophageal ganglion (SOG), and also supplies adjacent thoracic longitudinal muscles (Stolz et al., 2015). In addition, the intersegmental nerve complex innervates the glands by the posterior subesophageal nerve and the anterior prothoracic nerve in most species studied (Stolz et al., 2015). Between these distantly related groups (Goldberg et al., 2015), the peripheral nerve pattern is conserved. Notably, in *Peruphasma schultei* only the anterior subesophageal nerve innervates the defense glands, but not the intersegmental nerve complex (Stolz et al., 2015). Few neuron types located in the SOG and the prothoracic ganglion have axons in the Nervus anterior SOG (Stolz et al., 2015).

Here, we study the neuronal innervation of the defense glands in further detail in the species *Anisomorpha paromalus*, which is closely related to *A. buprestoides* (Bradler, 2009). The aim of this study is (1) to document the innervation pattern of the defense gland for a species from a genus which has a strong spraying defense behavior from prominent defense glands (Eisner, 1965), (2) to identify the particular neurons which innervate the defense gland muscles in nerves which also target adjacent muscles (Stolz et al., 2015), and (3) to compare the innervation in *A. paromalus* to the closely related *P. schultei* (both Pseudophasmatinae; Goldberg et al., 2015) for the functional specialization on the N. ant. SOG innervation. We use axonal tracing of individual nerve branches from the Nervus anterior SOG to differentiate the neuronal innervation of the defense gland and of the dorsal longitudinal muscles (or neck muscles, Honegger et al., 1984). Comparison of these motoneurons in stick insects to homologous neurons in related species of cockroaches (Davis, 1983) and locusts (Altman and Kien, 1979; Honegger et al., 1984) reveals neurons which have evolved with the development of the defense glands. This comparison of identified neurons (Goodman et al., 1979; Hoyle, 1983; Arbas et al., 1991; Kutsch and Breidbach, 1994) allows to identify the evolutionary novel nerve cells in stick insects which underlie chemical defense.

MATERIALS AND METHODS

Animals

Anisomorpha paromalus (Westwood, 1859) (Pseudophasmatinae) were reared in a crowded lab culture of females and males at the Institute for Animal Physiology, Justus-Liebig-University, Gießen. Animals were kept under a 12:12 light-dark regime. They were fed with *Ligustrum* leaves *ad libitum*. Only adult individuals were used in this study.

Scanning Electron Microscopy

The gland opening was documented by scanning electron microscopy from specimens stored in 70% ethanol (Carl Roth, Karlsruhe, Germany). Thoraces were isolated from the rest of the body and cut in the middle with scissors. They were dehydrated in a graded ethanol series (Carl Roth, Karlsruhe, Germany). The preparations were critical point-dried (BAL-TEC, Balzers, Liechtenstein) and sputter-coated with gold (SCD 004 SputterCoater, Balzers), and viewed and documented with a Phillips XL 20 SEM.

Dissection Procedures

Prior to preparation of the glands and the nervous system, insects were cold-anesthetized for 10 min at 4°C. The dissection procedures followed those established for other species (Stolz et al., 2015), cutting the insects open with scissors on the dorsal side of the thorax and head capsule, and flattening them out in glass dishes which were filled with Sylgard (Sylgard

184, Suter Kunststoffe AG, Fraunbrunnen, Switzerland) with insect pins. The esophagus and gut were removed with scissors, and the ganglia and peripheral nerves were thus exposed for neuroanatomical investigations from the dorsal side. The preparations were covered with *Carausius* saline with pH = 7.4 (0.00684 mol/l NaCl; 0.01744 mol/l KCl; 0.00748 mol/l $CaCl_2 \times 2 H_2O$; 0.01844 mol/l $MgCl_2 \times 6 H_2O$; 0.00198 mol/l Tris; Weidler and Diecke, 1969; Bässler, 1977). This dissection procedure was also followed in preparations for axonal tracing (see below).

Neuroanatomy and Axonal Tracing

Gland Innervation Pattern

To document the peripheral nerves innervating the defense gland, these structures were stained *in situ*. The preparations were shortly incubated for 20–40 s with Janus Green B solution (Sigma-Aldrich, St. Louis, Missouri; used 0.02% in *Carausius* saline). Janus Green B stains the fine peripheral nerves and other tissues. The Janus Green B solution was used at storage temperature of 4°C, and quickly washed out after incubation using *Carausius* saline.

Axonal Tracing Experiments

To reveal the gland innervation by specific nerves and the somata located in the central nervous system of neurons with axons in these nerves, axonal tracing was used. Again, the tracing procedures were carried out *in situ* following the dissection described above (for details see Stolz et al., 2015). Neurobiotin was used as tracing solution (5%, dissolved in Aqua dest.; Vector Laboratories, Burlingame, CA, USA). The different nerves taking up the tracing solution were cut with iridectomy scissors (see schematics in **Figures 7**, **8**). Preparations were incubated at 4°C for 4 days in a moist chamber. Ganglia were then taken out and fixed in 4% paraformaldehyde (Sigma Chemicals, St. Louis, Missouri, USA) dissolved in phosphate buffer (0.04 mol/l Na_2HPO_4; 0.00574 mol/l $NaH_2PO_4 \times 2 H_2O$) for 1 h. They were subsequently rinsed in phosphate buffer and stored in PBST buffer (0.1369 mol/l NaCl, 0.0027 mol/l KCl, 0.01 mol/l Na_2HPO_4, 0.00176 mol/l KH_2PO_4, all substances from Merck, Darmstadt, Germany; and 0.1% Triton X-100, Roth, Karlsruhe, Germany; with pH = 7.2). The uptake of neurobiotin in neurites and somata was visualized as described previously (Stolz et al., 2015) using the Avidin-Biotin kit (Vectastain ABC Kit PK-6100; Vector Laboratories, Burlington CA) and DAB solution (Vectastain DAB kit SK-4100; Vector Laboratories) according to manufacturers' instructions.

Histology of the Defense Glands

After axonal tracing, the defensive glands were dehydrated in a graded ethanol series (30% ethanol to 96% ethanol) followed by two changes of 99.9% 2-propanol, each step for several hours at room temperature. The tissues were then embedded in Histosec® (Merck, Darmstadt, Germany) and 10 µm sections were made with a Leitz rotary microtome and mounted on glass slides (SuperFrost™, Carl Roth, Karlsruhe, Germany). Sections were deparaffined with Roti®-Histol (Carl Roth, Karlsruhe, Germany) and rehydrated in a descending ethanol series.

For histological staining to analyze the gland muscles, the sections were also incubated in methanol for 5 min at room temperature and then stained in double concentrated Giemsa solution (Stock solution from Carl Roth, Karlsruhe, Germany) for 1 h. Excess staining solution was washed off with demineralized water, and the slides were next differentiated with 1% (v/v) acetic acid for 3 s and washed with demineralized water. In addition, gland sections were also analyzed without counter-staining. These sections were mounted directly after deparaffination (see below).

Microscopy and Documentation

In Situ Preparations of Peripheral Nerves with Vital Staining

The stained preparations covered with *Carausius* saline were viewed with a Leica dissection microscope and drawn with help of a Leica drawing mirror. The drawings were scanned and digitally redrawn using CorelDraw version 11 (Corel, Ottawa, Canada).

Preparations with Axonal Tracing

Glands were viewed in phosphate buffer with a Leica dissection microscope and documented by photographs from a Nikon Digital Sight DS-5M camera (1,280 × 960 pixel) attached to the microscope. Ganglia with filled nerves were dehydrated in a graded ethanol series (Carl Roth, Karlsruhe, Germany), cleared in methyl salicylate (Merck, Darmstadt, Germany). They were viewed with an Olympus BH-2 microscope, and documented by photographs from a Leica DFC 7000 T digital camera (1,920 × 1,440 pixel) connected to the microscope, using the Leica Application Suite V4.9.

Histological Sections

Histological sections were dehydrated in 100% xylol (Carl Roth) and mounted in Entellan® (Merck, Darmstadt, Germany). Photomicrographs were taken with a CV12 camera (Olympus K.K., Shinjuku, Japan) mounted on a BX50 microscope (Olympus K.K., Shinjuku, Japan). Series of single pictures were stitched together with the program AutoStitch v2.2 (Brown and Lowe, 2007).

Terminology

The terminology of peripheral nerves follows Marquardt (1940) and Honegger et al. (1984). The terminology for thoracic muscles follows Friedrich and Beutel (2008) and Wipfler et al. (2015) for the neopteran muscle groundplan in the thorax. For comparison to Orthoptera, we refer to the muscle descriptions and muscle terminology by Honegger et al. (1984).

Morphometric Analysis and Statistics

Ganglion areas and neuron soma areas were measured from digitized photographs of ganglia using the freeware program ImageJ (https://imagej.nih.gov/ij/). Since animals show a sexual dimorphism in size, we compared the data between sexes for SOG area, absolute soma size for two identified subesophageal neurons (ipsilateral neuron ILN and contralateral neuron CLN, see results), and the relative soma size for ILN and CLN. The relative soma size was calculated by dividing the absolute soma

size by the ganglion area of the respective ganglion. Statistical analysis used the software GraphPad Prism 4 (GraphPad, San Diego, CA). Data were tested for normal distribution using the Kolmogorov-Smirnov (KS) normality test. Since not all data were normally distributed, we further used the Mann-Whitney test to compare data from female and male individuals.

RESULTS

Defense Glands and Innervation Pattern

Anisomorpha paromalus shows a notable dimorphism in size between sexes with females being much larger than males (**Figure 1a**). In both sexes, the gland opening is located below a cuticular ridge at the anterio-dorsal edge of the pronotum (**Figure 1b**). This external opening of the ejaculatory duct was very small and surrounded by membranes (**Figure 1c**).

In situ preparations showed the paired defense glands in the dorsal prothorax (**Figures 2a$_i$,b$_i$**). In both sexes, the long glands span through the prothorax. For both sexes, the most obvious innervating nerve to the glands originates from the SOG (**Figures 2a$_{ii}$,b$_{ii}$**). This nerve is the subesophageal *Nervus anterior* (N. ant. SOG) which originates on each side of the SOG, runs under a cuticular apodeme on each side of the head and enters the prothorax toward the gland (**Figures 2a$_{ii}$,b$_{ii}$**). During the distance between the SOG and the gland, no further innervation targets occur. Close to the defense gland, the nerve splits into two nerve branches which contact the proximal gland surface. These two branches run on the dorsal and ventral side of the gland (for overview, see **Figures 2**, **3**; for details also **Figures 5a,c**). There are four dorsal longitudinal muscles in the prothorax of *A. paromalus* (**Figure 4**), and their overall organization resembles that reported for *C. morosus* (Jeziorski, 1918; Marquardt, 1940). Based on their position and anterior attachment points at an apodeme behind the head capsule, the two anterior muscles are Idlm1 (the median muscle) and Idlm2 (the lateral muscle) (Friedrich and Beutel, 2008). In *C. morosus*, the more posterior muscles are termed 3a and 3b (Jeziorski, 1918) or D3 and D4 (Marquardt, 1940). These muscles are more difficult to homologize, since in *C. morosus* some dorsal longitudinal muscles are absent in the prothorax (Idlm3, Idlm6; Jeziorski, 1918; Leubner et al., 2016). By their positions, the two posterior longitudinal muscles could represent Idlm5 and Idlm6 (Friedrich and Beutel, 2008), or two sets of fibers from Idlm5. Importantly, the major anterior dorsal longitudinal muscles are still present in *A. paromalus*, and locate next to the defense gland (**Figures 4**, **5**).

The innervation by N. ant. SOG is not exclusively on the gland, as a further nerve branch splits off from the dorsal branch which innervates a dorsal longitudinal neck muscle (**Figures 5b,c**). The muscle innervated together with the defense gland by N. ant. SOG (**Figures 5b,c**) is homologous to muscle Idlm2 in the neopteran groundplan (Friedrich and Beutel, 2008), and to the closely aligned muscles 50/51 in Orthoptera by its attachment sites and position (Altman and Kien, 1979; Honegger et al., 1984).

A further gland innervation originates from the intersegmental nerve complex, which is formed by three distinct nerves as they run toward the periphery: the *Nervus posterior* of the SOG (N. post. SOG), the *Nervus anterior* of the prothoracic ganglion (N. ant. T1), and the *Nervus transversus* (N. trans.) (**Figure 3**). From the nerve complex, a thin nerve branch splits off and contacts the defense gland. This nerve branch usually contacts the ventral branch of N. ant. SOG at the gland (**Figure 5d**). Some variability was found in the innervation by the intersegmental nerve complex, as an additional second branch from the intersegmental nerve complex could occur (**Figure 5e**) or two branches left the intersegmental nerve complex but fused into one branch which ultimately contacted the defense gland

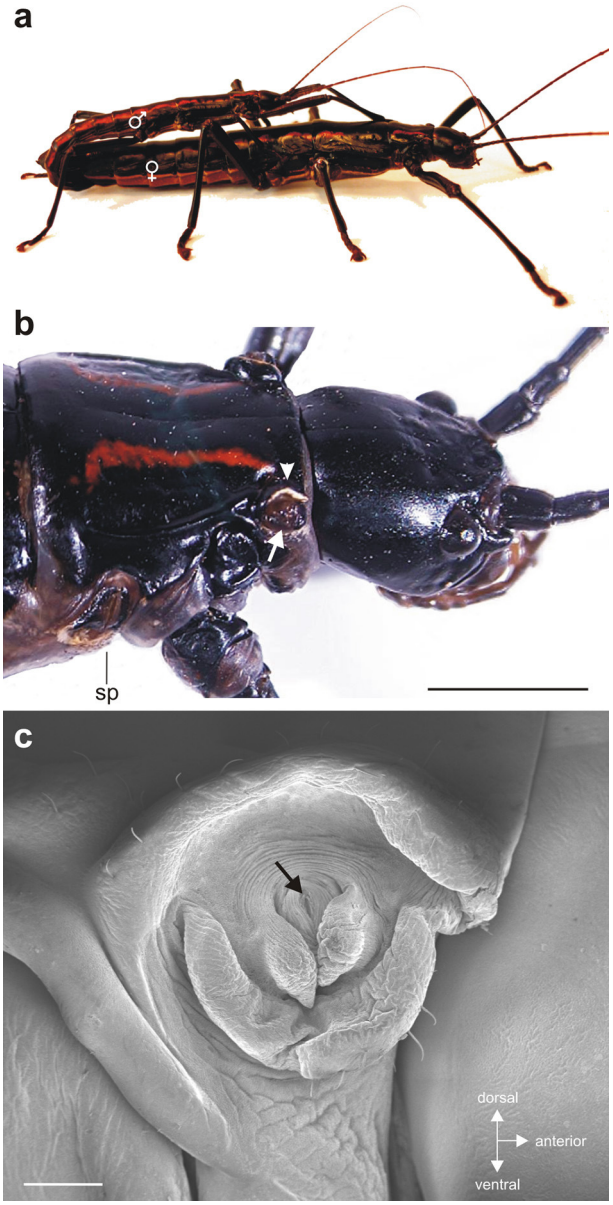

FIGURE 1 | (a) Couple of *Anisomorpha paromalus* with male on top and female below. **(b)** The gland opening (white arrow) is located below a cuticular ridge (arrowhead) at the anterio-dorsal edge of the pronotum. **(c)** Scanning electron micrograph of the small release opening (black arrow) surrounded by membranous structures. Scales: **(b)** = 4 mm; **(c)** = 250 μm.

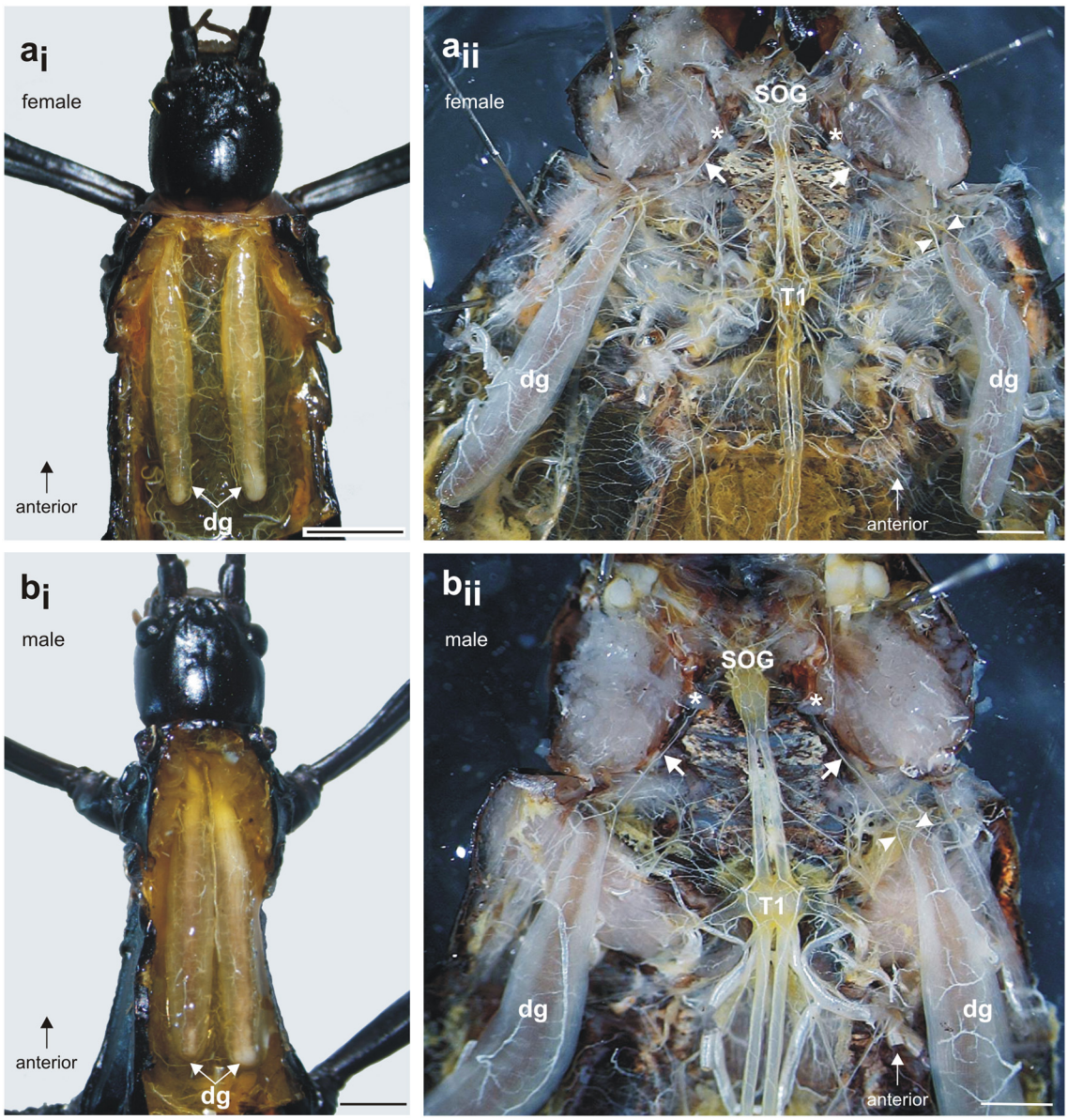

FIGURE 2 | Defense glands in *A. paromalus* **(a)** female and **(b)** male individuals. **(a_i, b_i)** Paired defense glands lay dorsally in the prothorax. **(a_{ii}, b_{ii})** The innervation by a prominent nerve from the subesophageal ganglion (SOG) is similar in both sexes: the nerve (white arrow) runs under a cuticular apodeme (asterisk) toward the anterior defense gland where it splits into two nerve branches which contact the gland surface (white arrowheads). Scales: female = 4 mm, male = 2 mm. dg, defense glands; T1, prothoracic ganglion; SOG, subesophageal ganglion.

(**Figure 5f**). This overall innervation pattern is identical to the species studied before (Stolz et al., 2015; Stolz, 2017).

Axonal tracing of different nerves was used to confirm the individual nerves innervating the gland muscles, in particular in the intersegmental nerve complex (**Figures 6a,e**, **Table 1**). The two branches of N. ant. SOG form a fine network of arborizations on the gland surface (**Figure 6b**). While the ventral and dorsal branch at the anterior gland run over the gland surface (**Figures 5a**, **6b**), histological sections of the middle of the gland showed that the two branches run between the outer longitudinal muscle layer and the inner ring muscle layer (**Figure 6c**). The longitudinal muscles are asymmetrically organized, with thicker longitudinal muscles at the ventral and dorsal side, and very thin longitudinal muscles at the medial and lateral side (**Figure 6c**). The secretory epithelium lines the inside of the gland (**Figure 6**). Sections revealed fine neuronal arborizations mainly in the outer longitudinal muscles (**Figure 6d**). A similarly clear innervation of the ring muscle fibers was not detectable.

In the intersegmental nerve complex, the fine nerve branch was also confirmed by anterograde axonal tracing toward the

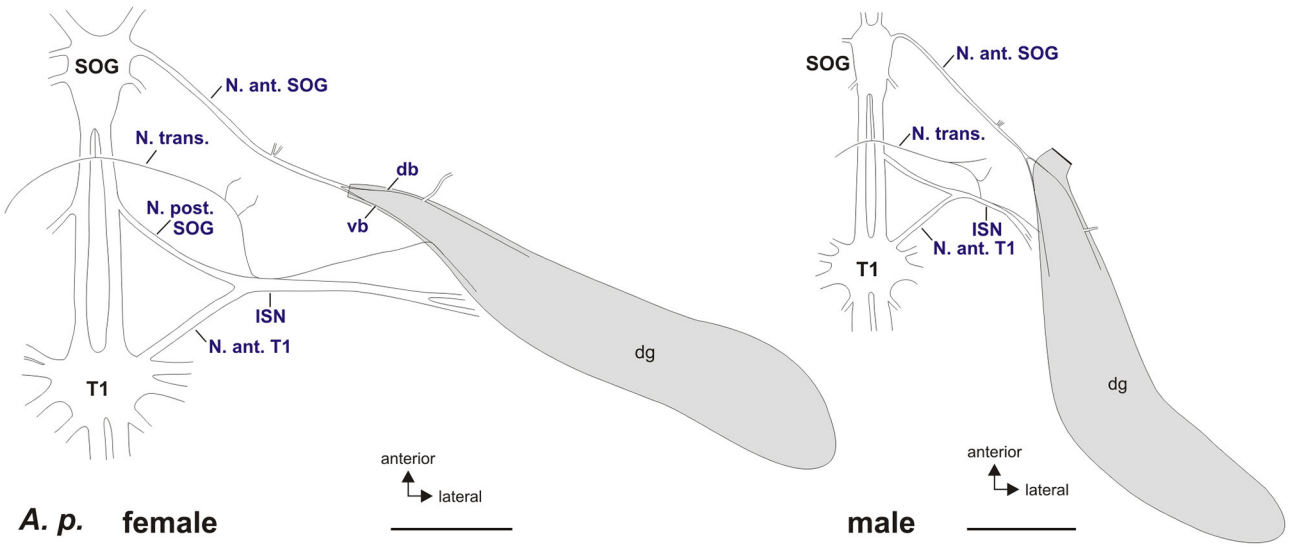

FIGURE 3 | Schematic of peripheral nerves contacting the defense glands in *A. paromalus* female **(left)** and male **(right)**. The defense glands are innervated by the Nervus anterior of the subesophageal ganglion (N. ant. SOG) and the intersegmental nerve complex (ISN) formed by the Nervus transversus (N. trans.), Nervus posterior of the subesophageal ganglion (N. post. SOG), and the Nervus anterior of the prothoracic ganglion (N. ant. T1) via a small nerve branch. The N. anterior SOG splits into a dorsal branch (db) and a ventral branch (vb) which contact the gland muscles. Scales = 2 mm. db, dorsal branch of N. anterior SOG; dg, defense glands; ISN, intersegmental nerve complex; N. ant. SOG, Nervus anterior of the subesophageal ganglion; N. ant. T1, Nervus anterior of the prothoracic ganglion; N. post. SOG, Nervus posterior of the subesophageal ganglion; N. trans., Nervus transversus; SOG, subesophageal ganglion; T1, prothoracic ganglion; vb, ventral branch of N. anterior SOG.

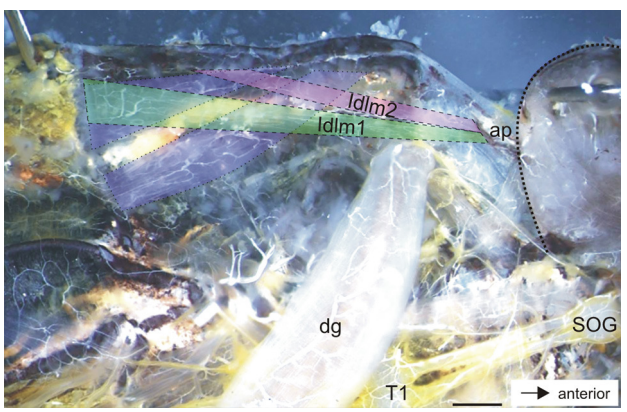

FIGURE 4 | Dorsal longitudinal neck muscles in the prothorax of *A. paromalus*. Dorsal longitudinal muscles are indicated by hatched lines and color coded for ldlm1 (green), ldlm2 (magenta), and two posterior muscles (blue). Dotted line indicates the outline of the head capsule. Scale = 1.5 mm. ap, apodeme; dg, defense gland; SOG, subesophageal ganglion; T1, prothoracic ganglion.

gland (**Figure 6f**). The nerve terminals occurred also on the gland surface but have a smaller innervation area. The different nerves of the intersegmental nerve complex were tested by individual tracing experiments. The obtained stainings showed an innervation by N. ant. SOG and N. post. T1, but not by N. transversus (**Table 1**). This overall innervation pattern is consistent with the innervation described for few other species (Stolz et al., 2015).

Identified Neurons Innervating the Defense Glands

We used retrograde axonal tracing on the N. ant. SOG and its nerve branches as well as the nerve branch of the intersegmental nerve complex to reveal the neurons with axons supplying the defense gland.

Tracing the complete N. ant. SOG (**Figure 7a**) stained three identified neuron types in the SOG (**Figure 7b$_i$**) and one in the prothoracic ganglion (T1) (**Figure 7b$_{ii}$**). The neurons in the SOG have been termed the ipsilateral neuron (ILN) which has the largest soma of the neuron types discussed here, the contralateral neuron (CLN), and the ventral medial neurons (VMN) with the smallest somata located at the ganglions ventral midline (**Figure 7b$_i$**) (see also Stolz et al., 2015). The number of VMNs can vary from 2 to 4 neurons but is in most preparations 3 VMNs. The neuron in the prothoracic ganglion has been termed the prothoracic intersegmental neuron (PIN) (Stolz et al., 2015). No difference in the neuron sets were found between the sexes.

We next used selective filling of N. ant. SOG nerve branches to distinguish between neurons innervating the defense glands, the longitudinal neck muscle Idlm2, or both. First, the ventral or dorsal nerve branches of N. ant SOG were carefully separated from the anterior gland surface (**Figure 7c**). For the ventral branch of N. ant. SOG (n = 15), the tracing revealed the subesophageal ILN and CLN (**Figure 7d**) as well as the prothoracic PIN (not shown). Among these neurons, the PIN was only stained in 50% of the preparations. This relatively rare staining was most likely due to the extended distance from tracing of N. ant. SOG close to the head capsule (**Figure 7a**)

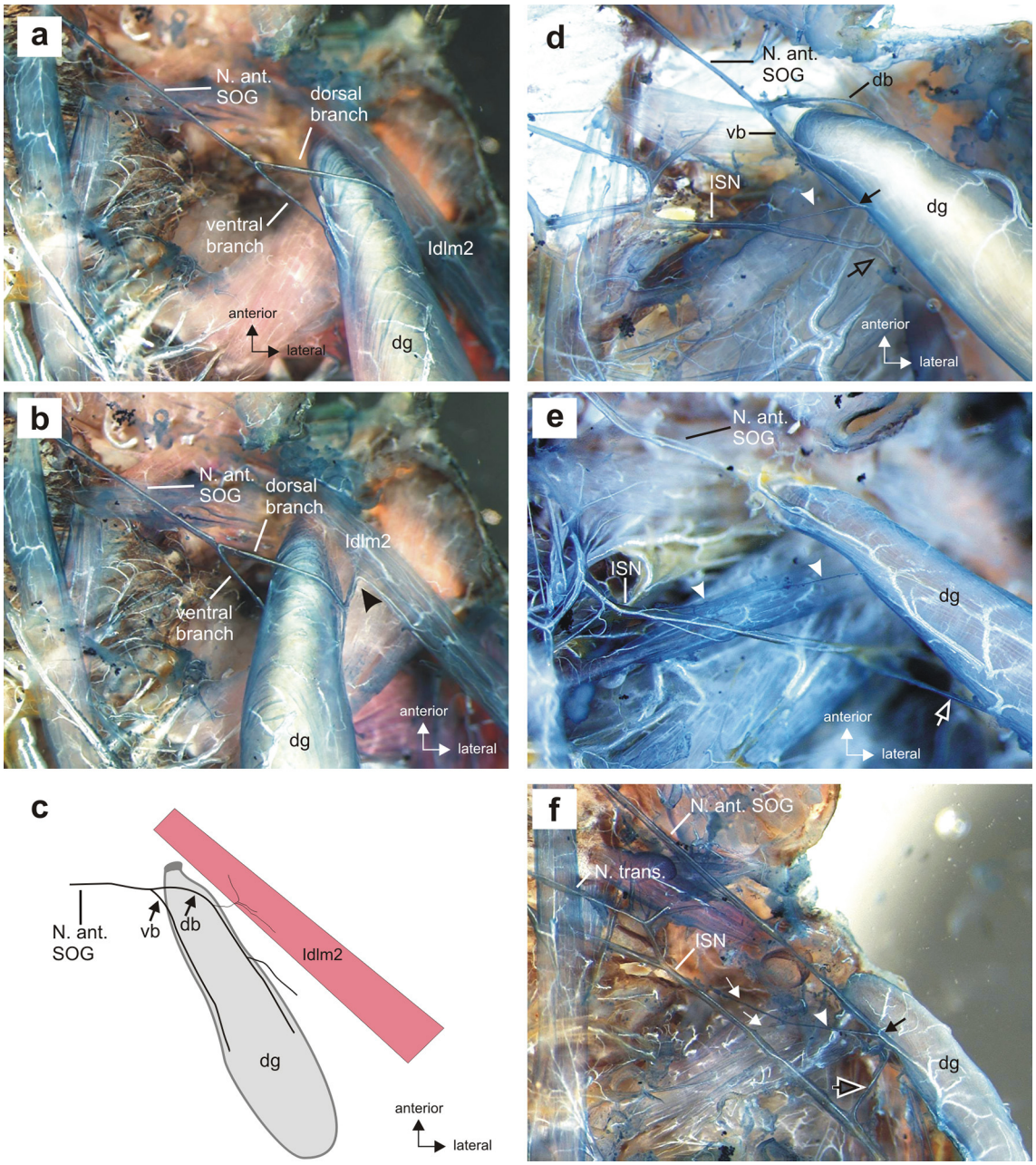

FIGURE 5 | Details of the gland innervation *in situ*. **(a)** Innervation of the defense gland (dg) by two branches of the N. anterior SOG, the dorsal and ventral branch, in dorsal view. **(b)** The dorsal branch innervates both the defense gland by the larger dorsal branch contacting the gland muscle and a dorsal longitudinal muscle (ldlm2) in the prothorax by a short side branch (black arrowhead), apparent with defense gland turned medially. Longitudinal neck muscle ldlm1 was removed during preparation. **(c)** Schematic of the shared innervation of dorsal longitudinal muscle (ldlm2) by the dorsal branch of the N. anterior SOG; the ventral branch exclusively innervates the defense gland. **(d)** The intersegmental nerve complex (ISN) usually contacts the defense gland by a fine nerve branch (white arrowhead). The ventral nerve branch (vb) and the nerve branch from the ISN connect at the gland surface (black arrow). The ISN extends laterally of the defense gland toward a longitudinal muscle, ldlm1 (black open arrow). **(e)** A second contact from the ISN can occur further distally on the gland surface (white open arrow). White arrowheads indicate the fine branch in more anterior position. **(f)** Two fine branches of the ISN (white arrows) can merge before contacting the gland as a single fiber (white arrowhead), with a shared contact zone with the N. anterior SOG (black arrow) on the gland surface. Note the ISN extending laterally toward the longitudinal muscle ldlm1 (black open arrow). db, dorsal branch of Nervus anterior SOG; dg, defense gland; dlm, dorsal longitudinal muscle; ISN, intersegmental nerve complex; N. ant. SOG, Nervus anterior of the subesophageal ganglion; N. transv., Nervus transversus; vb, ventral branch of N. anterior SOG.

to tracing the ventral branch at the defense gland (**Figure 7c**). The subesophageal VMNs were never stained by tracing the ventral nerve branch of N. ant. SOG which innervates the defense gland. For tracing of the dorsal nerve branch of N. ant SOG innervating the defense gland ($n = 7$), the ILN and CLN were also reliably stained (not shown). In two of these preparations of

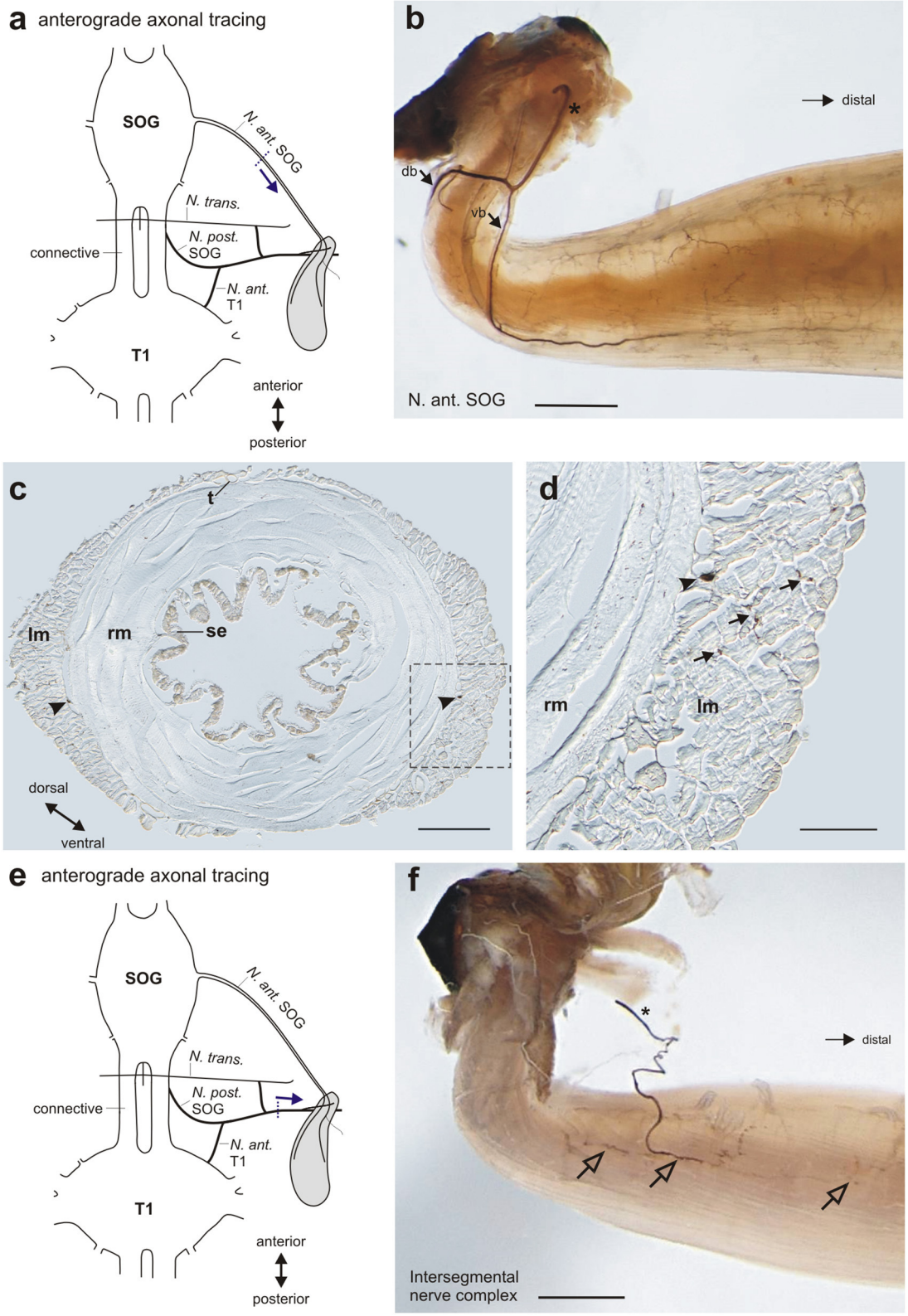

FIGURE 6 | Neural innervation of the defense gland shown by axonal tracing. **(a)** Schematic for the anterograde tracing of N. ant. SOG toward the defense gland. Dotted line indicates cut site of the nerve, arrow indicates the direction of axonal tracing. **(b)** Staining of nerve branches (dorsal branch db, ventral branch vb) and fine

(Continued)

FIGURE 6 | nerve arborization on the gland muscle after tracing of N. ant. SOG. Cut end of N. ant. SOG is indicated by asterisk. **(c)** Histological section at the middle of the gland shows the two nerve branches (arrowheads) between the outer longitudinal muscles (lm) and inner ring muscles (rm). Note the asymmetric organization of the outer, longitudinal muscle layer. Boxed area is shown in magnification in **(d)**. **(d)** Detail of muscle layers shows the stained nerve branch (arrowhead) at the border between longitudinal muscles (lm) and inner ring muscles (rm), and adjacent nerve endings in the outer longitudinal muscles (arrows). **(e)** Schematic for the anterograde tracing of the intersegmental nerve complex toward the defense gland. Dotted line indicates cut site of the nerve, arrow indicates the direction of axonal tracing. **(f)** Staining of the nerve branch from the intersegmental nerve complex (indicated by asterisk) and nerve arborizations on the gland muscle (open arrows) after tracing of the intersegmental nerve complex. Scales: **(b,f)** = 1 mm; **(c)** = 200 μm; **(d)** = 150 μm. db, dorsal branch of Nervus anterior SOG; lm, longitudinal muscles; N. ant. SOG, Nervus anterior SOG; N. ant. T1, Nervus anterior T1; N. post SOG, Nervus posterior SOG; N. trans., Nervus transversus; rm, ring muscles; SOG, subesophageal ganglion; se, secretory epithelium; t, trachea; T1, prothoracic ganglion; vb, ventral branch of Nervus anterior SOG.

TABLE 1 | Innervation of the defense gland by distinct nerves in *A. paromalus*.

Nerve	Innervation	*n*
Nervus anterior SOG	+	$n = 22$
INTERSEGMENTAL NERVE COMPLEX		
Nerve branch of intersegmental nerve complex	+	$n = 6$
Nervus posterior SOG	+	$n = 5$
Nervus anterior T1	+	$n = 5$
Nervus transversus	-	$n = 14$

(+) innervation supported by axonal tracing; (–) innervation not supported by axonal tracing.

the dorsal branch, the VMNs were also stained. Tracing the short nerve branch innervating the longitudinal neck muscle Idlm2 (**Figure 7e**; $n = 8$) stained the VMNs (**Figure 7f**), but no other neuron type. These selective backfills suggest that the ILN and CLN as well as the PIN innervate the defense gland, while the VMNs innervate the dorsal neck muscle Idlm2. The joint staining of ILN, CLN, and the VMNs in a subset of dorsal nerve branch fills was likely an artifact for the VMNs, due to the close proximity of the dorsal branch on the gland to the branch innervating the neck muscle. Based on the tracings of the ventral branch of the N. ant. SOG and the majority of the dorsal branch of the N. ant. SOG, the gland innervation by VMNs can be excluded. These findings provide evidence that distinct sets of neurons with axons in the N. ant. SOG innervate the defense gland (ILN, CLN, PIN) and the longitudinal neck muscle (VMNs).

Retrograde tracing of the nerve branch from the intersegmental nerve complex (**Figure 8a**) also revealed different neuron types in the SOG and the T1, by the N. post. SOG and the N. ant. T1. These experiments generally gave lower staining rates for the SOG, probably due to the thin nerve branch. In the SOG, a single contralateral neuron was stained (**Figure 8b**$_{i}$). In the prothoracic ganglion, a dorsal unpaired median neuron (DUM), one contralateral neuron, and one median neuron with a curved neurite were stained (**Figure 8b**$_{ii}$). Since the nerve branch from the intersegmental nerve complex contacts only the defense gland, the neurons revealed by tracing of this nerve branch can be assumed to innervate the gland.

Since we noted differences in the soma size for the ILN between individuals (**Figures 9a**$_{i}$,**a**$_{ii}$; see Supplementary Data), we measured the SOG sizes and somata sizes for ILN and CLN. Because the animals and also the subesophageal ganglia differ in sizes between sexes, we compared data from females and males. Since not all data tested showed normal distribution ($p = 0.0011$–0.1; KS distance $= 0.1070$–0.3480), we subsequently used the Mann-Whitney test for comparing data between the sexes. The absolute area of the SOG was significantly larger in females than in males (**Figure 9b**, females: $n = 15$, males: $n = 13$; one-tailed Mann-Whitney test: $p < 0.0001$, Mann-Whitney $U = 9.000$). For the ILN and CLN somata, we compared also absolute somata areas. The somata were significantly larger in females for both ILN somata (**Figure 9c**; females: $n = 15$, males: $n = 13$; one-tailed Mann-Whitney test: $p = 0.0362$, Mann-Whitney $U = 58.00$) and CLN somata (**Figure 9d**; females: $n = 10$, males: $n = 9$; one-tailed Mann-Whitney test: $p = 0.0175$, Mann-Whitney $U = 19.00$). To account for the size differences between sexes, we calculated relative somata sizes in relation to the ganglion area. Differences in relative somata sizes were not significant between sexes for the ILN (**Figure 9e**; females $n = 15$, males $= 13$; one-tailed Mann-Whitney test: $p = 0.4816$, Mann-Whitney $U = 96.00$) and the CLN (**Figure 9f**; females: $n = 10$, males: $n = 9$; one-tailed Mann-Whitney test: $p = 0.0912$; Mann-Whitney $U = 28$). We further tested for a correlation between ILN and CLN somata area and ganglion area. We found a statistically significant correlation between ILN somata area and SOG area for female *A. paromalus* ($n = 15$; one-tailed Spearman rank test: $p = 0.0099$, Spearman $r = -0.5929$), and between CLN somata area and SOG area for male *A. paromalus* ($n = 9$; one-tailed Spearman rank test: $p = 0.0484$, Spearman $r = 0.600$). However, no statistically significant correlation was found for male ILN ($n = 13$; one-tailed Spearman rank test: $p = 0.0872$, Spearman $r = 0.4011$) and for female CLN ($n = 10$; one-tailed Spearman rank test: $p = 0.3161$, Spearman $r = -0.1758$).

DISCUSSION

Innervation Pattern of the Defense Gland in *Anisomorpha paromalus*

The defense gland of *A. paromalus* is innervated by three distinct nerves, via the N. ant. SOG and the intersegmental nerve complex (N. post. SOG and N. ant. T1). The most prominent nerve is the N. ant. SOG, while the intersegmental nerve complex forms a fine nerve branch to the gland. This pattern is also found in other stick insects from different lineages (Timematidae: *Timema chumash, Timema petita,* Lonchodinae: *C. morosus,* Necrosciinae: *Sipyloidea sipylus*; Lanceocercata: *Extatosoma tiaratum*; Stolz et al., 2015; Stolz, 2017). The nerve pattern is thus identical across species irrespective of the particular mode of chemical defense, or even the lack of defensive secretions (in *C. morosus*;

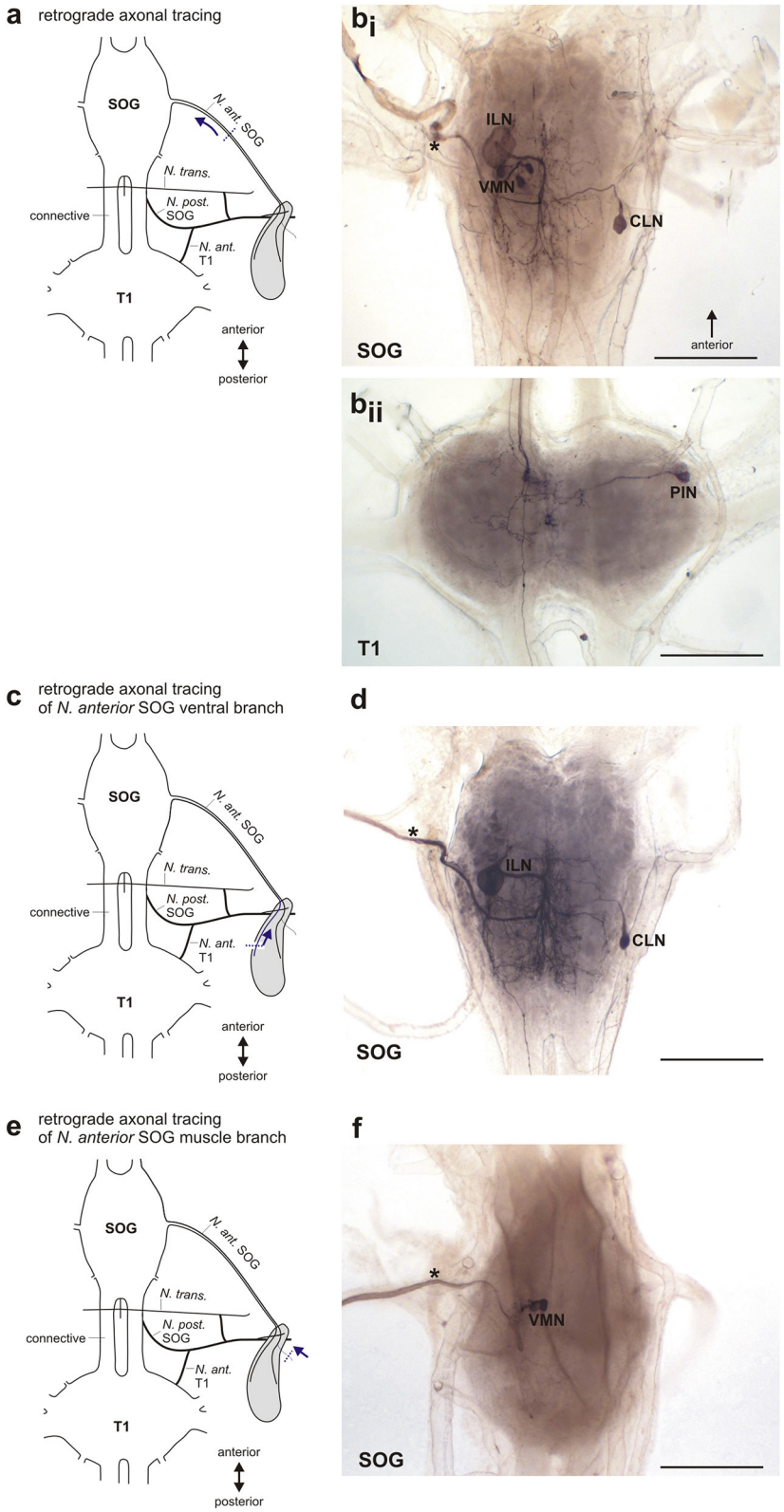

FIGURE 7 | Retrograde axonal tracing of the N. anterior SOG. **(a)** Schematic for the retrograde tracing of N. ant. SOG toward the central nervous system. Dotted line indicates cut site of the nerve, arrow indicates the direction of axonal tracing. **(b)** Stained neuron types after retrograde tracing of N. ant. SOG in the subesophageal

(Continued)

FIGURE 7 | ganglion **(b_i)** and prothoracic ganglion **(b_{ii})**. Traced nerve N. ant. SOG is indicated by asterisk. **(c)** Schematic for the retrograde tracing of the ventral branch of N. ant. SOG toward the central nervous system. Dotted line indicates cut site of the nerve, arrow indicates the direction of axonal tracing. **(d)** Stained neuron types after retrograde tracing of the ventral branch of N. ant. SOG (indicated by asterisk). **(e)** Schematic for the retrograde tracing of the nerve branch of N. ant. SOG innervating dorsal longitudinal muscle ldlm2 toward the central nervous system. Dotted line indicates cut site of the nerve, arrow indicates the direction of axonal tracing. **(f)** Stained neuron types after retrograde tracing of the nerve branch of N. ant. SOG innervating dorsal longitudinal muscle ldlm2 (indicated by asterisk). Scales = 500 μm. CLN, contralateral neuron; ILN, ipsilateral neuron; N. ant. SOG, Nervus anterior SOG; N. ant. T1, Nervus anterior T1; N. post. SOG, Nervus posterior SOG; N. trans., Nervus transversus; PIN, prothoracic intersegmental neuron; SOG, subesophageal ganglion; T1, prothoracic ganglion; VMN, ventral medial neurons.

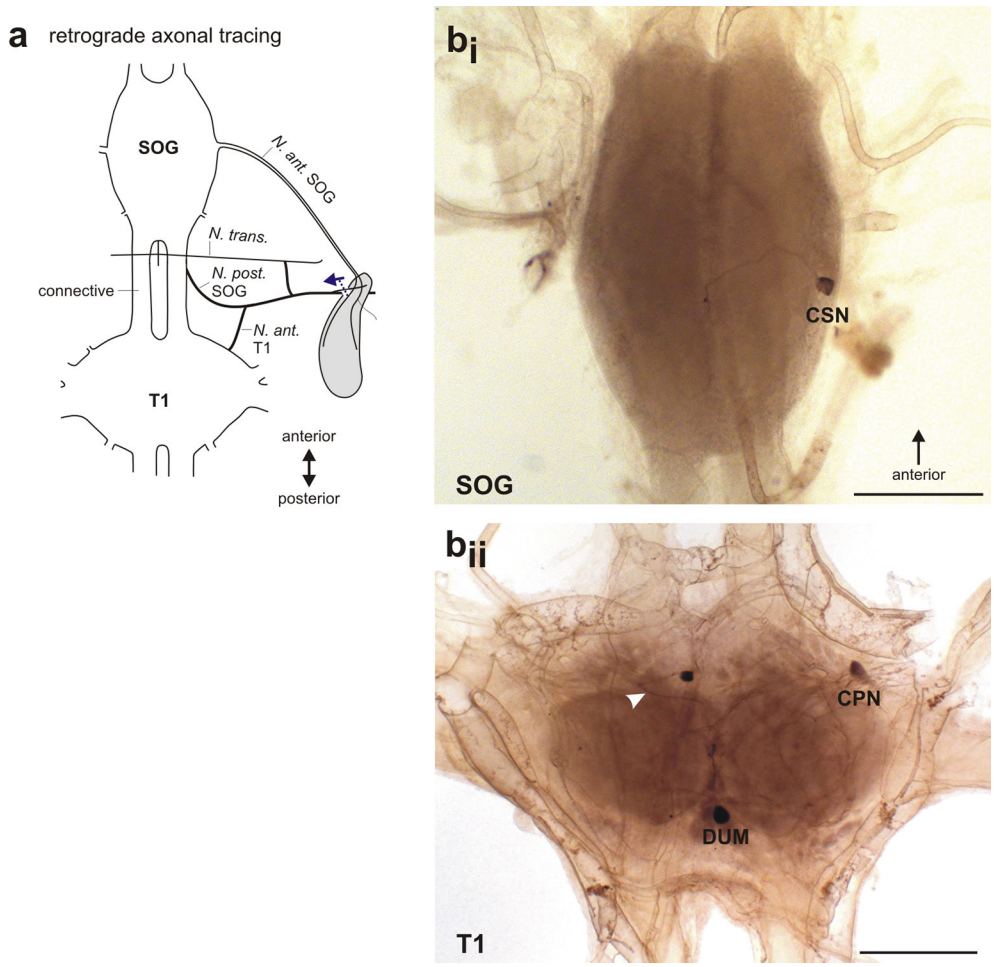

FIGURE 8 | Retrograde axonal tracing of the intersegmental nerve complex. **(a)** Schematic for the retrograde tracing of the intersegmental nerve complex toward the central nervous system. Dotted line indicates cut site of the nerve, arrow indicates the direction of axonal tracing. **(b)** Stained neuron types after retrograde tracing of the intersegmental nerve complex in (**b_i**) the subesophageal ganglion with one contralateral subesophageal neuron (CSN), and (**b_{ii}**) the prothoracic ganglion with a dorsal medial unpaired neuron (DUM), a contralateral prothoracic neuron (CPN), and a neuron located at the midline with a bending neurite (white arrowhead). Scale = 500 μm. CPN, contralateral prothoracic neuron; CSN, contralateral subesophageal neuron; DUM, dorsal unpaired median neuron; N. ant. SOG, Nervus anterior SOG; N. ant. T1, Nervus anterior T1; N. post. SOG, Nervus posterior SOG; N. trans., Nervus transversus; SOG, subesophageal ganglion; T1, prothoracic ganglion.

Carlberg, 1985a). Only in *P. schultei* (Pseudophasmatinae) is the innervation exclusively from the N. ant. SOG (Stolz et al., 2015). *Anisomorpha* species are very closely related to *P. schultei* (Goldberg et al., 2015), but the defense gland innervation is not specialized exclusively to the N. ant. SOG. Therefore, the innervation is only simplified in *P. schultei*. Other species including *A. paromalus* have an innervation by three distinct nerves (Stolz et al., 2015).

The peripheral nerve pattern is conserved also with respect to related taxa of Orthoptera (Honegger et al., 1984), Embioptera (Rähle, 1970), and Blattodea (Davis, 1983), where the nerves N. ant. SOG, N. post. SOG, and N. ant. T1 also innervate dorsal longitudinal ("neck") muscles. The transverse nerve as part of the intersegmental nerve complex does not innervate the defense gland in stick insects (present study; Stolz et al., 2015). In Orthoptera, it supplies

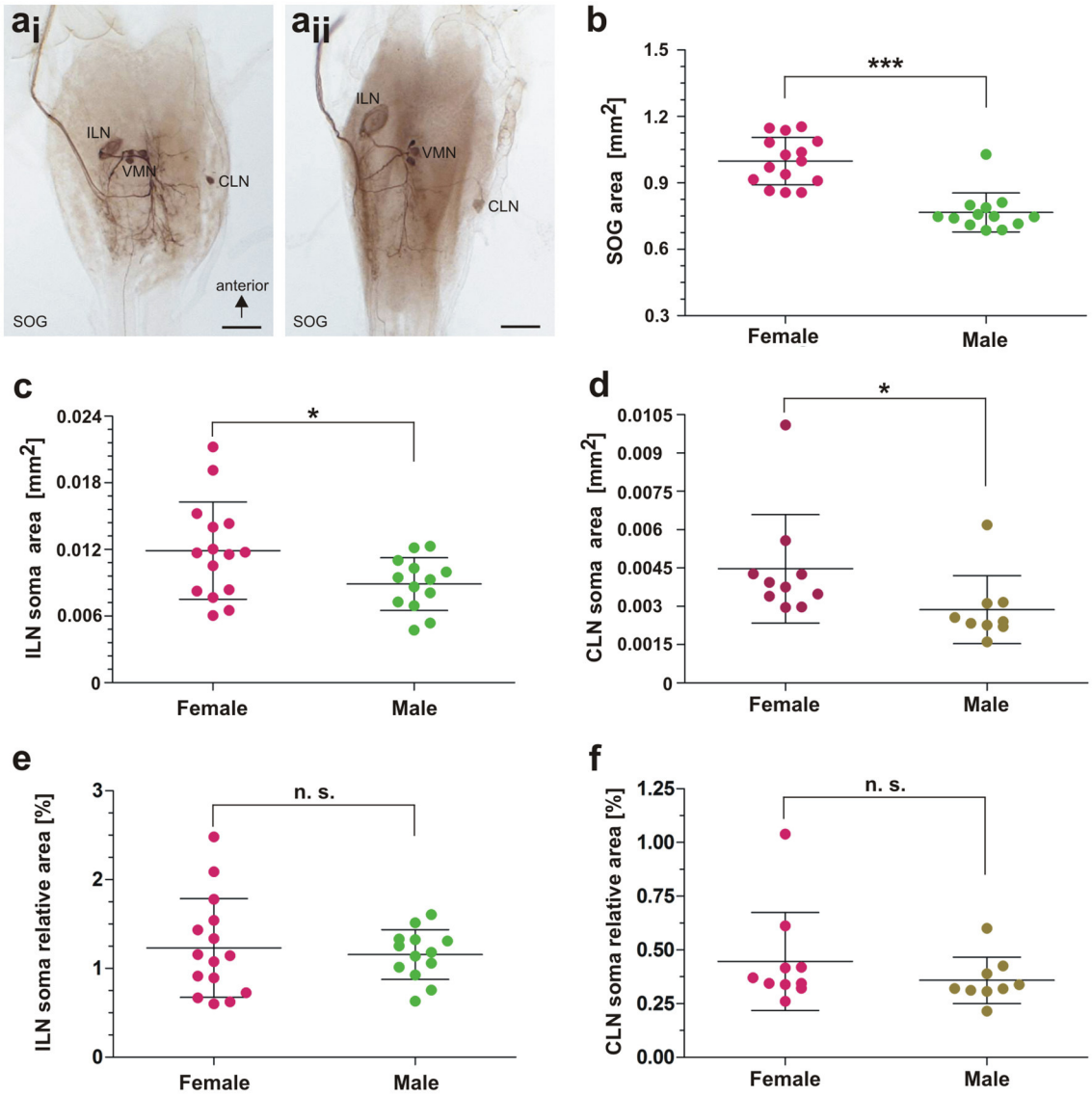

FIGURE 9 | Morphometrical analysis of neuronal elements. **(a)** Examples of ILN size differences between two male individuals. **(b)** Comparison of subesophageal ganglion area in females and males; Mann-Whitney test, $p < 0.0001$. **(c)** Comparison of ILN soma area in females and males; Mann-Whitney test, $p < 0.05$. **(d)** Comparison of CLN soma area in females and males; Mann-Whitney test, $p < 0.05$. **(e)** Comparison in ILN soma relative area in females and males; Mann-Whitney test, $p > 0.05$. **(f)** Comparison in CLN soma relative area in females and males; Mann-Whitney test, $p > 0.05$. Scales = 500 µm. For details, see main text. CLN, contralateral neuron; ILN, ipsilateral neuron; SOG, subesophageal ganglion; VMN, ventral median neurons. Statistics: *$0.05 > p > 0.01$; ***$p < 0.001$.

one to two smaller dorso-ventral muscles (Honegger et al., 1984).

Identified Neurons Innervating the Defense Gland and Evolutionary Novelties at the Cellular Level in a Conserved Innervation Pattern

Here, we conducted selective retrograde backfills of N. ant. SOG nerve branches from the defense gland or the Idlm2 neck muscle to identify the neurons which innervate gland muscles or thoracic neck muscles.

Tracing of the complete N. an. SOG reveals the ILN, CLN, VMNs, and PIN in the central nervous system (**Figure 7b**), as in other stick insects (Stolz et al., 2015). In *A. paromalus*, tracing the nerve branch of N. ant. SOG innervating the Idlm2 stains exclusively the VMNs. This neuron type is evolutionary conserved and innervates anterior dorsal longitudinal muscles in orthopteroid insects (Davis, 1983; Honegger et al., 1984), which we confirm also for stick insects (**Figure 7f**).

Tracing of the nerve branches on the defense gland reveals a subset of these neurons with ILN, CLN, and PIN. These neuron types are not present when tracing the homologous nerve 6 in Orthoptera (Altman and Kien, 1979; Honegger et al., 1984) or

the homologous tergal nerve in cockroaches (Davis, 1983). The selective backfills thus show that the defense gland and Idlm2 are supplied by distinct neurons. The ILN, CLN, and PIN are therefore evolutionary novel types of neurons, which evolved in Phasmatodea with the development of the defense gland (Stolz, 2017). Notably, in the most basal phasmatodean lineage *Timema* only the VMNs are present. The ILN varies in soma size between different species of stick insects, with a larger soma in species with spraying release of defense secretion (see Stolz et al., 2015). The prominent ILN is thus likely the main motoneuron to elicit the gland discharge. The ILN soma size in *A. paromalus* also supports this correlation. Comparisons of the ILN and CLN soma sizes showed no statistically consistent correlation to the ganglion sizes for females and males, as female CLN soma area and male ILN soma area showed no significant correlation to the ganglion area. Only the homogenous relative soma areas show that differences in ILN and CLN soma sizes between sexes likely depend on differences in the size of the SOG and hence body size (**Figures 9e,f**). In orthopteran insects, large muscles with a high number of fibers are also innervated by relatively large motoneurons (Burrows and Hoyle, 1972; Wolf, 2014). Size differences of the ILN and CLN motoneurons might thus also be influenced by the size of the defense gland or the muscle layers. Currently, we also investigate the neuropil areas and tracts with neurite projections from the ILN/CLN or VMNs in the stick insect SOG from selective backfill experiments to analyze the possible functional separation of these neuronal systems in the central nervous system (Stolz, Strauß, et al., in prep.).

The innervation of the defense gland by the intersegmental nerve complex is less prominent than the innervation by the N. ant. SOG, consisting of a rather fine nerve branch. Despite the small size (compared to the N. ant. SOG), it also contains neurites from four neuron types. Since this traced nerve branch from the intersegmental nerve complex contacts only the defense gland (**Figure 8a**), these neurons all innervate the defense gland. They include a known neuromodulatory neuron, the DUM neuron (e.g., Hoyle, 1978; Duch et al., 1999; Bräunig and Pflüger, 2001), and further motoneurons. The DUM neuron supplying the defense gland via N. ant. T1 was also found in *S. sipylus* (Stolz et al., 2015). It is also found to innervate longitudinal neck muscles in locusts in Nerve 1 (homologous to N. ant. T1; Honegger et al., 1984; Kutsch and Heckmann, 1995a) and in cockroaches in the homologous tergal nerve (Davis, 1983). Such DUM or DUM-like neurons innervating dorsal longitudinal muscles via the intersegmental nerve complexes in different ganglia are strongly conserved in insects (Heckmann and Kutsch, 1990, 1995). For the N. ant. T1, a single contralateral neuron or few contralateral neurons in the prothoracic ganglion, which innervate the longitudinal muscle Idlm1, also occur in locusts (Honegger et al., 1984; Kutsch and Heckmann, 1995a). In contrast to the N. ant. SOG, the intersegmental nerve complex reveals not only a conserved nerve, but also conserved neuron types to innervate the muscles in the defense gland. In several species of insects, larger sets of motoneurons innervate muscles via the intersegmental nerve complex (Storrer et al., 1986; Heckmann and Kutsch, 1995; Kutsch and Heckmann, 1995b; Goldammer et al., 2012). Few of such contralateral and median neurons might have been recruited during the evolution of the gland, resulting in a specialized system innervated by single representatives of several identified neuron types.

Gland Muscle Innervation and Muscle Homologies

The stick insect defense gland is mainly innervated by the prominent N. ant. SOG, but also by the intersegmental nerve complex. The innervation by nerves and neurons can be used to gain insights into the evolutionary origin of the longitudinal muscles in the defense gland (**Table 2**). In locusts, the closely aligned muscle pair 50/51 (Idlm2) is the only longitudinal neck muscle supplied by the N. ant. SOG, as shown by retrograde axonal tracing of peripheral nerves (Honegger et al., 1984). In crickets, an occasional additional innervation of muscle 65 (Idlm3) by the VMNs was interpreted as a likely staining artifact (Honegger et al., 1984). This innervation pattern suggests that the longitudinal gland muscle derives, at least partly, from the longitudinal neck muscle Idlm2. This is further supported by the shared innervation of the defense gland and Idlm2 by nerve branches from the N. ant. SOG reported here (**Figures 6b,c**). The intersegmental nerve complex of Orthoptera innervates the dorsal longitudinal muscle Idlm1 (Honegger et al., 1984), which is close to Idlm2 (Friedrich and Beutel, 2008; for *Timema*, see Stolz, 2017). In *A. paromalus* and other stick insects, the intersegmental nerves not only innervate the defense gland, but also Idlm1 (**Figures 5d,f**; Stolz, 2017). This substantiates that also Idlm1 has contributed to the longitudinal musculature of the defense gland. The more posterior dorsal longitudinal muscle with unclear homology to the neopteran groundplan (Friedrich and Beutel, 2008) are apparently not involved in the gland muscle set.

Both the N. ant. SOG and the intersegmental nerve thus innervate dorsal longitudinal muscles and gland muscle (**Figures 5**, **6**, **Table 2**). The shared innervation pattern of

TABLE 2 | Summary of identified motoneurons and their muscle targets in the defense gland system.

Nerve/Neuron type	Innervated muscle in stick insects	Innervated muscle in locusts	Innervated muscle in crickets
N. ANT. SOG			
VMNs	Idlm2	Idlm2	Idlm2; possibly also Idlm3
ILN	Defense gland	Neuron not present	Neuron not present
CLN	Defense gland	Neuron not present	Neuron not present
PIN	Defense gland	Neuron not present	Neuron not present
N. POST. SOG			
CSN	Defense gland	Neuron not present	Neuron not present
N. ANT. T1			
DUM	Defense gland	Present, but target muscle not specified	Axon present
CPN	Defense gland	Idlm1	Idlm1

Data from locusts and crickets after Honegger et al. (1984).

longitudinal muscles also found in Orthoptera suggests that both muscles, Idlm1 and Idlm2, have contributed to the longitudinal muscle fibers in the stick insect defense gland. Since the muscles persist in Phasmatodea, it is likely that sets of muscle fibers of both Idlm1 and Idlm2 contributed to forming the defense gland.

Histological sections from glands after axonal tracing confirm the innervation of longitudinal muscle fibers (**Figures 6c,d**). In frontal sections of the gland, the transversal fibers innervating ring muscles are more difficult to reveal. Innervation of the ring muscle might also be finer, but the position of the two main N. ant. SOG branches between the two muscle layers in the middle and distal gland indicates that both muscle layers are supplied by these branches. This would allow a simultaneous activation of muscle layers for fluid ejection.

CONCLUSION AND OUTLOOK

In sum, the defense gland in *A. paromalus* is innervated by a complex set of peripheral nerves (N. ant. SOG, N. post. SOG. N., ant. T1). The innervation pattern is identical to other stick insect species, including *C. morosus*, a species with relatively small defense glands which apparently does not produce defensive secretions. The nerves involved suggest that the defense gland muscles, at least in parts, derive from the longitudinal neck muscles Idlm1 and Idlm2. Selective backfills of nerve branches from N. ant. SOG to the gland or the dorsal longitudinal muscles reveal a functional specialization for both these systems with different motoneurons innervating the gland (ILN, CLN, PIN) and the dorsal longitudinal muscles (VMNs). The ILN, CLN, and PIN are evolutionary novel motoneurons. This suggests that they evolved with the evolutionary development of the defense gland. A similar pattern was shown for two neuron types from the intersegmental nerves. These neuroanatomical findings show that the conserved innervation pattern has allowed the evolution of the gland control by specialization of few additional motoneurons. It remains to be investigated further how the different nerves and neuron types independently or together activate and modulate the gland musculature, and how the muscle layers coordinate during contraction and fluid ejection.

AUTHOR CONTRIBUTIONS

Carried out experiments: JS, C-RvB, YvB. Carried out preparations: JS, KS. Analyzed data: JS, C-RvB, YvB, KS. Provided reagents and lab facilities: RL-H, TT. Assembled figures: JS. Drafted and wrote manuscript: JS. Edited manuscript: JS, C-RvB, YvB, KS, TT, RL-H. All authors read the manuscript and agreed with the publication.

ACKNOWLEDGMENTS

We thank Dr. Michael Gebhardt, Freising, for providing the *Anisomorpha* individuals for this study. We thank Julia Nothacker for providing additional *Anisomorpha* individuals. We thank Dr. Martin Hardt and Sabine Agel of the Imaging Unit at Justus-Liebig-Universität Gießen for excellent help with SEM. We thank two reviewers for very constructive and helpful comments which improved this manuscript.

SUPPLEMENTARY MATERIAL

The Supplementary Material for this article can be found online at: https://www.frontiersin.org/articles/10.3389/fevo.2017.00151/full#supplementary-material

REFERENCES

Altman, J. S., and Kien, J. (1979). Suboesophageal neurons involved in head movements and feeding in locusts. *Proc. R. Soc. Lond. B.* 205, 209–227. doi: 10.1098/rspb.1979.0061

Arbas, E. A., Meinertzhagen, I. A., and Shaw, S. R. (1991). Evolution in the nervous system. *Annu. Rev. Neurosci.* 14, 9–38. doi: 10.1146/annurev.ne.14.030191.000301

Bässler, U. (1977). Sense organs in the femur of the stick insect and their relevance to the control of position of the femur-tibia-joint. *J. Comp. Physiol.* 121, 99–113. doi: 10.1007/BF00614183

Bässler, U. (1983). *Neural Basis of Elementary Behavior in Stick Insects*. Berlin: Springer.

Bedford, G. O. (1978). Biology and ecology of the Phasmatodea. *Ann. Rev. Entomol.* 23, 25–149. doi: 10.1007/978-3-642-68813-3

Bouchard, P., Hsiung, C.-C., and Yaylayan, V. A. (1997). Chemical analysis of defense secretions of *Siyploidea sipylus* and their potential use as repellents against rats. *J. Chem. Ecol.* 23, 2049–2057. doi: 10.1023/B:JOEC.0000006488.58081.66

Bradler, S. (2009). Die Phylogenie der Stab- und Gespenstschrecken (Insecta: Phasmatodea). *Species Phyl. Evol.* 2, 1–139. doi: 10.17875/gup2009-710

Bräunig, P., and Pflüger, H. J. (2001). The unpaired median neurons of insects. *Adv. Insect Physiol.* 28, 185–266. doi: 10.1016/S0065-2806(01)28011-4

Brown, M., and Lowe, D. G. (2007). Automatic panoramic image stitching using invariant features. *Int. J. Comput. Vision* 74:59. doi: 10.1007/s11263-006-0002-3

Burrows, M., and Hoyle, G. (1972). Neural mechanisms underlying behavior in the locust *Schistocerca gregaria*. III. Topography of limb motorneurons in the metathoracic ganglion. *J. Neurobiol.* 4, 167–186. doi: 10.1002/neu.480040207

Carlberg, U. (1981). An analysis of the secondary defence reactions in stick insects (Phasmida). *Biol. Zentralblatt* 100, 295–303.

Carlberg, U. (1985a). Secondary defence in *Carausius morosus* (de Sinety) (Insecta: Phasmida). *Zool. Anz.* 215, 373–384.

Carlberg, U. (1985b). Chemical defense in *Extatosoma tiaratum* (Macleay) (Insecta, Phasmida). *Zool. Anz.* 214, 185–192.

Carlberg, U. (1985c). Chemical defense in *Anisomorpha buprestoides* (Houttuyn in Stoll) (Insecta, Phasmida). *Zool. Anz.* 215, 177–188.

Carlberg, U. (1986a). Phasmida: a biological review (Insecta). *Zool. Anz.* 216, 1–18.

Carlberg, U. (1986b). Chemical defense in *Sipyloidea sipylus* (Westwood) (Insecta, Phasmida). *Zool. Anz.* 217, 31–38.

Carlberg, U. (1987). Chemical defense in Phasmida vs Mantodea (Insecta). *Zool. Anz.* 218, 369–373.

Chow, Y. S. (2008). "Walkingstick defensive behavior and regeneration of appendages," in *Encyclopedia of Entomology*, *2nd Edn.*, ed J. L. Capinera (Springer:Netherlands), 4133–4135.

Chow, Y. S., and Lin, Y. M. (1986). Actinidine, a defensive secretion of stick insect, *Megacrania alpheus* Westwood (Orthoptera: Phasmatidae). *J. Entomol. Sci.* 21, 97–101. doi: 10.18474/0749-8004-21.2.97

Davis, N. T. (1983). Serial homologies of the motor neurons of the dorsal intersegmental muscles of the cockroach, *Periplaneta americana* (L.). *J. Morphol.* 176, 197–210. doi: 10.1002/jmor.1051760208

Dettner, K. (2015). "Toxins, defensive compounds and drugs from insects," in *Insect Molecular Biology and Ecology*, ed K. H. Hoffmann (Boca Raton FL: CRC Press), 39–93.

Dossey, A. T., Walse, S. S., and Edison, A. S. (2008). Developmental and geographical variation in the chemical defense of the walkingstick *Anisomorpha buprestoides*. *J. Chem. Ecol.* 34, 584–590. doi: 10.1007/s10886-008-9457-8

Dossey, A. T., Walse, S. S., Rocca, J. R., and Edison, A. S. (2006). Single insect NMR: a new tool to probe chemical biodiversity. *ACS Chem. Biol.* 1, 511–514. doi: 10.1021/cb600318u

Dossey, A. T., Whitaker, J. M., Dancel, M. C., Vander Meer, R. K., Bernier, U. R., Gottardo, M., et al. (2012). Defensive spirotekals from *Asceles glaber* (Ohasmatoidea): absolute configuration and effects on ants and mosquitoes. *J. Chem. Ecol.* 38, 1105–1115. doi: 10.1007/s10886-012-0183-x

Duch, C., Mentel, T., and Pflüger, H.-J. (1999). Distribution and activation of different types of octopaminergic DUM neurons in the locust. *J. Comp. Neurol.* 403, 119–134. doi: 10.1002/(SICI)1096-9861(19990105)403:1<119::AID-CNE9>3.0.CO;2-F

Eisner, T. (1965). Defensive spray of a phasmid insect. *Science* 148, 966–968. doi: 10.1126/science.148.3672.966

Eisner, T., Eisner, M., and Siegler, M. (2005). *Secret Weapons. Defenses of Insects, Spiders, Scorpions, and Other Many-Legged Creatures.* Cambridge, MA: Belknap.

Eisner, T., Morgan, R. C., Attygalle, A. B., Smedley, S. R., Herath, K. B., and Meinwald, J. (1997). Defensive production of quinoline by a phasmid insect (*Oreophoetes peruana*). *J. Exp. Biol.* 200, 2493–2500.

Friedrich, F., and Beutel, R. G. (2008). The thorax of *Zorotypus* (Hexapoda, Zoraptera) and a new nomenclature for the musculature of Neoptera. *Arthropod. Structure Dev.* 37, 29–54. doi: 10.1016/j.asd.2007.04.003

Goldammer, J., Büschges, A., and Schmidt, J. (2012). Motoneurons, DUM cells, and sensory neurons in an insect thoracic ganglion: a tracing study in the stick insect *Carausius morosus*. *J. Comp. Neurol.* 520, 230–257. doi: 10.1002/cne.22676

Goldberg, J., Bresseel, J., Constant, J., Kneubühler, B., Leubner, F., Michalik, P., et al. (2015). Extreme convergence in egg-laying strategy across insect orders. *Sci. Rep.* 5:7825. doi: 10.1038/srep07825

Goodman, C. S., Pearson, K. G., and Heitler, W. J. (1979). Variability of identified neurons in grasshoppers. *Comp. Biochem. Physiol. A* 64, 455–462. doi: 10.1016/0300-9629(79)90571-1

Grimaldi, D. G., and Engel, M. (2005). *Evolution of the Insects*. Cambridge: Cambridge University Press.

Happ, G. M., Strandberg, J. D., and Happ, C. M. (1966). The terpene-producing glands of a phasmid insect. *Cell Morphol. Histochem. J. Morphol.* 119, 143–160. doi: 10.1002/jmor.1051190204

Heckmann, R., and Kutsch, W. (1990). "Common neural "Bauplan" in Tracheata? Innervation of the dorsal longitudinal muscles," *in Brain – Perception – Recognition*, eds N. Elsner and G. Roth (Stuttgart: Thieme Verlag), 39.

Heckmann, R., and Kutsch, W. (1995). Motor supply of the dorsal longitudinal muscles II: comparison of motoneurone sets in Tracheata. *Zoomorphology* 115, 197–211. doi: 10.1007/BF00393800

Ho, H.-Y., and Chow, Y. S. (1993). Chemical identification of defensive secretion of stick insect, *Megacrania tsudai* Shiraki. *J. Chem. Ecol.* 19, 39–46. doi: 10.1007/BF00987469

Honegger, H.-W., Altman, J. S., Kein, J., Müller-Tautz, R., and Pollerberger, E. (1984). A comparative study of neck muscle motor neurons in a cricket and a locust. *J. Comp. Neurol.* 230, 517–535. doi: 10.1002/cne.902300404

Hoyle, G. (1978). The dorsal, unpaired, median neurones of the locust metathoracic ganglion. *J. Neurobiol.* 9, 43–57. doi: 10.1002/neu.480090105

Hoyle, G. (1983). "On the way to neuroethology: The identified neuron approach," in *Neuroethology and Behavioral Physiology. Roots and Growing Points*, eds F. Huber and H. Markl (Heidelberg: Springer), 9–25.

Jeziorski, L. (1918). Der Thorax von *Dixippus morosus* (Carausius). *Z. Wiss. Zool.* 117, 727–815.

Kutsch, W., and Breidbach, O. (1994). Homologous structures in the nervous systems of Arthropoda. *Adv. Insect Physiol.* 24, 1–113. doi: 10.1016/S0065-2806(08)60082-X

Kutsch, W., and Heckmann, R. (1995a). Motor supply of the dorsal longitudinal muscles, I: homonomy and ontogeny of the motoneurones in locusts (Insecta, Caelifera). *Zoomorphology* 115, 179–195. doi: 10.1007/BF00403172

Kutsch, W., and Heckmann, R. (1995b). "Homologous structures, exemplified by motoneurons of Mandibulata," in *The Nervous System of Invertebrates: An Evolutionary and Comparative Approach*, eds O. Breidbach and W. Kutsch (Basel: Birkhäuser), 221–248.

Leubner, F., Hörnschemeyer, T., and Bradler, S. (2016). The thorax of the cave cricket *Troglophilus neglectus*: anatomical adaptations in an ancient wingless insect lineage (Orthoptera: Rhaphidophoridae). *BMC Evol. Biol.* 16:39. doi: 10.1186/s12862-016-0612-5

Marquardt, F. (1940). Beiträge zur Anatomie der Muskulatur und der peripheren Nerven von Carausius (Dixippus) morosus. *BR. Zool. Jahrb. Anat. Ontog.* 66, 63–128.

Meinwald, J., Chadha, M. S., Hurst, J. J., and Eisner, T. (1962). Defense mechanisms of arthropods. 9. Anisomorphal, the secretion of a phasmid insect. *Tetrahedron Lett.* 3, 29–33. doi: 10.1016/S0040-4039(00)62038-5

Nentwig, W. (1990). Stick insects (Phasmida) as prey of spiders: size, palatability and defence mechanisms in feeding tests. *Oecologia* 82, 446–449. doi: 10.1007/BF00319784

Rähle, W. (1970). Untersuchungen an Kopf und Prothorax von *Embia ramburi* Rimsky-Korsakow 1906 (Embioptera, Embiidae). *Zool. Jahrb. Anat. Onto.* 87, 248–330.

Schmeda-Hirschmann, G. (2006). 4-Methyl-1-hepten-3-one, the defensive compound from *Agathemera elegans* (Philippi) (Phasmatidae) Insecta. Z. *Naturforschung* 61, 592–594. doi: 10.1515/znc-2006-7-820

Smith, R. M., Brophy, J. J., Cavill, G. W. K., and Davies, N. W. (1979). Iridodials and nepetalactone in the defensive secretion of the coconut stick insects, *Graeffea crouani*. *J. Chem. Ecol.* 5, 727–735. doi: 10.1007/BF00986557

Stolz, K. (2017). Functional morphology and neuronal innervation of the prothoracic defense gland in *Timema*. *Acta Zool.* doi: 10.1111/azo.12216. [Epub ahead of print].

Stolz, K., von Bredow, C.-R., von Bredow, Y. M., Lakes-Harlan, R., Trenczek, T. E., and Strauß, J. (2015). Neurons of self-defence: neuronal innervation of the exocrine defence glands in stick insects. *Front. Zool.* 12:29. doi: 10.1186/s12983-015-0122-0

Storrer, J., Bässler, U., and Mayer, S. (1986). Motoneurone im Meso- und Metathorakalganglion der Stabheuschrecke *Carausius morosus*. *Zool. Jahrb. Abt. Allg. Zool. Physiol.* Tiere 90, 359–374.

Strong, L. (1975). Defence glands in the giant spiny phasmid *Extatosoma tiaratum*. *J. Entomol.* 50, 65–72. doi: 10.1111/j.1365-3032.1975.tb00093.x

van de Kamp, T., dos Santos Rolo, T., Baumbach, T., and Greven, H. (2015). X-ray radiography of a spraying insect (Phasmatodea). *Entomol. Heute* 27, 37–44.

Weidler, D. J., and Diecke, F. P. J. (1969). The role of cations in conduction in the central nervous system of the herbivorous insect *Carausius morosus*. *Z. Vergl. Physiol.* 64, 372–399. doi: 10.1007/BF00340433

Wipfler, B., Klug, R., Ge, S. Q., Bai, M., Göbbels, J., Yang, X. K., et al. (2015). The thorax of Mantophasmatodea, the morphology of flightlessness, and the evolution of the neopteran insects. *Cladistics* 31, 50–70. doi: 10.1111/cla.12068

Wolf, H. (2014). Inhibitory motoneurons in arthropod motor control: organisation, function, evolution. *J. Comp. Physiol. A* 200, 693–710. doi: 10.1007/s00359-014-0922-2

Conflict of Interest Statement: The authors declare that the research was conducted in the absence of any commercial or financial relationships that could be construed as a potential conflict of interest.

The reviewer FL and handling Editor declared their shared affiliation.

frontiers in Ecology and Evolution

ORIGINAL RESEARCH
published: 24 May 2018
doi: 10.3389/fevo.2018.00069

The Evolution of Tarsal Adhesive Microstructures in Stick and Leaf Insects (Phasmatodea)

Thies H. Büscher[1], Thomas R. Buckley[2,3], Constanze Grohmann[1], Stanislav N. Gorb[1] and Sven Bradler[4]*

[1] Department of Functional Morphology and Biomechanics, Zoological Institute, Kiel University, Kiel, Germany, [2] Manaaki Whenua—Landcare Research, Auckland, New Zealand, [3] School of Biological Sciences, University of Auckland, Auckland, New Zealand, [4] Johann-Friedrich-Blumenbach-Institute of Zoology and Anthropology, University of Göttingen, Göttingen, Germany

Insects have developed specialized structures on their feet for adhering to surfaces, with stick and leaf insects or Phasmatodea exhibiting an unexpectedly high diversity of these structures. In Phasmatodea, attachment on different substrates is achieved by two types of pads on the legs: the euplantulae on the tarsomeres and the arolium on the pretarsus. The euplantulae are adhesive structures capable of adaptability to the substrate profile and generation of the required attachment strength. The diversity of euplantular microstructures of 56 species that represent all major lineages recognized within Phasmatodea and the whole biogeographical distribution of the group are examined using scanning electron microscopy (SEM). Nine different types of attachment structures can be distinguished whereby one, the nubby type, can be further divided into three different distinct types based on the specific ratio of each conical outgrowth. We mapped the morphological data from the SEM onto a phylogenetic tree we reconstructed based on molecular data. Previously, the evolution of different adhesive microstructures (AMs) on these pads has been suggested to reflect phylogenetic groups. However, different types of AMs are found within monophyletic groups, and our ancestral character state reconstruction suggests smooth euplantulae in the ground pattern of Euphasmatodea and multiple independent origins of other forms. The type of AM appears to be strongly associated with ecomorphs, e.g., smooth euplantular surfaces are more frequently found in tree-dwellers than in ground-dwellers, whilst the attachment pads of ground-dwelling species primarily bear conical cuticular outgrowths (nubby euplantulae).

Keywords: euplantulae, tarsal attachment, adhesive microstructures, phylogeny, cuticle, functional morphology

OPEN ACCESS

Edited by:
Mariana Mateos,
Texas A & M University, United States

Reviewed by:
Robert Friedman,
University of South Carolina, United States
Brian I. Crother,
Southeastern Louisiana University, United States

****Correspondence:***
Thies H. Büscher
tbuescher@zoologie.uni-kiel.de.

Specialty section:
This article was submitted to Phylogenetics, Phylogenomics, and Systematics, a section of the journal Frontiers in Ecology and Evolution

Received: *09 February 2018*
Accepted: *04 May 2018*
Published: *24 May 2018*

Citation:
Büscher TH, Buckley TR, Grohmann C, Gorb SN and Bradler S (2018) The Evolution of Tarsal Adhesive Microstructures in Stick and Leaf Insects (Phasmatodea). Front. Ecol. Evol. 6:69. doi: 10.3389/fevo.2018.00069

INTRODUCTION

The mesodiverse Phasmatodea are widespread, inhabiting nearly all temperate and tropical ecosystems worldwide (Günther, 1953; Bedford, 1978; Brock et al., 2017), but have only limited dispersal capabilities (Bradler et al., 2015). These exclusively phytophagous insects are well-camouflaged in their preferred habitats due to their masquerade imitating leafs or twigs (Bradler, 2009). While undergoing a fast radiation since the Cretaceous (Bradler et al., 2015) the

slowly migrating phasmids adapted to very local environmental settings. In a wide distributional range various ecological adaptations occurred independently in different lineages, causing different species inhabiting similar environments to display similar adaptations (e.g., Buckley et al., 2009; Dennis et al., 2015).

Since the wide distribution and occupancy of similar ecological niches has led to many convergences in Phasmatodea, many distinct morphological adaptations, such as specialized egg deposition modes, are more likely to form ecomorphological groups within this lineage than to reflect phylogenetic relationships (Buckley et al., 2009; Bradler et al., 2015; Goldberg et al., 2015). For instance, the exclusively ground dwelling tree lobsters (e.g., *Droycoccelus*, *Eurycantha*, *Canachus*) are shown to be polyphyletic, but adapted to specific environmental conditions, leading to many parallel evolvements. These formerly taxonomically associated species exhibit a very similar habitus, which is robust, dorsoventrally depressed and includes sturdy, armed legs. They dwell on the ground and all bury their eggs therein, usually with a secondary ovipositor (Buckley et al., 2009). Such a distinct ecological specification is attended by dissimilar substrata, species dwell on in their preferred habitats, and most probably includes adaptations of the attachment devices of these insects (Gottardo et al., 2015).

In order to adhere securely in the inhabited environment, phasmids possess specialized structures on their tarsi (**Figure 1**). Especially species living in the canopy depend on secure attachment to avoid potential damage from dropping to the ground (Schmitt et al., 2018). In addition to the pretarsal claws two main types of attachment pads are used in phasmids. The pretarsus is equipped with a pan-shaped toe pad (arolium) in every species. This particular attachment pad is suggested to create adhesion, if the tarsus is pulled from the surface (Labonte and Federle, 2013). On the proximal tarsomeres a small number of heel pads (euplantulae) are situated. Most species possess one euplantula on each of the four proximal tarsomeres enabling adjustment to the surface profile. In some species, a fifth euplantula is found on the distal tarsomere as well (Vallotto et al., 2016). In contrast to the arolium, the euplantulae generate large friction coefficients, when they are pressed onto the substrate due to shear forces, but create negligible adhesion (Busshardt et al., 2011, 2012; Labonte and Federle, 2013; Labonte et al., 2014).

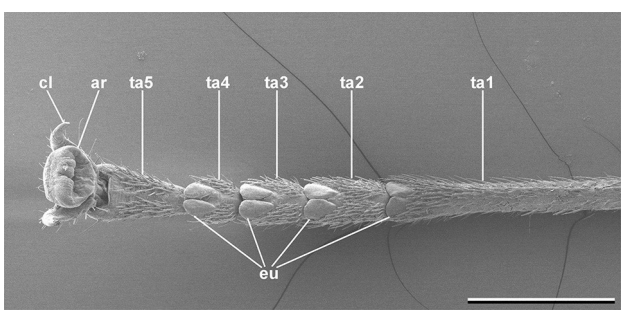

FIGURE 1 | Typical phasmatodean tarsus, *Clonaria conformans* (Gratidiini). cl, tarsal claw; ar, arolium; eu, euplantula; ta1-5, tarsomeres 1-5. Scale bar: 1 mm.

Attachment in insects is achieved in general by adaption to the surface profile in order to maximize the actual contact area. This is accomplished either by flexible setose structures, or by soft cuticle layers (Gorb, 2001, 2005; Bennemann et al., 2014). Both principles appear in different groups of insects (Beutel and Gorb, 2001; Grohmann et al., 2015). Hairy systems, consisting of deformable adhesive setae, are common in spiders (Gorb et al., 2006), beetles (Stork, 1980; Gorb and Gorb, 2002; Bullock and Federle, 2011), earwigs (Haas and Gorb, 2004), and flies (Bauchhenss, 1979; Gorb, 1998; Niederegger et al., 2002; Friedemann et al., 2014). The other system consists of cuticular pads, which bear no prominent ornamentation, such as setae, but might bear different adhesive microstructures (Beutel and Gorb, 2008). This type is common in Phasmatodea (Büscher and Gorb, 2017) and also found in Orthoptera (Gorb et al., 2000; Perez Goodwyn et al., 2006), Hymenoptera (Federle et al., 2001, 2002; Frantsevich and Gorb, 2004), and Blattodea (Clemente and Federle, 2008).

For hexapods in general, the structural diversity of the attachment devices has been demonstrated to reflect phylogenetic relationships and, for the Phasmatodea and their controversely discussed sister groups, potential evolutionary scenarios were postulated based on these traits (Beutel and Gorb, 2001, 2006, 2008). The presence of smooth arolia and euplantulae, without macroscopic adhesive structures, has been discussed with respect to a phylogenetic placement of Phasmatodea as sister group to Mantophasmatodea, emphasizing the morphological similarity of adhesive systems in both groups (Beutel and Gorb, 2008). Nevertheless, recent morphological and molecular approaches support the sister group relation of Embioptera and Phasmatodea (Ishiwata et al., 2011; Friedemann et al., 2012; Letsch et al., 2012; Letsch and Simon, 2013; Misof et al., 2014). Although the attachment pads of stick insects appear to be smooth on a macroscopical level, the basal splitting of *Timema* and Euphasmatoda (the remaining Phasmatodea excluding *Timema*), is supported by the ultrastructure of the arolium, which is covered with pointed acanthae in *Timema* and entirely smooth in the latter. This sister group relationship of *Timema* and Euphasmatodea is considered well supported (e.g., Bradler, 2009). Beutel and Gorb (2008) distinguished the pointed acanthae on the euplantulae of *Timema* and the nubby adhesive microstructures (AM) of the euphamatodeans *Aretaon asperrimus* and *Neohirasea maerens*. The nubs found in these two taxa were referred to as low aspect-ratio acanthae, but subsequent discussion regarding their structure used various different terms, including microtrichia (Gottardo and Heller, 2012) and bumps (Zill et al., 2014) without considering the cellular origin of these structures. Similar AM are found on the euplantulae of stick insects in a considerable diversity, as revealed in various taxonomic descriptions, biomechanic studies, and phylogenetic approaches. Five types of AM have been found so far: in addition to the pointed acanthae in *Timema*, nubs with two different aspect ratios are found in taxa from different lineages of euphasmatodeans. *Carausius morosus* possesses comparatively long nubs (Busshardt et al., 2012), while other stick insects from different lineages bear shorter nubs (Beutel and Gorb, 2008; Gottardo and Heller, 2012; Büscher

and Gorb, 2017). Some taxa possess entirely smooth euplantulae without any micromorphological ornamentation (Busshardt et al., 2012; Gottardo and Vallotto, 2014; Gottardo et al., 2015; Vallotto et al., 2016; Büscher and Gorb, 2017), and *Dallaiphasma eximius* revealed a hexagonal or plateau pattern (Gottardo, 2011). Although the structural diversity of phasmatodean AMs is known (Büscher et al., 2018) and the phylogenetic clustering of similar AMs is supposed to partly reflect the evolution of Phasmatodea (Gottardo et al., 2015; Büscher and Gorb, 2017), there is no recent study approaching the phylogenetic relationships of the different AMs. We therefore examine the diversity of euplantular AMs within Phasmatodea in correlation with the phylogeny of the species examined.

MATERIALS AND METHODS

Morphology

The euplantulae of 56 adult female specimens were examined using SEM. These species represent the major lineages currently recognized in Phasmatodea (see **Supplementary Data 1**: **Supplementary Table S1** for detailed information). Living specimens were bred in captivity until they reached adulthood. The insects were then anesthetized with CO_2 and then decapitated. The tarsi were cut off and fixated in a 2.5% solution of glutaraldehyde in PBS buffer and stored on ice on a shaker for 24 h. In the case, when no living specimens were available, dried specimens from collections were used. In order to restore the original condition of attachment pads, the cuticle has been softened. Therefore, the tarsi were removed and stored in a relaxing chamber for 24 h. Afterwards the tarsi were put into a 10% solution of lactic acid for 24–48 h until the attachment pads were restored into an adequate condition and then fixed in a 2.5% solution of glutaraldehyde in PBS buffer (Gladun and Gumovsky, 2006). Then specimens were stored in 70% ethanol, dehydrated in an ascending alcohol series and critical-point dried. Dried samples were mounted on aluminum stubs and sputter-coated with a 15 nm thick layer of gold-palladium. Samples were observed in the scanning electron microscope (SEM) Hitachi S4800 (Hitachi High-Technologies Corp., Tokio, Japan) at 7 kV of acceleration voltage.

Phylogenetic Analysis

DNA has been extracted and sequenced for 14 stick insect specimens. We combined these data with previously sequenced taxa (Buckley et al., 2009; Goldberg et al., 2015). Sampled taxa were chosen with a focus on the different ecomorphs, covering the entire geographic distribution of Phasmatodea and all extant stick insect lineages. We amplified regions of the mitochondrial cytochrome c-oxidase subunit I (COI) and II (COII) genes, and the nuclear histone subunit 3 (H3) and ribosomal large subunit RNA gene (28S) using methods described previously (Buckley et al., 2009). DNA sequences were edited in Geneious R10 (Kearse et al., 2012). Alignments were made using Muscle (Edgar, 2004) as implemented in Geneious R10. The alignments were partitioned into four sets of characters; mitochondrial 1st and 2nd codon positions, mitochondrial 3rd codon positions, H3 gene, and 28S gene. Use of a partitioned model allows us to account for the typically different substitution patterns between different genes and codon positions, especially the increased rate at the third codon positions. Model selection using the AIC in JModelTest v.2.1.3 (Darriba et al., 2012) was then performed independently on each partition. Phylogenetic reconstruction was then performed using MrBayes v3.2.6 (Ronquist et al., 2012). For prior distributions we used a flat Dirichlet distribution (1,1,1,1) on "ratepr," informative Dirichlet distribution (1,2,1,1,2,1) on "revmatpr," beta distribution (1,1) on "tratiopr," exponential distribution (1) on "shapepr," and an unconstrained exponential distribution (1) on "brlens," State frequencies were fixed at empirical values. We ran five independent analyses of 10 million generations, four chains, a sample frequency of 1000, and an MCMCMC temperature of 0.2. Output files were inspected in Tracer v1.6.0 (http://tree.bio.ed.ac.uk/software/tracer/) to ensure all effective sample sizes were >200 and MCMC chains were mixing appropriately. We also reconstructed phylogenetic relationships using maximum likelihood as implemented in Garli (Zwickl, 2006). We used the same partitioned substitution model as in the Bayesian analysis. The data were bootstrapped with 100 replicates and 1 search replicate per bootstrap. Ancestral character states were reconstructed using the Mkv model (Lewis, 2001) as implemented in Mesquite v3.4 (Maddison and Maddison, 2018). Ancestral states were estimated on the topology and branch lengths from the Bayesian analysis. The alignment used for the phylogenetic reconstruction is provided as a Nexus input file as **Supplementary Data Sheet 1**.

RESULTS

Morphology

The tarsus of stick insects generally consists of five tarsomeres (**Figure 1**). The pretarsus is equipped with two claws and an arolium. Tarsomeres 1–4 bear distal euplantulae in all species studied. In some species, an accessory euplantula is found on the fifth tarsomere. The whole tarsal morphology reveals no intraspecific difference, neither between different specimens, nor in the micromorphological features within the arolium and euplantulae, nor between different legs of the same individual, nor between different euplantulae on the same tarsus. We found nine types of AM among the examined species. Adult females of exemplary species for the corresponding AMs are shown in **Figure 2**. Smooth euplantular surfaces are the most frequently observed forms (**Figure 3A**), followed by conical outgrows of different aspect ratios (nubby, **Figures 3F–H**). Rare forms include flat pads (found in *Necroscia annulipes*, **Figure 3B**), plateaus (present in *Epidares nolimetangere* and *Dajaca monilicornis*, **Figures 3C,L**), coarse (found in *Kalokorinnis* and *Oreophoetes*, **Figure 3D**), maze (found in *Leiophasma*, **Figure 3E**), ridges (found in the Lanceocercata taxa *Argosarchus horridus* and *Megacrania phelaus*, **Figure 3I**), acanthae (only found in *Timema*, **Figure 3J**, Beutel and Gorb, 2008), and hairs (setae, present only in *Dinophasma saginatum*, **Figure 3K**). The AMs of every of these species is illustrated and described in detail in Büscher et al. (2018).

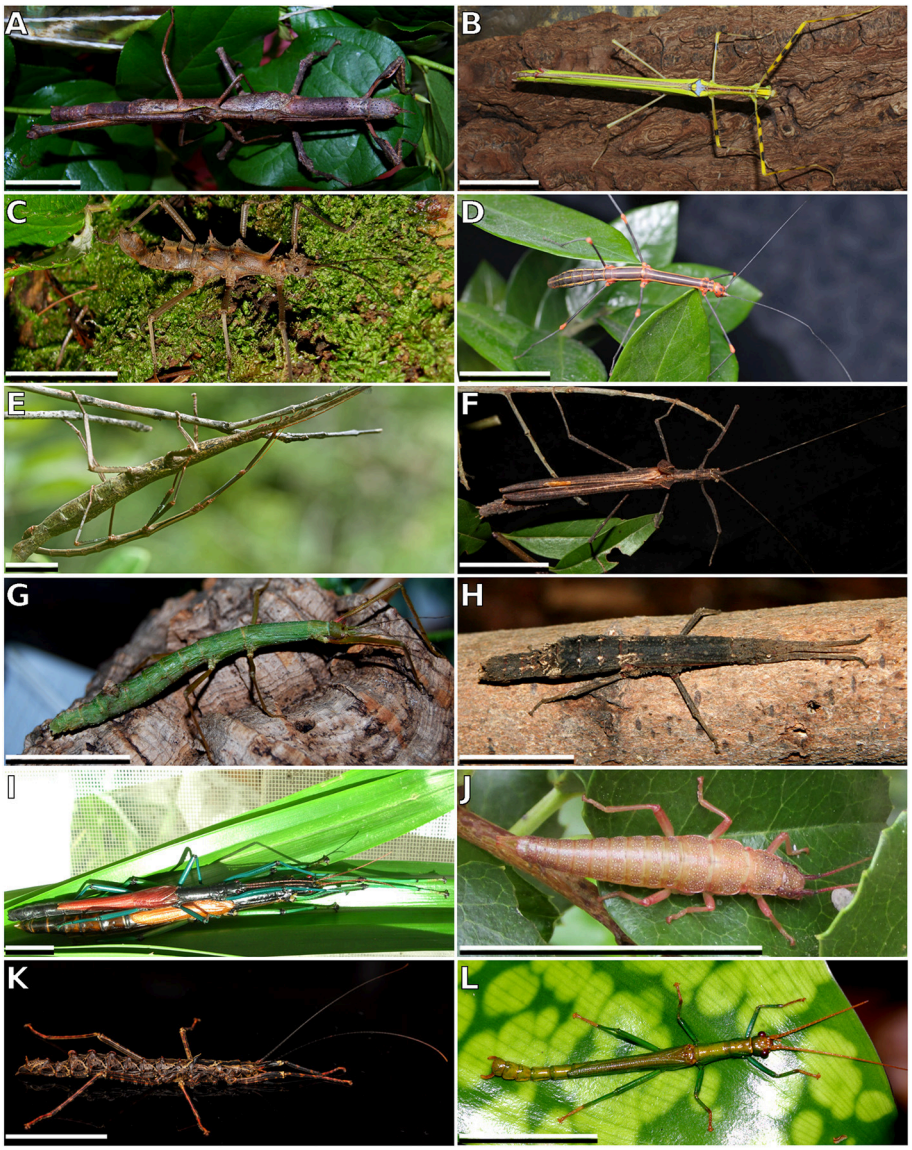

FIGURE 2 | Exemplary members of Phasmatodea. **(A)** *Cigarrophasma tessulatum*, couple, image provided by Daniel Dittmar. **(B)** *Necroscia annulipes*, female, image provided by Holger Dräger. **(C)** *Epidares nolimetangere*, female. **(D)** *Oreophoetes peruana*, female. **(E)** *Leiophasma* sp., couple, image provided by Paul Bertner. **(F)** *Pseudophasma velutinum*, female, image provided by Holger Dräger. **(G)** *Xylica oedematosa*, female, image provided by Daniel Dittmar. **(H)** *Orestes mouhotii*, female. **(I)** *Megacrania phelaus*, couple, image provided by Bruno Kneubühler. **(J)** *Timema* sp., female, image provided by Royce Cumming. **(K)** *Dinophasma saginatum*, female, image provided by Bruno Kneubühler. **(L)** *Dajaca monilicornis*, male, image provided by Luis Mata. Scale bars: 20 mm.

Phylogenetic Relationships

The DNA sequence alignment consisted of 762 base pairs (bp), 695, 328, and 615 from the COI, COII, H3, and 28S genes respectively. The maximum likelihood relative substitutions rates of mitochondrial 1st + 2nd codon positions, mitochondrial 3rd codon positions, H3 and 28S genes were 0.035, 4.732, 0.065, and 0.077 respectively. We observed strong support [Bayesian posterior probability (BPP) = 1] for several monophyletic groups that were also recovered in previous studies (**Figure 4**), including Necrosciinae, Phylliinae, Aschiphasmatinae, Pseudophasmatidae, Lanceocercata, and Anisacanthidae (*Leiophasma* + *Parectatosoma*). However, bootstrap (BS) values were somewhat lower with only Phylliinae, Aschiphasmatinae, and Anisacanthidae (*Leiophasma* + *Parectatosoma*) receiving 100% BS support. Clades not supported, but also monophyletic in accordance with previous studies (Bradler et al., 2014, 2015; Goldberg et al., 2015) are Clitumninae (BPP = 0.54, BS < 50%), Diapheromerinae (BPP = 0.53, BS = 72%), and Heteropteryginae (BPP = 0.74, BS < 50%). The three subgroups of the latter, Dataminae (*Epidares* + *Pylaemenes* + *Orestes*), Heteropteryginae (*Haaniella* + *Heteropteryx*), and Obriminae (*Aretaon* + *Sungaya*) are each highly supported with BPP

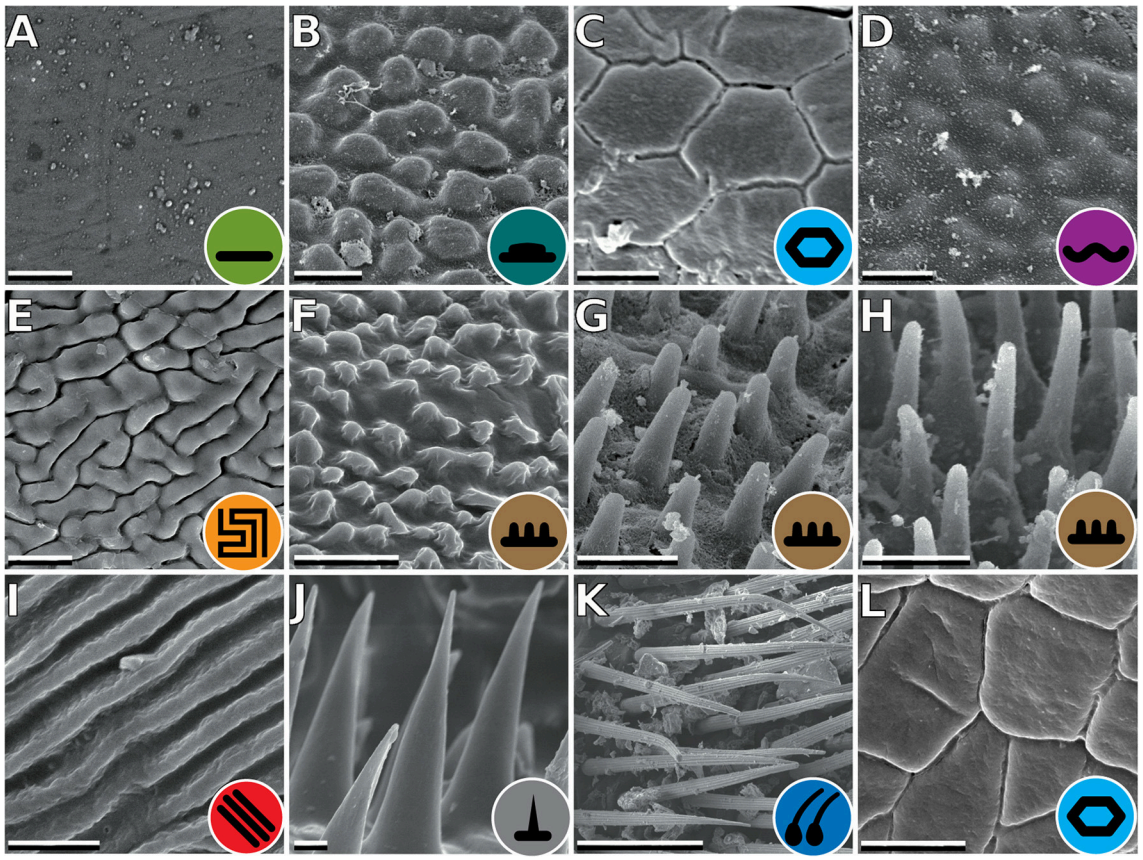

FIGURE 3 | Types of attachment microstructures in Phasmatodea. **(A)** Smooth, *Cranidium gibbosum*. **(B)** Flat pads, *Necroscia annulipes*. **(C)** Plateaus, *Epidares nolimetangere*. **(D)** Coarse, *Kalocorinnis wegneri*. **(E)** Maze, *Leiophasma* sp. **(F)** Nubby (small), *Pseudophasma velutinum*. **(G)** Nubby (median), *Xylica oedematosa*. **(H)** Nubby (long), *Orestes mouhotii*. **(I)** Ridges, *Megacrania phelaus*. **(J)** Acanthae, *Timema* sp. **(K)** Hairs, *Dinophasma saginatum*. **(L)** Plateaus, *Dajaca monilicornis*. Scale bars: **(A–J)**. 2 μm; **(K)**. 50 μm.

values of 1 and BS values of 98%, 100% and 100% respectively. Dataminae and Heteropteryginae are placed as sister taxa (BPP = 0.71, BS < 50%), which is in contrast to previous studies that suggest alternative topologies for these groups (Bradler et al., 2015; Goldberg et al., 2015). Further noteworthy results include a rather robust topology for Lanceocercata that largely corroborates earlier analyses, including a clade of taxa from New Caledonia (*Canachus*) + New Zealand (*Argosarchus* + *Clitarchus*) (BPP = 1, BS = 93%) and a sister group relationship between *Dimorphodes* and all remaining Lanceocercata, and with Cladomorphinae being sister clade to Stephanacridini (*Macrophasma*) + Lanceocercata (Buckley et al., 2009, 2010; Bradler et al., 2014, 2015). Necrosciinae also comprises Korinninae (*Kalokorinnis*) as suggested before (Goldberg et al., 2015) and *Conlephasma*, which has been discussed as being either related to Necrosciinae or Pseudophasmatidae (Gottardo and Heller, 2012) and is here unambiguously placed as sister group to *Neohirasea* + *Phaenopharos* (BPP = 1, BS = 92%) within Necrosciinae. A Malagasy clade consisting of *Achrioptera* + Anisacanthiade is well supported (BPP = 1, BS = 68%) as recovered before by Bradler et al. (2015). A further noteworthy result is the placement of the enigmatic African Bacillinae taxon *Xylica* as sister group to Aschiphasmatinae (BPP = 1, BS = 59%), which corroborates the finding of Buckley et al. (2009). One surprising result is our recovery of Phylliinae nested within Lonchodinae, albeit weakly supported. This is at odds with all previous phylogenetic analyses observing monophyletic Lonchodinae (Buckley et al., 2009; Bradler et al., 2014, 2015; Goldberg et al., 2015), and we attribute this result to a shortage of taxon sampling within these two subfamilies. The deeper nodes, e.g., the radiation of major phasmatodean lineages and enigmatic longstanding taxa like *Agathemera*, *Bacillus*, and *Bactrododema*, are poorly resolved and largely unsupported, which is a common observation for phylogenetic studies of Phasmatodea (Buckley et al., 2009; Bradler et al., 2014, 2015; Goldberg et al., 2015).

DISCUSSION

Evolution of Attachment Structures

The recovered phylogeny was largely consistent with current phylogenetic hypotheses on stick and leaf insects with the exception of the placement of Phylliinae within Lonchodinae, which is not well supported and probably an artifact due to the limited taxon sampling of the present study. The poorly resolved

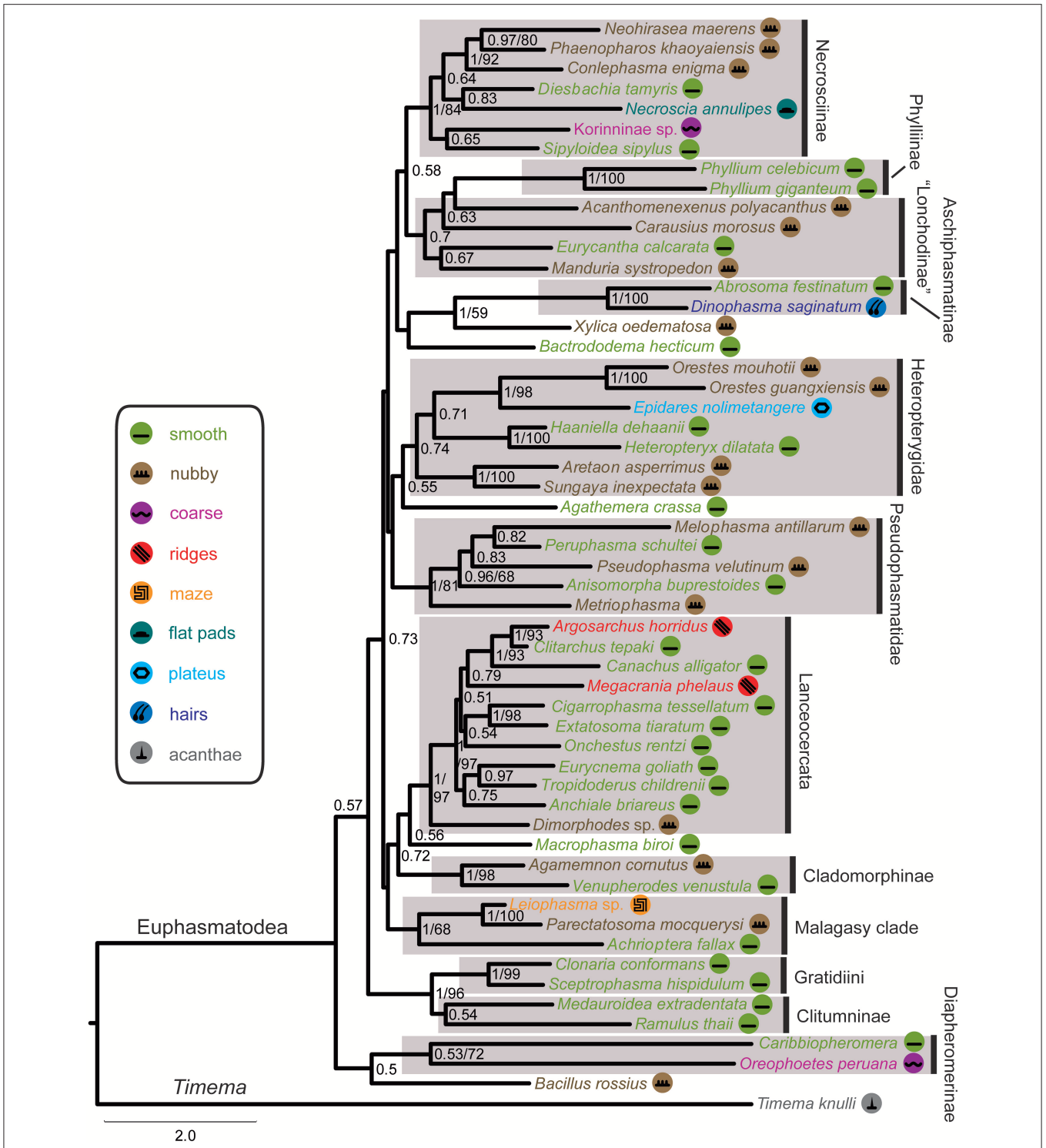

FIGURE 4 | Majority-rule consensus tree of investigated Phasmatodea resulting from Bayesian analysis of the combined molecular data. Posterior probabilities followed by bootstrap percentages are given at nodes. Symbols mapped on taxa and color code of tarsal structures/euplantulae type according to figure legend on the left.

radiation among the major phasmatodean lineages impedes a reliable ancestral character state reconstruction of euplantular adhesive structures for stick and leaf insects at the moment. Furthermore, the condition for this character complex in *Timema* (acanthae) is unlike in any of the investigated members of its sister group Euphasmatodea, which consequently does not allow

for an outgroup comparison. We are confident that one of the most frequent forms, smooth and nubby, which are also present in closely related groups like Orthoptera, Blattodea, and Embioptera (Gorb et al., 2000; Perez Goodwyn et al., 2006; Clemente and Federle, 2008; Büscher et al., 2018), represents the ground pattern of AM in Euphasmatodea, and indeed the ancestral state reconstructions favor smooth (**Figure 5**). We also conclude that the rare AM types are derived for the respective taxa, e.g., coarse for *Kalokorinnis* and *Oreophoetes*, plateaus for *Epidares*, maze for *Leiophasma*, and hairs (adhesive setae) for *Dinophasma*, and this is supported by the ancestral state reconstructions. Moreover, the euplantular structure ridges evolved twice within Lanceocercata, in *Argosarchus* and *Megacrania*. Our reconstructions support independent origins of the nubby types (**Figure 5**). In general, unambiguously monophyletic groups exhibit a diversity of structures, e.g., in Aschiphasmatinae the smooth (*Abrosoma*), hairy (*Dinophasma*), and plateaus (*Dajaca*) forms are found. While some closely related taxa possess the same euplantular types, such as nubby AMs in *Neohirasea*, *Phaenopharos*, and *Conlephasma* in Necrosciinae, or smooth AMs in *Anchiale*, *Eurycnema*, and *Tropidoderus* in Lanceocercata, the occurrence of specific AMs do not generally reflect phylogenetic relationships. Besides Clitumninae and Phylliinae, none of the well-supported major clades bears a uniform AM type. The type of AM appears to be associated with ecomorphs, e.g., smooth euplantular surfaces are more frequently found in slender tree-dwellers than in stout ground-dwellers, whilst the attachment pads of ground-dwelling species more often bear conical cuticular outgrowths with different aspect ratios. However, this does not entirely explain the distribution of AMs across phasmid taxa. For instance, Heteropterygidae are uniformly ground-dwelling phasmids, including egg-deposition into the soil, yet they exhibit varying types of adhesive structures: In Obriminae (*Aretaon*, *Sungaya*), the euplantular surface is nubby, whereas smooth euplantulae are found in Heteropteryginae (*Heteropteryx*, *Haaniella*). Yet, characterization of distinct ecomorphs still needs to be addressed based on substantiated criteria such as morphometrics and niche specialization. One further potential explanation of the presence of certain AMs is body size. Bigger species might exhibit smooth euplantulae more frequently, e.g., the large *Bactrododema*, *Eurycnema*, *Achrioptera*, and *Eurycantha*. Assumption of this potential trend gains further support by the fact that the smaller juvenile *Eurycantha* individuals still have nubby euplantulae while those of adults are smooth (Gottardo et al., 2015). Heteropteryginae bearing smooth euplantulae are generally bigger than Obriminae with nubby euplantulae. Then again, the ground-dwelling *Orestes* and *Epidares* are of the same small size and still possess different AMs.

Functional Relevance of Attachment Microstructures

The functional properties of the different AMs in Phasmatodea are only partially known so far. Experimental data are available for Phasmatodea only for the nubby and the smooth type (Busshardt et al., 2012; Labonte and Federle, 2013; Labonte et al., 2014), hence, the other remain hypothetical or are inferred from other taxa. The nubby AM is shown to be load sensitive and less susceptible to different surface roughnesses (Busshardt et al., 2012; Labonte and Federle, 2013; Labonte et al., 2014). Nubby attachment microstructures, if they are not the ground type of AMs, possibly evolved convergently in the different lineages as a response to a broad range of surfaces in the preferred habitats. In contrast, smooth AMs perform better on smooth surfaces (Busshardt et al., 2012). Many species possessing this AM live in trees and often are food plant specialists. These species possibly face rather smooth surfaces, whilst species with nubby structures possibly find a broader range of surface roughnesses on the ground. Other types of AMs might have evolved due to insect-plant interactions (e.g., Friedemann et al., 2015) or specific environmental conditions, e.g., specialized structured surfaces or wet surfaces (Grohmann et al., 2015). On wet surfaces, splitting the contact surface like in the flat pads, plateaus, and maze AMs possibly reduces hydroplaning and stick-slip motions. This effect has been shown for mushroom shaped and hexagonal bioinspired artificial surfaces (Varenberg and Gorb, 2007, 2009). Irregularly shaped microstructures, such as ridges, might have evolved due to food plant specialization. The anisotropy of the AM causes dissimilar adhesive forces with and against the structures (Filippov and Gorb, 2013) and might be used for generating propulsion on structured surfaces (Clemente et al., 2009). *Megacrania phelaus* feeds exclusively on plants with a parallel leaf venation (Hsiung, 2007). This food plant association possibly initiated the development of the structured AM in this species. The hairy system of attachment pads, herein only represented by *D. saginatum*, is reported to possess similar adhesion and friction forces to the smooth system (Bullock et al., 2008). The comparison of the adhesive pads of *C. morosus* and the dock beetle *Gastrophysa viridula* (Coleoptera: Chrysomelidae) suggested that fibrillary adhesive systems may be more efficient in terms of self-cleaning than smooth ones (Clemente et al., 2010).

CONCLUSION

Stick and leaf insects have more diverse euplantular microstructures than previously reported (Beutel and Gorb, 2008). Nine different types can be distinguished whereby the nubby type can be further divided into three different distinct types based on the specific ratio of each conical outgrowth. Hereby the different types of AMs do not follow a phylogenetic pattern, but rather depend on the ecological niche a species inhabits or its body size. Large canopy-dwellers more frequently appear to exhibit smooth euplantulae while smaller ground-dwellers apparently show nubby AMs. The morphological diversity found in each clade of phasmids suggests the convergent evolution or reversal of certain euplantular types. A high number of species is already illustrated and described in a comprehensive comparative analysis of the tarsal morphology in Phasmatodea (Büscher et al., 2018). To reliably reconstruct the evolution of these adhesive types, a denser taxon sampling and a better resolved phylogeny of these taxa are necessary.

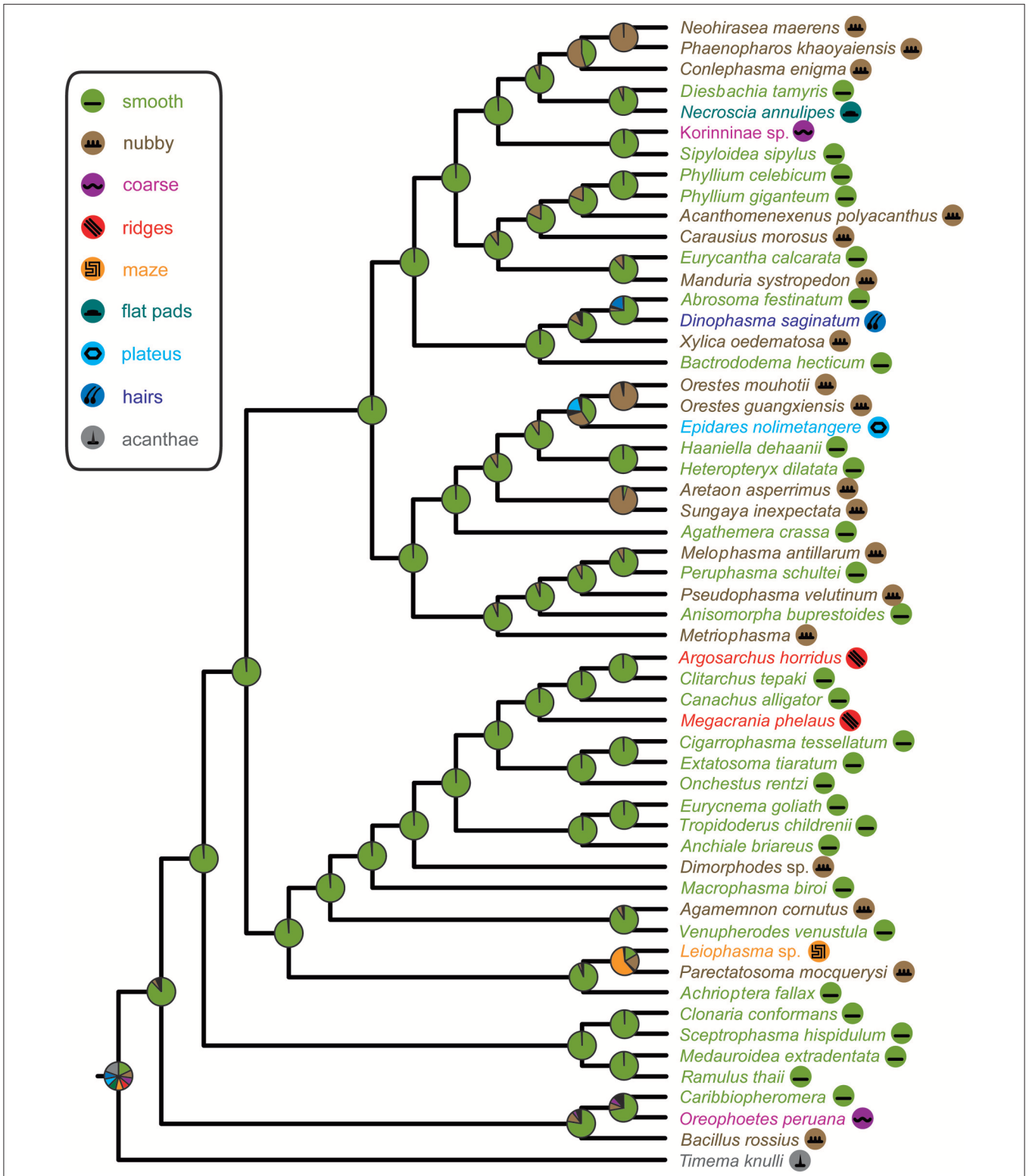

FIGURE 5 | Phasmatodea phylogeny and ancestral character state reconstruction of euplantular microstructures with pie charts representing relative ML support at ancestral nodes according to color code in figure legend.

DATA AVAILABILITY STATEMENT

All datasets analyzed for this study are included in the manuscript and the **Supplementary Material**. The DNA sequences used for the phylogenetic reconstruction can be found at GenBank [https://www.ncbi.nlm.nih.gov/genbank/] under the accession numbers listed in **Supplementary Table 1**. The alignment used for the phylogenetic reconstruction is provided as a Nexus input file as **Supplementary Data Sheet 1**.

AUTHOR CONTRIBUTIONS

THB, CG, SG, and SB designed research. THB generated SEM data and photographs. TRB obtained and analyzed molecular data. THB and SB wrote manuscript. TRB, CG, and SG contributed to manuscript editing. All authors have approved the final version of the manuscript.

FUNDING

This study was supported by the German Science Foundation (DFG grants BR 2930/3-1, BR 2930/4-1 and BR 2930/5-1 to SB).

ACKNOWLEDGMENTS

We thank Esther Appel and Alexander Kovalev (Department of Biomechanics and Functional Morphology, Kiel University, Germany) for support in microscopy and preservation. Bruno Kneubühler (Lucerne, Switzerland), Daniel Dittmar (Berlin, Germany), Royce Cumming (San Diego Natural History Museum, San Diego, USA), Paul Bertner (Winfield, Canada), Luis Mata (RMIT University, Melbourne, Australia), and Holger Dräger (Schwerin, Germany) are acknowledged for providing specimens and photographs. We acknowledge financial support by Land Schleswig-Holstein within the funding programme Open Access Publikationsfonds.

SUPPLEMENTARY MATERIAL

The Supplementary Material for this article can be found online at: https://www.frontiersin.org/articles/10.3389/fevo.2018.00069/full#supplementary-material

Supplementary Table 1 | Taxon sampling.

Supplementary Data Sheet | Nexus input file.

REFERENCES

Bauchhenss, E. (1979). Die Pulvillen von *Calliphora erythrocephala* Meig. (Diptera, Brachycera) als Adhäsionsorgane. *Zoomorphologie* 93, 99–123. doi: 10.1007/BF00994125

Bedford, G. O. (1978). Biology and ecology of the Phasmatodea. *Ann. Rev. Entomol.* 23, 125–149. doi: 10.1146/annurev.en.23.010178.001013

Bennemann, M., Backhaus, S., Scholz, I., Park, D., Mayer, J., and Baumgartner, W. (2014). Determination of the Young's modulus of the epicuticle of the smooth adhesive organs of *Carausius morosus* using tensile testing. *J. Exp. Biol.* 217, 3677–3687. doi: 10.1242/jeb.105114

Beutel, R. G., and Gorb, S. N. (2001). Ultrastructure of attachment specializations of hexapods (Arthropoda). Evolutionary patterns inferred from a revised ordinal phylogeny. *J. Zool. Syst. Evol. Res.* 39, 177–207. doi: 10.1046/j.1439-0469.2001.00155.x

Beutel, R. G., and Gorb, S. N. (2006). A revised interpretation of the evolution of attachment structures in Hexapoda with special emphasis on Mantophasmatodea. *Arthropod Syst. Phylogeny* 64, 3–25.

Beutel, R. G., and Gorb, S. N. (2008). Evolutionary scenarios for unusual attachment devices of Phasmatodea and Mantophasmatodea (Insecta). *Sys. Ent.* 33, 501–510. doi: 10.1111/j.1365-3113.2008.00428.x

Bradler, S. (2009). *Die Phylogenie der Stab- und Gespenstschrecken (Insecta: Phasmatodea)*. Göttingen: Universitätsverlag. 139.

Bradler, S., Cliquennois, N., and Buckley, T. R. (2015). Single origin of Mascarene stick insects: ancient radiation on sunken islands? *BMC Evol. Biol.* 15, 196. doi: 10.1186/s12862-015-0478-y

Bradler, S., Robertson, J. A., and Whiting, M. F. (2014). A molecular phylogeny of Phasmatodea with emphasis on Necrosciinae, the most species-rich subfamily of stick insects. *Sys. Ent.* 39, 205–222. doi: 10.1111/syen.12055

Brock, P. D., Büscher, T. H., and Baker, E. (2017). "Phasmida species file online: phasmida species file version 5.0/5.0," in *Species 2000 and ITIS Catalogue of Life*, eds eds Y. Roskov et al. (Leiden: Species 2000: Naturalis). Available online at: www.catalogueoflife.org/col

Buckley, T. R., Attanayake, D., and Bradler, S. (2009). Extreme convergence in stick insect evolution: phylogenetic placement of the Lord Howe Island tree lobster. *Proc. R. Soc. Lond. B* 276, 1055–1062. doi: 10.1098/rspb.2008.1552

Buckley, T. R., Attanayake, D.,Nylander, J. A. A., and Bradler, S. (2010). The phylogenetic placement and biogeographical origins of the New Zealand stick insects (Phasmatodea). *Sys. Ent.* 35, 207–225. doi: 10.1111/j.1365-3113.2009.00505.x

Bullock, J. M., and Federle, W. (2011). Beetle adhesive hairs differ in stiffness and stickiness: *in vivo* adhesion measurements on individual setae. *Naturwissenschaften* 98, 381–387. doi: 10.1007/s00114-011-0781-4

Bullock, J. M. R., Drechsler, P., and Federle, W. (2008). Comparison of smooth and hairy attachment pads in insects: friction, adhesion and mechanisms for direction-dependence. *J. Exp. Biol.* 211, 3333–3343. doi: 10.1242/jeb.020941

Büscher, T. H., and Gorb, S. N. (2017). Subdivision of the neotropical Prisopodinae Brunner von Wattenwyl 1893 based on features of tarsal attachment pads (Insecta: Phasmatodea). *Zookeys* 645, 1–11. doi: 10.3897/zookeys.645.10783

Büscher, T. H., Grohmann, C., Bradler, S., and Gorb, S. N. (2018). *Tarsal Attachment Pads in Phasmatodea (Hexapoda: Insecta). Zoologica*. Stuttgart: Schweizerbart Science Publishers.

Busshardt, P., Gorb, S. N., and Wolf, H. (2011). Activity of the claw retractor muscle in stick insects in wall and ceiling situations. *J. Exp. Biol.* 214, 1676–1684. doi: 10.1242/jeb.051953

Busshardt, P., Wolf, H., and Gorb, S. N. (2012). Adhesive and frictional properties of tarsal attachment pads in two species of stick insects (Phasmatodea) with smooth and nubby euplantulae. *Zoology* 115, 135–141. doi: 10.1016/j.zool.2011.11.002

Clemente, C. J., and Federle,W. (2008). Pushing versus pulling: division of labour between tarsal attachment pads in cockroaches. *Proc. R. Soc. Lond. B* 275, 1329–1336. doi: 10.1098/rspb.2007.1660

Clemente, C. J., Bullock, J. M., Beale, A., and Federle, W. (2010). Evidence for self-cleaning in fluid-based smooth and hairy adhesive systems of insects. *J. Exp. Biol.* 213, 635–642. doi: 10.1242/jeb.038232

Clemente, C. J., Dirks, J.-H., Barbero, D. R., Steiner, U., and Federle, W. (2009). Friction ridges in cockroach climbing pads: anisotropy of shear stress measured on transparent, microstructured substrates. *J. Comp. Physiol. A* 195, 805–814. doi: 10.1007/s00359-009-0457-0

Darriba, D., Taboada, G. L., Doallo, R., and Posada, D. (2012). JModelTest 2: more models, new heuristics and parallel computing. *Nat. Methods* 9, 772. doi: 10.1038/nmeth.2109

Dennis, A. B., Dunning, L. T., Sinclair, B. J., and Buckley, T. R. (2015). Parallel molecular routes to cold adaptation in eight genera of New Zealand stick insects. *Sci. Rep*. 5, 13965. doi: 10.1038/srep13965

Edgar, R. C. (2004). MUSCLE: multiple sequence alignment with high accuracy and high throughput. *Nucleic Acids Res*. 32, 1792–1797. doi: 10.1093/nar/gkh340

Federle, W., Brainerd, E. L., McMahon, T. A., and Hölldobler, B. (2001). Biomechanics of the movable pretarsal adhesive organ in ants and bees. *Proc. Natl. Acad. Sci. U.S.A*. 98, 6215–6220. doi: 10.1073/pnas.111139298

Federle, W., Riehle, M., Curtis, A. S., and Full, R. J. (2002). An integrative study of insect adhesion: mechanics and wet adhesion of pretarsal pads in ants. *Integr. Comp. Biol*. 42, 1100–1106. doi: 10.1093/icb/42.6.1100

Filippov, A., and Gorb, S. N. (2013). Frictional-anisotropy-based systems in biology: structural diversity and numerical model. *Sci. Rep*. 3, 1240. doi: 10.1038/srep01240

Frantsevich, L., and Gorb, S. (2004). Structure and mechanics of the tarsal chain in the hornet, *Vespa crabro* (Hymenoptera: Vespidae): implications on the attachment mechanism. *Arthropod. Struct. Dev*. 33, 77–89. doi: 10.1016/j.asd.2003.10.003

Friedemann, K., Kunert, G., Gorb, E. V., Gorb, S. N., and Beutel, R. G. (2015). Attachment forces of pea aphids (*Acyrthosiphon pisum*) on different legume species. *Ecol. Entomol*. 40, 732–740. doi: 10.1111/een.12249

Friedemann, K., Schneeberg, K., and Beutel, R. G. (2014). Fly on the wall – attachment structures in lower Diptera. *Syst. Ent.* 39, 460–473. doi: 10.1111/syen.12064

Friedemann, K., Wipfler, B., Bradler, S., and Beutel, R. G. (2012). On the head morphology of Phyllium and the phylogenetic relationships of Phasmatodea (Insecta). *Acta Zool.* 93, 184–199. doi: 10.1111/j.1463-6395.2010.00497.x

Gladun, D., and Gumovsky, A. (2006). The pretarsus in Chalcidoidea (Hymenoptera Parasitica). Functional morphology and possible phylogenetic implications. *Zool. Scripta* 35, 607–626. doi: 10.1111/j.1463-6409.2006.00245.x

Goldberg, J., Bresseel, J., Constant, J., Kneubühler, B., Leubner, F., Michalik, P., et al. (2015). Extreme convergence in egg-laying strategy across insect orders. *Sci. Rep*. 5, 7825. doi: 10.1038/srep07825

Gorb, S. N. (2001). *Attachment Devices of Insect Cuticle*. Dordrecht; Boston, MA; London: Kluwer Academic Publishers.

Gorb, E. V., and Gorb, S. N. (2002). Attachment ability of the beetle *Chrysolina fastuosa* on various plant surfaces. *Entomol. Exp. Appl*. 105, 13–28. doi: 10.1046/j.1570-7458.2002.01028.x

Gorb, S. N. (1998). The design of the fly adhesive pad. Distal tenent setae are adapted to the delivery of an adhesive secretion. *Proc. R. Soc. Lond. B* 265, 747–752. doi: 10.1098/rspb.1998.0356

Gorb, S. N. (2005). Uncovering insect stickiness: structure and properties of hairy attachment devices. *Am. Entomol.* 51, 31–35. doi: 10.1093/ae/51.1.31

Gorb, S., Jiao, Y., and Scherge, M. (2000). Ultrastructural architecture and mechanical properties of attachment pads in *Tettigonia viridissima* (Orthoptera Tettigoniidae). *J. Comp. Physiol. A* 186, 821–831. doi: 10.1007/s003590000135

Gorb, S. N., Niederegger, S., Hayashi, C. Y., Summers, A. P., Vötsch, W., and Walther, P. (2006). Biomaterials: silk-like secretion from tarantula feet. *Nature* 443, 407. doi: 10.1038/443407a

Gottardo, M. (2011). A new genus and new species of Philippine stick insects (Insecta: Phasmatodea) and phylogenetic considerations. *C. R. Biol*. 334, 555–563. doi: 10.1016/j.crvi.2011.04.003

Gottardo, M., and Heller, P. (2012). An enigmatic new stick insect from the Philippine Islands (Insecta: Phasmatodea). *C. R. Biol*. 335, 594–601. doi: 10.1016/j.crvi.2012.07.004

Gottardo, M., and Vallotto, D. (2014). External macro- and micromorphology of the male of the stick insect *Hermarchus leytensis* (Insecta: Phasmatodea) with phylogenetic considerations. *C. R. Biol*. 337, 258–268. doi: 10.1016/j.crvi.2014.02.005

Gottardo, M., Vallotto, D., and Beutel, R. G. (2015). Giant stick insects reveal unique ontogenetic changes in biological attachment devices. *Arthropod. Struct. Dev*. 44, 195–199. doi: 10.1016/j.asd.2015.01.001

Grohmann, C., Henze, M. J., Nørgaard, T., and Gorb, S. N. (2015). Two functional types of attachment pads on a single foot in the Namibia bush cricket *Acanthoproctus diadematus* (Orthoptera: Tettigoniidae). *Proc. R. Soc. Lond. B* 282, 20142976. doi: 10.1098/rspb.2014.2976

Günther, K. (1953). Über die taxonomische Gliederung und die geographische Verbreitung der Insektenordnung der Phasmatodea. *Beitr. Entomol.* 3, 541–563.

Haas, F., and Gorb, S. (2004). Evolution of locomotory attachment pads in the Dermaptera (Insecta). *Arthropod. Struct. Dev*. 33, 45–66. doi: 10.1016/j.asd.2003.11.003

Hsiung, C. C. (2007). Revision of the genus *Megacrania* Kaup (Cheleutoptera: Phasmatidae). *J. Orthoptera Res*. 16, 207–221. doi: 10.1665/1082-6467(2007)16[207:ROTGMK]2.0.CO;2

Ishiwata, K., Sasaki, G., Ogawa, J., Miyata, D., and Su, Z.-H. (2011). Phylogenetic relationships among insect orders based on three nuclear protein-coding gene sequences. *Mol. Phylogenet. Evol.* 58, 169–180. doi: 10.1016/j.ympev.2010.11.001

Kearse, M., Moir, R., Wilson, A., Stones-Havas, S., Cheung, M., Sturrock, S., et al. (2012). Geneious basic: an integrated and extendable desktop software platform for the organization and analysis of sequence data. *Bioinformatics* 28, 1647–1649. doi: 10.1093/bioinformatics/bts199

Labonte, D., and Federle, W. (2013). Functionally different pads on the same foot allow control of attachment: stick insects have load-sensitive "heel" pads for friction and shear-sensitive "toe" pads for adhesion. *PLoS ONE* 8, e81943. doi: 10.1371/journal.pone.0081943

Labonte, D., Williams, J. A., and Federle, W. (2014). Surface contact and design of fibrillar 'friction pads' in stick insects (*Carausius morosus*): mechanisms for large friction coefficients and negligible adhesion. *J. R. Soc. Interface* 11, 20140034. doi: 10.1098/rsif.2014.0034

Letsch, H. O., and Simon, S. (2013). Insect phylogenomics: new insights on the relationships of lower neopteran orders (Polyneoptera). *Sys. Ent*. 38, 783–793. doi: 10.1111/syen.12028

Letsch, H. O., Meusemann, K., Wipfler, B., Schütte, K., Beutel, R., and Misof, B. (2012). Insect phylogenomics: results, problems and the impact of matrix composition. *Proc. Roy. Soc. Lond. B* 279, 3282–3290. doi: 10.1098/rspb.2012.0744

Lewis, P. O. (2001). A likelihood approach to estimating phylogeny from discrete morphological character data. *Syst. Biol*. 50, 913–925. doi: 10.1080/106351501753462876

Maddison, W. P., and Maddison, D. R. (2018). *Mesquite: a Modular System for Evolutionary Analysis. Version 3.40*. (Accessed April 12, 2018).

Misof, B., Liu, S., Meusemann, K., Peters, R. S., Donath, A., Mayer, C., et al. (2014). Phylogenomics resolves the timing and pattern of insect evolution. *Science* 346, 763–767. doi: 10.1126/science.1257570

Niederegger, S., Gorb, S., and Jiao, Y. (2002). Contact behaviour of tenent setae in attachment pads of the blowfly *Calliphora vicina* (Diptera, Calliphoridae). *J. Comp. Physiol. A* 187, 961–970. doi: 10.1007/s00359-001-0265-7

Perez Goodwyn, P., Peressadko, A., Schwarz, H., Kastner, V., and Gorb, S. (2006). Material structure, stiffness, and adhesion: why attachment pads of the grasshopper (*Tettigonia viridissima*) adhere more strongly than those of the locust (*Locusta migratoria*) (Insecta: Orthoptera). *J. Comp. Physiol. A* 192, 1233–1243. doi: 10.1007/s00359-006-0156-z

Ronquist, F., Teslenko, M., van der Mark, P., Ayres, D. L., Darling, A., Höhna, S., et al. (2012). MrBayes 3.2: efficient Bayesian phylogenetic inference and model choice across a large model space. *Syst. Biol*. 61, 539–542. doi: 10.1093/sysbio/sys029

Schmitt, M., Büscher, T. H., Gorb, S. N., and Rajabi, H. (2018). How does a slender tibia resist buckling? The effect of material, structural and geometric characteristics on the buckling behaviour of the hindleg tibia in the postembryonic development of the stick insect Carausius morosus. *J. Exp. Biol.* 221:jep.173047. doi: 10.1242/jeb.173047

Stork, N. E. (1980). Experimental analysis of adhesion of *Chrysolina polita* (Chrysomelidae: Coleoptera) on a variety of surfaces. *J. Exp. Biol*. 88, 91–108.

Vallotto, D., Bresseel, J., Heitzmann, T., and Gottardo, M. (2016). A black-and-red stick insect from the Philippines - observations on the external anatomy and natural history of a new species of *Orthomeria*. *Zookeys* 559, 35–57. doi: 10.3897/zookeys.559.6281

Varenberg, M., and Gorb, S. (2007). Shearing of fibrillar adhesive microstructure: friction and shear-related changes in pull-off force. *J. R. Soc. Interface* 4, 721–725. doi: 10.1098/rsif.2007.0222

Varenberg, M., and Gorb, S. N. (2009). Hexagonal surface micropattern for dry and wet friction. *Adv. Mater.* 21, 483–486. doi: 10.1002/adma.200802734

Zill, S. N., Chaudhry, S., Exter, A., Büschges, A., and Schmitz, J. (2014). Positive force feedback in development of substrate grip in the stick insect tarsus. *Arthropod Struct. Dev.* 43, 441–455. doi: 10.1016/j.asd.2014.06.002

Zwickl, D. J. (2006). *Genetic Algorithm Approaches for the Phylogenetic Analysis of Large Biological Sequence Datasets under the Maximum Likelihood Criterion*. Ph.D. dissertation, The University of Texas, Austin, 115.

Conflict of Interest Statement: The authors declare that the research was conducted in the absence of any commercial or financial relationships that could be construed as a potential conflict of interest.

frontiers in Ecology and Evolution

ORIGINAL RESEARCH
published: 19 December 2018
doi: 10.3389/fevo.2018.00216

Evolution of Oviposition Techniques in Stick and Leaf Insects (Phasmatodea)

James A. Robertson[1,2]*, *Sven Bradler*[3] *and Michael F. Whiting*[2]

[1] National Identification Services, APHIS PPQ, United States Department of Agriculture, Beltsville, MD, United States, [2] Department of Biology and M. L. Bean Museum, Brigham Young University, Provo, UT, United States, [3] Department of Morphology, Systematics and Evolutionary Biology, Johann-Friedrich-Blumenbach Institute of Zoology and Anthropology, University of Göttingen, Göettingen, Germany

Stick and leaf insects (Phasmatodea) are large, tropical, predominantly nocturnal herbivores, which exhibit extreme masquerade crypsis, whereby they morphologically and behaviorally resemble twigs, bark, lichen, moss, and leaves. Females employ a wide range of egg-laying techniques, largely corresponding to their ecological niche, including dropping or flicking eggs to the forest floor, gluing eggs to plant substrate, skewering eggs through leaves, ovipositing directly into the soil, or even producing a complex ootheca. Phasmids are the only insects with highly species-specific egg morphology across the entire order, with specific egg forms that correspond to oviposition technique. We investigate the temporal, biogeographic, and phylogenetic pattern of evolution of egg-laying strategies in Phasmatodea. Our results unequivocally demonstrate that the ancestral oviposition strategy for female stick and leaf insects is to remain in the foliage and drop or flick eggs to the ground, a strategy that maintains their masquerade. Other major key innovations in the evolution of Phasmatodea include the (1) hardening of the egg capsule in Euphasmatodea; (2) the repeated evolution of capitulate eggs (which induce ant-mediated dispersal, or myrmecochory); (3) adapting to a ground or bark dwelling microhabitat with a corresponding shift in adult and egg phenotype and egg deposition directly into the soil; and (4) adhesion of eggs in a clade of Necrosciinae that led to subsequent diversification in oviposition modes and egg types. We infer at minimum 16 independent origins of a burying/inserting eggs into soil/crevices oviposition strategy, 7 origins of gluing eggs to substrate, and a single origin each of skewering eggs through leaves and producing an ootheca. We additionally discuss the systematic implications of our phylogenetic results. Aschiphasmatinae is strongly supported as the earliest diverging extant lineage of Euphasmatodea. Phylliinae and Diapheromerinae are both relatively early diverging euphasmatodean taxa. We formally transfer *Otocrania* from Cladomorphinae to Diapheromerinae and recognize only two tribes within Diapheromerinae: Diapheromerini **sensu nov.** and Oreophoetini **sensu nov.** We formally recognize the clade comprising Necrosciinae and Lonchodinae as Lonchodidae **stat. rev. sensu nov.**

Keywords: phylogeny, adaptive radiation, key innovation, Phasmida, classification, systematics, taxonomy

OPEN ACCESS

Edited by:
Anthony I. Cognato, Michigan State University, United States

Reviewed by:
Aaron D. Smith, Arizona State University, United States
Brian I. Crother, Southeastern Louisiana University, United States

***Correspondence:**
James A. Robertson
erotylid@gmail.com

Specialty section:
This article was submitted to Phylogenetics, Phylogenomics, and Systematics, a section of the journal Frontiers in Ecology and Evolution

Received: *06 September 2018*
Accepted: *29 November 2018*
Published: *19 December 2018*

Citation:
Robertson JA, Bradler S and Whiting MF (2018) Evolution of Oviposition Techniques in Stick and Leaf Insects (Phasmatodea). Front. Ecol. Evol. 6:216. doi: 10.3389/fevo.2018.00216

INTRODUCTION

Natural History

Stick and leaf insects (Phasmatodea) are among the most charismatic animals on earth. They are large, tropical, predominantly nocturnal herbivores, which exhibit extreme masquerade crypsis, whereby they phenotypically and behaviorally resemble twigs, bark, lichen, moss, and leaves (Bedford, 1978). Examples include the exquisite leaf-mimicking *Phyllium*, (**Figure 1A**), the robust, bark-like "tree lobsters" (e.g., *Dryococelus australis,* The Lord Howe tree lobster—likely the rarest documented insect on the planet, **Figure 1C**) (Priddel et al., 2003), and a large number of twig, stick, and branch mimics, including the recently described giant, *Phobaeticus chani*, the world's largest extant insect at just over two feet (56.7 cm) including legs (Hennemann and Conle, 2008). Despite being masters of masquerade among insects, phasmids are often chemically defended through a wide array of noxious chemicals secreted from specialized prothoracic glands when under threat (Eisner et al., 1997), and a few species have developed aposematic coloration (e.g., *Achrioptera fallax, Oreophoetes peruana, Orthonecroscia pulcherrima*). They are known for their ability to regenerate lost limbs (e.g., resulting from predation or complications during previous molts) during juvenile molts (Brusca et al., 2016). Many phasmids are facultatively parthenogenic, a feature likely tied to the poor dispersal ability of adults, particularly females, which are slow moving, often flightless, and when gravid, even winged species exhibit limited motility (Bradler and Buckley, 2018).

Female stick and leaf insects employ a wide range of egg-laying techniques, largely corresponding to their ecological niche (Carlberg, 1983; Sellick, 1997a,b) (**Figure 2**). Many species remain in the foliage during oviposition and passively drop or actively flick single eggs from their ovipositor to the ground. Others carefully fix their eggs to plant substrate with glue (**Figure 2D**) or even by skewering them through leaves (**Figure 2E**). Some species, including the robust tree lobsters, carefully place their eggs directly into crevices (e.g., bark) or the soil (**Figure 2C**). An anomaly for the order, a recently discovered species produces a complex egg case or ootheca that contains numerous eggs in a highly ordered fashion (**Figure 2F**) (Goldberg et al., 2015).

Whereas, the diversity of oviposition strategies within Phasmatodea is ecologically fascinating and likely evolutionarily significant, the diversity of form exhibited in the eggs themselves is simply extraordinary (**Figure 3**). Phasmids are the only insects with blatant species-specific egg morphology across the entire order, with specialized egg forms adapted to oviposition technique. For example, eggs that are directly buried into the soil (**Figure 3E'**) are typically tapered at the posterior pole in a bullet-like fashion, modified for ease of burial (e.g., *Orxines*, *Acacus*, *Centrophasma*, and *Diesbachia)* or are slightly tapered and cylindrical in shape (e.g., *Heteropteryx*) (Sellick, 1997a). Eggs skewered to leaves are modified with a collard spine-like extension at the posterior pole that is used to pierce the leaf and hold up the egg (**Figure 3S**). A major guild of eggs exclusive to groups of species that drop or flick their eggs to the ground bear a capitulum—a lipid-rich, detachable, knob-like extension of the operculum (lid of the egg) that serves as the signal adaptation for inducing ant-mediated dispersal (**Figures 3A–N**) (Moore, 1993; Stanton et al., 2015). Capitulate eggs represent a key innovation for phasmid dispersal and occur in disparate lineages and biogeographic regions worldwide (Compton and Ware, 1991; Hughes and Westoby, 1992; Windsor et al., 1996). Eggs that are attached to plant substrate (usually leaves) with glue are more variable in form. Generally, adhesion is on the ventral surface of the egg with the eggs attached singly (e.g., *Sceptrophasma*, *Sipyloidea*). But in a few genera (e.g., *Calvisia*, *Trachythorax*) eggs are attached in groups, with eggs additionally glued to the anterior or posterior surface of adjacent eggs (Sellick, 1997a).

Given the taxonomic occurrence of phasmid oviposition strategies, multiple origins of various techniques are likely throughout the order. Goldberg et al. (2015) provided an initial investigation of phasmid oviposition modes primarily to place the anomalous ootheca-producing species in an ecological and phylogenetic context. Their analysis strongly supported the recovery of this species among the ecologically- and species-rich Necrosciinae. However, their taxon sampling was not crafted to explore the evolution of egg-laying techniques across phasmid diversity. The evolutionary significance and the temporal, biogeographic, and phylogenetic pattern of evolution of egg-laying strategies in Phasmatodea remain unclear.

Systematics

Phasmatodea stands out as one of the few insect orders to lack a phylogenetically based classification (Bradler and Buckley, 2018). Günther (1953) classified Phasmatodea into a number of subfamilies and tribes, and this classification gained broad acceptance (Bradley and Galil, 1977; Kevan, 1977, 1982). However, subsequent phylogenetic analyses based on morphological (Tilgner, 2002; Bradler, 2009) and molecular data (Whiting et al., 2003; Buckley et al., 2009; Bradler et al., 2014, 2015; Büscher et al., 2018) clearly demonstrate that we lack a meaningful higher-level classification for phasmids. Due to the widespread phenotypic convergence associated with extreme masquerade crypsis and corresponding microhabitat (Buckley et al., 2009; Bradler et al., 2015), it is not surprising that morphology-based classification schemes have failed to reflect the evolutionary history of the group.

Molecular-based phylogenetic studies have largely been limited and focused on biogeographically-restricted taxa such as New Zealand stick insects (e.g., Trewick et al., 2008; Buckley et al., 2010), Mascarene phasmids (Bradler et al., 2015), Mediterranean taxa (e.g., Ghiselli et al., 2007; Scali et al., 2012, 2013), the genus *Timema* in Southern North America (Law and Crespi, 2002; Schwander et al., 2011), and the primarily Indo-Malayan subfamily Necrosciinae (Bradler et al., 2014; Goldberg et al., 2015). In the present study we use the most broadly sampled molecular data set to date to investigate the temporal, biogeographic, and phylogenetic pattern of evolution of egg-laying strategies in Phasmatodea and infer their evolutionary significance. We further discuss systematic implications and

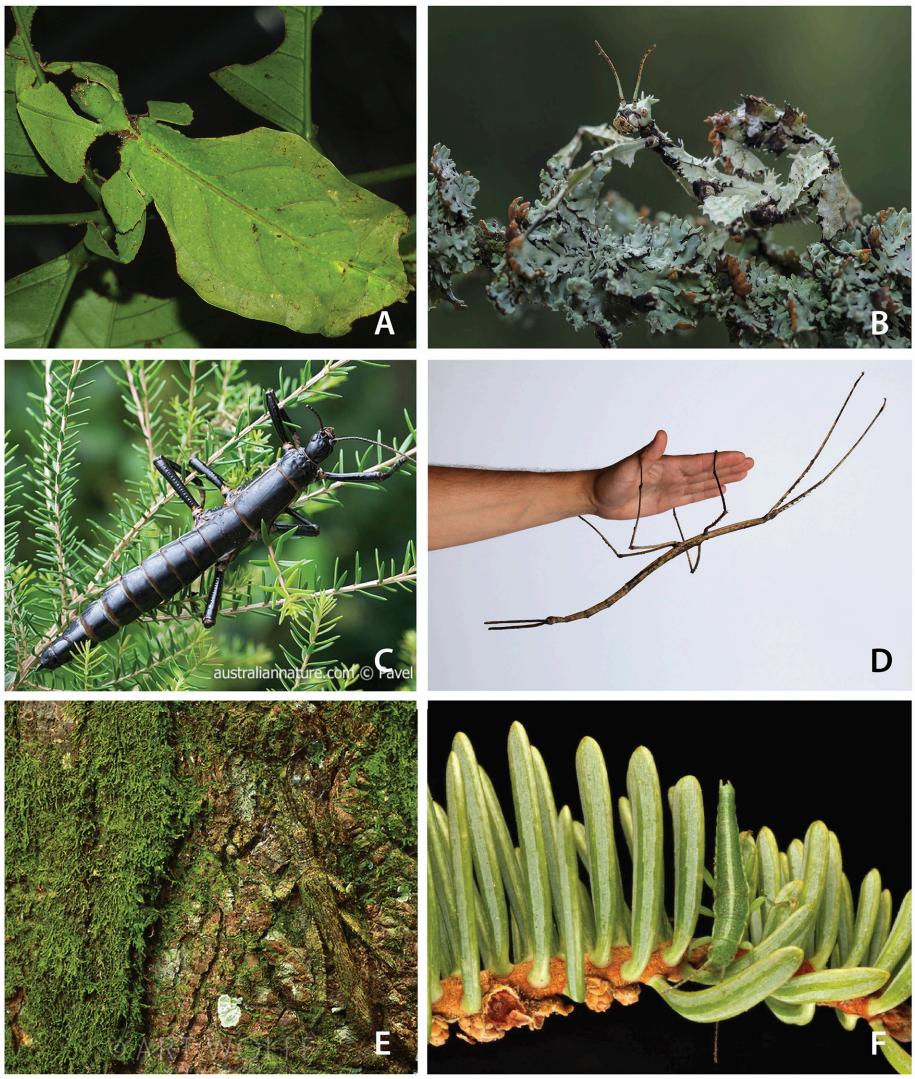

FIGURE 1 | A glimpse of stick and leaf insect diversity and masquerade crypsis. **(A)** A leaf insect, *Phyllium* (photograph by Bernard Dupont, used by permission). **(B)** *Extatasoma tiaratum* (photograph by Miroslaw Wasinski, used by permission). **(C)** The Lord Howe stick insect, *Dryococelus australis*, the rarest known insect on the planet (photograph by Pavel German, used by permission). **(D)** *Ctenomorpha gargantuan*, measuring 56.5 cm in length (photograph by the Museum of Victoria, used by permission). **(E)** *Prisopus* sp. (photograph by Art Wolfe, used by permission). **(F)** *Timema cristinae* (photograph by Moritz Muschick, used by permission).

make formal emendations to phasmid classification in light of the current molecular phylogenetic consensus.

METHODS

Taxon and Gene Sampling

A global sampling comprising 284 phasmid exemplars representing all major lineages and ca. 32% (150 of 473) of the generic diversity and a single representative of Embioptera (*Metoligotoma*) as an outgroup (see Misof et al., 2014) was used in the present study (**Supplementary Table S1**). We sampled regions of 7 genes to infer the evolutionary history of Phasmatodea: nuclear 18S rRNA (18S), 28S rRNA (28S) and histone subunit 3 (H3), and mitochondrial 12S rRNA (12S), 16S rRNA (16S), cytochrome-c oxidase subunit I (COI) and cytochrome-c oxidase subunit II (COII). Molecular data were acquired via traditional PCR and Sanger sequencing following methods outlined previously (Bradler et al., 2014; Robertson et al., 2015), or from previously published data available on GenBank (Buckley et al., 2009, 2010; Bradler et al., 2014, 2015; Goldberg et al., 2015). Sequences new to this study are deposited in GenBank under accession numbers MK291527-MK291924, MK296739-MK296749, and MK297240-MK297296.

Alignment and Data Partitions

The protein encoding genes H3 and COI were length invariant and thus alignment of these genes was trivial, based on conservation of amino acid (AA) reading frame. COII however

FIGURE 2 | Phasmid oviposition techniques and eggs. **(A)** Ovipositor and mature egg of *Diapheromera femorata*. Photo © Alex Wild, used by permission. **(B)** Capitulate eggs of *Eurycnema goliah*. Photo by Piotr Naskrecki, used by permission. **(C)** *Dryococelus australis* depositing eggs in soil. Photo by Rohan Cleave, Zoos Victoria, Australia, used by permission. **(D)** *Neoclides* sp. gluing eggs to branch. Photo by Albert Kang, used by permission. **(E)** *Asceles* eggs skewered into leaf. Photo by Thierry Heitzmann, used by permission. **(F)** Korinninae nymph emerging from ootheca. Photo by Bruno Kneubühler, used by permission.

contained a length variable region in the coding sequence. Using Mesquite 3.31 (Maddison and Maddison, 2017), COII was translated into AA sequence and aligned using MUSCLE (Edgar, 2004) as implemented in Mesquite. The COII nucleotide sequences were then aligned via Mesquite to match the aligned AA sequences. Ribosomal genes were aligned using an online implementation of MAFFT 7 (Katoh and Toh, 2008) http://mafft.cbrc.jp/alignment/server/ applying the G-INS-I strategy. Resulting alignments were visually inspected to check for ambiguously aligned regions and alignment artifacts. Multiple ambiguously aligned expansion regions were removed from the 28S alignment using GBlocks (Talavera and Castresana, 2007) with options for a "less stringent selection."

We used PartitionFinder 2 (Lanfear et al., 2016) to simultaneously select the best-fit partitioning scheme and corresponding nucleotide substitution models for our data. The data were initially partitioned with ribosomal markers partitioned by gene and protein encoding genes partitioned by codon position. The analysis was run using a greedy search scheme (search = greedy), with all models considered (models = all). The corrected Akaike information criteria (AICc) was used to evaluate the fit of competing models. Alignments of the individual markers (12S: 463 bp; 16S: 600 bp; COI: 762 bp; COII: 621 bp; 18S: 1871 bp; 28S: 1608 bp; H3: 327 bp) were concatenated using Sequence Matrix 1.7.8 (Vaidya et al., 2011). PartitionFinder separated the data into 5 subsets as follows: 12S+16S (HKY+I+G+X), 18S+28S (GTR+I+G+X), codon positions 1+2 (GTR+I+G+X), COX position 3 (GTR+I+G), and H3 position 3 (GTR+I+G+X). Subsequent analyses were performed using this partitioned combined data set comprising 6,252 bp.

Phylogeny and Divergence Time Estimation

Phylogenetic analyses were performed on the Cipres Science Gateway (Miller et al., 2010) (www.phylo.org/). Exploratory RAxML analyses (Stamatakis et al., 2005) were executed on initial data sets including individual gene alignments to monitor potential contamination and assess gene performance, and on the combined data to assess terminal inclusion for constrained nodes in the divergence time analyses (see below). We performed RAxML rapid bootstrapping with a

FIGURE 3 | Stick and leaf insect eggs illustrating the breadth of their phenotypic diversity. Eggs depicted in the top two rows have capitula. Corresponding taxonomic names are provided in **Supplementary Table S3**. Photos by François Tetaert, used by permission.

subsequent ML search (Stamatakis et al., 2005) executing 500–1000 bootstrap inferences using a GTR+G model [as recommended in Stamatakis et al. (2008; the RAxML 7.0.3 manual)]. FigTree 1.4 (Rambaut, 2012) was used to visualize the resulting trees.

Phylogeny and divergence time estimation was performed simultaneously in BEAST 2 (v2.4.5) (Bouckaert et al., 2014) using 5 unambiguous crown-group phasmid fossils as minimum calibration points that we were able to assign to specific nodes on the tree using synapomorphy-based anatomical evidence (Bradler et al., 2015) (**Supplementary Table S2**). The analysis was run using a lognormal distributed relaxed clock model with a Yule speciation prior. Clock and tree parameters were linked across all data partitions. Fossil calibrations were implemented using a lognormal prior distribution with a log-mean of 1.0 and log-SD of 1.0. Five separate analyses comprising 80–100 million generations each, with parameters sampled every 4,000 generations, were run to ensure convergence. Convergence and sufficiently high effective sample sizes (ESSs) of parameter estimates were verified in Tracer v1.6 (Rambaut et al., 2014). The initial 5,000 trees sampled were discarded as burnin and TreeAnnotator v1.8.4 (Rambaut and Drummond, 2016) was used to calculate a maximum credibility tree from the posterior 15001 trees. FigTree 1.4 (Rambaut, 2012) was used to visualize the resulting tree.

Oviposition Strategies

We scored oviposition strategies for our taxonomic sampling using the following 5 (unordered) states (**Supplementary Table S1**):

0: Drop or flick eggs
1: Bury/insert eggs into soil or crevices
2: Glue eggs to substrate
3: Pierce eggs into leaves
4: Produce ootheca

Twenty-two of the 285 (ca. 7%) taxa investigated were scored as missing data (?) for oviposition technique due to unknown natural history information for these species. Even so, our data provide more than sufficient taxonomic and geographic coverage to infer general patterns regarding the timing and geographic pattern of evolution of egg laying techniques in stick and leaf insects. Ancestral state reconstruction of egg-laying strategies was performed in Mesquite 3.31 (Maddison and Maddison, 2017) using parsimony unambiguous optimization.

RESULTS AND DISCUSSION

The Evolution of Oviposition Strategies

The diversity exhibited in phasmid ova and oviposition strategies is striking. Our results unequivocally demonstrate that the ancestral oviposition strategy for stick and leaf insects is to remain in the foliage and drop or flick eggs to the ground (**Figures 4–6**) as suggested previously (Bradler, 2009; Goldberg et al., 2015), contradicting earlier assumptions that favored a ground-dwelling ecomorph to represent the ancestral character state (Carlberg, 1987). The phasmid egg capsule is a defining phenotypic character for Phasmatodea. It includes the presence of both a detachable lid-like operculum at its anterior pole through which the first instar nymph emerges, and an interior, air-containing plate that is demarcated externally by the micropylar plate (Sellick, 1997b). In Euphasmatodea (all phasmids excluding *Timema*) the egg capsule is greatly hardened. The eggs of *Timema* are soft but the females coat them with pulverized soil or sand that hardens to provide modest outer protection. The greatly hardened egg capsule of Euphasmatodea represents a key innovation in phasmid evolution, equipping the eggs to withstand an otherwise potentially perilous fall from the canopy, float extended periods of time (e.g., >1 year) on sea water (Kobayashi et al., 2014) and pass through the intestine of birds (Suetsugu et al., 2018) without compromising viability. The Western Nearctic genus *Timema* includes 21 species and Euphasmatodea just over 3,000 species (Bradler and Buckley, 2018). The striking disparity in species richness between these sister clades strongly suggests significant ecological opportunity [e.g., acquisition of key innovations, colonization of new habitat, extinction of antagonists (Yoder et al., 2010)] obtained in Euphasmatodea, and whereas there are certainly many selective factors at play (e.g., horizontal gene transfer of pectinases Shelomi et al., 2016), the evolution of a hardened egg capsule in Euphasmatodea is foremost.

Adult female stick insects lay eggs over a period of several months at a rate of one to several per day (Goldberg et al., 2015). During periods of active oviposition the sound of phasmid eggs dropping to the forest floor is reminiscent of the onset of rain (Beier, 1968). The ground plan oviposition technique of dropping/flicking eggs represents a boon for maintaining their masquerade as females are not required to move in search of specific oviposition sites, but can remain put, invisible to threat. Dropping/flicking eggs is not only employed by the earliest diverging (extant) lineages (e.g., Aschiphasmatinae, Phylliinae, Diapheromerinae) but occurs in the majority of phasmid species worldwide. In fact, all inferred transitions away from this ancestral oviposition strategy to a new technique occur in taxa well nested within major phasmid lineages (see below). Droppers and flickers occur in all biogeographic regions where phasmids occur.

Phasmids have limited dispersal ability (Compton and Ware, 1991) and are generally considered non-volant (Bradler et al., 2015). Roughly 60% of phasmid species exhibit greatly reduced wings or lack wings altogether in the adult form (Whiting et al., 2003) and even winged forms may not exhibit sustained flight (Maginnis, 2006). Various stick and leaf insects have evolved three key innovations to compensate for the loss of motility associated with the phenotypic and behavioral consequences of extreme masquerade: polyphagy, parthenogenesis, and myrmecochory. In general, flightless species are polyphagous (linked to their limited motility) whereas volant species (e.g., Necrosciinae) exhibit a more restricted diet and are regarded as host plant specialists (Blüthgen et al., 2006). Roughly 10% of phasmids exhibit varying forms of facultative parthenogenesis (e.g., *Parabacillus, Bacillus, Clonopsis*) including species hybrid parthenogens (Note that hybridogenetic females can escape hybridity back to Mendelian reproduction in just one generation Scali, 2009).

Another major key innovation in phasmid diversification appears to be the evolution of capitulate eggs, which facilitate ant-mediated dispersal, or myrmecochory (Compton and Ware, 1991; Hughes and Westoby, 1992; Windsor et al., 1996; Stanton et al., 2015). Capitula are phenotypically and functionally analogous to elaiosomes of angiosperm seeds. In fact, capitula and elaiosomes have a similar chemical profile, thus stick insects, and flowering plants utilize the same chemical signaling pathway to exploit ant behavior (Stanton et al., 2015). Selective benefits for myrmecochorous stick insects overlap with those for angiosperms including distance dispersal as a way of escaping clumping of offspring and rapid removal as a protection against predation and fire, but also parasitism by wingless parasitoid wasps that specialize on phasmid eggs (Compton and Ware, 1991). Like elaiosomes (Lengyel et al., 2009, 2010), capitula vary tremendously in form and given their taxonomic occurrence have likely evolved independently in geographically disparate lineages (Sellick, 1997a,b).

We infer at minimum 16 independent shifts to a burying/inserting eggs into soil/crevices oviposition strategy (**Figures 4–6**). All but one of these transitions represents a shift from the ancestral condition of dropping or flicking eggs (the one exception is *Diesbachia* and allies, see below). Depositing eggs into the soil or crevices of bark represents a major departure from simply dropping eggs from the canopy. Such major shifts in oviposition mode typically correspond to a major shift in microhabitat, egg phenotype, and often, adult phenotype. For example, most of the shifts to deposition in soil/crevices correspond to adapting to a ground or bark

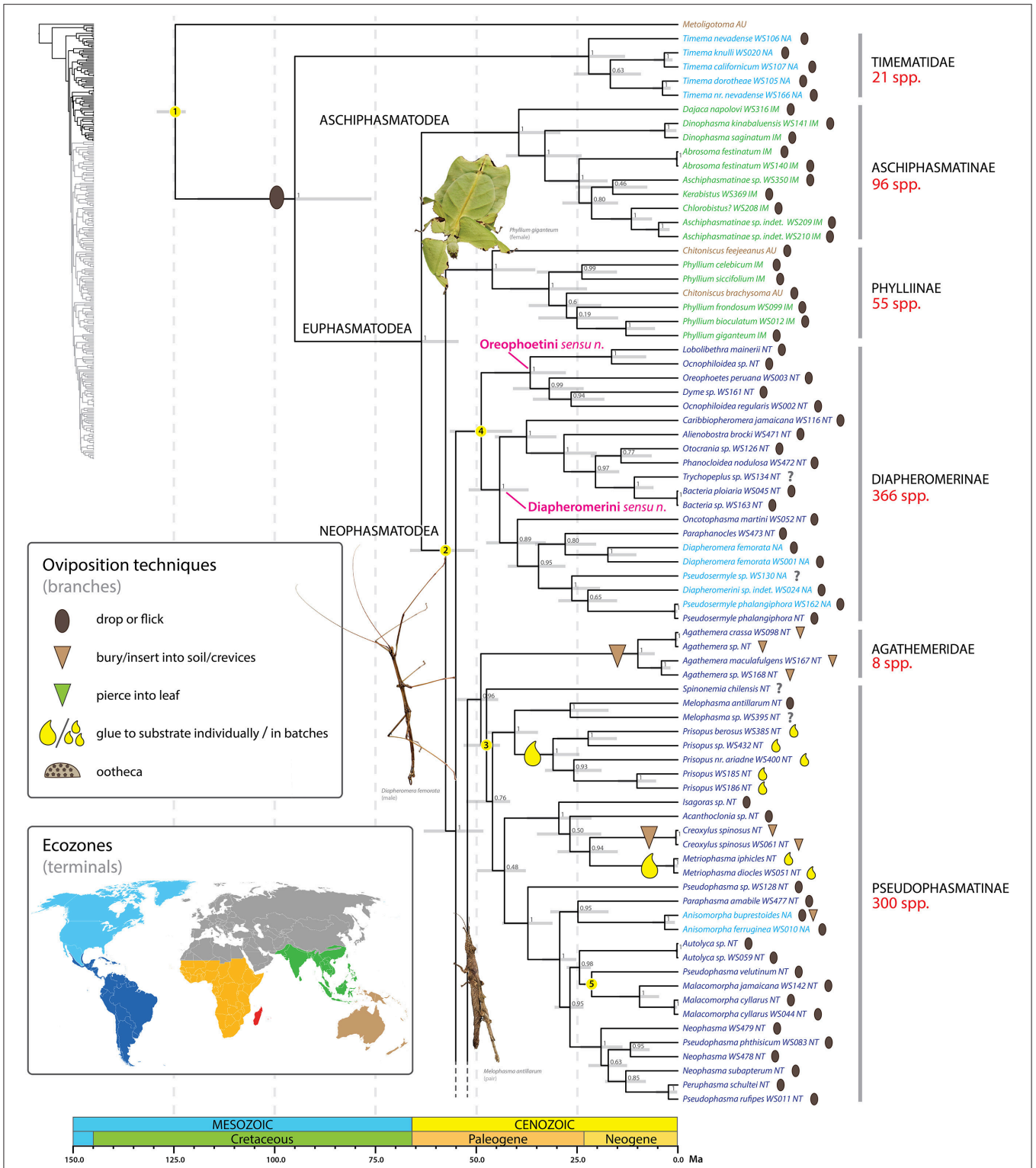

FIGURE 4 | Chronogram of Phasmatodea (part 1 of 3). The full time tree is shown to the left with the emboldened region enlarged and colored for discussion. Fossil calibration points are denoted with numbered yellow circles (see **Supplementary Table S2**). Ninety-five percentage confidence intervals around node ages are indicated by gray bars. Bayesian posterior probability confidence intervals are listed for each node. Terminals are colored by ecozone following the inset. Oviposition technique for each sampled species is shown to the right of the terminal according to the inset, with inferred transitions optimized and marked on the branches. Photos of stick and leaf insects by Melinda Fawver (*Diapheromera femorata*), Isselee (*Phyllium giganteum*), Bruno Kneubühler (*Melophasma antillarum*) modified for use, used by permission.

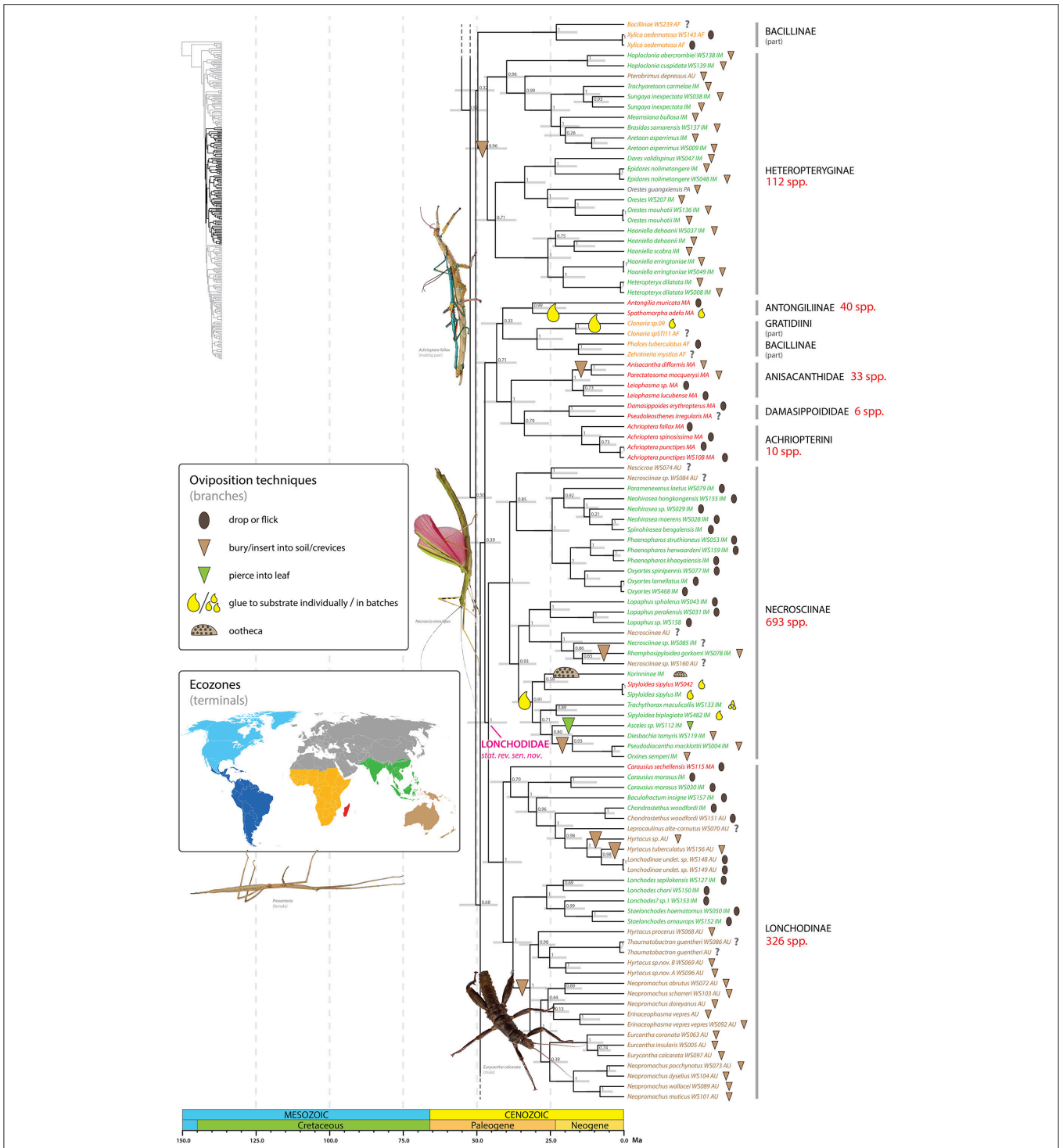

FIGURE 5 | Chronogram of Phasmatodea (part 2 of 3). The full time tree is shown to the left with the emboldened region enlarged and colored for discussion. See **Figure 1** caption for details. Photos of stick and leaf insects by Igor Siwanowicz (*Achrioptera fallax*), Isselee (*Necroscia annulipes*), Bruno Kneubühler (*Prosentoria*) modified for use, Valentino2 (*Eurycantha calcarata*), used by permission.

dwelling microhabitat, with a corresponding robust adult phenotype and egg deposition directly into the soil. These eggs are typically cylindrical, bullet-shaped, or otherwise modified for ease of burial (e.g., **Figures 3Z,A',E'**). Extreme examples include two independent shifts, one in *Dryococelus australis* and another within a New Zealand clade including *Trapezaspis*,

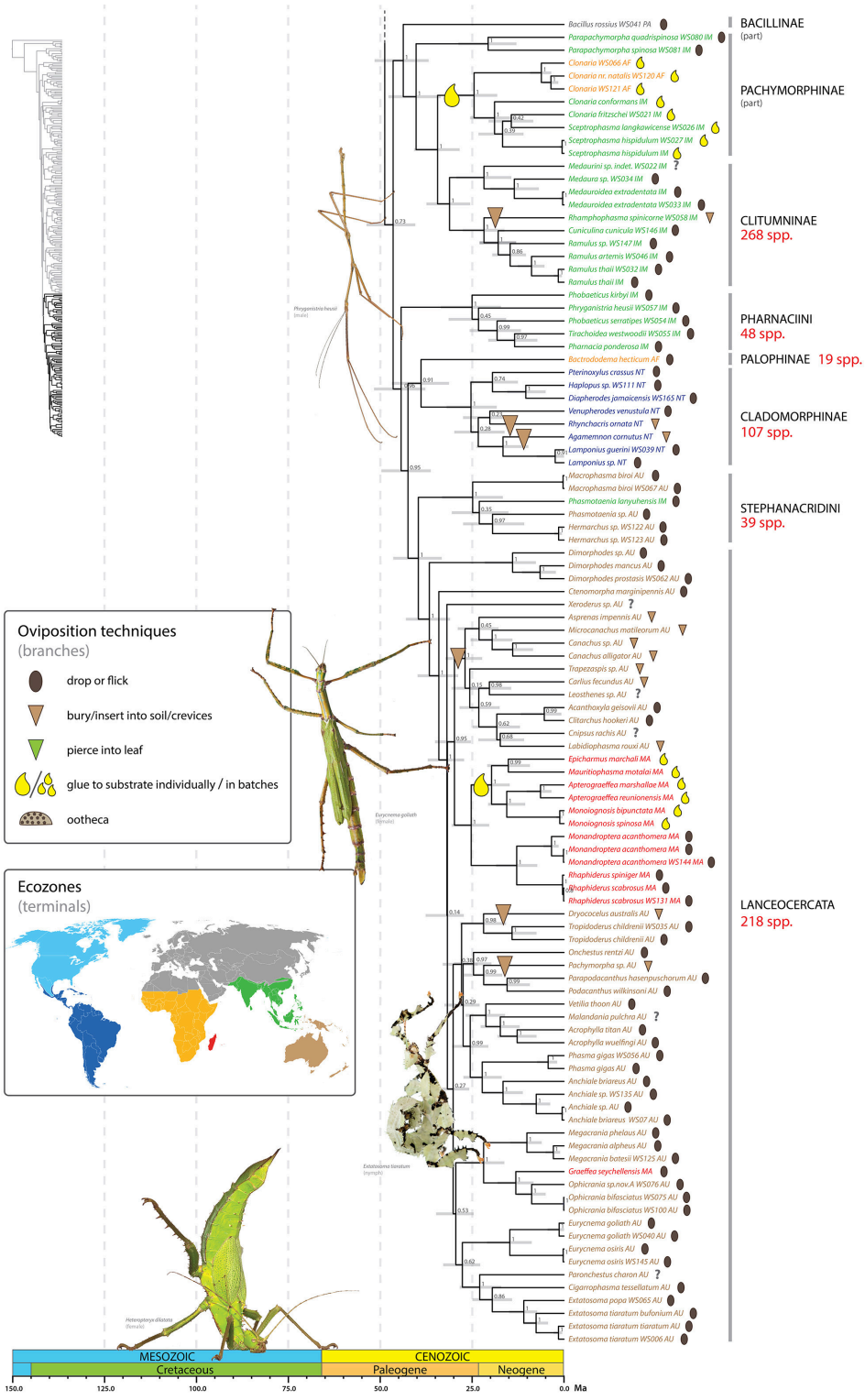

FIGURE 6 | Chronogram of Phasmatodea (part 3 of 3). The full time tree is shown to the left with the emboldened region enlarged and colored for discussion. See **Figure 1** caption for details. Photos of stick and leaf insects by Finalion (*Eurycnema goliath*), Laetitia Bourgois (*Extatosoma tiaratum*), Magnus Forsberg (*Heteropteryx dilatata*), Bruno Kneubühler (*Phryganistria heusii*) modified for use, used by permission.

Microcanachus, and *Canachus* (**Figure 6**). These are clear instances of adapting to a ground dwelling microhabitat, with a corresponding robust tree lobster phenotype (Buckley et al., 2009) and egg deposition directly into the soil. This trend is also evident in several other taxa including the Eurycanthomorpha (Bradler, 2009) of Lonchodinae (**Figure 5**) and, to a lesser degree, the Heteropteryginae, and the South American genus *Agathemera* (**Figure 4**).

At least one shift to egg deposition into soil/crevices, inferred in the most recent common ancestor of the Heteropteryginae, resulted in a radiation of over 100 species (**Figure 5**). Heteropteryginae are distributed primarily in Indo-Malaysia, with only a few Australasian or Palearctic species. We estimate Heteropteryginae diverged from its sister taxon some time between 56 and 44 Ma (ca. 50 Ma) and began to radiate between 53 and 40 Ma (ca. 46.4 Ma). This lineage comprises species generally exhibiting a robust phenotype compared to the quintessential stick-like phasmids and includes the massive Jungle Nymph, *Heteropteryx dilatata*.

Adhering eggs to substrate evolved at least seven times throughout phasmid diversification (**Figures 4–6**). We infer two independent shifts to gluing eggs among the Neotropical Pseudophasmatinae in the taxa *Prisopus* and *Metriophasma* (**Figure 4**). Other shifts occur in Antongiliinae, two disparate clades of Gratidiini (Pachymorphinae), Necrosciinae, and Mascarene Lanceocercata. Most of the inferred shifts to a gluing oviposition strategy apparently did not result in marked subsequent diversification. However, one exception may be the Afrotropical and Indomalaysian clade comprising species of *Clonaria*, and *Sceptrophasma* (Gratidiini) (**Figure 6**). It is difficult to estimate the species-richness of this clade due to the fact that *Clonaria* (or Gratidiini) is recovered as polyphyletic, with some Afrotropical species distantly removed, recovered sister to *Phalces* and *Zehntneria.* In addition to the problematic generic boundaries, the species diversity of *Clonaria* is not well-accounted for.

Necrosciinae is the most species-rich and ecologically diverse lineage in the order treated at the subfamily rank; the ca. 700 species collectively employ all modes of phasmid oviposition (**Figure 5**). *Rhamphosipyloidea gorkomi* buries its eggs, but the oviposition mode of closely related taxa is unknown and thus so are the evolutionary transitions leading to this shift to depositing eggs in soil. One lineage comprising Korinninae sp., *Trachythorax*, *Diesbachia* and allies, *Asceles*, and several species of *Sipyloidea* exhibits a diverse range of oviposition strategies. It is unclear what selective pressures may have promoted this diversification, but we infer an initial shift from dropping/flicking to adhesion at the base of this lineage. Following this shift to gluing eggs singly, multiple instances of evolutionary novelty are evident. The general reproduction strategy of Phasmatodea regardless of oviposition mode is to deposit eggs singly thereby avoiding aggregating their offspring. In some taxa, including *Trachythorax*, *Neoclides* (not sampled in present study), and others, the females glue their eggs in loose single layer clusters (Goldberg et al., 2015). We recovered the ootheca producing Korinninae sister to *Sipyloidea* spp. that glue their eggs singly. Because the production of ootheca is a remarkable departure from the remaining phasmid oviposition strategies, reconstructing the ancestral states and evolutionary transitions leading to this shift is of great interest. The analyses of Goldberg et al. (2015) support *Asceles,* which skewer their eggs into leaves, as the sister to Korinninae. It is unclear under this sister group hypothesis what the ancestral oviposition condition might be. The evolution of an ootheca oviposition strategy from an ancestral mode of adhesion as supported by our results is an intuitive pathway since the sticky glandular secretion would already be in place (see Goldberg et al., 2015). We recovered a clade with moderate support (PP = 80) formed by sister taxa each exhibiting a novel mode of oviposition from the ancestral adhesion strategy. One of these lineages includes taxa that insert their eggs into soil or crevices of bark (e.g., *Diesbachia*, *Pseudodiacantha*, *Orxines*). Interestingly, the other lineage is *Asceles,* which pierces their eggs into leaves (**Figure 2E**).

Phasmatodea Systematics

Our molecular phylogeny represents the most extensively sampled estimate of the phasmid tree of life to date, in terms of the unique lineages, number of terminals, and number of loci. Our results present many significant relationships, some proposed previously and some novel. Corroborating earlier studies (Buckley et al., 2009; Bradler et al., 2014, 2015; Goldberg et al., 2015; Büscher et al., 2018), our results indicate a general pattern of strong branch support for the major lineages and toward the tips of the tree but only moderate support at some of the deeper relationships (**Figures 4–6**). Even so, we are encouraged that compared to previous molecular analyses (e.g., Buckley et al., 2009; Bradler et al., 2014, 2015; Goldberg et al., 2015; Büscher et al., 2018) the backbone relationships are in general recovered with higher support, an observation likely tied to increased taxon and gene sampling. The observed pattern of major diversification of lineages over a relatively short period of time may be the signature of an ancient rapid radiation of major phasmatodean lineages (see also Bradler, 2015; Bradler and Buckley, 2018).

We recovered an early subdivision of the Euphasmatodea into Aschiphasmatinae and all remaining stick and leaf insects with maximum support (PP = 1) (**Figure 4**). Aschiphasmatinae are enigmatic stick insects. They have been recovered as the earliest or one of the earliest diverging extant lineages of Euphasmatodea based on morphological (Tilgner, 2002) and molecular phylogenetic analyses (Buckley et al., 2009; Bradler et al., 2015). Engel et al. (2016) regarded this lineage as Aschiphasmatodea, with the remainder of the Euphasmatodea forming the Neophasmatodea. Within Aschiphasmatinae, *Dajaca* is the sister group to all remaining Aschiphasmatinae, thus reflecting its subdivision into Dajacini and Aschiphasmatini as suggested by Bragg (2001). However, Aschiphasmatidae sensu Bragg (2001) (= Aschiphasmatinae + Korinninae) is not supported since the species-poor Korinninae is recovered as a subordinate lineage of Necrosciinae as shown previously (Goldberg et al.,

2015). Anatomical features supporting Neophasmatodea include galealobulus (maxillary lobe at base of galea) present (absent in *Timema* and Aschiphasmatinae), pro-spina absent (present in *Timema* and Aschiphasmatinae) (Tilgner, 2002).

The Phylliinae, or leaf insects, are strongly supported as the earliest diverging lineage of Neophasmatodea (**Figure 4**). This placement is consistent with the recent molecular study of Bradler et al. (2015), and additional studies employing a narrower taxon sampling regime also recover Phylliinae as a relatively early diverging lineage within Euphasmatodea (Buckley et al., 2009; Kômoto et al., 2011). This Old World lineage includes the 47 million year old fossil *Eophyllium messelense* (Wedmann et al., 2007), one of the oldest known extinct euphasmatodeans. Members of Phylliinae possess a unique egg morphology, making them distinct from most other phasmids. The edge of the micropylar plate is broken up into strips creating a fringe around its border (Sellick, 1997b). Fringed plates also occur in the Datamini (Heteropteryginae).

In contrast to some earlier studies that recovered paraphyletic Diapheromerinae at the euphasmatodean base (Whiting et al., 2003; Bradler et al., 2014 in part), we observe monophyletic New World Diapheromerinae (with the inclusion of *Otocrania,* see below) (**Figure 4**). However, our topology does not reflect the current classification (Phasmida Species File, Brock et al., 2017) of Diapheromerinae into the three subgroups Oreophoetini (*Oreophoetes*), Ocnophilini (*Ocnophiloidea*), and Diapheromerini (the remaining Diapheromerinae taxa in our tree). Instead, we recover with maximum support (PP = 1) a clade comprising *Lobolibethra*, *Dyme*, *Oreophoetes*, and polyphyletic *Ocnophiloidea* and this clade forms the sister group to the remaining Diapheromerinae. Perhaps a more significant result is the placement of *Otocrania* (formerly incorrectly assigned to Cladomorphinae) among the Diapheromerinae with strong support indicating its true affinity within Diapheromerinae. Further work is needed to delimit meaningful groups within Diapheromerinae reflective of their evolutionary history, but for now we formally transfer *Otocrania* to Diapheromerinae and recognize only two tribes within the subfamily, Diapheromerini **sensu nov.** and Oreophoetini **sensu nov**.

***Diapheromerini*, Kirby 1904 sensu nov.**

Type genus. *Diapheromera* Gray, 1835: [18]

Diagnosis. The tribe Diapheromerini **sensu nov.** is well-supported by molecular data (see above), but to date very few anatomical apomorphies have been identified for the group. Most Diapheromerini **sensu nov.** produce eggs with a matrix (non-stalked) capitulum.

Included taxa. Diapheromerini **sensu nov.** comprises the majority of the species diversity within the subfamily, including most taxa previously classified as Diapheromerini (except *Dyme* and *Lobolibethra*; see below) and *Otocrania,* formerly regarded as Cladomorphinae.

***Oreophoetini*, Zompro 2001 sensu nov.**

Type genus. *Oreophoetes* Rehn, 1904: [56]

Diagnosis. The tribe Oreophoetini **sensu nov.** is well-supported by molecular data (see above), but to date no morphological characters have been identified that unite the group. Oreophaetini **sensu nov.** produce eggs lacking a capitulum and are restricted to the Neotropics.

Included taxa. Oreophoetini **sensu nov.** includes *Oreophoetes*, *Ocnophiloidea* Zompro, *Lobolibethra,* and *Dyme*. Other taxa formerly included in Oreophoetini (e.g., *Oreophoetophasma* Zompro) *Ocnophiloidea* (*Dubiophasma* Zompro, *Exocnophila* Zompro, *Ocnophila* Brunner von Wattenwyl, *Parocnophila* Zompro) but not sampled in this or previous molecular phylogenetic studies are considered *incertae sedis*.

Another strongly supported Neotropical clade (PP = 0.96) comprises the species poor South American *Agathemera* and Heteronemiini + the species rich Pseudophasmatidae (**Figure 4**), often referred to as Pseudophasmatinae (Bradler et al., 2014, 2015; Goldberg et al., 2015). These taxa were considered as Pseudophasmatinae by Günther (1953), but its subgroups *Agathemera*, Heteronemiini (= Bacunculini sensu Günther, 1953) and Prisopodini were subsequently removed from Pseudophasmatinae (or Pseudophasmatidae, Zompro, 2004). Based on morphological evidence, *Agathemera* was repeatedly placed as sister group to all remaining Euphasmatodea (Klug and Bradler, 2006; Bradler, 2009; Friedemann et al., 2012), but this hypothesis is in sharp contrast to all molecular studies which support *Agathemera* as a subordinate euphamatodean taxon (Whiting et al., 2003; Buckley et al., 2009; Bradler et al., 2014, 2015; Goldberg et al., 2015; Büscher et al., 2018), albeit with no consensus regarding its placement among the remaining stick insects. Zompro (2004) erected the subfamily Prisopodinae for *Prisopus* and related species (e.g., *Melophasma*) and the family Prisopodidae for Prisopodinae + Korinninae. *Prisopus* and allies are enigmatic taxa. We recovered Prisopodini nested within Pseudophasmatinae (see also Goldberg et al., 2015), but in some analyses it was supported as an early divergent neophasmatodean lineage far removed from Pseudophasmatinae. The internal phylogeny of Pseudophasmatidae does not reflect the current classification following the Phasmida Species File (Brock et al., 2017, mainly based on Zompro, 2004). The subgroup Xerosomatinae is supported (PP = 1) but not its subdivision into tribes, e.g., Xerosomatini (represented here by *Acanthoclonia* and *Creoxylus*) and Prexaspini (represented by *Isagoras* and *Metriophasma*) (see also Bradler et al., 2015). It is also evident from our results that the eponymous and species-rich genus *Pseudophasma* is polyphyletic.

Represented in the present study by 24 exemplars, the Heteropteryginae (or Heteropterygidae, Zompro, 2004) are supported as monophyletic (**Figure 5**). Multiple heteropterygine taxa (e.g., Datamini) exhibit relatively high rates of sequence divergence across the sampled genes as reflected in their long

branches and unstable position in Euphasmatodea when the taxon sampling is limited. With increased taxon sampling of Heteropteryginae we observe increased support for its monophyly. For example, early molecular analyses that included three to four exemplars (Whiting et al., 2003; Buckley et al., 2009) did not recover a monophyletic Heteropteryginae, whereas subsequent studies with increased sampling have (Goldberg et al., 2015; Büscher et al., 2018). The heteropterygine tribes Datamini, Heteropterygini, and Obrimini are each recovered with high support (PP = 1, 1, 0.96 respectively), but the relationships between these three tribes are not well-supported, with Datamini forming the sister group to Heteropterygini (PP = 0.71). The other two studies that included exemplars of all three tribes each recovered a unique scenario of tribal relationships (Bradler et al., 2015; Goldberg et al., 2015; Büscher et al., 2018). Our results further illustrate several taxonomic shortcomings within Heteropteryginae on a lower scale. For example, the Tisamenini as recently erected by Hennemann et al. (2016), represented here by *Hoploclonia* and *Pterobrimus*, are paraphyletic. What's more, *Hoploclonia abercrombiei* was recently synonimyzed with *H. cuspidata* (Seow-Choen, 2016), but the genetic distance spanning these two taxa (reflected by relative branch lengths) clearly indicates they are distinct species (**Figure 5**); *H. abercrombiei* should be brought out of synonymy accordingly. Similarly, the genus *Haaniella* is paraphyletic with respect to *Heteropteryx dilatata* (see also Goldberg et al., 2015), the later strongly supported as the sister taxon to *H. erringtoniae*. If these relationships are confirmed in subsequent analyses *Haaniella* or parts of it will need to be synonymized with *Heteropteryx*. Only a few superficial characters have been used to separate the monotypic *Heteropteryx* from *Haaniella* including *Heteropteryx* having a strongly conical and elevated head, distinct spines on the abdominal terga of females, a shortened mesothorax in the male form, and specific coloring in both sexes (Hennemann et al., 2016). The remarkable similarity in form of the eggs of some *Haaniella* species and *Heteropteryx* strongly indicates their close affinity.

We recovered an African-Malagasy clade with low to moderate support (PP = 0.71) (**Figure 5**). The clade comprises two Malagasy lineages recovered with high support: Antongiliinae (*Antongilia* + *Spathomorpha*) (PP = 0.99) and Anisacanthidae + Damasippoidini + Achriopterini (PP = 1). The one subordinate African lineage (PP = 1) consists of the Gratidiini (Pachymorphinae) taxa *Clonaria* (part) and *Zehntneria* and the Bacillinae taxon *Phalces*. Bradler et al. (2015) also recovered this African clade with maximum support. Neither Bacillinae nor Pachymorphinae are recovered as monophyletic. The polyphyly of these two subfamilies has been demonstrated in previous studies as well (Buckley et al., 2009). Some of the sampled Bacillinae species (or Bacillidae species sensu Zompro, 2004) (e.g., *Xylica oedematosa, Bacillus rossius*) exhibit long branches and their respective phylogenetic positions tend to be unstable across analyses. For example, one African Antongiliinae/Bacillinae clade containing *Xylica* and allies (PP = 1) was recovered with negligible support (PP = 0.32) as the sister group to Heteropteryginae. In contrast, previous molecular studies have recovered *Xylica oedematosa* as the earliest divergent lineage of Euphasmatodea (Bradler et al., 2015), or part of that lineage (Buckley et al., 2009). Note that the clade comprising *Xylica oedematosa* and allies was recovered in preliminary analyses of these data with *Parapachymorpha*, Gratidiini (in part), and Clitumninae (excluding Pharnaciini); this instability is reflected by the poor branch support along the base of the tree spanning these alternative placements. Antongiliinae as erected by Zompro (2004) and currently recognized in the Phasmida Species File (Brock et al., 2017), represented here by *Antongilia* and *Xylica*, is not supported. In contrast to Bradler et al. (2015), we recovered *Antongilia muricata* and *Spathomorpha adefa* as sister taxa (PP = 0.99) lending support to a single colonization hypothesis rather than independent colonization of Madagascar by these taxa.

A sister group relationship between Necrosciinae and Lonchodinae has been repeatedly shown (Bradler et al., 2014; Goldberg et al., 2015) and is corroborated here based on a significantly enlarged taxon sampling with maximum support (PP = 1) (**Figure 5**). Necrosciinae and Lonchodinae are both characterized by the presence of long antennae and the absence of the area apicalis on the tibiae (Günther, 1953; Bradley and Galil, 1977). Both subfamilies are currently treated as members of different families (Necrosciinae as part of Diapheromeridae and Lonchodidae as part of Phasmatidae) in the Phasmida Species File (Brock et al., 2017), highlighting the inadequacy of this database to represent the higher-level phylogenetic relationships among stick and leaf insects despite its utility at the species level. We formally recognize the clade comprising Necrosciinae and Lonchodinae at the family level as Lonchodidae **stat. rev. sensu nov.**

***Lonchodidae* Brunner von Wattenwyl, 1893 stat. rev. sensu nov.**

Type genus. *Lonchodes* Gray, 1835: [19]

Diagnosis. Lonchodidae **stat. rev. sensu nov.** are strongly supported by molecular data (see above) but only vaguely characterized by morphology including the following combination of features: Adults with antennae long, and area apicalis on tibiae absent. Lonchodidae **stat. rev. sensu nov.** are distributed in Indomalaysia, Australasia, Madagascar, and related islands, and with very few species occurring in the Palaearctic.

Included taxa. Lonchodidae **stat. rev. sensu nov**. comprises all taxa included in the current concept of the constituent subfamilies Lonchodinae and Necrosciinae as set forth in Bradler et al. (2014).

The species-rich genus *Sipyloidea* is clearly polyphyletic with species recovered in multiple clades within Necrosciinae (**Figure 5**). Most higher phasmid taxa exhibit high levels of endemism. In sharp contrast, the genus *Sipyloidea* as presently constituted is widely distributed, with species occurring in Madagascar, Africa, Indo-Malaysia, and Australasia. Our results clearly reject the hypothesis that *Sipyloidea* is a species-rich

genus with a broad geographic distribution, but rather represents several unique lineages with restricted geographic distributions.

Within Lonchodinae, the Eurycanthomorpha comprising the New Guinean tree lobsters (*Eurycantha* spp.) and allies (Buckley et al., 2009; Bradler et al., 2015; Büscher et al., 2018) are recovered with maximum support (PP = 1). However, our results indicate that several lonchodine genera are polyphyletic, including *Carausius*, *Hyrtacus*, and *Neopromachus*.

We recovered with maximum support a wingless lineage comprising *Bacillus rossius*, *Parapachymorpha,* Gratidiini (in part: *Clonaria* spp., *Sceptrophasma*), Clitumnini and Medaurini (**Figure 6**). Whereas, this clade represents a grouping that has not been formally recognized, variations of it have been suggested repeatedly (Hennemann and Conle, 2008; Bradler, 2009; Buckley et al., 2009; Bradler et al., 2014, 2015). Based on phylogenetic inference of morphological data, Bradler (2009) recovered two disparate clades, one comprising *Bacillus rossius* + Gratidiini (*Clonaria*, *Sceptrophasma*) and the other formed by Clitumnini, Medaurini, and *Parapachymorpha*. Molecular phylogenetic studies strongly support the grouping of Clitumnini (e.g., *Ramulus*), Medaurini (without *Parapachymorpha*), and African and Southeast Asian Gratidiini (Bradler, 2009; Buckley et al., 2009; Bradler et al., 2014, 2015; Büscher et al., 2018). Traditionally, Gratidiini was classified as Pachymorphinae based on the presence of short antennae, whereas Clitumnini and Medaurini were placed in Phasmatinae. Both subfamilies are clearly polyphyletic (Bradler, 2009; Buckley et al., 2009; Bradler et al., 2014). Hennemann and Conle (2008) established the subfamily Clitumninae, comprising Clitumnini + Medaurini (including *Parapachymorpha*) + Pharnaciini. However, Clitumninae are not recovered as monophyletic in the present analysis. Instead Clitumnini and Medaurini (without *Parapachymorpha*) are sister taxa (PP = 1) with the African and Southeast Asian Gratidiini subtending them (PP = 1). *Parapachymorpha* forms the sister taxon (PP = 1) of this undisputed clade and *Bacillus rossius* is recovered as the sister to the whole group (PP = 1). Pharnaciini is strongly supported as more closely related to Lanceocercata and allies than to Medaurini and Clitumnini (see below).

Pharnaciini contains a number of giant-sized stick insects including the recently described *Phobaeticus chani*. Our sampling includes two species of *Phobaeticus*, *P. kirbyi,* and *P. serratipes*, but our results suggest the genus as presently constituted is not monophyletic, with *P. serratipes* strongly supported (PP = 0.99) as the sister group to *Tirachoidea* + *Pharnacia*. In our analysis (see **Figure 6**) the tribe Pharnaciini forms the sister group (PP = 0.96) to the clade [(Cladomorphinae + *Bactrododema*) + (Stephanacridini + Lanceocercata)]. This diverse grouping comprises a lineage that has been repeatedly shown in the past, albeit with differing placements of *Bactrododema* (Buckley et al., 2009, 2010; Bradler et al., 2014, 2015; Goldberg et al., 2015; Büscher et al., 2018).

The internal relationships of Lanceocercata (**Figure 6**) are recovered with varying support and generally corroborate those recovered in previous studies (Buckley et al., 2009, 2010; Bradler et al., 2014, 2015; Goldberg et al., 2015; Büscher et al., 2018). The genus *Dimorphodes* forms the sister group (PP = 1) to all remaining Lanceocercata (PP = 1). *Ctenomorpha marginipennis* and *Xeroderus* represent additional early divergent taxa. Within Lanceocercata a New Caledonia/New Zealand clade is recovered (PP = 1) (Buckley et al., 2010) as well as a Mascarene lineage (PP = 1). We further find support for monophyletic Platycraninae (PP = 1), the coconut stick insects. The sister taxon to *Dryococelus australis,* The Lord Howe stick insect, remains unclear with no consensus across analyses (Buckley et al., 2009, 2010; Bradler et al., 2015; Goldberg et al., 2015); candidates include *Eurycnema* (Buckley et al., 2009), *Ctenomorpha* + *Eurycnema* (Buckley et al., 2009) and Platycraninae (Bradler et al., 2015). We recovered a strongly supported (PP = 0.98) sister grouping of *Dryococelus australis* and the fully winged *Tropidoderus childrenii* from the East Coast of Australia.

Clearly much work is needed to delimit meaningful groups within Phasmatodea reflective of their evolutionary history. Corroborating previous phylogenetic studies (see above), our results highlight the limitations of the current classification scheme for Phasmatodea and the need for future phylogenetic revision and reassessment of concepts and boundaries of higher taxa. The relationships among several major phasmid lineages remain unsettled. Even so, we are encouraged with our results of having recovered major phasmatodean divergences with significant support [e.g., Aschiphasmatinae and Phylliinae as early divergent taxa of Euphasmatodea; Diapheromerinae sensu nov.; Pseudophasmatinae s.l.; Necrosciinae + Lonchodinae; Clitumnini, Medaurini, Gratidiini and allies; ((Cladomorphinae + *Bactrododema*) + (Stephanacridini + Lanceocercata))] and look forward to continued progress by the phasmid community.

DATA AVAILABILITY STATEMENT

All datasets analyzed for this study are included in the manuscript and the **Supplementary Material.** Oviposition mode data is provided in **Supplementary Table S1**. The DNA sequences used for phylogenetic inference can be found at GenBank [http://www.ncbi.nlm.nih.gov/genbank] under accession numbers MK291527-MK291924, MK296739-MK296749, and MK297240-MK297296. The alignment used for the phylogenetic reconstruction is provided as a Nexus input file as **Supplementary Data Sheet 1.**

AUTHOR CONTRIBUTIONS

JR, SB, and MW designed the research. JR generated and analyzed molecular data. JR, SB, and MW wrote the manuscript. JR generated the artwork. All authors have approved the final version of the manuscript.

FUNDING

This research was funded in part by the National Science Foundation (DEB- 1557114 to MW, JR, and SB; DEB-1256976 to Wendy Moore and JR) and by the German Science Foundation (BR 2930/5-1 to SB).

ACKNOWLEDGMENTS

We recognize and are grateful for the support of the following people and agencies that have enhanced the value of this work. Christoph Seiler (Altlussheim, Germany), Seth Bybee (BYU), Joe McHugh (UGA), Gavin Svenson (CMNH), provided valuable specimens for this research. Yelena Pacheco helped generate sequence data for several critical taxa. Rohan Cleave, Melinda Fawver, Pavel German, Thierry Heitzmann, Isselee, Albert Kang, Bruno Kneubühler, Moritz Muschick, Piotr Naskrecki, Igor Siwanowicz,François Tetaert, Miroslaw Wasinski, Alex Wild, Art Wolfe, Valentino2, and the Museum of Victoria provided use of their stunning photos of stick and leaf insects. Special thanks go to Mark Miller and the CIPRES Science Gateway.

SUPPLEMENTARY MATERIAL

The Supplementary Material for this article can be found online at: https://www.frontiersin.org/articles/10.3389/fevo.2018.00216/full#supplementary-material

Supplementary Table S1 | Taxon and data sampling for the present study. Identification of voucher specimens new to this study was performed or confirmed by SB.

Supplementary Table S2 | Fossil Calibrations used in the divergence time estimate in BEAST2.

Supplementary Table S3 | Corresponding taxonomic names for the stick and leaf insect eggs pictured in **Figure 3**.

Supplementary Data Sheet 1 | Nexus input file.

REFERENCES

Bedford, G. O. (1978). Biology and ecology of the Phasmatodea. *Ann. Rev. Entomol.* 23, 125–149.

Beier, M. (1968). "Phasmida (Stab- oder Gespenstheuschrecken)," in *Handbuch der Zoologie, IV, 2, Vol. 10,* eds J.-G. Helmcke, D. Starck, and H. Wermuth (Berlin: Walter de Gruyter and Company), 1–56.

Blüthgen, N., Metzner, A., and Ruf, D. (2006). Food plant selection by stick insects (Phasmida) in a Bornean rain forest. *J. Trop. Ecol.* 22, 35–40. doi: 10.1017/S0266467405002749

Bouckaert, R., Heled, J., Kühnert, D., Vaughan, T., Wu, C.-H., Xie, D., et al. (2014). BEAST 2: a software platform for bayesian evolutionary analysis. *PLoS Comput. Biol.* 10: e1003537. doi: 10.1371/journal.pcbi.1003537

Bradler, S. (2009). Phylogenie der Stab- und Gespenstschrecken (Phasmatodea). *Spec. Phyl. Evol.* 2, 3–139. doi: 10.17875/gup2009-710

Bradler, S. (2015). Der phasmatodea tree of life: Überraschendes und Ungeklärtes in der Stabschrecken-Evolution. *Entomologie heute* 27, 1–23.

Bradler, S., and Buckley, T. R. (2018). "Biodiversity of Phasmatodea" in *Insect Biodiversity: Science and Society, Volume II*, eds R. G. Foottit and P. H. Adler (Hoboken, NJ: Wiley-Blackwell), 281–313.

Bradler, S., Cliquennois, N., and Buckley, T. R. (2015). Single origin of Mascarene stick insects:ancient radiation on sunken islands? *BMC Evol. Biol.* 15:196. doi: 10.1186/s12862-015-0478-y

Bradler, S., Robertson, J. A., and Whiting, M. F. (2014). A molecular phylogeny of Phasmatodea with emphasis on Necrosciinae, the most species-rich subfamily of stick insects. *Syst. Entomol.* 39, 205–222. doi: 10.1111/syen.12055

Bradley, J. C., and Galil, B. S. (1977). The taxonomic arrangement of the Phasmatodea with keys to the subfamilies and tribes. *Proc. Entomol. Soc. Washington* 79, 176–208.

Bragg, P. E. (2001). *Phasmids of Borneo.* Borneo; Kota: Natural History Publications Kinabalu, 772.

Brock, P. D., Büscher, T. H., and Baker, E. (2017). "Phasmida species file online: phasmida species file version 5.0/5.0," in *Species 2000 and ITIS Catalogue of Life*, eds Y. Roskov, G. Ower, T. Orrell, D. Nicolson, N. Bailly, P. M. Kirk, T. Bourgoin, R. E. DeWalt, W. Decock, E. van Nieukerken, J. Zarucchi, and L. Penev (Leiden: Species 2000; Naturalis). Available online at: www.catalogueoflife.org/col

Brusca, R. C., Moore, W., and Shuster, S. M. (2016). *Invertebrates, 3rd Edn.* Sunderland, MA: Sinauer Associates, 500.

Buckley, T. R., Attanayake, D., and Bradler, S. (2009). Extreme convergence in stick insect evolution: phylogenetic placement of the Lord Howe Island tree lobster. *Proc. R. Soc. Lond. B* 276, 1055–1062. doi: 10.1098/rspb.2008.1552

Buckley, T. R., Attanayake, D., Nylander, J. A. A., and Bradler, S. (2010). The phylogenetic placement and biogeographical origins of the New Zealand stick insects (Phasmatodea). *Syst. Entomol.* 35, 207–225. doi: 10.1111/j.1365-3113.2009.00505.x

Büscher, T. H., Buckley, T. R., Grohmann, C., Gorb, S. N., and Bradler, S. (2018). The evolution of tarsal adhesive microstructures in stick and leaf insects (Phasmatodea). *Front. Ecol. Evol.* 6:69. doi: 10.3389/fevo.2018.00069

Carlberg, U. (1983). A review of different types of egglaying in the Phasmida in relation to the shape of the eggs and with a discussion on their taxonomic importance (Insecta). *Biol. Zentralblatt* 102, 587–602.

Carlberg, U. (1987). "Evolutionary and ecological aspects on ovarian diversity in Phasmida,"in *Evolutionary Biology of Orthopteroid Insects*, ed B. Baccetti (Chichester: Ellis Horwood Ltd.), 174–176.

Compton, S. G., and Ware, A. B. (1991). Ants disperse the elaiosome-bearing Eggs of an African stick insect. *Psyche* 98, 207–213.

Edgar, R. C. (2004). MUSCLE: Multiple sequence alignment with high accuracy and high throughput. *Nucleic Acid Res.* 32, 1792–1797. doi: 10.1093/nar/gkh340

Eisner, T., Morgan, R. C., Attygalle, A. B., Smedley, S. R., Herath, K. B., and Meinwald, J. (1997). Defensive production of quinoline by a phasmid insect (*Oreophoetes peruana*). *J. Exp. Biol.* 200, 2493–2500.

Engel, M. S., Wang, B., and Alqarni, A. S. (2016). A thorny, 'anareolate' stick-insect (Phasmatidae s.l.) in Upper Cretaceous amber from Myanmar, with remarks on diversification times among Phasmatodea. *Cret. Res.* 63, 45–53. doi: 10.1016/j.cretres.2016.02.015

Friedemann, K., Wipfler, B., Bradler, S., and Beutel, R. G. (2012). On the head morphology of *Phyllium* and the phylogenetic relationships of Phasmatodea (Insecta). *Act. Zool.* 93, 184–199. doi: 10.1111/j.1463-6395.2010.00497.x

Ghiselli, F., Milani, L., Scali, V., and Passamonti, M. (2007). The *Leptynia hispanica* species complex (Insecta Phasmida): polyploidy, parthenogenesis, hybridization and more. *Mol. Ecol.* 16, 4256–4268. doi: 10.1111/j.1365-294X.2007.03471.x

Goldberg, J., Bresseel, J., Constant, J., Kneubühler, B., Leubner, F., Michalik, P., et al. (2015). Extreme convergence in egg-laying strategy across insect orders. *Sci. Rep.* 5:7825. doi: 10.1038/srep07825

Günther, K. (1953). Über die taxonomische Gliederung und geographische Verbreitung der Insektenordnung der Phasmatodea. *Beitr. Entomol.* 3, 541–563.

Hennemann, F. H., and Conle, O. V. (2008). Revision of Oriental Phasmatodea: the tribe Pharnaciini, Günther, 1953, including the description of the world's longest insect, and a survey of the family Phasmatidae Gray, 1835 with keys to the subfamilies and tribes (Phasmatodea: "Anareolatae": Phasmatidae). *Zootaxa* 1906, 1–316. Available online at: https://www.mapress.com/zootaxa/2008/f/z01906p316f.pdf

Hennemann, F. H., Conle, O. V., Brock, P. D., and Seow-Choen, F. (2016). Revision of the Oriental subfamily Heteropteryginae Kirby, 1896, with a re-arrangement of the family Heteropterygidae and the descriptions of five new species of *Haaniella* Kirby, 1904. *(Phasmatodea: Areolatae: Heteropterygidae). Zootaxa* 4159, 1–219. doi: 10.11646/zootaxa.4159.1.1

Hughes, L., and Westoby, M. (1992). Capitula on stick insects and elaiosomes on seeds: convergent adaptations for burial by ants. *Funct. Ecol.* 6, 642–648.

Kômoto, N., Yukuhiro, K., Ueda, K., and Tomita, S. (2011). Exploring the molecular phylogeny of phasmids with whole mitochondrial genome sequences. *Mol. Phylogenet. Evol.* 58, 43–52. doi: 10.1016/j.ympev.2010.10.013

Katoh, K., and Toh, H. (2008). Recent developments in the MAFFT multiple sequence alignment program. *Brief. Bioinformatics* 9, 276–285. doi: 10.1093/bib/bbn013

Kevan, D. K. McE. (1977). The higher classification of orthopteroid insects: a general view. *Lyman Entomol. Mus. Res. Lab. Memoirs* 4, 1–31.

Kevan, D. K. McE. (1982). "Phasmatoptera," in *Synopsis and Classification of Living Organisms*, *Vol. 2*. ed S. F. Parker (New York, NY: McGraw-Hill), 379–383.

Klug, R., and Bradler, S. (2006). The pregenital abdominal musculature in phasmids and its implications for the basal phylogeny of Phasmatodea (Insecta: Polyneoptera). *Organ. Divers. Evol.* 6, 171–184. doi: 10.1016/j.ode.2005.08.004

Kobayashi, S., Usui, R., Nomoto, K., Ushirokita, M., Denda, T., and Izawa, M. (2014). Does egg dispersal occur via the ocean in the stick insect genus *Megacrania* (Phasmida: Phasmatidae)? *Ecol. Res.* 29, 1025–1032. doi: 10.1007/s11284-014-1188-4

Lanfear, R., Frandsen, P. B., Wright, A. M., Senfeld, T., and Calcott, B. (2016). PartitionFinder 2: new methods for selecting partitioned models of evolution for molecular and morphological phylogenetic analyses. *Mol. Biol. Evol.* 34, 772–773. doi: 10.1093/molbev/msw260

Law, J. H., and Crespi, B. J. (2002). The evolution of geographic parthenogenesis in *Timema* walking-sticks. *Mol. Ecol.* 11, 1471–1489. doi: 10.1046/j.1365-294X.2002.01547.x

Lengyel, S., Gove, A. D., Latimer, A. M., Majer, J. D., and Dunn, R. R. (2009). Ants sow the seeds of global diversification in flowering plants. *PLOS ONE* 4:e5480. doi: 10.1371/journal.pone.0005480

Lengyel, S., Gove, A. D., Latimer, A. M., Majer, J. D., and Dunn, R. R. (2010). Convergent evolution of seed dispersal by ants, and phylogeny and biogeography in flowering plants: a global survey. *Perspect. Plant Ecol. Evol. Syst.* 12, 43–55. doi: 10.1016/j.ppees.2009.08.001

Maddison, W. P., and Maddison, D. R. (2017). *Mesquite: A Modular System for Evolutionary Analysis*. Version 3.31 Available online at: http://mesquiteproject.org

Maginnis, T. L. (2006). Leg regeneration stunts wing growth and hinders flight performance in a stick insect (*Sipyloidea sipylus*). *Proc. R. Soc. Lond. B* 273, 1811–1814. doi: 10.1098/rspb.2006.3508

Miller, M. A., Pfeiffer, W., and Schwartz, T. (2010). "Creating the CIPRES Science Gateway for inference of large phylogenetic trees," in *Proceedings of the Gateway Computing Environments Workshop (GCE)* (New Orleans, LA), 1–8.

Misof, B., Liu, S., Meusemann, K., Peters, R. S., Donath, A., Mayer, C., et al. (2014). Phylogenomics resolves the timing and pattern of insect evolution. *Science* 346, 763–767. doi: 10.1126/science.1257570

Moore, P. D. (1993). How to get carried away. *Nature* 361, 304–305.

Priddel, D., Carlile, N., Humphrey, M., Fellenberg, S., and Hiscox, D. (2003). Rediscovery of the 'extinct' Lord Howe Island stick-insect (*Dryococelus australis* (Montrouzier)) (Phasmatodea) and recommendations for its conservation. *Biodivers. Conserv.* 12, 1391–1403. doi: 10.1023/A:1023625710011

Rambaut, A. (2012). *FigTree v1.4*. Available online at: http://tree.bio.ed.ac.uk/software/figtree/

Rambaut, A., and Drummond, A. J. (2016). *TreeAnnotator v1.8.4*. Available online at: http://www.beast2.org/

Rambaut, A., Suchard, M. A., Xie, D., and Drummond, A. J. (2014). *Tracer v1.6*. Available online at: http://beast.bio.ed.ac.uk/Tracer

Robertson, J. A., Slipinski, A., Moulton, M., Shockley, F., Giorgi, A., Lord, N. P., et al. (2015). Phylogeny and classification of Cucujoidea and the recognition of a new superfamily Coccinelloidea (Coleoptera: Cucujiformia). *Syst. Entomol.* 40, 745–778. doi: 10.1111/syen.12138

Scali, V. (2009). "Stick insects: parthenogenesis, polyploidy and beyond," in *Life and Time: The Evolution of Life and its History*, eds S. Casellato, P. Burighel, and A. Minelli (Padova: Cleup), 171–192.

Scali, V., Milani, L., and Passamonti, M. (2012). Revision of the stick insect genus *Leptynia*: description of new taxa, speciation mechanism and phylogeography. *Contrib. Zool.* 81, 25–42. Available online at:http://www.ctoz.nl/vol81/nr01/a02

Scali, V., Milani, L., and Passamonti, M. (2013). Description and ecology of new *Pijnackeria* stick insects: four bisexual species and a triploid parthenogen with their phyletic relationships. *J. Zool. Syst. Evol. Res.* 51, 213–226. doi: 10.1111/jzs.12018

Schwander, T., Henry, L., and Crespi, B. J. (2011). Molecular evidence for ancient asexuality in *Timema* stick insects. *Curr. Biol.* 21, 1129–1134. doi: 10.1016/j.cub.2011.05.026

Sellick, J. T. (1997a). The range of egg capsule morphology within the Phasmatodea and its relevance to the taxonomy of the order. *Ital. J. Zool.* 64, 97–104.

Sellick, J. T. (1997b). Descriptive terminology of the phasmid egg capsule, with an extended key to the phasmid genera based on egg structure. *Syst. Entomol.* 22, 97–122.

Seow-Choen, F. (2016). *A Taxonomic Guide to the Stick Insects of Borne*. Borneo; Kota Kinabalu: Natural History Publications, 454.

Shelomi, M., Danchin, E. G. J., Heckel, D., Wipfler, B., Bradler, S., Zhou, X., et al. (2016). Horizontal gene transfer of pectinases from bacteria preceded the diversification of stick and leaf insects. *Sci. Rep.* 6:26388. doi: 10.1038/srep26388

Stamatakis, A., Hoover, P., and Rougemont, J. (2008). A rapid bootstrap algorithm for the RAxML Web-Servers. *Syst. Biol.* 57, 758–771. doi: 10.1080/10635150802429642

Stamatakis, A., Ludwig, T., and Meier, H. (2005). RAxML-III: a fast program for maximum likelihood-based inference of large phylogenetic trees. *Bioinformatics* 21, 456–463. doi: 10.1093/bioinformatics/bti191

Stanton, A. O., Dias, D. A., and O'Hanlon, J. C. (2015). Egg dispersal in the Phasmatodea: convergence in chemical signalling strategies between plants and animals? *J. Chem. Ecol.* 41, 689–695. doi: 10.1007/s10886-015-0604-8

Suetsugu, K., Funaki, S., Takahashi, A., Ito, K., and Yokoyama, T. (2018). Potential role of bird predation in the dispersal of otherwise flightless stick insects. *Ecology* 99, 1504–1506. doi: 10.1002/ecy.2230

Talavera, G., and Castresana, J. (2007). Improvement of phylogenies after removing divergent and ambiguously aligned blocks from protein sequence alignments. *Syst. Biol.* 56, 564–577. doi: 10.1080/10635150701472164

Tilgner, E. H. (2002). *Systematics of Phasmida*. Dissertation, University of Georgia, Athens, GA.

Trewick, S. A., Morgan-Richards, M., and Collins, L. J. (2008). Are you my mother? Phylogenetic analysis reveals orphan hybrid stick insect genus is part of a monophyletic New Zealand clade. *Mol. Phylogenet. Evol.* 48, 799–808. doi: 10.1016/j.ympev.2008.05.025

Vaidya, G., Lohman, D., and Meier, R. (2011). SequenceMatrix: concatenation software for the fast assembly of multi-gene datasets with character set and codon information. *Cladistics* 27, 171–180. doi: 10.1111/j.1096-0031.2010.00329.x

Wedmann, S., Bradler, S., and Rust, J. (2007). The first fossil leaf insect: 47 million years of specialized cryptic morphology and behavior. *Proc. Natl. Acad. Sci. U.S.A.* 104, 565–569. doi: 10.1073/pnas.0606937104

Whiting, M. F., Bradler, S., and Maxwell, T. (2003). Loss and recovery of wings in stick insects. *Nature* 421, 264–267. doi: 10.1038/nature01313

Windsor, D. M., Trapnell, D. W., and Amat, G. (1996). The egg capitulum of a Neotropical walkingstick, *Calynda biscuspis*, induces aboveground egg dispersal by the ponerine ant, *Ectatomma ruidum*. *J. Inst. Behav.* 9, 353–367.

Yoder, J. B., Clancey, E., Des Roches, S., Eastman, J. M., Gentry, L., Godsoe, W., et al. (2010). Ecological opportunity and the origin of adaptive radiations. *J. Evol. Biol.* 23, 1581–1596. doi: 10.1111/j.1420-9101.2010.02029.x

Zompro, O. (2004). Revision of the genera of the Areolatae, including the status of *Timema* and *Agathemera* (Insecta, Phasmatodea). *Verhandl. Naturw. Ver. Hamburg* 37, 1–327.

Conflict of Interest Statement: The authors declare that the research was conducted in the absence of any commercial or financial relationships that could be construed as a potential conflict of interest.

frontiers in Ecology and Evolution

ORIGINAL RESEARCH
published: 02 April 2019
doi: 10.3389/fevo.2019.00105

When Giant Stick Insects Play With Colors: Molecular Phylogeny of the Achriopterini and Description of Two New Splendid Species (Phasmatodea: *Achrioptera*) From Madagascar

Frank Glaw[1], *Oliver Hawlitschek*[1], *Andreas Dunz*[1], *Julia Goldberg*[2] *and Sven Bradler*[2]*

[1] Zoologische Staatssammlung München (ZSM-SNSB), München, Germany, [2] Johann-Friedrich-Blumenbach-Institut für Zoologie und Anthropologie, Georg-August-Universität Göttingen, Göttingen, Germany

OPEN ACCESS

Edited by:
Anthony I. Cognato,
Michigan State University,
United States

Reviewed by:
Bjarte Henry Jordal,
University of Bergen, Norway
Rebecca Barr Simmons,
University of North Dakota,
United States

***Correspondence:**
Sven Bradler
sbradle@gwdg.de

Specialty section:
This article was submitted to Phylogenetics, Phylogenomics, and Systematics, a section of the journal Frontiers in Ecology and Evolution

Received: 05 December 2018
Accepted: 15 March 2019
Published: 02 April 2019

Citation:
Glaw F, Hawlitschek O, Dunz A, Goldberg J and Bradler S (2019) When Giant Stick Insects Play With Colors: Molecular Phylogeny of the Achriopterini and Description of Two New Splendid Species (Phasmatodea: Achrioptera) From Madagascar. Front. Ecol. Evol. 7:105. doi: 10.3389/fevo.2019.00105

Achrioptera is a taxon of extremely large and exceptionally colorful stick insects endemic to Madagascar and the Comoros Archipelago. We studied the phylogenetic position of the Achriopterini, comprising the genera *Achrioptera* and *Glawiana*, based on a multigene phylogeny and concluded that it is a sister group to other Madagascan phasmids (Anisacanthidae) rather than to Neotropical or Australo-Pacific groups as was suggested in a previous study based on morphology. Our results also point to unresolved relationships (potential paraphyly of *Achrioptera*), taxonomic issues (elevation of *A. punctipes cliquennoisi* to species level), and detection of cryptic diversity (in *A. impennis*), demonstrating the need of additional research. A DNA barcoding approach based on COI sequences of *Achrioptera* species revealed a clear discrimination between closely related and morphologically similar species. Applying integrative taxonomy using multiple lines of evidence, we demonstrated that the well-known species with blue males from Montagne des Français and Foret d'Orangea in the far north of Madagascar, previously attributed to *Achrioptera fallax*, represents a new species, which we describe as *Achrioptera manga* sp. nov. based on morphological, chromatic, and genetic (mitochondrial and nuclear) differences. We also describe a second new giant species from this massif: *Achrioptera maroloko* sp. nov. is among the largest insects (females reaching up to 24 cm total length) and differs from its sister species *A. spinosissima* from western Madagascar in morphology, coloration, and substantial DNA barcode divergence. These magnificent new species confirm the significance of the Montagne des Français area as a hotspot of biodiversity and microendemism. The biogeographic pattern of the species pair *A. fallax*/*A. manga* is paralleled by species pairs of reptiles and amphibians suggesting a similar evolutionary history. Finally, we discuss the sexual dichromatism of

Achrioptera species with conspicuous males and mostly cryptic females. As possible reasons, we consider female mate choice and divergent habits of males and females, but aposematism combined with toxic substances produced in defense glands or accumulated in the insect's body from nutritional plants are more plausible explanations for this phenomenon.

Keywords: *Achrioptera*, aposematic coloration, biogeography, DNA barcoding, Madagascar, mate choice, new species, multigene phylogeny

INTRODUCTION

Madagascar is one of the largest islands and a global biodiversity hotspot (Myers et al., 2000; Goodman and Benstead, 2003). Its biota has evolved in isolation from other major landmasses for more than 65 million years, making it a prime model region to explore mechanisms of evolutionary diversification (Vences et al., 2009). Insular environments (including large islands) generally favor the evolution of unusual morphology and behavior, including extreme sexual dimorphism, miniaturization, and gigantism (e.g., Lomolino, 2005; Meiri et al., 2008; Miralles et al., 2017).

Stick insects (order Phasmatodea) are widespread herbivores in tropical environments and famous for their excellent plant mimesis. Walking leaves (family Phylliidae) almost perfectly mimic green leaves of plants, whereas most other stick insects are brownish and imitate branches and twigs. Mimesis effectively reduces the predation risk of these insects and—together with other key innovations (Shelomi et al., 2016)—might have significantly contributed to the evolutionary success of the Phasmatodea. Most of the ca. 3,100 known species (Bradler and Buckley, 2018) are entirely cryptically colored. The warning colors of the few aposematic taxa are often restricted to the hindwings (alae) and become only visible when the insects are threatened and display their open wings (Bedford, 1978). This display can be associated with other behaviors including stridulation (e.g., in *Achrioptera*) or spraying chemical defense liquids from glands in the prothorax (e.g., in *Peruphasma schultei*). Only very few aposematic phasmid species show their coloration also when undisturbed (e.g., *Oreophoetes peruana*, Eisner et al., 1997), including the adult males of several large *Achrioptera* species, which permanently present their extremely colorful bodies to the environment. Remarkably, their juvenile stages and their much larger females are cryptically colored.

Over the last decades, substantial progress in the alpha-taxonomy of phasmids has led to the discovery and description of many new species (e.g., Conle et al., 2011) especially from tropical environments, and large-scale molecular studies of phasmids have started to elucidate their phylogenetic relationships (Buckley et al., 2009, 2010; Bradler et al., 2014, 2015; Robertson et al., 2018). However, the stick insects of many regions remain poorly studied and, despite a significant increase of publications in recent years (Hennemann and Conle, 2004; Cliquennois, 2007, 2008), the knowledge of Malagasy Phasmatodea is exceptionally poor. This is also reflected in the low number of described species (77 species according to Brock et al., 2017, Phasmida Species File online) and by the absence of any summarizing paper or book chapter (e.g., this insect group is not covered by Goodman and Benstead, 2003). The only exception is the charismatic genus *Achrioptera* Coquerel, 1861, which is widespread in Madagascar and has one endemic species on the Comoro Islands. This genus, which includes the largest insects of Madagascar, was revised by Hennemann and Conle (2004), who recognized nine species and provided hypotheses on the phylogenetic relationships of the Achriopterini based on morphological characters. These authors already studied two *Achrioptera* species from Montagne des Français in north Madagascar and identified them as *A. spinosissima* (Kirby, 1891) and *A. fallax* Coquerel, 1861, respectively, interpreting the slight differences to previously known populations from other localities as intraspecific variation. Subsequent fieldwork, captive breeding, as well as additional morphological and molecular studies, led to the paper presented here. We investigate the phylogenetic position and internal phylogeny of the Achriopterini based on a multigene approach and apply DNA barcoding for the identification of species within this group. Based on an integrative approach, using multiple lines of evidence, we describe two new giant species from the far north of Madagascar with extremely colorful males and discuss possible evolutionary scenarios to explain these unusual traits.

MATERIALS AND METHODS

Morphological Measurements

For better comparison, the terminology and morphological description scheme follows the *Achrioptera* revision of Hennemann and Conle (2004). Since these authors studied all available type specimens in the genus *Achrioptera* in great detail, we refrained from re-examining the type material and relied on the identification keys in this revision for the diagnosis of the new species described herein. Bragg (1997) was used for clarification when the definitions of terms were unclear. All specimens of the newly described species that were studied are stored in the Zoologische Staatssammlung München (ZSM) and the Mention Zoologie et Biodiversité Animale of the University of Antananarivo (UADBA). We used field numbers of F. Glaw (FGZC) and M. Vences (ZCMV) to identify all type specimens and other individuals used for this study. For morphological measurements we used a

digital caliper to the nearest 0.1 mm and a ruler to the nearest 1.0 mm.

Molecular Laboratory Work and Computational Analyses

We extracted genomic DNA from eggs or muscle tissue using the NucleoSpin® Tissue kit (Macherey-Nagel) following the standard protocol provided by the manufacturer. Following the protocol used in our previous studies (Buckley et al., 2009, 2010; Goldberg et al., 2014; Bradler et al., 2015) we amplified two mitochondrial (COI, COII) and nuclear gene regions (H3, 28S), ∼2.3 kb in total, for 33 new samples. We sequenced COI of 32 further specimens using the primers Jerry (Simon et al., 1994) and TOM1 (Ribera et al., 2010) with the protocol of Hebert et al. (2003). We then edited and quality-checked sequences and generated an alignment of a combination of newly and previously sequenced taxa (see **Supplementary Tables S1,S2**) in Geneious v7.0.1 (available at http://www.geneious.com) and BioEdit v.7.05.3 (Hall, 1999) and then aligned datasets of individual genes in Muscle v.3.6 (Edgar, 2004). We employed the Akaike information criteria (AIC) as implemented in Modeltest v3.745 to select a suitable model of sequence evolution for the combined data.

We separately analyzed two datasets: (1) The DNA barcoding dataset consisting of 49 sequences of *Achrioptera* and *Glawiana* with *Heteropteryx dilatata* as outgroup, and (2) the multigene dataset comprising sequences of 71 taxa of Phasmatodea. The multigene dataset was rooted with the North American stick insect taxon *Timema*, which has been repeatedly demonstrated to form the sister group of all remaining stick and leaf insects (= Euphasmatodea) (Whiting et al., 2003; Klug and Bradler, 2006; Bradler, 2009; Tomita et al., 2011; Gottardo et al., 2012). Phylogenetic trees of both datasets were reconstructed with the GTR substitution model selected for all partitions using Maximum Likelihood (ML) analyses in MEGA 5.2.2 (Tamura et al., 2011) and Bayesian Inference (BI) analyses in MrBayes 3.1.247 (Ronquist and Huelsenbeck, 2003). ML analyses used 1,000 bootstrap repeats. BI used four independent Markov Chain Monte Carlo (MCMC) runs for 10 million generations with a burn-in of 25% and a tree sampling frequency of 1,000. Trees sampled after burn-in of the four runs were merged and used to construct a 50% majority rule consensus tree.

Newly obtained DNA sequences were deposited on GenBank and are listed in **Supplementary Tables S1,S2**.

Registration of Nomenclature

The electronic version of this article in Portable Document Format (PDF) will represent a published work according to the International Commission on Zoological Nomenclature (ICZN), and hence the new names contained in the electronic version are effectively published under that Code from the electronic edition alone. This published work and the nomenclatural acts it contains have been registered in ZooBank, the online registration system for the ICZN. The ZooBank LSIDs (Life Science Identifiers) can be resolved and the associated information viewed through any standard web browser by appending the LSID to the prefix http://zoobank.org/. The LSID for this publication is: urn:lsid:zoobank.org:pub:8DAF68FE-4BDA-4511-B9B0-20B7E1CEB3CD. The online version of this work will be archived and made available from the following digital repositories: Biotaxa (http://biotaxa.org/).

RESULTS AND DISCUSSION

DNA Barcoding and Multigene Phylogeny of the Achriopterini

The final DNA barcoding tree (**Figure 1**) comprised 49 sequences of 416 bp each. Base frequencies were not significantly different from equal (Chi-square tests, $df = 123$; $p = 1.0$). The final alignments are available on DRYAD (http://www.datadryad.org/). ML and BI topologies were largely congruent, though BI did not resolve the monophyly of *Achrioptera fallax* vs. *A. manga* sp. nov. Otherwise, barcoding data revealed a clear distinction between all studied taxa including the new species described herein. Pairwise sequence divergences are provided in **Supplementary Table S3**.

The multigene tree (**Figure 2**) consisted of up to 2.3 kb of nuclear and mitochondrial sequence data for each specimen, depending on gene coverage. We observed excellent support (1.0 BPP) for Aschiphasmatinae, Cladomorphinae, Diapheromerinae, Lanceocercata, Pseudophasmatinae, and Stephanacridini in agreement with previous studies (Whiting et al., 2003; Buckley et al., 2009, 2010; Bradler et al., 2014; Goldberg et al., 2015; Büscher et al., 2018; Robertson et al., 2018). Lonchodinae sensu Bradler et al. (2014) were also supported (0.97 BPP). In contrast to Whiting et al. (2003), Bradler et al. (2014, 2015), Goldberg et al. (2015), and Robertson et al. (2018), Necrosciinae (represented by *Sipyloidea* and *Oxyartes* + *Phaenopharos*) were recovered as polyphyletic. The sister group relationship between Lanceocercata and Stephanacridini was supported (0.92 BPP) as previously suggested (Buckley et al., 2009, 2010; Bradler et al., 2014). Diapheromerinae as sister group to the majority of phasmatodean lineages (0.96 BPP) is in accordance with results obtained by Whiting et al. (2003) and Bradler et al. (2014). The early branches are entirely formed by wingless taxa (*Timema*, *Bacillus*, Diapheromerinae, *Zehntneria*, *Spinonemia,* and *Sceptrophasma*), a pattern also observed by Whiting et al. (2003). *Agathemera* was recovered as sister group to Cladomorphinae (1.0 BPP). The Heteropteryginae were supported as monophyletic (0.99 BPP). Its subgroups Datamini and Heteropteryginae were also well-supported (1.0 BPP). However, Obrimini was recovered as paraphyletic in respect of Datamini with *Hoploclonia* as sister to the latter (1.0 BPP).

Both the Achriopterini and Anisacanthidae were supported as monophyletic (1.0 BPP) and as sister groups to each other (1.0 BPP), as suggested earlier (Bradler et al., 2015; Goldberg et al., 2015; Büscher et al., 2018). We recovered Achriopterini + Anisacanthidae to be a sister group of Heteropteryginae (1.0 BPP). Within Anisacanthidae, the genera *Amphiphasma* and *Xerantherix* appear to be well-established (1.0 BPP), whereas *Leiophasma* was recovered as paraphyletic. Within Achriopterini, we found no support for a sister group

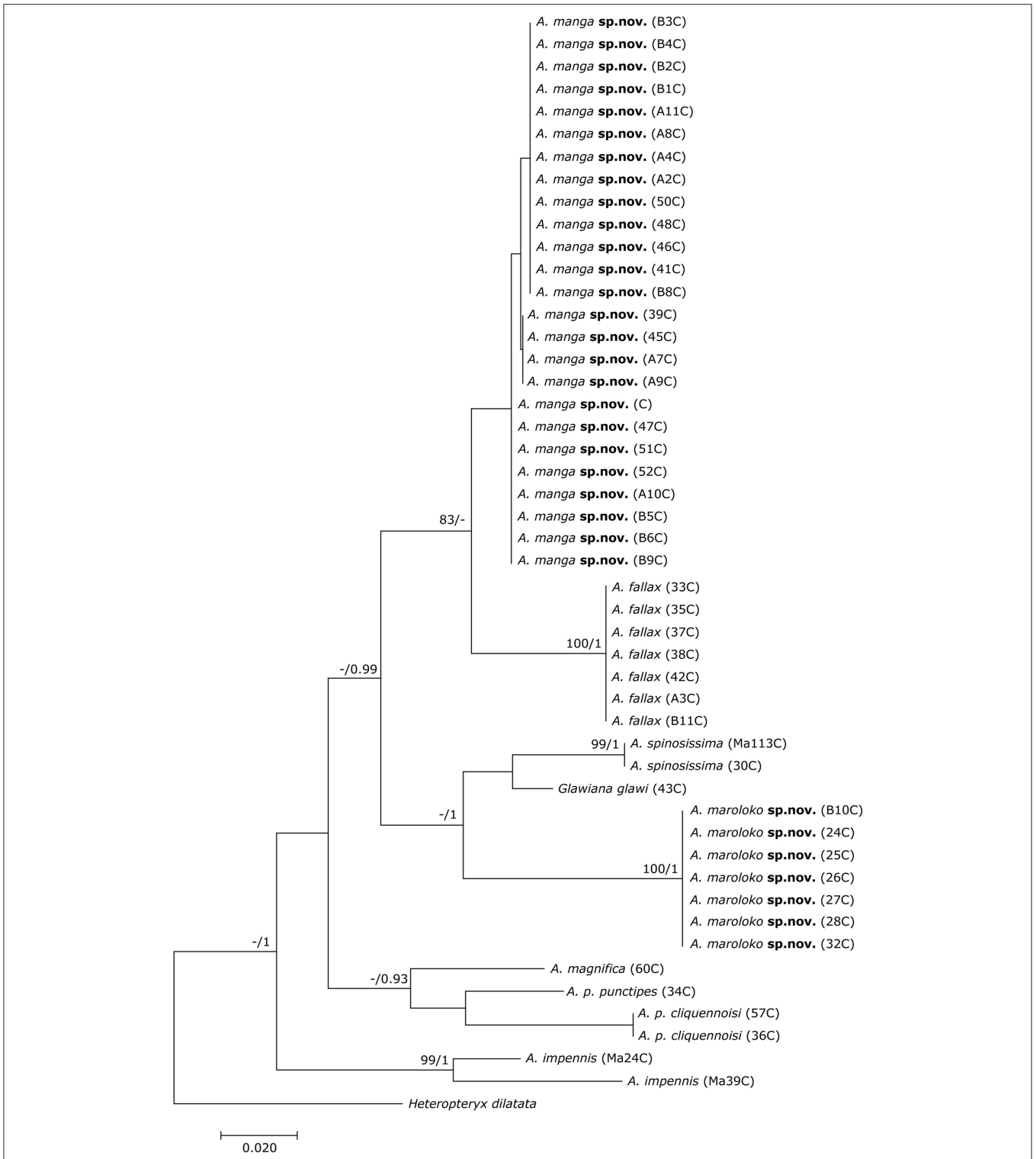

FIGURE 1 | Phylogenetic tree of 48 individuals of *Achrioptera* and *Glawiana*, based on DNA barcode sequences of a fragment of the mitochondrial COI gene (Bayesian inference). *Heteropteryx dilatata* was used as outgroup. ML Bootstrap / BI Posterior Probability support values are given above branches.

relationship between *Achrioptera* and the monotypic *Glawiana*, the latter being possibly more closely related to *A. impennis*. However, due to lack of support, the phylogenetic position of *Glawiana* could not be conclusively established. The remaining *Achrioptera* spp. formed a well-supported lineage (1.0 BPP) with three pairs of sister taxa (1.0 BPP each): (1) *A. fallax*

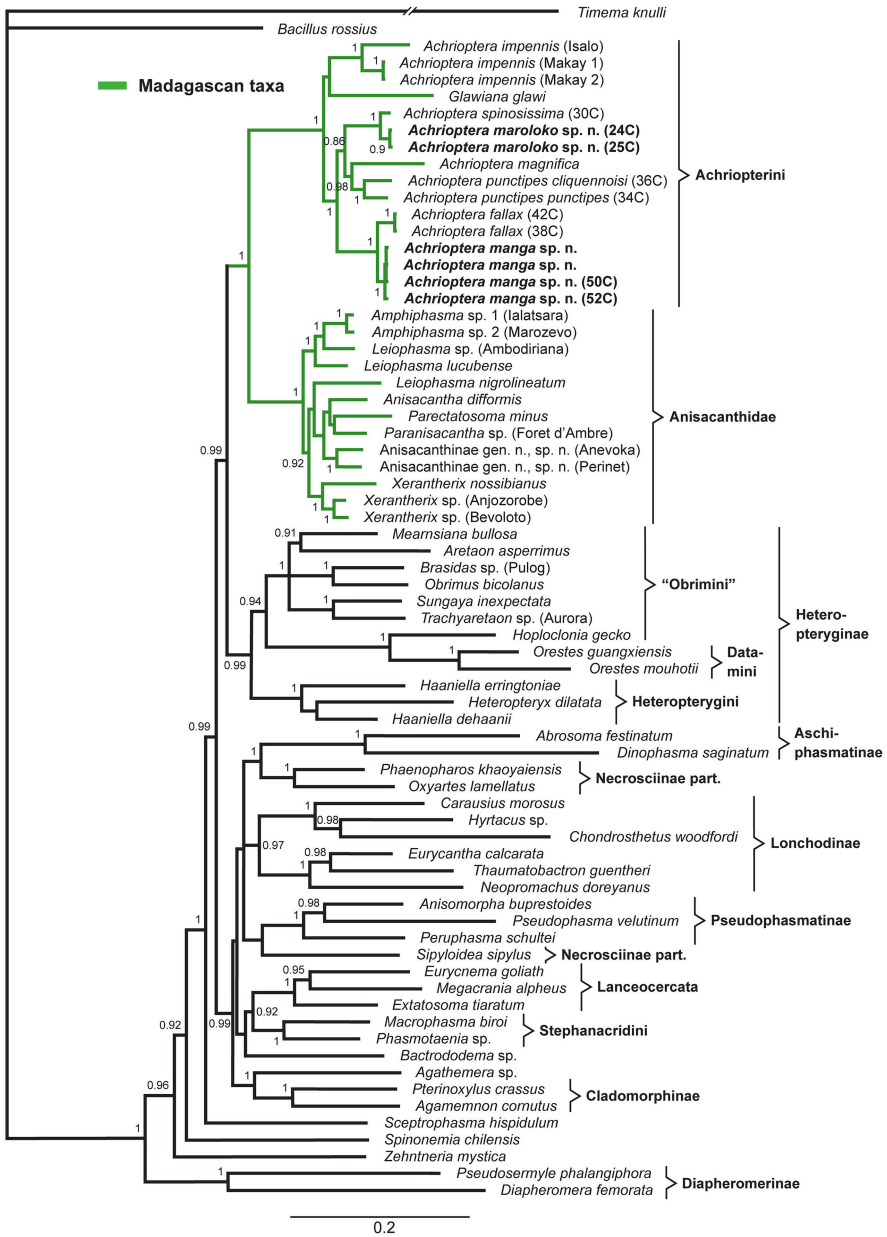

FIGURE 2 | Bayesian phylogenetic tree of 71 phasmatodean specimens showing relationships of the Achriopterini (based on ca. 2.3 kb of mitochondrial and nuclear sequence data). Bayesian Posterior Probability (PP) is given as support value above nodes.

+ *A. manga* sp. nov., (2) *A. magnifica* + *A. punctipes*, and (3) *A. maroloko* sp. nov. + *A. spinosissima*. Within this clade, *A. fallax* + *A. manga* sp. nov. are sisters to the remaining four species. *A. impennis* from Makay and from Isalo show distinct genetic differentiation in both mitochondrial and nuclear genes, suggesting that they may belong to different species. The same is true for the two subspecies *A. punctipes punctipes* and *A. p. cliquennoisi*. We therefore elevate the subspecies *A. punctipes cliquennoisi* to species level (*A. cliquennoisi*).

Identity, Morphology, Coloration, and Reproduction of *Achrioptera fallax*

Achrioptera fallax was described by Coquerel (1861) from the type locality "Port Leven," a coastal locality in northeast Madagascar, which is apparently close to the small island Nosy Manambiby (12°46′00″S, 49°47′00″E), one of the northernmost islands in the Nosy Ankao group (Goodman et al., 2017). Hennemann and Conle (2004) could not trace the male holotype of *A. fallax* in the collection of the Museum nationale d'histoire naturelle (MNHN) in Paris, but the original description by

Coquerel (1861) is accompanied by an excellent color figure of the holotype (reproduced in **Figure 3A**), which clearly shows its morphological and chromatic characteristics. Photographs of males from Ankarana, Andrafiamena, and Daraina agree with the holotype in coloration whereas the populations from further north differ substantially in color (**Figures 3B**, **4D**). Based on the distinctive color differences of males from northern and southern populations, the name *A. fallax* can be unambiguously applied to the greenish southern populations whereas no name is available for the blueish northern form, which will be described below.

Females of *A. fallax* were first described by Hennemann and Conle (2004), but four of the five females studied by them (those from Orangea, Montagne des Français, and Diego Suarez) are from northern populations and therefore refer to the new species described below, whereas the remaining fifth female has no locality data. We therefore characterize the only available adult female specimen from a southern population (*A. fallax* sensu stricto, FGZC 1853 from Ankarana, **Figure 4C**): total length (head plus body) 207 mm, including subgenital plate 216 mm. Generally very similar to the females of the northern populations (*A. manga* sp. nov.) as described by Hennemann and Conle (2004), but generally with more spines (7 spines on pronotum, 17 spines on head, 4 spines on tergum II, 7 spines on sternum III, 1 spine on sternum IV, 1 distinct pair of spines on sternum 7) and a light brown base of the spines on head and thorax. Photographs of another female from Daraina (Bekaraoka, **Figure 4B**) show at least 2 spines on the pronotum, many spines on head, 4 spines on tergum II, 4 spines on tergum III, and also a light brown base of the spines on head and thorax.

The female from Ankarana (collected on 13 February 2008) laid several eggs, which appeared very similar but slightly thicker than eggs of *A. manga*. Eggs were incubated at room temperature. Most juveniles hatched (usually in the early morning) after ca. 120–140 days and appeared slightly darker and slightly larger (ca. 19 mm total length) than those of *A. manga*. Juveniles were fed with bramble leaves. Both males and females became adult as early as 3 months after hatching (faster than *A. manga*). Newly molted adult males were cryptically colored (brown) and reached the final coloration (greenish body with yellow lateral stripe) after ca. 1 week. Two young males secreted a blue liquid (probably hemolyph) from articulations of the limbs for unknown reasons. The first adult female did not show any spines on the pronotum (in contrast to its mother). Subsequently, all insects died for unknown reason and the specimens were lost.

Achrioptera manga sp. nov.

(**Figures 4D,E**)

ZooBank LSID: urn:lsid:zoobank.org:act:0D7185AB-E205-4CFC-962F-DB0D681E0471urn:lsid:zoobank.org:act:0D7185AB-E205-4CFC-962F-DB0D681E0471

Holotype: FGZC 4058 (ZSM DNA Bank Pha-FG-058), adult dried male in good condition, reared in captivity in 2008 from eggs of one of the three females (ZCMV 5356–5358), which were collected at Foret d'Orangea, near Antsiranana, north Madagascar in 2007.

Paratypes: FGZC 4056, adult dried female, collected at Montagne des Français (12°20′02″S, 49°21′31″E, ca. 100 m a.s.l.), near Antsiranana, north Madagascar in February 2004, by F. Glaw, Jaques, Jaquesamis, M. Puente, and R. Randrianiaina; FGZC 1334 and FGZC 4057, two adult males, collected in the Foret d'Orangea, by F. Glaw, P. Bora, H. Enting, Jaques, J. Köhler, and A. Knoll in March 2007; ZCMV 5356–5358, three dried adult females, and UADBA uncataloged, adult female, same locality and collectors as FGZC 1334, collected in February or March 2007; FGZC 1775, adult male, fixed and preserved in ethanol, collected in foret d'Orangea (pitfall line 2), on 22 February 2008 by S. Megson; FGZC 1896, adult male, fixed and preserved in ethanol, collected in Montagne des Français, base camp, on 1 March 2008 by Jaques. The following paratypes were all reared from several eggs laid by the three females ZCMV 5356–5358 from Orangea and bred in several generations in captivity by F. Glaw: FGZC 4059–4068 and FGZC 4104–4125, all adult females; FGZC 4069–4075, FGZC 4078–4102, all adult males; FGZC 4127–4135, all juveniles.

Diagnosis: Females differ (according to the identification key of Hennemann and Conle, 2004, in which they are treated under the name *A. fallax*) from known females of all other *Achrioptera* species except *A. spinosissima*, *A. fallax* and *A. maroloko* sp. nov. (females are unknown from *A. pygmaea* and *A. lobipes*) by a pair of small spines on the prosternum (normally present vs. absent); from *A. spinosissima* and *A. maroloko* sp. nov. by smaller body length (<220 mm) and shorter alae (<30 vs. >50 mm). Females of *A. manga* sp. nov. differ from those of the most similar *A. fallax* by differences in coloration of the anal region of the alae (proximally blackish with indistinct reticulations, bordered by a dark red band distally vs. proximally gray with darker reticulations, bordered by a light red band distally), by a reddish base of the spines on head and thorax (**Figure 4E**) vs. light brown (**Figure 4C**), and generally by fewer spines (0 vs. 2–7 on pronotum, 0–10 vs. 17 on head, mostly 2 (rarely 4) vs. 4 on sternum II, 0–3 vs. 4–7 on sternum III, 0 vs. 1 on sternum IV).

Males differ (according to the identification key of Hennemann and Conle, 2004) from known males of all other *Achrioptera* species (males are unknown from *A. gracilis* and *A. griveaudi*) as follows: From *A. impennis* by fully developed alae (vs. rudimentary, hardly visible alae) and by blue dorsal body coloration (vs. cryptic brown coloration); from *A. pygmaea* and *A. lobipes* by larger body length (>129 vs. <96 mm); from *A. spinosissima* and *A. maroloko* sp. nov. by unarmed pronotum, prosternum and sterna IV–VI (vs. spinose); from *A. fallax* by blue dorsal body coloration (vs. green), by orange ventral parts of femora (vs. yellow), and by coloration of anal region of alae (proximally gray, distally light red to rosy, overall with dark reticulations, becoming less distinct distally vs. proximally blackish, distally dark red, with indistinct reticulation); from all other species (including the junior synonyms *A. intermedia* and *A. composita*, see Redtenbacher, 1908; Carl, 1913) by short alae (<20 mm vs. >33 mm).

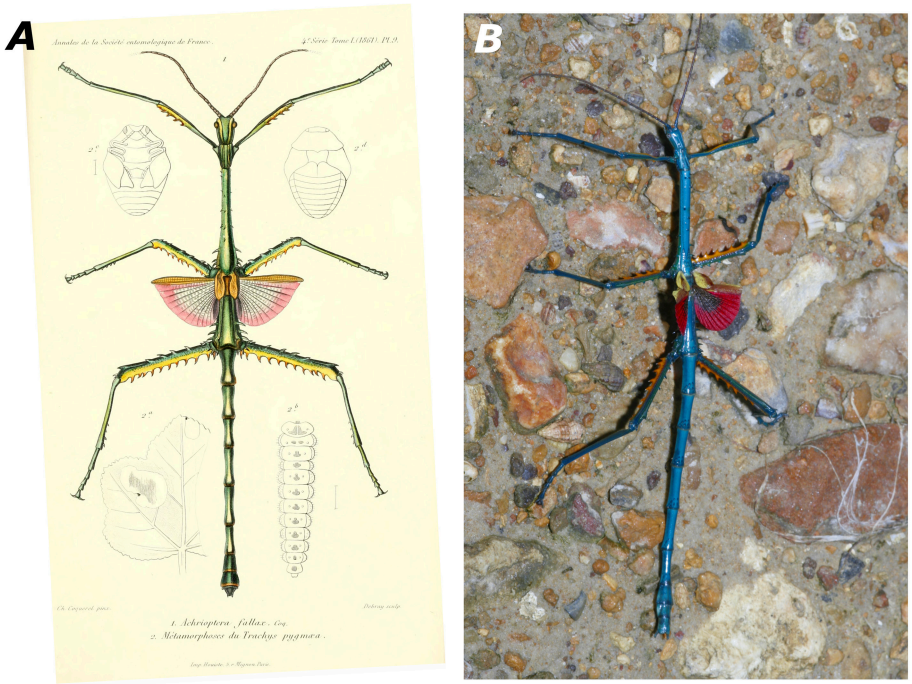

FIGURE 3 | (A) Male holotype of *Achrioptera fallax* from Port Leven (specimen probably lost) as depicted in the original description (Coquerel, 1861, Pl. 9, Figure 1). **(B)** Male paratype of *A. manga* sp. nov. (FGZC 1334) from Foret d'Orangea. With the discovery that the name *A. fallax* has to be applied to the green rather than to the blue species, the epithet "fallax" (meaning spurious) is now finally and truly fitting.

In addition to the morphological and chromatic differences, *A. manga* differs from its sister species *A. fallax* by distinct differentiation in mitochondrial and nuclear genes (**Figures 1**, **2**).

Description of the male holotype FGZC 4058: dried specimen in good condition. Total length (from tip of head to end of abdomen) 154.7 mm; head length 6.2 mm. Body slender (maximum body width 5.4 mm) with long antennae (slightly bent 43.9 mm, stretched length ∼45 mm) reaching to posterior margin of mesonotum. Short tegmina (8.1 mm) and short alae (19.5 mm from insertion of tegmina to end of folded alae). Body surface glabrous and smooth.

Coloration of dried holotype: overall color of body and legs bluish green; ventral surfaces of femora including carinae and spines bright orange. Tibiae and dorsal surface including spines of femora bluish green. All femora irregularly covered with minute white dots. Head with a thin white median line in posterior half, and two lateral lines on each side of which the inner is much more prominent and broader than the outer, starting above the eyes and running along the complete length of the head capsule; another very short white line directly behind the eye. Antennae brownish, scapus, and pedicellus bluish green. Pronotum with a bold, longitudinal white stripe along lateral margins with an incomplete transverse connection, forming a "H-like" marking. Median segment with indistinct, irregular whitish markings. Eyes brownish. Folded tegmina yellowish with a brownish lateral margin, broadening knob-like distally. Folded alae yellowish with broad brown margin.

Head: elongate, 1.5× longer than wide, cylindrical, slightly narrowing toward posterior margin. Dorsal side of head flat and smooth. Eyes strongly convex and prominently projecting from head capsule. Antennae with 28 segments. Scapus and pedicellus almost quadrate, pedicellus smaller than scapus.

Thorax: pronotum slightly longer than head, 2.0× longer than wide, and with a pair of lateral gland openings at front margin. Pronotum and prosternum without spines. Mesothorax elongate, 2.5× longer than length of head and pronotum combined, slightly broadened at posterior margin. Mesonotum anteriorly with two small spines, mesosternum with five small spines posteriorly, and mesopleurae with each one slightly backcurving spine in posterior quarter. Metasternum densely covered with long pointed spines. Spines of meso- and metapleurae large, slightly backcurving, arranged in one longitudinal line of nine spines on each side. Tegmina oval, narrowing toward base. Alae not reaching posterior margin of median segment.

Abdomen: segments II–VI cylindrical, slightly medially constricted. VII slightly shorter than VI, distinctly medially constricted and of bone-like appearance. Sternum II with a posterior pair of medium sized, straight spines, and an additional isolated spine in the middle of the sternum. Terga VIII strongly widening toward posterior margin, trapezoidal, slightly more than half the length of VII. IX 2/3 of the size of VIII. Tergum X as long as IX, almost 1.5× longer than wide, posterior margin raised and with a broad but flat medial notch. Cerci obtuse, slightly projecting over abdominal tergum X. Vomer broad, triangular, lateral margins raised.

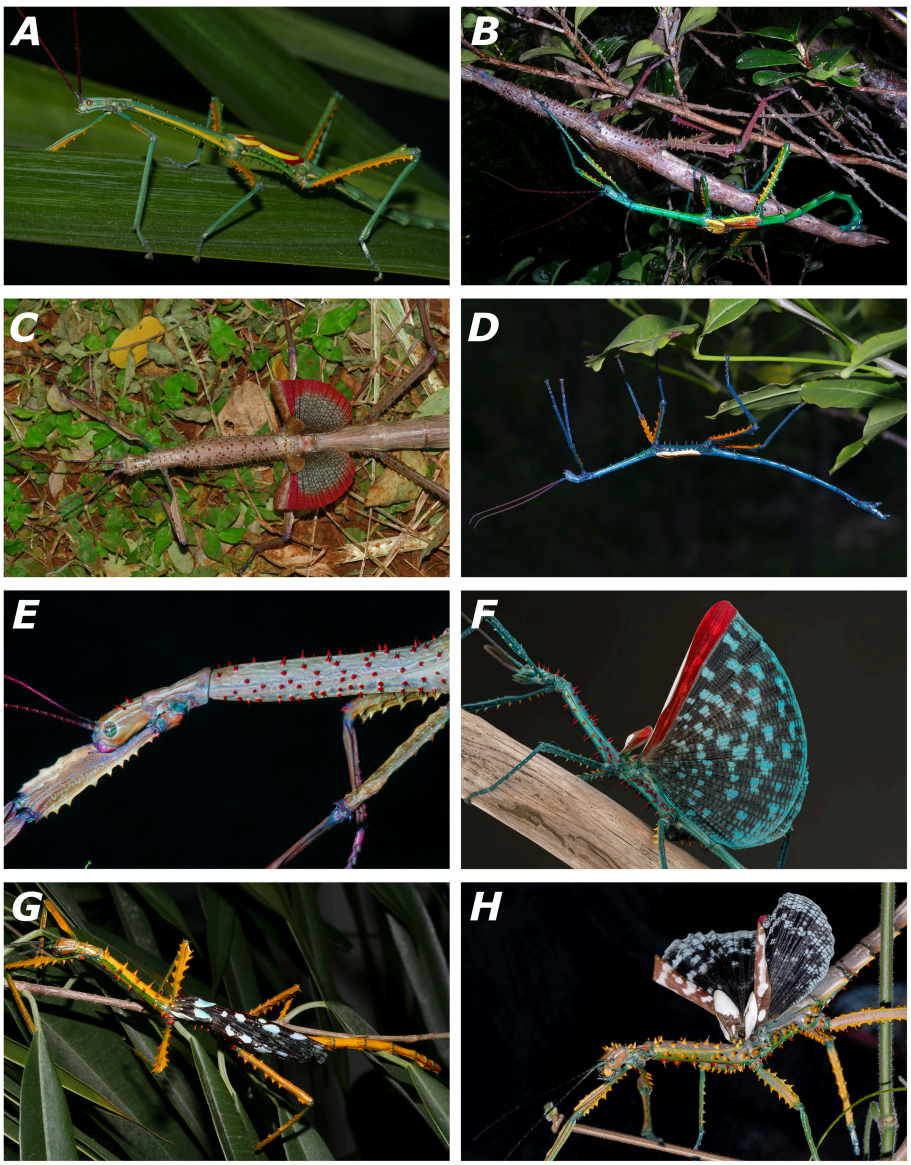

FIGURE 4 | Living specimens of the newly described species of *Achrioptera*. **(A)** *A. fallax*, adult male, captive-bred, reared from eggs of a female from Ankarana (FGZC 1853); **(B)** *A. fallax*, mating couple from Daraina (Bekaraoka) (photo by Louis Nusbaumer); **(C)** *A. fallax*, adult female with exposed wings from Ankarana National Park (FGZC 1853); **(D)** *A. manga*, adult male paratype (FGZC 1334) from Foret d'Orangea; **(E)** *A. manga*, adult female; **(F)** *A. spinosissima*, adult male reared from eggs collected at Marofandilia, near the type locality in west Madagascar (photo by Bruno Kneubühler); **(G)** *A. maroloko* sp. nov., adult male paratype (FGZC 4052) reared from eggs collected at Montagne des Français in dorsolateral view; **(H)** *A. maroloko*, adult female paratype (FGZC 4055), bred in captivity from ancestors of Montagne des Français (photo by Moritz Grubenmann).

Legs: all slender, mid-legs projecting over tergum III, hind-legs reaching posterior margin of abdominal tergum VII. Carinae of profemora raised and smooth. Probasitarsus longer than following two tarsomeres combined. Mesofemora laterally compressed, ventral carinae with seven large, irregular spines, postero-dorsal carina with five spines. Ventral carinae of mesotibiae very minutely tuberculate, dorsal carinae smooth. Metafemora broadened, ventral carinae with 8–10 very prominent, long and pointed spines, dorsal carinae each with 3–4 spines in basal half. Each dorsal carina with an enlarged and slightly lobe-like apical tooth. Ventral carinae of metatibiae with several minute teeth in apical half, dorsal carinae smooth. Meso- and metabasitarsus longer than the following two tarsomeres combined, ventral carinae usually with a single, minute tooth.

Description of the female paratype ZCMV 5356: dried specimen in good condition. Total length (from tip of head to end of subgenital plate) 204.1 mm; head length 9.8 mm. Body moderately slender (maximum body width 8.8 mm) with long antennae (slightly bent 46.1 mm, stretched length ∼48 mm; left antenna partly missing) almost reaching to posterior margin of

mesonotum. Short tegmina (13.2 mm) and short alae (29.4 mm from insertion of tegmina to end of folded alae). Body surface glabrous, thorax spinose.

Coloration of dried specimen after several years of preservation in ethanol: general color of body and legs in various shades of brown and gray. Head brown with seven white longitudinal lines, region between the eyes brown without lines. Eyes brownish. Antennae, scapus, and pedicellus brown. Pronotum largely light gray to whitish with five longitudinal brown lines in the posterior half. Mesonotum brownish, darker than abdomen, posterior region with whitish speckles. Spines on body orange brown with dark tips. Tegmina and alae brown with distinctly lighter yellowish veining.

Head: elongate, 1.7× longer than wide, cylindrical, slightly narrowing toward posterior margin. Dorsal side of head flat with one distinct spine. Eyes strongly convex and prominently projecting from head capsule. Antennae with 29 segments. Scapus and pedicellus almost quadrate, pedicellus smaller than scapus.

Thorax: pronotum slightly shorter than head, 1.5× longer than wide. Pronotum with a pair of lateral gland openings at front margin, without spines. Prosternum with a pair of small spines. Mesothorax elongate, 2.0× combined length of head and pronotum, slightly convex in dorsal view, broadest in middle, all over and densely set with numerous pointed spines. Metasternum very densely covered with long pointed spines. Spines of meso- and metapleurae large, slightly backcurving, spines of metapleurae arranged in two longitudinal lines of seven spines on each side, spines of ventral line pointing downwards. Tegmina oval, narrowing toward base. Alae reaching exactly posterior margin of median segment.

Abdomen: segments II–VI cylindrical, parallel-sided, slightly decreasing in width posteriorly. VII slightly shorter than VI. Sternum II with a posterior pair of medium sized, straight spines. Sternum III similar, but only right spine visible, very small, left spine indistinct. Sternum VII with narrow pair of distinct spines. Tergum VIII mediolaterally compressed, slightly less than half the length of VII. IX slightly less than half size of previous. Tergum X as long as IX, with a clear median keel in posterior half, slightly truncate. Cerci not reaching posterior margin of abdominal tergum X. Subgenital plate keeled, but becoming more flattened toward pointed apex, projecting over tergum X by almost the length of the three terminal terga combined (projecting part 15.1 mm).

Legs: all slender, mid-legs projecting over tergum III, hind-legs projecting over posterior margin of tergum VI. Antero-dorsal carina of profemora strongly raised and with five rough, truncate serrations, postero-ventral carina with 11 medium-sized spines. Carinae of protibiae raised and smooth. Probasitarsus longer than following two tarsomeres combined. Mesofemora laterally compressed, ventral carinae with 8 large, irregular spines, antero-dorsal carina with 2 and postero-dorsal carina with 4 (left)/5 (right) spines. Each dorsal carina with an enlarged slightly lobe-like apical tooth. Ventral carinae of mesotibiae with five small spines in apical half, slightly serrate in basal half, dorsal carinae smooth. Metafemora broadened, ventral carinae with 9–10 very prominent, long and pointed spines, dorsal carinae each with 5–4 spines in basal half. Each dorsal carina with an enlarged slightly lobe-like apical tooth, that of the postero-dorsal carina larger. Ventral carinae of metatibiae with five spines in apical half, dorsal carinae smooth. Meso- and metabasitarsus longer than following two tarsomeres combined, ventral carinae of metabasitarsus usually with a single, minute tooth.

Variation: the color of the dried specimens, which were originally preserved in alcohol (FGZC 1334, 4056, 4057, 5356, 5357, 5358), has faded to cream with distally yellow alae. The colors of specimens still stored in 70% ethanol (FGZC 1775, 1896) have faded to dark brown. The coloration of the freshly dried specimens is mostly similar to the types described in detail. In addition to the orange or deeply yellow ventral surfaces of the femora their basis can have a red band. The number of spines on the head is always 0 in males (0–10 in females) and on the pronotum always 0 in males and females. A pair of spines on the prosternum is present in most *A. manga* females, but can also be absent (this character is used in the identification key of Hennemann and Conle, 2004). The body length varies from 129 to 157 mm in males (total length 135–164 mm) and 176–209 mm in females (total length 189–227 mm).

Eggs: eggs were already described, measured and figured by Hennemann and Conle (2004) based mainly on 14 eggs from a female from Montagne des Français (FGZC 4056) and one dehydrated egg extracted from the ovipositor of a female from Orangea, both here attributed to *A. manga*.

Etymology: the specific epithet "manga" is an adjective in Malagasy language and means blue, referring to the predominantly blue body color of males. It is used here as an invariable noun in apposition.

Distribution and conservation status: *Achrioptera manga* has a small distribution range and is currently only known from Montagne des Français (50 km^2) and the adjacent Foret d'Orangea (16.4 km^2) in far northern Madagascar. Both areas are covered by deciduous dry forest and were threatened by heavy logging until several years ago, but now Montagne des Français appears to be a well-protected communal reserve (F. Glaw, pers. obs. in August 2016) and recently the Orangea region was protected as "Nouvelle aire protégée Oronjia" (http://www.fapbm.org/beneficiaires/nouvelle-aire-protegee-doronjia), indicating that *A. manga* might not be "Critically Endangered" at current. Hennemann and Conle (2004) mapped an additional (unvouchered) locality of *A. fallax* in the Sambirano region, which might indeed refer to *A. fallax* if it can be confirmed. These autors also listed *A. fallax* specimens from two additional localities, in particular one male from Tsivory and one male from Toirory and located both localities in southern Madagascar. Tsivory is indeed a large village in southeastern Madagascar (−24.068419°, 46.074708°), whereas we could not locate the position of Toirory. For biogeographical reasons we consider these southern localities as unlikely to refer to *A. manga*, but we cannot exclude that (1) species morphologically similar to *A. fallax* and *A. manga* occur in southern Madagascar, (2) localities with these names exist in the north or (3) the historical localities were misspelled. The localities Port Leven, Daraina, Andrafiamena and Ankarana refer to *A. fallax*.

Reproduction and behavior in capitivity: eggs laid by the three females ZCMV 5356–5358 in February/March 2007 were incubated at room temperature and most juveniles hatched after 120–140 days, with the exception of one juvenile, which only hatched more than 8 months after egg deposition. Both males and females became adult ca. 4.5–5 months after hatching. Newly hatched adult males were cryptically colored (brown) and fully reached their blue coloration after ca. 1 week when they also started first mating attempts. We assume that most (or even all) *A. manga* currently in culture are descendants of the three paratypes ZCMV 5356–5358, which represented three different COI haplotypes (see **Figure 1**). When threatened or disturbed, both males and females can open their colorful alae and produce stridulating noises.

Achrioptera maroloko sp. nov.

(**Figures 4G,H**)

ZooBank LSID: urn:lsid:zoobank.org:act:52DC7014-DEB7-4095-B56C-2C2D9AB2B26B

Remark: the two wild-captured female paratypes from Montagne des Français (FGZC 4053 and 4051) and some of their eggs were already described and depicted by Hennemann and Conle (2004: Figures 81, 82) in their section "Variation" of *Achrioptera spinosissima*. These authors already noticed that these two females differ from the holotype of *A. spinosissima* (and photographs of further females) from the Morondava region in western Madagascar by (l) fewer spines of the mesothorax; (2) posterior spines of head indistinct or lacking; (3) spine on posterolateral angle of abdominal terga II–VI more prominent; (4) smaller number of serrations on the postero-ventral carina of the profemora; (5) white longitudinal line on costal region of alae indistinct, bold white markings instead and (6) pattern of anal region of alae less regular, darker toward bases and black markings of anal areas 1–2 more prominent. Furthermore, the pronotum of both specimens lacks the posterior pair of spines and in one even lacks the anterolateral spines, both seen in the holotype.

Holotype: FGZC 4049 (ZSM DNA Bank Pha-FG-025), adult dried female, reared in captivity from eggs of the female paratype (FGZC 4053), which was collected in 2003 at Montagne des Français (12°18′45″S 49°20′23″E, 100–200 m a.s.l.), north Madagascar.

Paratypes: FGZC 4053, adult female, originally fixed and preserved in ethanol (coloration faded) and subsequently dried, collected at Montagne des Français (12°18′45″S 49°20′23″E, 100–200 m a.s.l.), north Madagascar in February or March 2003 by F. Glaw and Jaqueamis; FGZC 4051 (ZSM DNA Bank Pha-FG-028), adult female (slightly damaged by ants), originally fixed and preserved in ethanol (coloration faded) and subsequently dried, collected at Montagne des Français (southwest of Andavakoera, no coordinates available), north Madagascar on 28 February 2004 by F. Glaw, M. Puente, R. D. Randrianiaina and Jaques; FGZC 4050 (ZSM DNA Bank Pha-FG-026), adult female, reared in captivity from eggs of the female FGZC 4053; FGZC 4052 (ZSM DNA Bank Pha-FG-024), adult male, reared in captivity from eggs of the female FGZC 4051; FGZC 4055, adult female, fixed and preserved in ca. 70% ethanol (grandparents collected at Montagne des Français), reared in captivity by Moritz Grubenmann from parthenogenetically produced eggs laid by either FGZC 4050 or FGZC 4049.

Additional material: FGZC 4054 (ZSM DNA Bank Pha-FG-032), juveniles, preserved in ethanol, captive-bred (mother from Montagne des Français); two dried juveniles without number (offspring of FGZC 4053, hatched in January or February 2004); 6 eggs (one of these eggs sampled: ZSM DNA Bank Pha-FG-027), offspring of FGZC 4053, hatched in January or February 2004; 5 boxes with numerous eggs (partly hatched), offspring of FGZC 4053, one of the eggs unsuccessfully sampled (ZSM DNA Bank Pha-FG-029).

Diagnosis: females differ (according to the identification key of Hennemann and Conle, 2004) from known females of all other species of *Achrioptera* except *A. spinosissima*, *A. fallax* and *A. manga* (females are unknown from *A. pygmaea* and *A. lobipes*) by a pair of small spines on prosternum (vs. no spines on prosternum) and from *A. gracilis* (155 mm), *A. griveaudi* (185 mm), *A. impennis* (144–182 mm), and *A. magnifica* (156.5–176 mm) by larger size (206–219 mm body length). In addition, they can be distinguished from the poorly known *A. griveaudi* by the presence of 4–6 spines on the pronotum (vs. absence), and from *A. p. punctipes* and *A. p. cliquennoisi* by numerous differences in the coloration of body and wings (e.g., dorsal spines on body yellowish vs. bright green). They differ from *A. fallax* and *A. manga* sp. nov. by reduced alae (vs. fully developed) and from *A. spinosissima* by anal region of alae with dark proximal zone vs. regular pattern of light and dark blotches throughout both proximal and distal zones; possibly by fewer spines on the mesothorax and slightly more colorful body. Further differences in comparison to the holotype of *A. spinosissima* were noticed by Hennemann and Conle (2004) and are provided above.

Males differ (according to the identification key of Hennemann and Conle, 2004) from known males of all other species of *Achrioptera* (males are unknown from *A. gracilis* and *A. griveaudi*) as follows: from *A. impennis* by fully developed alae (vs. rudimentary, hardly visible alae) and by yellow dorsal base coloration on body and limbs (vs. cryptic brown coloration); from *A. pygmaea* and *A. lobipes* by larger body length (>150 mm vs. <96 mm); and from all other species of *Achrioptera* (including the junior synonyms *A. intermedia* and *A. composita*, see Redtenbacher, 1908; Carl, 1913) except *A. spinosissima* by spinose pronotum, prosternum and sterna IV–VI (vs. unarmed). The single male of *A. maroloko* (**Figure 4G**) differs from *A. spinosissima* (**Figure 4F**) by strong differences in coloration (dorsal coloration in life of body and all femora predominantly yellow vs. blue, see **Figures 4F,G**; mesonotum with yellow spines vs. red spines), dorsal side of head without spines but with a single minute and indistinct tubercle (vs. dorsal side of head with 5–9 distinct spines of red color, **Figures 4F,G**), pronotum with single pair of yellow spines (vs. pronotum with 2–7 red spines); and anal region of alae with dark proximal zone vs. regular pattern of light and dark blotches throughout both proximal and distal zones.

In addition to the morphological and chromatic differences, *A. maroloko* differs from its sister species *A. spinosissima* by distinct differentiation of mitochondrial genes (**Figures 1**, **2**).

Description of the female holotype FGZC 4049: dried specimen in good condition. Total length (from tip of head to end of subgenital plate, body slightly bent, subgenital plate slightly bent upwards) 226.4 mm (approximate total length 232.0 mm); head length 10.9 mm. Body moderately slender (maximum body width 12.1 mm) with long antennae (50.4 mm, incomplete) not reaching to posterior margin of mesonotum. Short tegmina (18.4 mm) and fully developed alae (62.1 mm from insertion of tegmina to end of folded ala). Body surface glabrous, head and thorax densely spinose, abdomen smooth dorsally, spinose ventrally.

Coloration of dried holotype: general color of body in various shades of brown and gray. Head cream with a median white line on vertex and each one white line running from posterior edge of eye to posterior end of head on each side. Eyes brownish. Antennae dark greenish, scapus, and pedicellus slightly lighter. Pronotum cream, with one indistinct dorsolateral band of more than 1 mm width per side. Mesonotum reddish brown, lighter than abdomen, with one indistinct white, narrow mid-dorsal line. Abdomen greenish brown. Coxae reddish ventrally. Pro- and mesotibiae, and pro- and mesotarsi dark green; tibiae and basitarsi with numerous irregular white spots. Pro- and mesofemora olive green with indistinct white dots arranged in one regular line between carinae. Metatibiae and metatarsi dull olive green with very indistinct white dots. Metafemora dark brown. Spines on mesonotum with dark base, darker tip, and orange ring in between. Spines on head and pronotum similar, but less distinct. Costal region of tegmina white (positioned laterally in folded wing), anal region brownish proximally, whitish distally. Costal region of alae reddish with lighter rosy blotches. Anal region dark brown, slightly transparent and with numerous transparent pale turquoise spots arranged in irregular transverse bands; spots becoming larger and more numerous toward the outer margin. Anal regions 1–2 with two distinct, elongate rectangular blackish markings.

Head: slightly elongate, 1.4× longer than wide, slightly narrowing toward posterior margin. Dorsal side of head with five spines on each side. Eyes strongly convex and prominently projecting from head capsule. Antennae broken, left antenna with 16 segments. Scapus and pedicellus almost quadrate, pedicellus smaller than scapus.

Thorax: pronotum slightly longer than head, 1.6× longer than wide. Pronotum with a pair of lateral gland openings and 4 spines at anterior margin and a pair of spines near the middle. Prosternum with a pair of small spines. Mesothorax elongate, 2.0× combined length of head and pronotum, parallel sided, slightly broadening posteriorly, all over and densely set with numerous long and pointed spines. Spines on metasternum arranged in five partly irregular pairs. Spines of meso- and metapleurae large, spines of metapleurae arranged in two longitudinal lines of six spines on each side, posterior most pair reduced, spines of ventral line pointing downwards. Tegmina oval, narrowing toward base, costal region always folded downward. Alae almost reaching posterior margin of abdominal tergum III.

Abdomen: segments II–VII cylindrical, parallel-sided. VII slightly shorter than VI. Sterna II to VII with 2 pairs of medium sized, straight spines. Sternum III similar, but only right spine visible, very small, left spine indistinct. Sternum VII with narrow pair of distinct spines. Terga II–V with a ± prominent spine on the posterolateral edge. Tergum VIII mediolaterally compressed, about 2/3 the length of VII. IX slightly less than half size of previous. Tergum X 1/3 longer than IX, with a moderately distinct median keel in posterior half, slightly broadening toward apex, posterior margin rounded. Cerci distinct, spine-like, not projecting over posterior margin of tergum X. Subgenital plate keeled, but becoming more flattened toward pointed apex, projecting far over tergum X.

Legs: all moderately slender, hind-legs projecting over posterior margin of abdominal tergum VI. Antero-dorsal carina of profemora with 5 distinct serrations, postero-ventral carina with 10 medium-sized spines. Inner carina of profemora smooth, with one proximal small spine. Carinae of protibiae raised, undulate. Probasitarsus longer than following two tarsomeres combined. Mesofemora laterally compressed, ventral carinae with 6–8 large, irregular spines, dorsal carinae with 7–8 large spines. Ventral carinae of mesotibiae with 6–7 minute spines, dorsal carinae slightly undulate. Metafemora broadened, ventral carinae with 9–10 large spines, dorsal carinae each with 8–9 spines. Ventral carinae of metatibiae with 9–10, dorsal carinae smooth. Meso- and metabasitarsus longer than following two tarsomeres combined, ventral carinae of metabasitarsus with 2 minute teeth.

Description of the male paratype FGZC 4052: dried specimen in moderate condition (right ala damaged, right protarsus missing). Medium-sized, total length (from tip of head to end of abdomen) 155.1 mm; head length 7.4 mm. Body slender (maximum body width 6.6 mm) with long antennae (48.5 mm, incomplete) reaching beyond posterior margin of mesonotum. Short tegmina (14.9 mm) and fully developed alae (49.8 mm from insertion of tegmina to end of folded ala). Body surface glabrous, head smooth, thorax densely spinose, abdomen smooth dorsally, spinose ventrally.

Coloration of dried paratype: body and legs with areas of dark green and of dull orange to brown, legs covered with minute white spots. All femora dull orange. All tibiae with shades of dark green and of dull orange, portion of orange higher in pro- and metatibiae than in mesotibiae. All tarsi dark green. Head with a thin white median line in posterior half, and two white lateral lines on each side. Upper line starting above the eyes, much more prominent and broader than lower but fading toward posterior end of head. Lower line starting at posterior end of eyes and running along complete length of head capsule. Antennae dark green, scapus and pedicellus slightly lighter. Pronotum with a bold, longitudinal white stripe along lateral margins with an incomplete transverse connection, forming an incomplete 'H-like' marking. Distinct brown blotch between the eyes. Eyes brownish. Mesonotum dull orange dorsally, green toward the lateral margins. Mesopleurae yellowish. Mesosternum green laterally, wine red ventrally. Metanotum dark brown,

metasternum green laterally, ventrally with a very dark red zone covered with darker red spines. Costal region of tegmina white (positioned laterally in folded wing), anal region brown with a distal whitish to turquoise marking. Costal region of alae wine red with lighter rosy to whitish blotches increasing in size distally. Anal region dark brown, slightly transparent and with numerous transparent pale turquoise spots arranged in irregular transverse bands; spots becoming larger and more numerous toward the outer margin. Anal regions 1–2 with three distinct, elongate rectangular blackish markings. Distal part of right wing damaged.

Head: slightly elongate, 1.5× longer than wide, cylindrical, slightly narrowing toward posterior margin. Dorsal side of head flat and smooth, with a single minute and indistinct tubercle. Eyes strongly convex and prominently projecting from head capsule. Antennae incomplete, 17 segments in left antenna. Scapus and pedicellus almost quadrate, pedicellus smaller than scapus.

Thorax: pronotum slightly longer than head, 1.5× longer than wide. Pronotum with a pair of lateral gland openings at front margin, with one dorsal pair of spines, prosternum with one ventral pair of very small spines. Mesothorax elongate, 2× combined length of head and pronotum, slightly broadened at posterior margin, all over covered with numerous long pointed spines (paired on mesosternum). Metapleurae and metasternum densely covered with long pointed spines, spines on metasternum longer and directed ventrally. Tegmina oval, narrowing toward base. Alae reaching abdominal tergum IV.

Abdomen: segments II–VI cylindrical, slightly medially constricted. VII as long as VI, distinctly medially constricted and of bone-like appearance. Sterna II–VII with a pair of medium-sized spines at the middle of the segment, II–VI with an additional pair at posterior end of segment. Pleura II–VI on each side with a single small lateral spine at posterior end, reduced on VI. Terga VIII half the length of VII, strongly widening toward posterior margin, trapezoidal. IX 3/4 of the size of previous, narrowing toward posterior margin. Tergum X longer than VIII and IX, distal margin concave, with a slight dorsal median keel. Cerci spiniform, directed ventrally, not projecting over tergum X. Vomer indistinctly triangular, lateral margins light brownish, slightly raised.

Legs: all slender, hind legs reaching to anterior margin of abdominal tergum IX. Antero-dorsal carina of profemora with four rough serrations, postero-ventral carina with 10 long and straight pointed spines (decreasing in length toward apex of femora). All carinae of protibiae indistinct, without serrations or spines. Mesofemora laterally compressed, carinae with 5–7 large spines. Ventral carinae of mesotibiae with six very small spines, dorsal carinae smooth. Ventral carinae of metafemora with 7–9 prominent, pointed spines. Dorsal carina of right led with irregularly arranged spines, of left leg almost smooth with 2 minute spines. Ventral carinae of metatibiae with 6–7 medium-sized spines, dorsal carinae smooth. Meso- and metabasitarsus longer than following two tarsomeres combined, ventral carinae usually with a single, minute tooth.

Variation: the colors of the two dried females that were originally preserved in alcohol (FGZC 4051 and 4053), and that of FGZC 4055 (still stored in 70% ethanol) have faded. The coloration of FGZC 4050 (a dried female) is similar to the holotype. The number of spines on the head of females varies from 6 to 10 and on the pronotum from 4 to 6. The three dried female paratypes vary in body length from 206 to 219 mm, and in total length from 227 to 242 mm. The single male paratype (FGZC 4052) is described in detail above.

Eggs: eggs were already described, measured and depicted by Hennemann and Conle (2004) based on eggs from Montagne des Français, here attributed to *A. maroloko*.

Etymology: the specific epithet "maroloko" is an adjective in Malagasy language and means colorful, but is used here as an invariable noun in apposition.

Reproduction and behavior in capitivity: ca. 20 eggs were obtained from the female captured in February/ March 2003 (FGZC 4053) and incubated in a plastic dish on a wet sponge at room temperature. Almost exactly 1 year later four brown juveniles hatched, but two of them died a few days later. The two remaining juveniles were fed successfully with leaves of bramble, dog roses and in later stages also with oaks. Larger juveniles were brown with branch-like skin texture and displayed a characteristic resting position (resulting in mimesis of a branch): the mid legs (mesofemora and mesotibia) were folded and adpressed along the body and both front legs were stretched forward in parallel. In this position the insects became very similar to a small branch and almost disappeared from human perception. After the penultimate ecdysis of the two female juveniles rudimentary spines became recognizable on the head. All juvenile stages displayed a cryptic brown, branch-like, coloration, but after the last ecdysis the insects became colorful with fully developed spines. Disturbed adult females opened their colorful alae and sometimes also lifted their front legs and secreted liquid from the prothoracic defense glands, but did no longer show the mimetic resting position of the juveniles.

The first female (either FGZC 4049 or FGZC 4050) had its penultimate ecdysis on 1 July and the ultimate ecdysis on 28 July (<5 months after hatching). It started laying of (parthenogenetically produced) eggs 38 days later (on 4 September) and laid ca. 504 eggs in the following 198 days (resulting in an average of 2.5 eggs per day) until its death on 20 March 2005, more than 12 months after hatching. The second female (ultimate ecdysis ca. 28 August) started egg laying on 11 October and laid at least 449 eggs in the following 198 days (on average 2.27 eggs per day) until its death on 26 April 2005, more than 13 months after hatching. The parthenogenetically produced eggs of these two females partly hatched, but the juveniles refused to feed and died quickly. However, at least one of the parthogenetically produced juveniles (FGZC 4055) was successfully reared to an adult female by M. Grubenmann and returned to the ZSM after its death. Eggs obtained from the female FGZC 4051, collected on 28 February 2004, were initially incubated at room temperature and later transferred to an incubator for reptile eggs. Seven juveniles hatched between 11 January and 6 April 2005, ca. 10–13 months (but mostly 12 months) after egg laying. Most juveniles refused to feed and died quickly, but FGZC 4052 was successfully reared to an adult male.

Distribution and conservation status: *Achrioptera maroloko* is currently only known from Montagne des Français in northern Madagascar (**Figure 5**). This limestone massif is covered by

deciduous dry forest and was threatened by heavy logging until a few years ago, but now appears to be a well-protected communal reserve (F. Glaw, pers. obs. in August 2016). Despite intensive surveys of this massif by the first author and other herpetologists in the period 2000–2016, including numerous nocturnal search excursions, we encountered only two females (although a third female was discovered by N. Cliquennois, pers. comm.), suggesting that this splendid stick insect has low population densities and/or a very cryptic habits, perhaps in the canopy of higher trees. However, based on additional localities listed in Hennemann and Conle (2004) and photographs on the internet, the species complex including *A. maroloko* and *A. spinosissima* might be widespread in the dry forest areas of northern and western Madagascar. Photographs taken by C. Foucault in the Anjajavy reserve (−15.005819, 47.23413) in northwestern Madagascar (see http://www.inaturalist.org/taxa/429526-Achrioptera-spinosissima), showing a dark proximal zone of the alae and a relatively colorful body of females, suggest that this population might belong to *A. maroloko* rather than to *A. spinosissima*. A "giant green and red *Achrioptera* walking stick" was mentioned by Preston-Mafham (1991: 203) for the Ampijoroa Forestry (Ankarafantsika National Park) and could also refer to *A. maroloko*. However, the actual area of occupancy and the range limits of both species are unknown and can only be clarified by future studies. We therefore suggest considering the IUCN conservation of *A. maroloko* status as Data Deficient.

Sexual Dichromatism in *Achrioptera* and the Conspicuous Coloration of Males

Most phasmids resemble sticks and, typically, their coloration is highly cryptic. Only very few species show conspicuous coloration when undisturbed, though some use their conspicuously colored wings to startle potential predators. The genus *Achrioptera* is an exception, since the males of most large species permanently present their extremely colorful bodies to the environment and potential predators. There are several possible explanations for this phenomenon, including the following:

1. Female mate choice: only adult males of *Achrioptera* species are conspicuously colored, while females and juveniles show the typical brown colors that have a strong camouflaging effect and help them mimicking sticks. This could indicate that the male coloration has a signaling function in sexual selection. However, there is no behavioral data that suggests any form of female mate choice in *Achrioptera* and without an efficient defense mechanism the conspicuous coloration would be prone to strong natural selection by predators, making this explanation unlikely.
2. Cryptic functionality of aposematic coloration combined with different habits of males and females: while appearing conspicuous to the human eye, the green and yellow-black male colorations of *A. fallax* and *A. maroloko* (**Figure 4**) may also have a cryptic function for individuals moving among leaves. In searching for mates, males may be more vagile, which reduces the effect of the stick mimesis that works well for the more sedentary females and juveniles. Disruptive coloration may be more beneficial than mimesis in this case. However, at least for the blue males of *A. manga* and *A. spinosissima* it appears unlikely that their coloration can provide any substantial camouflage in the foliage.
3. Aposematism combined with toxic substances produced in defense glands: *Achrioptera* species possess a pair of prothoracic defense glands, which is a defining autapomorphic character of Phasmatodea and is supposed to be present in all stick and leaf insects (Bradler and Buckley, 2018). These glands are usually well-developed in species exhibiting aposematic coloration [e.g., *Oreophoetes*, (Eisner et al., 1997); *Peruphasma*, (Stolz et al., 2015)] and contain repellent substances synthesized by the insects. When disturbed or threatened, both male and female *Achrioptera* open their colorful wings and often produce stridulating noise simultaneously, which might confuse potential predators and warn them about defensive substances. However, this does not explain why males are conspicuously colored when unthreatened whereas females and juveniles show a cryptic coloration. In *Parectatosoma*, a member of the closely related Anisacanthidae, highly effective defensive substances are produced (Dossey et al., 2007), but no studies have been conducted yet to detect potential repulsive or toxic substances in *Achrioptera* spp.
4. Aposematism combined with accumulation of toxic substances from nutritional plants: cryptically colored organism groups like phasmids or frogs are under strong coloration-based selection pressure and accordingly, their freedom in the evolution of deviant colorations is usually very limited. Some frogs (e.g., in the Neotropical family Dendrobatidae and in the genus *Mantella* from Madagascar) are famous exceptions and display a wide variety of conspicuous and aposematic color pattern (Vences et al., 2003a; Brown et al., 2011). Several studies have demonstrated that the aposematically colored frogs contain potent skin toxins (e.g., Daly et al., 1996) and their chemical components are ingested and accumulated with their food (e.g., ants and termites). Their conspicuous coloration therefore serves as a warning signal of toxicity and enables these frogs relatively safe diurnal activity. A similar mechanism could be hypothesized for the conspicuous coloration of *Achrioptera* males. Many species of toxic plants occur in the dry forests of Madagascar including Montagne des Français (Lavranos et al., 2001) and *Achrioptera* might have acquired the ability to digest toxic leaves and to accumulate toxic substances in their bodies, making them uneatable for most predators and allowing them to evolve extreme body colorations like the blue *A. manga*. Blue body color has also evolved in Neotropical poison frogs (Wollenberg et al., 2006) and such a color change can, at least in frogs, happen rather rapidly in aposematic species (Wang and Shaffer, 2008).

The mechanisms producing warning colorations are diverse and phenotypes are often multifunctional, and subject to biotic and abiotic selection pressures (Briolat et al., 2018). In the absence of substantial data on mate selection, habits, predators, natural food plants, toxins produced by defense glands and possible accumulation of toxins of any *Achrioptera* species, finding

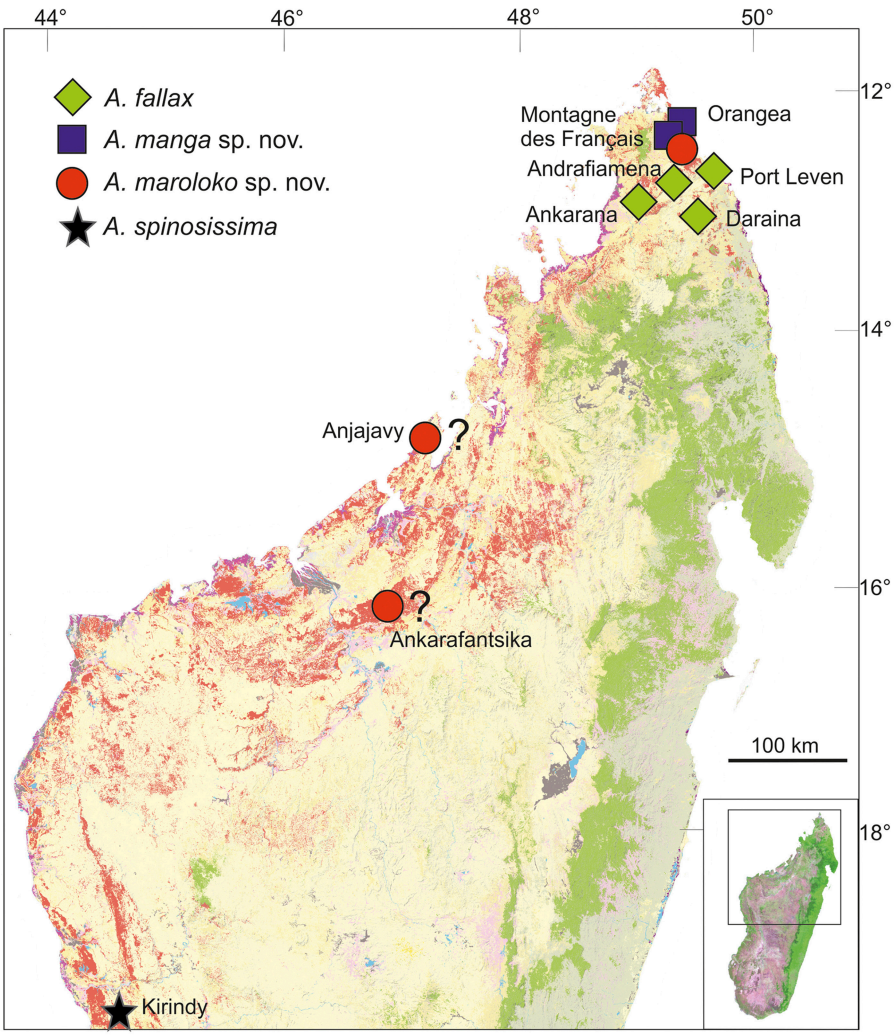

FIGURE 5 | Distribution of *Achrioptera fallax*, *A. manga* sp. nov., *A. maroloko* sp. nov., and *A. spinosissima*. The localities Ankarafantsika and Anjajavy are uncertain. Orange (dry forest) and green (rainforest) show remaining primary vegetation in 2003–2006, modified from the Madagascar Vegetation Mapping Project (http://www.vegmad.org).

evidence for these ideas and hypotheses, may prove difficult and substantial efforts would be required, also because more than one factor may have played a role in the evolution of this remarkably conspicuous coloration.

Origin and Systematic Position of Achriopterini and Anisacanthidae

Traditionally, the genus *Achrioptera* was considered to represent a monotypic tribe, Achriopterini, among the species-rich subfamily Phasmatinae (Günther, 1953). However, Phasmatinae has been demonstrated to represent an artificial assemblage, recovered repeatedly as polyphyletic in numerous phylogenetic studies (Whiting et al., 2003; Bradler, 2009; Buckley et al., 2009, 2010; Dunning et al., 2013; Bradler et al., 2014). In more recent molecular phylogenies, *Achrioptera* is placed as a sister group to the likewise Malagasy stick insect lineage Anisacanthidae (Bradler et al., 2015; Goldberg et al., 2015). Furthermore, a second genus of the Achriopterini, *Glawiana*, was described (Hennemann and Conle, 2004), and the Achriopterini was discussed either as sister group to the Australo-Pacific Stephanacridini or to the Neotropical *Pterinoxylus* (Cladomorphinae) (Hennemann and Conle, 2004). We found no support for a close relationship of *Achrioptera* to either of these groups, namely to *Macrophasma* + *Phasmotaenia* (Stephanacridini) or to *Pterinoxylus* (Cladomorphinae). Instead, Achriopterini is strongly corroborated as a sister group to Anisacanthidae. With both taxa being endemic to Madagascar and the adjacent Comoro Islands, this finding makes sense from a biogeographic point of view. Nonetheless, this result is particularly noteworthy, since Anisacanthidae and Achriopterini are considered to belong to the two different suborders of Phasmatodea, Areolatae, and Anareolatae (Günther, 1953; Zompro, 2004; Cliquennois, 2007, 2008). This traditional subdivision is based on the presence (areolate) or absence

(anareolate) of the area apicalis, a demarcated triangular area located ventrally on the apex of the tibiae (Günther, 1953). Numerous previous studies demonstrated that neither Areolatae nor Anareolatae are monophylectic (Whiting et al., 2003; Bradler, 2009; Buckley et al., 2009; Kômoto et al., 2011, 2012; Tomita et al., 2011; Bradler et al., 2014), yet a close relationship between the anareolate Achriopterini and the areolate Anisacanthidae has never been assumed before based on morphological evidence and comes as a major surprise.

Remarkably, the sister groups Achriopterini and Anisacanthidae display an obvious lack of balance in the degree of splitting at the genus and subfamily levels. Although branch lengths between terminal taxa in the studied Achriopterini are generally similar or even longer than in the studied Anisacanthidae (**Figure 2**), Achriopterini includes only two genera whereas the studied Anisacanthidae includes six described (plus one unnamed) genera and is furthermore divided into three different subfamilies (Anisacanthinae including *Anisacantha*, *Paranisacantha*, *Parectatosoma*, and a presumably unnamed genus; Leiophasmatinae including *Amphiphasma* and *Leiophasma*; and Xerantherinae including *Xerantherix*). Future studies are needed to clarify if this lack of balance correlates with conservatism of morphological evolution in the Achriopterini or indicates shortcomings of the current taxonomy of these groups (e.g., due to oversplitting in the Anisacanthidae). Furthermore, both groups have traditionally been placed at different taxonomic levels (as family in Anisancanthidae and as tribe in Achriopterini), and should be adjusted to the same level once their relationships are sufficiently resolved.

Furthermore, we recovered the areolate Oriental Heteropteryginae to be a sister group of the Malagasy Achriopterini + Anisacanthidae, leading to the assumption of an independent secondary loss of the area apicalis in Achriopterini. The presence of the area apicalis is considered to represent the plesiomorphic condition among stick insects (Bradler, 2009). The hypothesis of a close relationship between Anisacanthidae and Heteropteryginae, with Anisacanthini forming a subgroup of Heteropteryginae, is old (Günther, 1953; Klante, 1976), but was revised by Zompro (2004) who excluded Anisacanthini from Heteropteryginae. This assumption gained acceptance in subsequent studies (Cliquennois, 2007, 2008) and is also supported here.

Hennemann and Conle (2004) argued that Achriopterini "is an evolutionary rather old and unspecialized group of Phasmatodea" due to the animal's large size, long abdomen, strong sexual dimorphism, and presence of wings. These authors proposed a middle to late Jurassic origin of the Achriopterini, when Madagascar was still connected to India, Antarctica and Australia. In contrast, Bradler et al. (2015) estimated a much younger divergence time of 50–35 my between a phylogenetically highly subordinate *Achrioptera* and Anisacanthidae. Our phylogenetic analysis also resolved Achriopterini to be deeply nested among Phasmatodea as part of a previously unexpected Malagasy radiation. Large size and strong sexual dimorphism as exhibited by Achriopterini might represent a secondary modern trait rather than the plesiomorphic condition within Phasmatodea. Recent descriptions of fossil stick insects further corroborate this assumption, as Mesozoic forms were rather small, ranging from 24 to 56 mm, and lacked noteworthy sexual dimorphism (Nel and Delfosse, 2011; Wang et al., 2014).

Large-Scale Biogeography

A sister-group relationship between Heteropteryginae and Achriopterini + Anisacanthidae indicates a single colonization of Madagascar after transoceanic dispersal from the Asian region, as demonstrated before for various plant and animal species (Warren et al., 2009).

However, this sister group relationship was not suggested before, and Bradler et al. (2015) recovered a monophyletic lineage comprising Anisacanthidae + Achriopterini + further Malagasy species and some African and South American taxa, which could indicate a colonization from Africa (most recently also corroborated by Robertson et al., 2018). Traditionally, the gross phylogeny of Phasmatodea was explained by continental drift vicariance (Günther, 1953). Lately, this view was challenged by molecular clock analyses (Buckley et al., 2009; Bradler et al., 2015), favoring a much younger origin of extant taxa (probably after the Tertiary–Cretaceous transition or K-T boundary, ∼66 Ma). Consequently, a high number of transoceanic dispersal events must have shaped the present distribution of stick and leaf insects. The historical biogeography of Malagasy phasmatodeans needs to be addressed in future studies including a more comprehensive taxon sampling from Africa and Madagascar, two largely understudied regions in regards of phasmid systematics.

Apart from unpublished observations (Cliquennois pers. comm.) *Achrioptera griveaudi* is the only known Comoran species of the genus. It is only known from two female specimens, which were extracted from the stomach of a bird (*Leptosomus discolor*) at Moheli Island (Paulian, 1960). The volcanic Comoro archipelago consists of oceanic islands surrounded by deep waters, excluding past physical contact to other land masses through fluctuating sea levels (Vences et al., 2003b). Aside from an unlikely aerial transmarine transport by birds (e.g., as a lost or digested prey with surviving eggs; Suetsugu et al., 2018) overseas dispersal from north Madagascar is thus the most plausible hypothesis to explain the presence of this endemic and flightless species on the Comoros and its similarity with *A. maroloko*. This dispersal mechanism was also used by many other Comoran endemics, including amphibians and reptiles, and is facilitated by prevailing ocean currents (Vences et al., 2003b; Hawlitschek et al., 2017a,b).

Regional Biogeography and Conservation

Northern Madagascar is a mosaic of different geological formations, including old limestone massifs, volcanoes, coastal sands, and other structures. Depending on the topography, climate and vegetation vary substantially as well, ranging from grassland and dry deciduous forest at low altitudes to montane rainforest at high elevations of Montagne d'Ambre. These and other factors have contributed to a remarkable species diversity and endemism in this area. However, the region of Montagne des Français/Orangea has an exceptionally high degree of microendemism, including many species of plants, amphibians

and reptiles (Lavranos et al., 2001; D'Cruze et al., 2007; Glaw et al., 2012), and even one microendemic family of blind-snakes (Wegener et al., 2013). The distribution maps of *A. fallax* and *A. manga* (**Figure 5**) point to the existence of a biogeographical border between the Montagne des Français/Orangea region in the north and the adjacent limestone massifs (Ankarana-Andrafiamena-Analamera) further south. Similar distribution patterns of numerous allopatrically distributed sister species pairs suggests a general biogeographic border for different organism groups, such as geckos of the genus *Paroedura* (Jackman et al., 2008), snakes of the genus *Madagascarophis* (Glaw et al., 2013; Ruane et al., 2016), and dwarf frogs of the genus *Stumpffia* (Köhler et al., 2010).

The Montagne des Français region is currently a hotspot for conservation priorities. The massif was unprotected and affected by heavy logging until several years ago (D'Cruze et al., 2007), but is now an apparently well-protected community-based reserve. The hitherto unprotected, degraded forest of Orangea is now being transformed into the National Park Oronjia. The protection of this area is of particular concern not only for the survival of the microendemic *A. manga*, but also harbors the highest density of critically endangered reptiles in Madagascar (Jenkins et al., 2014) and is home to *Lepilemur septentrionalis*, one of the most threatened primate species in the world (Ranaivoarisoa et al., 2013).

The two new giant insects described in this paper are among the most spectacular insects in the world. The blue *A. manga*, hitherto known as *A. fallax*, has become one of the most famous stick insects after its first successful husbandry and breeding. It is highly desired in the phasmid community and has already served as a model for artwork, paintings, T-shirt prints and others during the past few years. *A. maroloko*, perhaps even more impressive because of its enormous size, its large spines, and its splendid coloration, might be similarly attractive. These splendid phasmids could therefore be used as flagship species to promote local ecotourism in their habitats, awareness of the unique biodiversity of Madagascar, and the need for its protection.

DATA AVAILABILITY

The datasets generated for this study can be found in NCBI GenBank, https://www.ncbi.nlm.nih.gov/genbank/ (the numerous single accession numbers are to be found in **Supplementary Tables S1, S2**).

AUTHOR CONTRIBUTIONS

FG, OH, and SB designed the study. FG, OH, AD, JG, and SB collected the data and wrote the paper. FG, OH, AD, and JG analyzed the data. All authors read, commented on, and approved the final version of the manuscript.

FUNDING

This work was financially supported by the Volkswagen Foundation, the European Association of Zoos and Aquaria and by Act for Nature to FG, and by the German Science Foundation (DFG grant BR 2930/2-1 and BR 2930/5-1) to SB.

ACKNOWLEDGMENTS

We are grateful to numerous friends and colleagues: to Moritz Grubenmann for rearing parthenogenetic *A. maroloko*; to Olivier Arnoult, Nicolas Cliquennois, Moritz Grubenmann, Bruno Kneubühler, and Louis Nusbaumer for providing photographs; to Neil D'Cruze, Falk Sebastian Eckhardt, Arne Hartig, and Bruno Kneubühler for providing crucial tissue samples; to Parfait Bora, Neil D'Cruze, Hildegard Enting, Michael Franzen, Jaques, Jaqueamis, Peter Kappeler, Angelika Knoll, Jörn Köhler, Marta Puente, Steven Megson, and Roger-Daniel Randrianirina for their help in the field work; to York Pareik for his hospitality; to Nicolas Cliquennois, Oskar Conle, Frank Hennemann, Bruno Kneubühler, and Miguel Vences for stimulating discussions; to Tanja Kothe and Bärbel Stock for the preparation of numerous specimens and to Klaus Schönitzer for access to the collection. We are grateful to the Malagasy authorities who kindly issued research and export permits.

SUPPLEMENTARY MATERIAL

The Supplementary Material for this article can be found online at: https://www.frontiersin.org/articles/10.3389/fevo.2019.00105/full#supplementary-material

Supplementary Table S1 | Specimens and samples used for DNA barcoding (COI) GenBank accession numbers.

Supplementary Table S2 | Specimens and samples used for the multigene phylogeny with GenBank accession numbers for each gene.

Supplementary Table S3 | Pairwise genetic distances among sequences of Achrioptera taxa in the COI DNA barcoding fragment.

REFERENCES

Bedford, G. O. (1978). Biology and ecology of the Phasmatodea. *Ann. Rev. Entomol.* 23, 125–149. doi: 10.1146/annurev.en.23.010178.001013

Bradler, S. (2009). Die Phylogenie der Stab- und Gespenstschrecken (Insecta: Phasmatodea). *Spec. Phyl. Evol.* 2, 3–139. doi: 10.17875/gup2009-710

Bradler, S., and Buckley, T. R. (2018). "Biodiversity of phasmatodea," in *Insect Biodiversity: Science and Society*, Vol. II, eds R. G. Foottit and P. H. Adler (Hoboken, NJ: Wiley-Blackwell), 281–313.

Bradler, S., Cliquennois, N., and Buckley, T. R. (2015). Single origin of the Mascarene stick insects: ancient radiation on sunken islands? *BMC Evol. Biol.* 15:196. doi: 10.1186/s12862-015-0478-y

Bradler, S., Robertson, J. A., and Whiting, M. F. (2014). A molecular phylogeny of Phasmatodea with emphasis on Necrosciinae, the most species-rich subfamily of stick insect. *Syst. Entomol.* 39, 205–222. doi: 10.1111/syen.12055

Bragg, P. E. (1997). A glossary of terms used to describe phasmids. *Phasmid Stud.* 6, 24–33.

Briolat, E. S., Burdfield-Steel, E. R., Paul, S. C., Rönkä, K. H., Seymoure, B. M., Stankowich, T., et al. (2018). Diversity in warning coloration: selective paradox or the norm? *Biol. Rev.* 94, 388–414. doi: 10.1111/brv.12460

Brock, P. D., Büscher, T., and Baker, E. (2017). *Phasmida Species File Online*. Available online at: http://phasmida.Speciesfile.org, version 5.0/5.0 (accessed December 30, 2017).

Brown, J. L., Twomey, E., Amézquita, A., de Souza, M. B., Caldwell, J. P., Lötters, S., et al. (2011). A taxonomic revision of the Neotropical poison frog genus *Ranitomeya* (Amphibia: Dendrobatidae). *Zootaxa* 3083, 1–120. doi: 10.11646/zootaxa.3083.1.1

Buckley, T. R., Attanayake, D., and Bradler, S. (2009). Extreme convergence in stick insect evolution: phylogenetic placement of the Lord Howe Island tree lobster. *Proc. R. Soc. B* 276, 1055–1062. doi: 10.1098/rspb.2008.1552

Buckley, T. R., Attanayake, D., Nylander, J. A. A., and Bradler, S. (2010). The phylogenetic placement and biogeographical origins of the New Zealand stick insects (Phasmatodea). *Sys. Ent.* 35, 207–225. doi: 10.1111/j.1365-3113.2009.00505.x

Büscher, T. H., Buckley, T. R., Grohmann, C., Gorb, S. N., and Bradler, S. (2018). The evolution of tarsal adhesive microstructures in stick and leaf insects (Phasmatodea). *Front. Ecol. Evol.* 6:69. doi: 10.3389/fevo.2018.00069

Carl, J. (1913). Phasmides_nouveaux_ou_peu_connus_du_Musém de Genève. *Rev. Suisse Zool.* 21, 1–56. doi: 10.5962/bhl.part.37151

Cliquennois, N. (2007). Aperçu général de la diversité des phasmes de Madagascar (Insecta, Phasmatodea). *Bull. Arthropoda* 32, 3–16. Available online at: https://www.researchgate.net/publication/265848904Apercu_general_de_la_diversite_des_phasmes_de_Madagascar_Insecta_Phasmatodea

Cliquennois, N. (2008). Révision des Anisacanthidae, famille endémique de phasmes de Madagascar (Phasmatodea: Bacilloidea). *Ann. Soc. Entomol. Fr.* 44, 59–85. doi: 10.1080/00379271.2008.10697545

Conle, O. V., Hennemann, F. H., and Gutièrrez, Y. (2011). *The Stick Insects of Colombia*. Norderstedt: Books on Demand.

Coquerel, C. (1861). Orthoptères de bourbon et de Madagaskar. *Ann. Soc. Entomol. Fr.* 4, 495–499, pl. 9.

Daly, J. W., Andriamaharavo, N. R., Andriantsiferana, M., and Myers, C. W. (1996). Madagascan poison frogs (*Mantella*) and their skin alkaloids. *Am. Museum Novitates* 3177, 1–34.

D'Cruze, N., Sabel, J., Green, K., Dawson, J., Gardner, C., Robinson, J., et al. (2007). The first comprehensive survey of amphibians and reptiles at Montagne des Français, Madagascar. *Herpetol. Conserv. Biol.* 2, 87–99.

Dossey, A. T., Walse, S. S., Conle, O. V., and Edison, A. S. (2007). Parectadial, a monoterpenoid from the defensive spray of *Parectatosoma mocquerysi*. *J. Nat. Prod.* 70, 1335–1338. doi: 10.1021/np070151g

Dunning, L. T., Thomson, G., Dennis, A. B., Sinclair, B. J., Newcomb, R. D., and Buckley, T. R. (2013). Positive selection in glycolysis among Australasian stick insects. *BMC Evol. Biol.* 13:215. doi: 10.1186/1471-2148-13-215

Edgar, R. C. (2004). MUSCLE: a multiple sequence alignment method with reduced time and space complexity. *BMC Bioinformatics* 5:113. doi: 10.1186/1471-2105-5-113

Eisner, T., Morgan, R. C., Attygalle, A. B., Smedley, S. R., Herath, K. B., and Meinwald, J. (1997). Defensive production of quinoline by a phasmid insect (*Oreophoetes peruana*). *J. Exp. Biol.* 200, 2493–2500.

Glaw, F., Köhler, J., Townsend, T. M., and Vences, M. (2012). Rivaling the world's smallest reptiles: discovery of miniaturized and microendemic new species of leaf chameleons (*Brookesia*) from northern Madagascar. *PLoS ONE* 7:e31314. doi: 10.1371/journal.pone.0031314

Glaw, F., Kucharzewski, C., Köhler, J., Vences, M., and Nagy, Z. T. (2013). Resolving an enigma by integrative taxonomy: *Madagascarophis fuchsi* (Serpentes: Lamprophiidae), a new opisthoglyphous and microendemic snake from northern Madagascar. *Zootaxa* 3630, 317–322. doi: 10.11646/zootaxa.3630.2.7

Goldberg, J., Bresseel, J., Constant, J., Kneubühler, B., Leubner, F., Michalik, P., et al. (2015). Extreme convergence in egg-laying strategy across insect orders. *Sci. Rep.* 5:7825. doi: 10.1038/srep07825

Goldberg, J., Knapp, M., Emberson, R. M., Townsend, J. I., and Trewick, S. A. (2014). Species radiation of carabid beetles (Broscini: Mecodema) in New Zealand. *PLoS ONE* 9:e86185. doi: 10.1371/journal.pone.0086185

Goodman, S. M., Anbdou, Y., Andriamiarantsoa, Y., Fisher, B. L., Griffiths, O., Keitt, B., et al. (2017). Results of a biological inventory of the Nosy Ankao island group, Parc National de Loky-Manambato, northeastern Madagascar. *Malagasy Nat.* 11, 1–59. Available online at: https://hal.archives-ouvertes.fr/hal-01493362/document

Goodman, S. M., and Benstead, J. P. (eds.) (2003). *The Natural History of Madagascar*. Chicago, IL; London: University of Chicago Press.

Gottardo, M., Mercati, D., and Dallai, R. (2012). The spermatogenesis and sperm structure of *Timema poppensis* (Insecta: Phasmatodea). *Zoomorph.* 131, 209–223. doi: 10.1007/s00435-012-0158-z

Günther, K. (1953). Über die taxonomische Gliederung und geographische Verbreitung der Insektenordnung der Phasmatodea. *Beitr. Entomol.* 3, 541–563.

Hall, T. A. (1999). BioEdit: a user-friendly biological sequence alignment editor and analysis program for Windows 95/98/NT. *Nucl. Acids. Symp. Ser.* 41, 95–98.

Hawlitschek, O., Ramirez Garrido, S., and Glaw, F. (2017a). How marine currents influenced the widespread natural overseas dispersal of reptiles in the Western Indian Ocean region. *J. Biogeogr.* 44, 1435–1440. doi: 10.1111/jbi.12940

Hawlitschek, O., Toussaint, E. F. A., Gehring, P.-S., Ratsoavina, F. M., Cole, N., Crottini, A., et al. (2017b). Gecko phylogeography in the Western Indian Ocean region: the oldest clade of *Ebenavia inunguis* lives on the youngest island. *J. Biogeogr.* 44, 409–420. doi: 10.1111/jbi.12912

Hebert, P. D., Cywinska, A., Ball, S. L., and deWaard, J. R. (2003). Biological identifications through DNA barcodes. *Proc. R. Soc. Lond. B* 270, 313–321. doi: 10.1098/rspb.2002.2218

Hennemann, F. H., and Conle, O. V. (2004). Revision of the tribe Achriopterini Bradley & Galil, 1977, with the description of a new genus, three new species and a new subspecies from Madagascar (Phasmatodea: Phasmatidae: Phasmatinae). *Mitt. Münch. Ent. Ges.* 94, 5–54.

Jackman, T. R., Bauer, A. M., Greenbaum, E., Glaw, F., and Vences, M. (2008). Molecular phylogenetic relationships among species of the Malagasy-Comoran gecko genus *Paroedura* (Squamata: Gekkonidae). *Mol. Phylogenet. Evol.* 46, 74–81. doi: 10.1016/j.ympev.2007.10.018

Jenkins, R. K., Tognelli, M. F., Bowles, P., Cox, N., Brown, J. L., et al. (2014). Extinction risks and the conservation of Madagascar's reptiles. *PLoS ONE* 9:e100173. doi: 10.1371/journal.pone.0100173

Kômoto, N., Yukuhiro, K., and Tomita, S. (2012). Novel gene rearrangements in the mitochondrial genome of a webspinner, *Aposthonia japonica* (Insecta: Embioptera). *Genome* 55, 222–233. doi: 10.1139/g2012-007

Kômoto, N., Yukuhiro, K., Ueda, K., and Tomita, S. (2011). Exploring the molecular phylogeny of phasmids with whole mitochondrial genome sequences. *Mol. Phylogenet. Evol.* 58, 43–52. doi: 10.1016/j.ympev.2010.10.013

Kirby, W. F. (1891). On the Phasmidae of Madagascar, with the description of a new genus and species in the collection of the British Museum. *Ann. Mag. Nat. Hist.* 8, 150–152. doi: 10.1080/00222939109460409

Klante, H. (1976). Die "Wandelnden Blätter". Eine taxonomische Revision der Gattung *Phyllium* Ill. (Insecta Orthoptera, Phasmatoptera). *Zool. Beitr.* 22, 49–79.

Klug, R., and Bradler, S. (2006). The pregenital abdominal musculature in phasmids and its implications for the basal phylogeny of Phasmatodea (Insecta: Polyneoptera). *Org. Divers. Evol.* 6, 171–184. doi: 10.1016/j.ode.2005.08.004

Köhler, J., Vences, M., D'Cruze, N., and Glaw, F. (2010). Giant dwarfs: discovery of a radiation of large-bodied 'stump-toed frogs' from karstic cave environments of northern Madagascar. *J. Zool.* 282, 21–38. doi: 10.1111/j.1469-7998.2010.00708.x

Lavranos, J. J., Röösli, W., and Hoffmann, R. (2001). Montagne des Français - an ultimate paradise in Madagascar. *Cactus Succulent J.* 73, 4–11.

Lomolino, M. V. (2005). Body size evolution in insular vertebrates: generality of the island rule. *J. Biogeogr.* 32, 1683–1699. doi: 10.1111/j.1365-2699.2005.01314.x

Meiri, S., Cooper, N., and Purvis, A. (2008). The island rule: made to be broken? *Proc. R. Soc. B* 275, 141–148. doi: 10.1098/rspb.2007.1056

Miralles, A., Macleod, A., Rodríguez, A., Ibáñez, A., Jiménez-Uzcategui, G., Quezada, G., et al. (2017). Shedding light on the Imps of Darkness: an integrative taxonomic revision of the Galápagos marine iguanas (genus *Amblyrhynchus*). *Zool. J. Linn. Soc.* 20, 1–33. doi: 10.1093/zoolinnean/zlx007

Myers, N., Mittermeier, R. A., Mittermeier, C. G., da Fonseca, G. A., and Kent, J. (2000). Biodiversity hotspots for conservation priorities. *Nature* 403, 853–858. doi: 10.1038/35002501

Nel, A., and Delfosse, E. (2011). A new Chinese Mesozoic stick insect. *Acta Pal. Pol.* 56, 429–432. doi: 10.4202/app.2009.1108

Paulian, R. (1960). Notes d'Entomologie Comorienne. I. *Rev. Entomol. Moçambique* 3, 271–278.

Preston-Mafham, K. (1991): *Madagascar. A Natural History*. Oxford; New York, NY: Facts on File, Inc.

Ranaivoarisoa, J. F., Zaonarivelo, J. R., Lei, R., Johnson, S. E., and Wyman, T. M., Mittermeier, et al. (2013). Rapid survey and assessment of the Northern Sportive Lemur, *Lepilemur septentrionalis*, in northern Madagascar. *Primate Conserv*. 27, 23–31. doi: 10.1896/052.027.0109

Redtenbacher, J. (1908). *Die Insektenfamilie der Phasmiden, III. Phasmidae Anareolatae (Phibalosomini, Acrophyllini, Necrosciini)*. Leipzig: Wilhelm Engelmann. p. 341–589, pls. 16–27.

Ribera, I., Fresneda, J., Bucur, R., Izquierdo, A., Vogler, A. P., Salgado, J. M., et al. (2010). Ancient origin of a Western Mediterranean radiation of subterranean beetles. *BMC Evol. Biol.* 10:29. doi: 10.1186/1471-2148-10-29

Robertson, J. A., Bradler, S., and Whiting, M. F. (2018). Evolution of oviposition techniquesin stick and leaf insects (Phasmatodea). *Front. Ecol. Evol.* 6:216. doi: 10.3389/fevo.2018.00216

Ronquist, F., and Huelsenbeck, J. P. (2003). MrBayes 3: Bayesian phylogenetic inference under mixed models. *Bioinformatics* 19, 1572–1574 doi: 10.1093/bioinformatics/btg180

Ruane, S., Burbrink, F. T., Randriamahatantsoa, B., and Raxworthy, C. J. (2016). The cat-eyed snakes of Madagascar: phylogeny and description of a new species of *Madagascarophis* (Serpentes: Lamprophiidae) from the Tsingy of Ankarana. *Copeia* 104, 712–721. doi: 10.1643/CH-15-346

Shelomi, M., Danchin, E. G., Heckel, D., Wipfler, B., Bradler, S., Zhou, X., et al. (2016). Horizontal gene transfer of pectinases from bacteria preceded the diversification of stick and leaf insects. *Sci. Rep.* 6:26388. doi: 10.1038/srep26388

Simon, C., Frati, F., Beckenbach, A. T., Crespi, B., Liu, H., and Flook, P. K. (1994). Evolution, weighting, and phylogenetic utility of mitochondrial gene sequences and a compilation of conserved polymerase chain reaction primers. *Ann. Entomol. Soc. Am.* 87, 651–701. doi: 10.1093/aesa/87.6.651

Stolz, K., von Bredow, C.-R., von Bredow, Y. M., Lakes-Harlan, R., Trenczek, T. E., and Strau,ß, J. (2015). Neurons of self-defence: neuronal innervation of the exocrine defence glands in stick insects. *Front. Zool.* 12:29. doi: 10.1186/s12983-015-0122-0

Suetsugu, K., Funaki, S., Takahashi, A., Ito, K., and Yokoyama, T. (2018). Potential role of bird predation in the dispersal of otherwise flightless stick insects. *Ecology* 99, 1504–1506. doi: 10.1002/ecy.2230

Tamura, K., Peterson, D., Peterson, N., Stecher, G., Nei, M., and Kumar, S. (2011). MEGA5 molecular evolutionary genetics analysis using maximum likelihood, evolutionary distance, and maximum parsimony methods. *Mol. Biol. Evol.* 28, 2731–2739. doi: 10.1093/molbev/msr121

Tomita, S., Yukuhiro, K., and Kômoto, N. (2011). The mitochondrial genome of a stick insect *Extatosoma tiaratum* (Phasmatodea) and the phylogeny of polyneopteran insects. *J. Ins. Biotech. Sericol.* 80, 79–88.

Vences, M., Kosuch, J., Boistel, R., Haddad, C. F. B., La Marca, E., Lötters, S., et al. (2003a). Convergent evolution of aposematic coloration in Neotropical poison frogs: a molecular phylogenetic perspective. *Org. Divers. Evol.* 3, 215–226. doi: 10.1078/1439-6092-00076

Vences, M., Vieites, D. R., Glaw, F., Brinkmann, H., Kosuch, J., Veith, M., et al. (2003b). Multiple overseas dispersal in amphibians. *Proc. R. Soc. Lond. B* 270, 2435–2442. doi: 10.1098/rspb.2003.2516

Vences, M., Wollenberg, K. C., Vieites, D. R., and Lees, D. C. (2009). Madagascar as a model region of species diversification. *Trends Ecol. Evol.* 24, 456–465. doi: 10.1016/j.tree.2009.03.011

Wang, I. J., and Shaffer, H. B. (2008). Rapid color evolution in an aposematic species: a phylogenetic analysis of color variation in the strikingly polymorphic strawberry poison-dart frog. *Evolution* 62, 2742–2759. doi: 10.1111/j.1558-5646.2008.00507.x

Wang, M., Béthoux, O., Bradler, S., Jacques, F., Cui, Y., and Ren, D. (2014). Under cover at pre-angiosperm times: a cloaked phasmatodean insect from the Early Cretaceous Jehol biota. *PLoS ONE* 9:e91290. doi: 10.1371/journal.pone.0091290

Warren, B. H., Strasberg, D., Bruggemann, J. H., Prys-Jones, R. P., and Thébaud, C. (2009). Why does the biota of the Madagascar region have such a strong Asiatic flavour? *Cladistics* 26, 526–538. doi: 10.1111/j.1096-0031.2009.00300.x

Wegener, J. E., Swoboda, S., Hawlitschek, O., Franzen, M., Wallach, V., Vences, et al. (2013). Morphological variation and taxonomic reassessment of the endemic Malagasy blind snake family Xenotyphlopidae (Serpentes, Scolecophidia). *Spixiana* 36, 269–282.

Whiting, M. F., Bradler, S., and Maxwell, T. (2003). Loss and recovery of wings in stick insects. *Nature* 421, 264–267. doi: 10.1038/nature01313

Wollenberg, K. C., Veith, M., Noonan, B. P., and Lötters, S. (2006). Polymorphism versus species richness - systematics of large *Dendrobates* from the Eastern Guiana Shield (Amphibia: Dendrobatidae). *Copeia* 2006, 623–629. doi: 10.1643/0045-8511(2006)6[623:PVSROL]2.0.CO;2

Zompro, O. (2004). Revision of the genera of the Areolatae, including the status of *Timema* and *Agathemera* (Insecta, Phasmatodea). *Verh. Naturwiss. Ver. Hamburg* 37, 1–327.

Conflict of Interest Statement: The authors declare that the research was conducted in the absence of any commercial or financial relationships that could be construed as a potential conflict of interest.

frontiers in Ecology and Evolution

ORIGINAL RESEARCH
published: 05 April 2019
doi: 10.3389/fevo.2019.00101

Olfactory Proteins in *Timema* Stick Insects

Darren J. Parker[1,2]*, *Jelisaveta Djordjevic*[1] *and Tanja Schwander*[1]

[1] Department of Ecology and Evolution, University of Lausanne, Lausanne, Switzerland, [2] Swiss Institute of Bioinformatics, Lausanne, Switzerland

Most animals use olfaction to obtain important information from the environment, including the presence of food or mates. Insects detect odorants through receptors that are expressed in the sensory neurons of the olfactory sensilla, which cover the surface of the antennae. The olfactory capacities of an insect thus depend largely on the repertoire of the odorant receptors. Here, we study the repertoire of olfactory proteins in the stick insect *Timema cristinae*. We first generate transcriptomes from the antennae of adult males and females and identify, via homology searches, putative olfactory proteins of three different families: odorant binding proteins, odorant receptors, and chemosensory proteins (CSPs). We then attempt to categorize olfactory proteins likely involved in sexual communication by comparing gene expression between adults and juveniles, as well as between males and females. Notably, the olfactory proteins involved in the perception of food or abiotic environmental components, should be expressed in both adults and juveniles. By contrast, the olfactory proteins involved in sexual communication, such as the detection of sex pheromones, should be expressed in adults and often comprise different repertoires in males and females. Finally, we also tested whether olfactory proteins in general and the subset, with putative roles in sexual communication in particular, are under relaxed selection in the asexual species *T. monikensis,* a close relative of *T. cristinae*. We found that olfactory proteins are typically differentially expressed between juveniles and adults, but there is little overlap of differential expression between developmental stages and the level of sex bias in adults. Furthermore, while we find evidence that olfactory proteins are indeed under relaxed selection in the asexual species, there is no evidence that this is necessarily the case for olfactory genes with a putative role in sexual communication. Nevertheless, the list of olfactory genes generated in our study provides a useful tool for future studies on olfaction in *Timema* and other stick insects.

Keywords: timema, gene expression, olfacation, selection, antennae

OPEN ACCESS

Edited by:
Sven Bradler,
University of Göttingen, Germany

Reviewed by:
Francesca Romana Dani,
University of Florence, Italy
Dmitry Yurievich Sherbakov,
Limnological Institute (RAS), Russia

***Correspondence:**
Darren J. Parker
darrenJames.Parker@unil.ch

Specialty section:
This article was submitted to Phylogenetics, Phylogenomics, and Systematics, a section of the journal Frontiers in Ecology and Evolution

Received: *30 November 2018*
Accepted: *13 March 2019*
Published: *05 April 2019*

Citation:
Parker DJ, Djordjevic J and Schwander T (2019) Olfactory Proteins in Timema Stick Insects. Front. Ecol. Evol. 7:101. doi: 10.3389/fevo.2019.00101

INTRODUCTION

Olfaction, the sense of smell, is of critical importance for survival and reproduction in insects. For the majority of species studied, it is the main sense that guides the location of resources, mate recognition, selection of oviposition sites and predator avoidance (Pickett and Glinwood, 2007; Leal, 2013). In stick insects, experiments on different species have demonstrated the role of olfactory cues for the selection of suitable host plant species, as well as for sexual communication and intra-and interspecific mate discrimination (Nosil et al., 2007; Schwander et al., 2013a; Burke et al., 2015; Myers et al., 2015; Riesch et al., 2017).

In contrast, the molecular mechanisms underlying the detection and processing of olfactory cues for host plant selection or mate discrimination remain unexplored. This constrains studies of how olfaction contributes to adaptive divergence between stick insect populations and species.

The two organs insects primarily used to detect odors are the antennae and maxillary palps (specialized mouthparts). These organs comprise large numbers of olfactory receptor neurons which house receptors for scent molecules in their cell membrane (reviewed in Pelosi et al., 2006). Specifically, the detection of odors depends on different protein families, with odorant-binding proteins (OBPs), chemosensory proteins (CSPs), and odorant receptors, playing a key role (Hallem et al., 2006; Touhara and Vosshall, 2009; Leal, 2013). Odorant-binding and CSPs are involved in the first step of the recognition of chemical signals, by binding to hydrophobic molecules from the environment and delivering them to the receptors (Hallem et al., 2006; Touhara and Vosshall, 2009; Leal, 2013). However, members of these protein families are also involved in functions not linked to the detection of odors. Members of the chemosensory protein family in particular have more diverse functions in chemoreception, growth, and development (Pelosi et al., 2018).

Here, we provide a first step toward developing a better understanding of the mechanisms underlying olfaction in stick insects, by generating a catalog of olfactory proteins that are expressed in the antennae of the stick insect *Timema cristinae*. *Timema*, the sister group of all remaining stick and leaf insects (Euphasmatodea) (Whiting et al., 2003; Tilgner, 2009), are a small group of stick insects native to the western part of the United States of America and Mexico (Vickery and Sandoval, 2001). Previous work on *Timema* has shown that olfaction plays an important role in mate discrimination, both within and between species (Nosil et al., 2007; Arbuthnott and Crespi, 2009; Schwander et al., 2013a; Riesch et al., 2017).

We first annotated OBPs, CSPs, and odorant receptors in a previously published reference transcriptome of *T. cristinae* and screened for their expression in the antennae of juvenile and adult individuals of both sexes. We then combined two approaches in an attempt to distinguish between olfactory proteins likely involved in sexual communication vs. proteins likely involved in odor detection linked to host plants and other environmental cues (or in functions not related to olfaction). For the first approach, we identified olfactory proteins with a higher expression in adults than in juveniles, as only adults react to pheromone and hydrocarbon stimuli of the opposite sex (Schwander et al., 2013b). Functions such as host plant selection, predator avoidance and the detection of other cues from the environment are not expected to differ extensively between juveniles and adults given that different developmental stages live on the same individual host plant and are exposed to similar predator guilds (Sandoval, 1993). For the second approach, we took advantage of the fact that several functionally apomictic asexual species are known in the genus *Timema* (Schwander and Crespi, 2009).

A previous study showed that females in asexual species feature reduced pheromone production and altered surface smells, likely because selection favored the reduction of costly sexual traits in asexual species where such traits are not required for reproduction (Schwander et al., 2013b). Thus, olfactory proteins involved sexual communication are expected to be under relaxed (or even negative) selection in asexual species, while olfactory proteins involved in vital functions are expected to be maintained. By combining these two approaches, we generated a list of olfactory genes which will be a useful tool for future studies on olfaction in *Timema* and other stick insects.

METHODS

Identifying Odorant-Related Genes

We identified OBPs, CSPs, and odorant receptors (ORs) in a previously published reference transcriptome of *T. cristinae* (Bast et al., 2018) using a blast approach. Protein reference sequences were downloaded from the protein database at NCBI, found by searching the titles for the following terms: "Odorant binding," "Chemosensory protein," or "Odorant receptor" for the following insect taxa: Drosophila melanogaster, Tribolium castaneum, Orthoptera, Hemiptera, and Blattodea (for a full list of accession numbers, see **Supplementary Table 2**). We also used the putative OBP, CSP, and OR sequences of *Clitarchus hookeri* provided in Wu et al. (2016), and OR sequences of *Phyllium siccifolium* provided in Missbach et al. (2014).

The protein reference sequences were blasted (tblastn) to the whole *T. cristinae* transcriptome, keeping only hits with an e-value of $< 1 \times 10^{-5}$. From these, sequences with significant hits were classed as putative OBPs, CSPs, or ORs. If a sequence had hits from different sequence groups (OBPs, CSPs, or ORs), the sequence was then classified to the group which provided the greatest number of significant blast for that sequence. Note identical Protein reference sequences were discarded before blasting.

Antennal Samples

Antenna transcriptomes were generated from individuals collected as second or third instars in the field (spring 2018, field site coordinates 34.514781, −119.779256) and then reared in the laboratory for ∼4 weeks in net cages on *Ceanothus thyrsiflorus*. Fourth instar juveniles and virgin adults of both sexes (collected 5 days after their final molt) were collected simultaneously and CO_2 anesthetized before dissections.

Total RNA was extracted from the whole antennae of four individuals per developmental stage and sex. This was done by first freezing the tissue in liquid nitrogen, followed by the addition of Trizol (Life Technologies) and crushing with beads (Sigmund Lindner). The homogenized tissue was then treated with chloroform and ethanol and the aqueous layer transferred to RNeasy MinElute Columns (Qiagen). Following the RNeasy Mini Kit protocol, potential DNA in the sample was digested, RNA was eluted into water and stored at 80°C. RNA quantity and quality was measured using NanoDrop (Thermo Scientific) and Bioanalyzer (Agilent). RNA extracts were pooled and fragmented to 120 nt for strand-specific library preparation. Paired-end sequencing with a read length of 100 bp was performed on a

HiSeq 2500 platform at the CIG (Center of Integrative Genomics, Lausanne, Switzerland).

Expression Analyses

To quantify gene expression of olfactory genes in the antennae, we mapped reads to the reference transcriptome using Kallisto (v. 0.43.1) (Bray et al., 2016) with the following options: –bias –rf-stranded. Before mapping, adapter sequences were trimmed from raw reads with CutAdapt (Martin, 2011). Reads were then quality trimmed using Trimmomatic v 0.36 (Bolger et al., 2014), clipping leading or trailing bases with a phred score of <10 from the read, before using a sliding window from the 5′ end to clip the read if 4 consecutive bases had an average phred score of <20. Any reads with a sequence length of <80 after trimming were discarded. Any unpaired reads after this trimming were then also discarded.

Expression analyses were performed using the Bioconductor package EdgeR (v. 3.18.1) (Robinson et al., 2010) in R (v. 3.4.1) (R Core Team, 2017). Firstly, gene-level counts were obtained from the transcript-level estimates using the tximport package (Soneson et al., 2015). Genes with a low expression in the antennae samples (transcripts per million (TPM) <0.5 in 2 or more libraries) were excluded from the expression analyses. Normalization factors for each library were computed using the TMM method in EdgeR. To estimate dispersion, we then fit a generalized linear model (GLM) with negative binomial distribution with developmental stage, sex, and their interaction as explanatory variables. To identify genes that differed in expression between developmental stages and between the sexes, we used a quasi-*F* test to determine the significance for each gene by comparing appropriate model contrasts. *P*-values were then corrected for multiple tests using Benjamini and Hochberg's algorithm (Benjamini and Hochberg, 1995), with statistical significance set to 5%.

Sequence Evolution of Olfactory Genes in the Asexual Species *T. monikensis*

To test for differences in the rate of evolutionary divergence between olfactory genes and other genes in the asexual species *T. monikensis*, we calculated dN/dS ratios for each of the one-to-one orthologs between *T cristinae, T. monikensis,* and *T. californicum* (outgroup species) using the ortholog matrix from Bast et al. (2018). All of the one-to-one orthologs were aligned with prank (v.100802, codon-mode) (Löytynoja and Goldman, 2005) and then curated with Gblocks (v. 0.91b, type = codons, minimum block length = 4) (Talavera and Castresana, 2007). These alignments were then used as input for codeml of the PAML package (Yang, 2007) to generate maximum likelihood estimates of dN/dS for the *T. monikensis* terminal branch in the phylogeny (using the "free model"). Note we did not use a more complex model for examining differences in evolutionary rate (e.g., branch-site models) as we are interested in identifying genes which have increased accumulation of deleterious changes due to the reduced purifying selection (indicated by an increase in dN/dS), rather than genes showing evidence of positive selection. dN/dS estimates where dS = 0 or dN/dS > 1 were discarded. Differences of dN/dS between gene categories were assessed using a Wilcoxon test in R.

TABLE 1 | Number of Olfactory genes found in *T. cristinae*.

Gene type	*N*	*N* expressed in antennae
OBP	44	39
CSP	31	31
OR	57	52
Total	132	122

N are the numbers annotated in the reference transcriptome via homology searches, most of which are expressed in the antennae. OBP, odorant binding protein; CSP, chemosensory protein; OR, odorant receptor.

RESULTS

We identified a total of 132 putative olfactory genes in *T. cristinae*, 122 of which were expressed at least at a low level in the antennae (**Table 1**, **Supplementary Table 1**). Factors influencing antennal expression pattern of olfactory genes varied by olfactory gene type, with sex inferencing OBP expression more than the developmental stage, and vice versa for CSPs and ORs (**Figure 1**). The majority of olfactory genes (68%) showed a significant change in expression between developmental stages in males and/or females (OBPs: 28/39, CSPs: 23/31, ORs: 32/52) while only a minority of them were sex-biased in adults (OBPs: 18/39, CSPs: 7/31, ORs: 16/52).

Olfactory genes evolve significantly faster than genes with other functions in the asexual species *T. monikensis* (**Figure 2A**). However, the comparison is only significant if the three gene categories are pooled; only ORs show significantly elevated rates of evolution if the three gene categories are analyzed separately (**Figure 2B**). Note, a similar result was found when using dN/dS values for *T. cristinae* (**Supplementary Figure 1**). We were only able to calculate a dN/dS ratio for 58 of the 122 expressed olfactory genes (47%), in large part due to a lack of orthologous sequences. This percentage is not specific to olfactory genes as we obtained a similar percentage for non-olfactory genes (45%) (**Supplementary Table 1**).

We then assessed whether any genes featured patterns consistent with expectations for olfactory genes involved in sexual communication. This would be the case for genes featuring increased expression in adults, sex-bias and an elevated rate of evolution. However, when we combined expression shifts between developmental stages, sex bias and evolutionary rates of olfactory genes (**Figure 3**) we found no genes that fit these predictions of olfactory genes.

DISCUSSION

We identified putative genes for olfactory proteins in *Timema cristinae* and studied their expression in antennae. These proteins include 44 odorant binding proteins, 31 CSPs, and 57 odorant receptors. The number of olfactory proteins identified in *T. cristinae* is higher than in other phasmids whose olfactory repertoire has been studied [*Clitarchus hookeri*: OBP = 10, CSP = 12, and OR = 16 (Wu et al., 2016), and in *Phyllium siccifolium*: OR = 30 (Missbach et al., 2014)], for unknown reasons. Such differences in olfactory protein numbers are

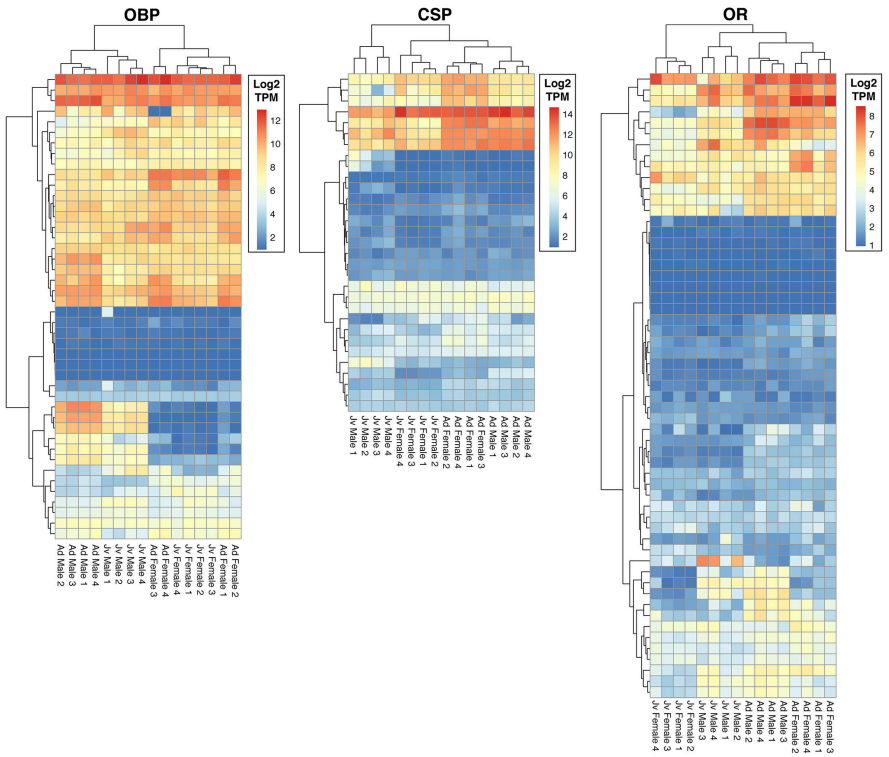

FIGURE 1 | Heatmaps of expression of olfactory genes in antennae of juvenile and adult males and females of *Timema cristinae*. OBP, odorant binding proteins; CSP, chemosensory proteins; OR, odorant receptors. Jv, Juvenile; Ad, Adult.

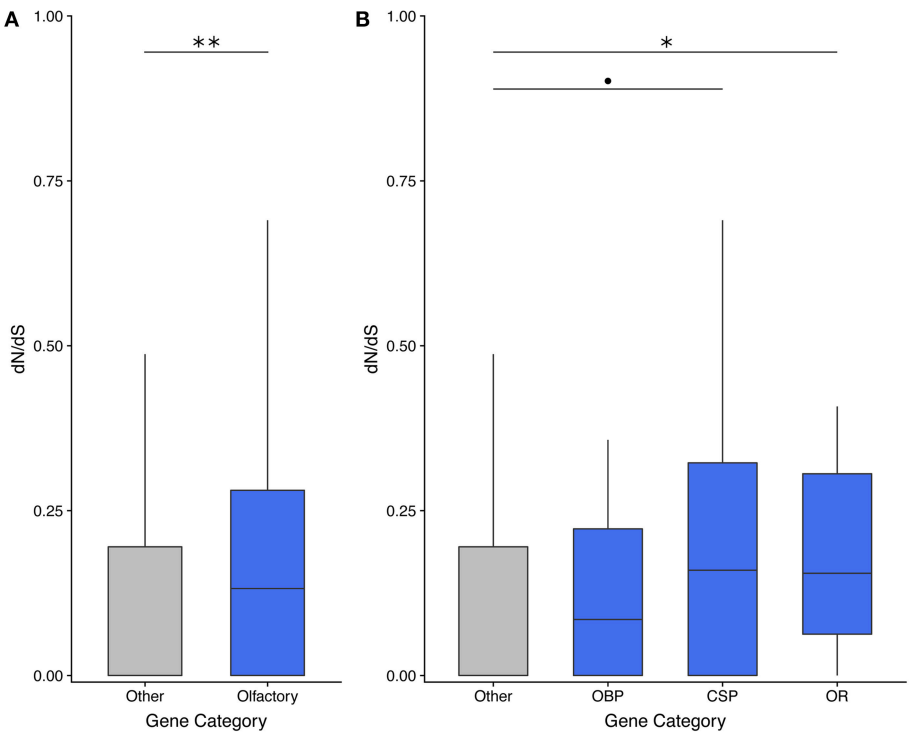

FIGURE 2 | dN/dS analyses reveal that olfactory genes evolve faster than genes with other functions in the asexual species *T. monikensis*. OBP, odorant binding proteins; CSP, chemosensory proteins; OR, odorant receptors. Codes for levels of significance are 0.01 "**," 0.05 "*,"0.1 "•" from a Wilcoxon test.

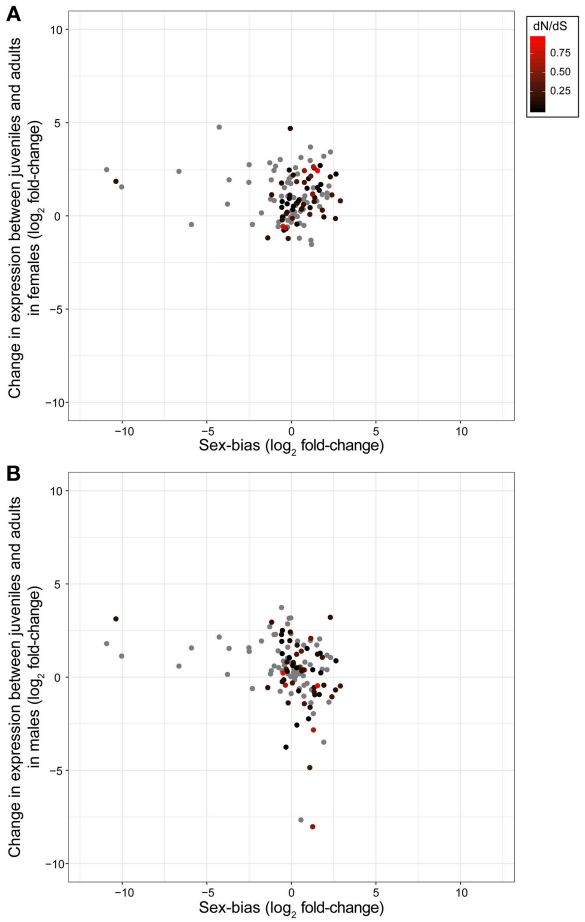

FIGURE 3 | Expression changes of olfactory genes between *T. cristinae* developmental stages in females **(A)** and males **(B)**, and between adult males and females. Olfactory genes involved in sexual communication are expected to mostly be expressed in adults and feature sex-biased expression. They are further expected to be under relaxed selection in asexual species (red points, see legend) where sexual communication no longer occurs. (No dN/dS rates could be determined for the gray points because of lack of polymorphism or orthology). None of the candidate olfactory genes identified in *T. cristinae* clearly fit with these expectations. Positive values for sex-bias indicate higher expression in females, and positive values for expression between developmental stages indicate higher expression in adults.

unlikely to be driven primarily by differences in study design as all studies used an RNA-seq approach which included antennal tissue. Despite this, the number of genes in these different gene families are known to vary extensively among insects (Brito et al., 2016; Pelosi et al., 2018), and in the vast majority of species, there are no studies designed to identify the subset of these genes that are directly involved in odorant reception vs. those are involved in other functions. As a consequence, the diversification of genes in different olfactory gene families does not inform the complexity of the chemical communication system in a given species.

We expected that olfactory proteins involved in sexual functions such as the detection of pheromones should be expressed mostly in adults and not in juveniles, and generally feature sex biased expression. However, there was no set of olfactory proteins that fit this description and we found no relation between expression shifts in juveniles and adults and the level of sex bias. There was also no group of olfactory genes featuring particularly fast evolutionary rates in the asexual species, as could be expected for olfactory genes involved in sexual communication. A possible explanation for the lack of a pattern in our data is that we used homology of known insect olfactory proteins to identify olfactory proteins in *Timema*. This approach constrains the set of analyzed proteins to those that are relatively conserved among distantly related species. However, proteins involved in sexual communication often diverge very rapidly between species (e.g., Picimbon and Gadenne, 2002; Guo and Kim, 2007; Sánchez-Gracia et al., 2009). Therefore, the lack of pattern in our data may stem from the fact that our set of proteins may largely lack the set involved in sexual functions. An additional complication may be that our study only examined gene expression levels, but not protein expression levels. It is therefore possible that our study could have missed important differences in expression levels if there was extensive post-translational regulation. Future work examining both protein and gene expression levels are needed to investigate this.

Olfactory proteins overall evolve faster in the asexual species *T. monikensis* than proteins with other functions. We were able to detect such accelerated evolution in spite of the fact that there is little power to detect rate variations among genes in asexuals. Gene level selection is relatively inefficient in asexuals given all alleles co-segregate as a single linkage block in the absence of meiosis and outcrossing. The implications are that the differences in selection pressures, acting on olfactory proteins vs. other proteins in *T. monikensis*, must be quite extensive. Because we could not identify subsets of olfactory proteins likely associated with sexual functions, we could not test whether rapid evolution of olfactory proteins overall is a consequence of relaxed selection for sexual functions in asexuals, or whether it reflects the fact that olfactory proteins are relatively "dispensable" overall. The fact that we also observed an elevated rate of sequence evolution for olfactory proteins in the sexual species *T. cristinae* suggests the latter, however, it is also likely that sexual selection may increase the dN/dS of olfactory proteins in sexual species (e.g., Guo and Kim, 2007; Sánchez-Gracia et al., 2009). There is extensive evidence for relaxed and/or negative selection on sexual phenotypes in asexual species (van der Kooi and Schwander, 2014). By contrast, it has thus far been difficult to detect corresponding signatures in genes underlying sexual traits, perhaps because sexual trait decay proceeds largely via an altered expression of certain gene networks, rather than the pseudogenization of specific genes. Only a single study, on an asexual wasp species, detected a disproportionate accumulation of deleterious mutations in genes likely involved in male functions (Kraaijeveld et al., 2016). However, this wasp produces haploid eggs via meiosis and diploidy in the eggs is restored secondarily via fusion of the daughter cells of the first mitotic division (so-called gamete duplication). This allows for both, gene-specific selection (because normal meiosis occurs) as well as the rapid fixation of beneficial mutations (because they are immediately homozygous).

In conclusion, we found that putative olfactory proteins are typically differentially expressed between juveniles and adults in *T. cristinae*, but there is little overlap of differential expression between developmental stages and the level of sex bias in adults. Furthermore, while we found evidence that olfactory proteins are indeed under relaxed selection in the asexual species *T. monikensis*, there is no evidence that this is necessarily the case for olfactory genes with a putative role in sexual communication. Nevertheless, the list of olfactory genes generated in our study provides a useful tool for future studies on olfaction in *Timema* and other stick insects.

DATA AVAILABILITY

Raw reads have been deposited in the SRA with the following accession numbers: SRR8182935-SRR8182950.

AUTHOR CONTRIBUTIONS

TS and DP designed the study. TS collected samples. DP and JD analyzed the data with input TS. DP and TS wrote the manuscript with input from all authors.

FUNDING

This study was supported by Swiss FNS grants PP00P3_170627 and CRSII3_160723.

SUPPLEMENTARY MATERIAL

The Supplementary Material for this article can be found online at: https://www.frontiersin.org/articles/10.3389/fevo.2019.00101/full#supplementary-material

REFERENCES

Arbuthnott, D., and Crespi, B. J. (2009). Courtship and mate discrimination within and between species of *Timema* walking-sticks. *Anim. Behav.* 78, 53–59. doi: 10.1016/j.anbehav.2009.02.028

Bast, J., Parker, D. J., Dumas, Z., Jalvingh, K. M., Tran Van, P., Jaron, K. S., et al. (2018). Consequences of asexuality in natural populations: insights from stick insects. *Mol. Biol. Evol.* 35, 1668–1677. doi: 10.1093/molbev/msy058

Benjamini, Y., and Hochberg, Y. (1995). Controlling the false discovery rate: a practical and powerful approach to multiple testing. *J. R. Stat. Soc. Series B Stat. Methodol.* 57, 289–300. doi: 10.1111/j.2517-6161.1995.tb02031.x

Bolger, A. M., Lohse, M., and Usadel, B. (2014). Trimmomatic: a flexible trimmer for Illumina sequence data. *Bioinformatics* 30, 2114–2120. doi: 10.1093/bioinformatics/btu170

Bray, N. L., Pimentel, H., Melsted, P., and Pachter, L. (2016). Near-optimal probabilistic RNA-seq quantification. *Nat. Biotechnol.* 34, 525–527. doi: 10.1038/nbt.3519

Brito, N. F., Moreira, M. F., and Melo, A. C. A. (2016). A look inside odorant-binding proteins in insect chemoreception. *J. Insect. Physiol.* 95, 51–65. doi: 10.1016/j.jinsphys.2016.09.008

Burke, N. W., Crean, A. J., and Bonduriansky, R. (2015). The role of sexual conflict in the evolution of facultative parthenogenesis: a study on the spiny leaf stick insect. *Anim. Behav.* 101, 117–127. doi: 10.1016/j.anbehav.2014.12.017

Guo, S., and Kim, J. (2007). Molecular evolution of *Drosophila* odorant receptor genes. *Mol. Biol. Evol.* 24, 1198–1207. doi: 10.1093/molbev/msm038

Hallem, E. A., Dahanukar, A., and Carlson, J. R. (2006). Insect odor and taste receptors. *Annu. Rev. Entomol.* 51, 113–135. doi: 10.1146/annurev.ento.51.051705.113646

Kraaijeveld, K., Anvar, S. Y., Frank, J., Schmitz, A., Bast, J., Wilbrandt, J., et al. (2016). Decay of sexual trait genes in an asexual parasitoid wasp. *Genome Biol. Evol.* 8, 3685–3695. doi: 10.1093/gbe/evw273

Leal, W. S. (2013). Odorant reception in insects: roles of receptors, binding proteins, and degrading enzymes. *Annu. Rev. Entomol.* 58, 373–391. doi: 10.1146/annurev-ento-120811-153635

Löytynoja, A., and Goldman, N. (2005). An algorithm for progressive multiple alignment of sequences with insertions. *Proc. Natl. Acad. Sci. U.S.A.* 102, 10557–10562. doi: 10.1073/pnas.0409137102

Martin, M. (2011). Cutadapt removes adapter sequences from high-throughput sequencing reads. *EMBnet J.* 17, 10–12. doi: 10.14806/ej.17.1.200

Missbach, C., Dweck, H. K., Vogel, H., Vilcinskas, A., Stensmyr, M. C., Hansson, B. S., et al. (2014). Evolution of insect olfactory receptors. *Elife* 3:e02115. doi: 10.7554/eLife.02115

Myers, S. S., Buckley, T. R., and Holwell, G. I. (2015). Mate detection and seasonal variation in stick insect mating behaviour (Phamatodea: *Clitarchus hookeri*). *Behaviour* 152, 1325–1348. doi: 10.1163/1568539X-00003281

Nosil, P., Crespi, B. J., Gries, R., and Gries, G. (2007). Natural selection and divergence in mate preference during speciation. *Genetica* 129, 309–327. doi: 10.1007/s10709-006-0013-6

Pelosi, P., Iovinella, I., Zhu, J., Wang, G., and Dani, F. R. (2018). Beyond chemoreception: diverse tasks of soluble olfactory proteins in insects. *Biol. Rev. Camb. Philos. Soc.* 93, 184–200. doi: 10.1111/brv.12339

Pelosi, P., Zhou, J. J., Ban, L. P., and Calvello, M. (2006). Soluble proteins in insect chemical communication. *Cell. Mol. Life Sci.* 63, 1658–1676. doi: 10.1007/s00018-005-5607-0

Picimbon, J. F., and Gadenne, C. (2002). Evolution of noctuid pheromone binding proteins: identification of PBP in the black cutworm moth, *Agrotis ipsilon*. *Insect Biochem. Mol. Biol.* 32, 839–846. doi: 10.1016/S0965-1748(01)00172-2

Pickett, J. A., and Glinwood, R. T. (2007). "Chemical ecology," in *Aphids as Crop Pests*, eds H. F. van Emden and R. Harrington (Wallingford: CAB International Press), 235–260.

R Core Team (2017). *R: A Language and Environment for Statistical Computing*. Available online at: https://www.R-project.org/ (accessed March 23, 2019).

Riesch, R., Muschick, M., Lindtke, D., Villoutreix, R., Comeault, A. A., Farkas, T. E., et al. (2017). Transitions between phases of genomic differentiation during stick-insect speciation. *Nat. Ecol. Evol.* 1:0082. doi: 10.1038/s41559-017-0082

Robinson, M. D., McCarthy, D. J., and Smyth, G. K. (2010). edgeR: a Bioconductor package for differential expression analysis of digital gene expression data. *Bioinformatics* 26, 139–140. doi: 10.1093/bioinformatics/btp616

Sánchez-Gracia, A., Vieira, F. G., and Rozas, J. (2009). Molecular evolution of the major chemosensory gene families in insects. *Heredity* 103, 208–216. doi: 10.1038/hdy.2009.55

Sandoval, C. P. (1993). *Geographic, Ecological and Behavioral Factors Affecting Spatial Variation in Color Morph Frequency in the Walking-Stick, Timema Cristinae*. Ph.D. Thesis, University of California, Santa Barbara, CA.

Schwander, T., Arbuthnott, D., Gries, R., Gries, G., Nosil, P., and Crespi, B. J. (2013a). Hydrocarbon divergence and reproductive isolation in *Timema* stick insects. *BMC Evol. Biol.* 13:151. doi: 10.1186/1471-2148-13-151

Schwander, T., and Crespi, B. J. (2009). Multiple direct transitions from sexual reproduction to apomictic parthenogenesis in *Timema* stick insects. *Evolution* 63, 84–103. doi: 10.1111/j.1558-5646.2008.00524.x

Schwander, T., Crespi, B. J., Gries, R., and Gries, G. (2013b). Neutral and selection-driven decay of sexual traits in asexual stick insects. *Proc. Biol. Sci.* 280:20130823. doi: 10.1098/rspb.2013.0823

Soneson, C., Love, M. I., and Robinson, M. D. (2015). Differential analyses for RNA-seq: transcript-level estimates improve gene-level inferences. *F1000Res.* 4:1521. doi: 10.12688/f1000research.7563.1

Talavera, G., and Castresana, J. (2007). Improvement of phylogenies after removing divergent and ambiguously aligned blocks from protein sequence alignments. *Syst. Biol.* 56, 564–577. doi: 10.1080/10635150701472164

Tilgner, E. H. (2009). "Phasmida: Stick and Leaf Insects," in *Encyclopedia of Insects, 2nd Edn.*, eds V. H. Resh and R. T. Cardé (London: Elsevier), 765–766.

Touhara, K., and Vosshall, L. B. (2009). Sensing odorants and pheromones with chemosensory receptors. *Annu. Rev. Physiol.* 71, 307–332. doi: 10.1146/annurev.physiol.010908.163209

van der Kooi, C. J., and Schwander, T. (2014). On the fate of sexual traits under asexuality. *Biol. Rev. Camb. Philos. Soc.* 89, 805–819. doi: 10.1111/brv.12078

Vickery, V. R., and Sandoval, C. P. (2001). Descriptions of three new species of *Timema* (Phasmatoptera: Timematodea: Timematidae) and notes on three other species. *J. Orthoptera Res.* 10, 53–61. doi: 10.1665/1082-6467(2001)010[0053:DOTNSO]2.0.CO;2

Whiting, M. F., Bradler, S., and Maxwell, T. (2003). Loss and recovery of wings in stick insects. *Nature* 421, 264–267. doi: 10.1038/nature01313

Wu, C., Crowhurst, R. N., Dennis, A. B., Twort, V. G., Liu, S., Newcomb, R. D., et al. (2016). *De novo* transcriptome analysis of the common New Zealandstick insect *Clitarchus hookeri* (Phasmatodea) reveals genes involved in olfaction, digestion and sexual reproduction. *PLoS ONE* 11:e0157783. doi: 10.1371/journal.pone.0157783

Yang, Z. (2007). PAML 4: phylogenetic analysis by maximum likelihood. *Mol. Biol. Evol.* 24, 1586–1591. doi: 10.1093/molbev/msm088

Conflict of Interest Statement: The authors declare that the research was conducted in the absence of any commercial or financial relationships that could be construed as a potential conflict of interest.

frontiers in Ecology and Evolution

ORIGINAL RESEARCH
published: 07 October 2019
doi: 10.3389/fevo.2019.00345

Old World and New World Phasmatodea: Phylogenomics Resolve the Evolutionary History of Stick and Leaf Insects

Sabrina Simon[1], Harald Letsch[2], Sarah Bank[3], Thomas R. Buckley[4,5], Alexander Donath[6], Shanlin Liu[7], Ryuichiro Machida[8], Karen Meusemann[6,9,10], Bernhard Misof[6], Lars Podsiadlowski[6], Xin Zhou[7], Benjamin Wipfler[11] and Sven Bradler[3]**

[1] Biosystematics Group, Wageningen University and Research, Wageningen, Netherlands, [2] Department of Botany and Biodiversity Research, University of Vienna, Vienna, Austria, [3] Department of Animal Evolution and Biodiversity, Johann-Friedrich-Blumenbach Institute for Zoology and Anthropology, University of Göttingen, Göttingen, Germany, [4] New Zealand Arthropod Collection, Manaaki Whenua–Landcare Research, Auckland, New Zealand, [5] School of Biological Sciences, The University of Auckland, Auckland, New Zealand, [6] Center for Molecular Biodiversity Research, Zoological Research Museum Alexander Koenig, Bonn, Germany, [7] Beijing Advanced Innovation Center for Food Nutrition and Human Health, College of Plant Protection, China Agricultural University, Beijing, China, [8] Sugadaira Research Station, Mountain Science Center, University of Tsukuba, Nagano, Japan, [9] Evolutionary Biology and Ecology, Institute for Biology I (Zoology), University of Freiburg, Freiburg, Germany, [10] Australian National Insect Collection, Commonwealth Scientific and Industrial Research Organisation National Research Collections Australia, Canberra, ACT, Australia, [11] Center for Taxonomy and Evolutionary Research, Zoological Research Museum Alexander Koenig, Bonn, Germany

OPEN ACCESS

Edited by:
Mariana Mateos,
Texas A&M University, United States

Reviewed by:
Jesús A. Ballesteros,
University of Wisconsin-Madison, United States
Marco Gottardo,
University of Siena, Italy

***Correspondence:**
Sven Bradler
sbradle@gwdg.de
Sabrina Simon
info@sabrina-simon.com

Specialty section:
This article was submitted to Phylogenetics, Phylogenomics, and Systematics, a section of the journal Frontiers in Ecology and Evolution

Received: *23 May 2019*
Accepted: *28 August 2019*
Published: *07 October 2019*

Citation:
Simon S, Letsch H, Bank S, Buckley TR, Donath A, Liu S, Machida R, Meusemann K, Misof B, Podsiadlowski L, Zhou X, Wipfler B and Bradler S (2019) Old World and New World Phasmatodea: Phylogenomics Resolve the Evolutionary History of Stick and Leaf Insects. Front. Ecol. Evol. 7:345. doi: 10.3389/fevo.2019.00345

Phasmatodea comprises over 3,000 extant species and stands out as one of the last remaining insect orders for which a robust, higher-level phylogenetic hypothesis is lacking. New research suggests that the extant diversity is the result of a surprisingly recent and rapid radiation that has been difficult to resolve with standard Sanger sequence data. In order to resolve the early branching events of stick and leaf insects, we analyzed transcriptomes from 61 species, including 38 Phasmatodea species comprising all major clades and 23 outgroup taxa, including all other Polyneoptera orders. Using a custom-made ortholog set based on reference genomes from four species, we identified on average 2,274 orthologous genes in the sequenced transcriptomes. We generated various sub-alignments and performed maximum-likelihood analyses on several representative datasets to evaluate the effect of missing data and matrix composition on our phylogenetic estimates. Based on our new data, we are able to reliably resolve the deeper nodes between the principal lineages of extant Phasmatodea. Among Euphasmatodea, we provide strong evidence for a basal dichotomy of Aschiphasmatodea and all remaining euphasmatodeans, the Neophasmatodea. Within the latter clade, we recovered a previously unrecognized major New World and Old World lineage, for which we introduce the new names Oriophasmata tax. nov. ("Eastern phasmids") and Occidophasmata tax. nov. ("Western phasmids"). Occidophasmata comprise Diapheromerinae, Pseudophasmatinae, and *Agathemera*, whereas all remaining lineages form the Oriophasmata, including Heteropterygidae, Phylliinae, *Bacillus*, Lonchodidae (Necrosciinae + Lonchodinae), Clitumninae, Cladomorphinae, and Lanceocercata. We furthermore performed a divergence time analysis and reconstructed the historical biogeography for stick and

leaf insects. Phasmatodea either originated in Southeast Asia or in the New World. Our results suggest that the extant distribution of Phasmatodea is largely the result of dispersal events in a recently and rapidly diversified insect lineage rather than the result of vicariant processes.

Keywords: phasmids, transcriptomes, historical biogeography, Polyneoptera, Euphasmatodea

INTRODUCTION

Exploring large-scale patterns of species diversity in time and space is a major research goal for evolutionary biology. Understanding the evolutionary processes generating these patterns requires broad comparative investigations of phenotypic attributes across taxa combined with well-corroborated phylogenies.

In recent years, numerous large-scale, highly resolved phylogenies for several insect lineages have been published and these have led to workable classifications for nearly all major groups traditionally referred to as insect orders, for instance, major groups of Polyneoptera (Wipfler et al., 2019), Blattodea (Evangelista et al., 2019), true bugs (Heteroptera) and other hemipteroid lineages (Johnson et al., 2018), Hymenoptera (Peters et al., 2017), Coleoptera (Zhang et al., 2018), Lepidoptera (Breinholt et al., 2018), and dipteran lineages (Pauli et al., 2018). Stick and leaf insects (Phasmatodea) however, stand out as one of the last remaining insect lineages traditionally referred to as orders for which a robust higher-level phylogenetic hypothesis is still lacking, as highlighted in numerous textbooks (e.g., Grimaldi and Engel, 2005; Tilgner, 2009; Beutel et al., 2014; Gullan and Cranston, 2014). Most recently, phasmatodean systematics were described as "muddled" and "burdened with much paraphyly and polyphyly" by Engel et al. (2016). This shortcoming largely impedes the study of evolutionary patterns within this group and yet, stick insects are an emerging model system in evolutionary biology (Brand et al., 2018, for overview, see also Bradler and Buckley, 2018).

Stick and leaf insects form a mesodiverse group of large, mostly nocturnal terrestrial herbivores with a mainly tropical and subtropical distribution. They exhibit impressive forms of camouflage directed against visually hunting predators by imitation of various parts of plants, such as twigs, bark and leaves (**Figure 1**). Over 3,100 described species are distributed across nearly 500 genera (Bradler, 2015; Bradler and Buckley, 2018). The relative large number of genera, of which around 175 are monotypic, reflects the degree of disparity regarding the morphological diversity found in Phasmatodea.

Over recent decades, the debate dealing with phasmatodean systematics was mostly devoid of an explicit phylogenetic basis. Instead, unmethodical classifications and numerous artificial groupings at various taxonomic ranks (e.g., Bradley and Galil, 1977; Zompro, 2004; Brock and Marshall, 2011) resulted in a highly chaotic taxonomy with incorrectly appointed taxa still recognized in the current Phasmida Species File database (Brock et al., 2017).

This situation has now been improved by numerous phylogenetic analyses of molecular datasets being published (Whiting et al., 2003; Buckley et al., 2009, 2010; Bradler et al., 2014, 2015; Goldberg et al., 2015; Robertson et al., 2018). However, datasets initially were too restricted to allow reliable conclusions for broader phasmatodean systematics. For instance, Whiting et al. (2003) and Buckley et al. (2009) did not recover monophyletic groups, such as Heteropterygidae, that have now been strongly supported as monophyletic with increased taxon sampling (Bradler et al., 2015; Goldberg et al., 2015; Robertson et al., 2018). Even the analyses of mitochondrial genomes (Kômoto et al., 2011, 2012; Tomita et al., 2011; Zhou et al., 2017) did not allow for any general systematic conclusion due to their non-representative, negligible taxon sampling.

In other cases, geographical distribution rather than morphological similarity appeared to reflect the evolutionary relationships among stick and leaf insects. Thus, phylogenetic inferences of the phasmatodean faunas of New Caledonia, New Zealand, the Mascarene Archipelago and Madagascar (Buckley et al., 2009, 2010; Bradler et al., 2015; Robertson et al., 2018) rendered several traditional groupings as polyphyletic.

In summary, the published studies based on Sanger-sequencing approaches have resulted in some sound topologies in regard to shallower nodes, but were unable to resolve the deeper nodes of the presumed rapid radiation of Phasmatodea (Bradler et al., 2014). Therefore, much of the early evolutionary history, such as the relationships between families, subfamilies, and some perpetually enigmatic taxa such as *Agathemera*, was difficult to address in the past and is still a matter of debate (Bradler and Buckley, 2018).

In order to illuminate these previously unresolved deep nodes of phasmatodean phylogeny and to test previous conflicting topologies, we conducted a phylogenomic study based on 27 novel transcriptomes of a representative set of stick and leaf insects and combined these with previously published transcriptomes of 11 phasmatodeans and 23 outgroup polyneopterans (Misof et al., 2014; Wipfler et al., 2019). We estimated divergence times for our new phylogeny using a validated set of fossils as calibration points (Bradler et al., 2015) and reconstructed the historical biogeography using explicit models. Whereas in the past phylobiogeographic research addressing Phasmatodea was restricted to specific geographic areas such as Australia, New Caledonia, and New Zealand (Buckley et al., 2010), our present study is the first to formally infer the historical biogeography for the whole order, albeit with the shortcoming of lacking some African taxa.

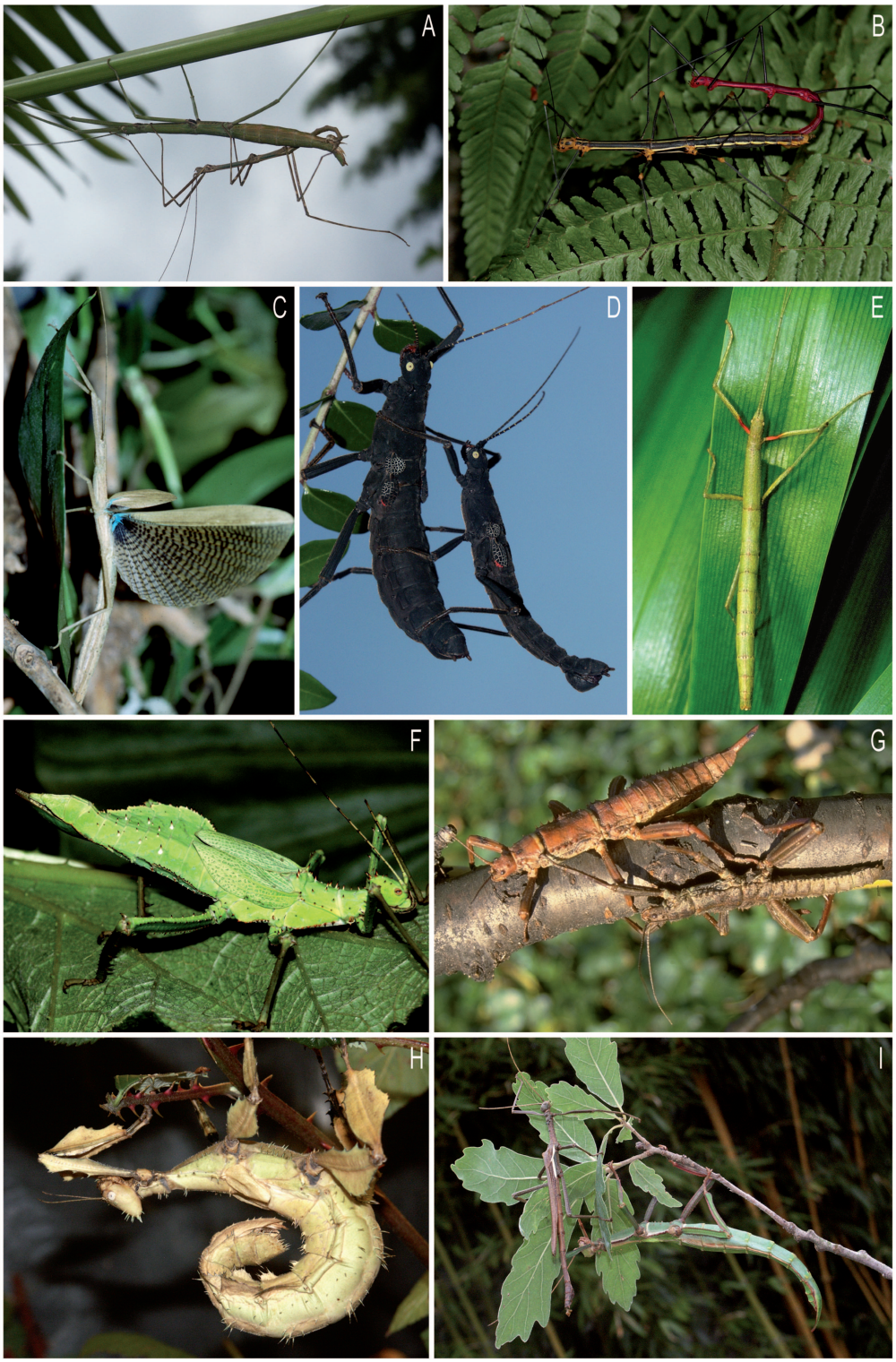

FIGURE 1 | Various members of Neophasmatodea: **(A–D)**: Occidophasmata; **(E–I)**: Oriophasmata. **(A)**, couple of *Pseudosermyle phalangiphora*, Diapheromerinae (Mexico); **(B)**, couple of *Oreophoetes peruana*, Diapheromerinae (Peru); **(C)**, female of *Metriophasma diocles*, Pseudophasmatinae (Panama); **(D)**, couple of *Peruphasma schultei*, Pseudophasmatinae (Peru); **(E)**, female of *Carausius morosus*, Lonchodinae (India); **(F)**, female of *Heteropteryx dilatata*, Heteropterygidae (Malaysia); **(G)**, couple of *Eurycantha calcarata*, Lonchodinae (New Guinea); **(H)**, female of *Extatosoma tiaratum*, Lanceocercata (Australia); **(I)**, couple of *Diapherodes gigantea*, Cladomorphinae (Grenada). Photos by Christoph Seiler, Altlussheim, Germany.

METHODS

Dataset Generation

Our dataset comprised 38 species representing all major clades of Phasmatodea and 23 outgroup species including all other Polyneoptera orders (**Supplementary Table S1**). Data was derived from transcriptomes, except for the termite *Zootermopsis nevadensis* for which we used the official gene set obtained from a whole genome project (Terrapon et al., 2014). For most species, we sampled the RNA from the head and thorax of adult specimens (see **Supplementary Table S1.1**). Further detailed information (e.g., sex, collection date, collector, etc.) can be found at the National Center for Biotechnology Information (NCBI) under the 1KITE umbrella project and the respective BioSample number (**Supplementary Table S1.1**). RNA extraction and cDNA library preparation, transcriptome sequencing (HiSeq 2000 platform with 150 bp paired-end (PE) reads), and *de novo* assembly (SOAPdenovo-Trans-31kmer; Xie et al., 2014) were conducted at the Beijing Genomics Institute (BGI) Shenzhen and are described in detail by Peters et al. (2017). Transcriptome quality assessment, removal of contaminants and submission to the NCBI Sequence Read Archive (SRA) as well as to the Transcriptome Shotgun Assembly (TSA) database were conducted as described in Peters et al. (2017) and under the 1KITE umbrella project (**Supplementary Tables S1.1, S1.2**).

The phylogenomic pipeline is described in detail in Evangelista et al. (2019) (**Supplementary Material**). Briefly, for the identification of orthologous transcripts we used the custom-made ortholog set, specifically designed for Polyneoptera taxa and comprising 3,247 orthologous genes/groups (OGs) for the four reference species *Ephemera danica*, *Ladona fulva*, *Zootermopsis nevadensis*, and *Rhodnius prolixus*. Transcripts of each query taxon were assigned to these ortholog groups (OGs) with Orthograph v.0.5.4 (Petersen et al., 2017) with following settings: max-blast-searches = 50; blast-max-hits = 50; extend-orf = 1; substitute-u-with = X. We identified on average 2,274 OGs in the transcriptomes (minimum: 637; maximum: 2,861) (**Supplementary Table S2**). OGs were aligned applying the L-INS-i algorithm of MAFFT v.7.221 (Katoh and Standley, 2013) at the translational (amino-acid) level. Each multiple sequence alignment (MSA) was quality assessed and outliers were removed using the procedure outlined by Misof et al. (2014) but using the -addfragments algorithm implemented in MAFFT. Subsequently, we excluded the sequences of three reference species *Ephemera danica*, *Ladona fulva,* and *Rhodnius prolixus* since we aimed to include only Polyneoptera taxa for the phylogenetic inference, and removed columns resulting in only gaps. Subsequently, MSAs of nucleotides (nt) corresponding to the amino-acid (aa) MSAs were generated with a modified version of the software PAL2NAL (Suyama et al., 2006; see Misof et al., 2014). We further used the Pfam-A database release 28.0 (Punta et al., 2012) in conjunction with the software pfam_scan.pl v.1.5 and HMMER (Eddy, 2011; http://hmmer.org/), Domain-identification-v1.3 and Domain-parser-v1.4.1-dist, to identify regions in the MSAs annotated as protein clans, families, single domains or non-annotated regions (so called voids, see also Bank et al., 2017). In parallel, we identified putative alignment ambiguities or randomized MSA sections within each aa MSA with Aliscore v.1.2 (Misof and Misof, 2009) (options -e -r) and combined this information with the results from the protein domain identification step to generate a supermatrix. We followed two approaches to create matrices for the phylogenetic analyses: (1) we used MARE v.0.1.2-rc (Misof et al., 2013) to remove taxa or partitions with lowest average information content (IC) from the aa supermatrix, yielding a selected optimal subset (SOS) (for rationale see also Meusemann et al., 2010) and defining all phasmatodeans as taxon constraints; thus, they were not dropped from the matrix (AA_{SOS}: 61 taxa, 837,567 aa positions, 2,773 partitions); (2) we only kept partitions with IC $>$ 0 as identified by MARE removing partitions with an IC $=$ 0 from the aa and nt supermatrix. Thus, we further increased data coverage by including only data blocks, i.e., that contained sequence information for at least one representative of specified taxonomic groups (**Supplementary Table S3**) resulting in a decisive aa dataset (sensu Dell'Ampio et al., 2014; $AA_{decisive}$: 61 taxa, 387,987 aa positions, 388 partitions). The specified taxonomic groups for Phasmatodea represented uncontroversial monophyletic groups according to previously published studies. For the corresponding decisive nt dataset we subsequently evaluated whether or not our datasets have evolved under globally stationary, reversible, and homogeneous (SRH) conditions with SymTest v.2.0.47 (Ho and Jermiin, 2004) (see for rationale also Evangelista et al., 2019). We applied the in SymTest implemented Bowker Test on the 1st, 2nd, and 3rd codon position separately, on the 1st + 2nd, and on all codon positions. Further downstream analyses were performed on the decisive nucleotide dataset keeping the 2nd codon position only ($NT_{decisive}$: 61 taxa, 387,987 nt positions, 388 partitions), as this showed smaller among-lineage heterogeneity compared to the other nt datasets (see **Supplementary Figure S1**).

For the two amino-acid datasets, we additionally evaluated the coverage with respect to pairwise sequence coverage of unambiguous data using AliStat v.1.6 (https://github.com/thomaskf/AliStat) (see also Misof et al., 2014; Wong et al., 2017). Details are provided in **Supplementary Figure S2**.

Phylogenetic Analyses

Prior to the tree inference, we optimized our partitioning scheme and searched for the best-scoring substitution models for the two aa datasets (AA_{SOS} and $AA_{decisive}$) by using PartitionFinder v.2.0.0 (prerelease 10) (http://www.robertlanfear.com/partitionfinder/; Lanfear et al., 2014, 2016) in combination with RaxML v.8.2.4 (Stamatakis, 2014) (options –rcluster –rcluster-max 6000 (for AA_{SOS}) –rcluster-max 2000 (for $AA_{decisive}$) –rcluster-percent 100 -q -p 24 –weights 1,1,0,1 –all-states –min-subset-size 100). We further restricted the PartitionFinder search to 11 amino-acid substitution models as these are the most selected models for empirical studies on Hexapoda (Misof et al., 2014; Peters et al., 2017; Pauli et al., 2018), namely LG+G, WAG+G, DCMUT+G, JTT+G, BLOSUM62+G, LG+G+F, WAG+G+F, DCMUT+G+F, JTT+G+F, BLOSUM62+G+F, LG4X (Yang, 1994; Gu et al., 1995; Müller and Vingron, 2000; Whelan and Goldman, 2001;

Veerassamy et al., 2003; Kosiol and Goldman, 2005; Le and Gascuel, 2008; Soubrier et al., 2012).

In order to find the best-scoring substitution model for each partition of the nt dataset ($NT_{decisive}$), we applied ModelFinder as implemented in IQ-TREE v.1.5.1 (Kalyaanamoorthy et al., 2017) (options –m TESTNEWONLY –gmedian). Please note that the boundaries of the partitions identified on amino-acid level are equivalent to the boundaries we kept for the decisive nucleotide dataset.

Phylogenetic relationships were inferred under the maximum likelihood (ML) optimality criterion as implemented in IQ-TREE v.1.3.11 and v.1.4.4 (Nguyen et al., 2015; Chernomor et al., 2016) and by using the best-scoring amino-acid substitution matrix for each partition (option–spp). We performed 50 independent ML tree searches with a random start tree for all three datasets, taking the median for each rate category (–gmedian) and an increased number of unsuccessful iterations before stopping (–numstop 200). Note that for each independent tree search, there were in total 100 initial random trees generated. To assess the number of unique topologies present within the 50 inferred trees, we used the software UniqueTree v.1.9. For each dataset, the 50 independently inferred tree showed all the same, i.e., one unique topology. However, there were topological differences between these three topologies, see discussion below.

Branch support was estimated via non-parametric bootstrapping of 100 bootstraps alignments in IQ-TREE and mapped onto the ML tree with the best log-likelihood. To assess the minimum number of replicates needed for a reliable estimation of bootstrap support, we subsequently used the "autoMRE" bootstrap convergence criterion (Pattengale et al., 2010) as implemented in RAxML with default settings. Bootstrap convergence was reached after 50 replicates for all three datasets in all tests.

Analyses of Phylogenetic Signal

In addition to the non-parametric bootstrap support, we determined support for the deeper phylogenetic relationships with the aid of Four-cluster Likelihood Mapping (FcLM) (Strimmer and von Haeseler, 1997), see Simon et al. (2018) and Supplementary Information in Misof et al. (2014) for details on the strategy. We applied the FcLM analyses on the decisive amino-acid dataset ($AA_{decisive}$) and tested all major relationships of the Phasmatodea lineages (see **Supplementary Figure S3**). For all 17 splits/relationships in question, we defined four groups and included only partitions for which at least one representative species of each of the four addressed groups was present. Taxa that did not address a particular hypothesis were discarded from the alignment (see **Supplementary Table S4** for included species, group definitions, and number of drawn quartets). For two incongruent nodes based on the tree inferences (see section Results and Discussion), we additionally checked for confounding signal due to among-lineage heterogeneity, non-random substitution processes and/or distribution of missing data using the FcLM approach with permuted datasets with phylogenetic signal destroyed. FcLM analyses were performed using IQ-TREE v.1.4.2 (Nguyen et al., 2015).

Divergence Time Estimations

For divergence time estimations, we used five fossils (**Table 1**) representing the oldest known fossils for the respective groups. The reported calibration points thus provide a lower limit to the age of each group. We modeled all fossil constraints as an exponential distribution with a rigid lower bound equal to the age of the fossils and a soft upper bound so that 95% of the distribution lies between the age of the fossil and the end of the Triassic (201.3 million years ago [mya], fossil 1), the end of the Jurassic (144.9 mya, fossil 2), and the end of the Paleogene (66.4 mya, fossils 3–5). For the root, a rather conservative prior estimate of the divergence date was specified, using a uniform distribution with rigid lower and upper bound indicated by the begin of the Permian (298.8 mya) and the end of the Jurassic. For the divergence date inference, we compiled a reduced version of the decisive amino-acid dataset ($AA_{decisive}$) only containing sites with unambiguous data for at least 95% of the 61 taxa ($AA_{decisive95}$) comprising 31,298 aa positions. To reduce computational effort, we chose an unpartitioned dating analysis. Divergence time estimates were performed in the program BEAST v.1.8.2 (Drummond et al., 2012) with a JTT+G+I substitution model, an uncorrelated lognormal relaxed clock, and a Yule tree prior. The JTT+G+I substitution model was determined in ModelFinder as implemented in IQ-TREE as best-scoring model of the available models implemented in BEAST for the reduced unpartitioned dataset. Markov Chain Monte Carlo analyses were conducted on the fixed topology obtained by the IQ-TREE ML analyses. Four separate runs for 50 million generations were conducted and sampled every 5,000 generations. The first 10 million generations of each run were discarded as burn-in as indicated by the software Tracer v.1.7.6 (Rambaut et al., 2018), which was also used to inspect convergence and mixing of parameters and the effective sample sizes (ESS). Post-burn-in samples were combined across all four runs to summarize parameter estimates and were used to construct a maximum clade credibility tree with median node heights in TreeAnnotator v.1.8.2 (Drummond et al., 2012). All BEAST analyses were conducted using the CIPRES portal (Miller et al., 2015).

Ancestral Range Reconstruction

For the reconstruction of ancestral ranges, we determined five areas according to the current distribution of the 38 extant phasmatodean species and following Wallace's zoogeographical regions by Holt et al. (2013): New World (Nearctic + Neotropical), Palearctic, Madagascan, Australian (including Oceanian), and Oriental. Based on the dated phylogenetic tree and allowing a maximum of two areas to be occupied, biogeographic models were compared using the maximum likelihood approach implemented in the R package BioGeoBEARS v.1.1.2 (Matzke, 2013, 2018). To cover a variety of different settings concerning dispersal, extinction, sympatry, and vicariance, we conducted the analysis using three models, namely, the Dispersal-Extinction-Cladogenesis model (DEC) and the likelihood interpretations of the models DIVA and BayArea (DIVALIKE and BAYAREALIKE). BayArealike features a parameter for widespread sympatry, DEC one for subset

TABLE 1 | Fossil Calibrations used in the divergence time estimate (modified from Robertson et al., 2018), fossils numbered according to **Figure 2**.

Fossil	Life stage	References	Formation	Minimum age offset (mya)	Soft upper bound (mya)	Distribution mean (mya)	Calibration node	Comments
Renphasma sinica	Adult	Nel and Delfosse, 2011	Yixian Formation, Liaonign, China	122	201.3	26.5	Divergence of Embioptera and Phasmatodea (**fossil 1**)	Unambiguous crown group phasmatodean due to presence of the vomer between a pair of unsegmented cerci
Echinosomiscus primoticus	Adult	Engel et al., 2016	Upper Cretaceous Amber, Myanmar	98.8	144.9	15.4	(**fossil 2**)	Euphasmatodea with uncertain affinity (presumed male Neophasmatodea)
Eophyllium messelense	Adult	Wedmann et al., 2007	Messel Germany deposits	47	66.4	6.5	Phyllinae (**fossil 3**)	Unambiguous crown leaf insect
Eophasma spp.	Egg	Poinar, 2011	Eocene Clarno Formation Nut Beds of Oregon	44	66.4	7.5	Pseudophasmatinae (**fossil 4**)	Euphasmatodean eggs most similar to Anisomorphini (Pseudophasmatinae)
Clonistria sp.	Egg	Poinar, 2011	Dominican amber, Hispaniola	20	66.4	15.5	Diapheromerinae (**fossil 5**)	Unambiguous Diapheromerinae egg due to vesicular/matrix capitulum

sympatry, and DIVALIKE one for widespread vicariance. Each model was also run with the +J parameter accounting for jump dispersal and founder-event speciation (Matzke, 2014). The best fitting model was assessed with the Likelihood-Ratio-Test (LRT), the Akaike Information criterion (AIC) and corrected AIC (AICc).

RESULTS AND DISCUSSION

Phylogenetic Relationships

Overall, our phylogenomic reconstruction received strong support in all analyses and significantly alters previous ideas regarding the evolutionary history of Phasmatodea, but at the same time corroborates clades that appeared well-supported in past molecular studies, both within and outside Phasmatodea (see **Figure 3** for comparison). All trees were rooted with the clade Zoraptera + Dermaptera according to Wipfler et al. (2019). Previously observed topologies by Wipfler et al. (2019) were fully corroborated, e.g., Plecoptera as sister group to a polyneopteran clade comprising Orthoptera, Blattodea, Mantodea, Phasmatodea, Embioptera, Mantophasmatodea, and Grylloblattodea. We also received in all three tree inferences support for Dictyoptera (Mantodea + Blattodea) as sister group to Xenonomia (Grylloblattodea + Mantophasmatodea) + Eukinolabia (Embiotera + Phasmatodea) (**Figure 2**; **Supplementary Figures S4**, **S5**). The only notable topological differences between the three phylogenetic analyses were observed within Embioptera in regard to the position of *Rhagadochir*, and within Phasmatodea in regard to the positions of the two phasmatodean taxa *Agathemera* and *Heteropteryx* (see discussion below). Results of all FcLM analyses testing all major nodes connecting Phasmatodea are mainly compatible with the ML tree reconstructions showing that they are robust against taxon sampling (**Supplementary Figure S6**). There are only two exceptions, which are further discussed and evaluated in **Supplementary Data Sheet 1**.

Within Phasmatodea, the species-poor *Timema* (= Timematodea) with 21 described species in western North America and species-rich Euphasmatodea (over 3,000 described species with worldwide distribution) form the basal sister groups, as has been demonstrated in a plethora of studies before (for an overview see Bradler and Buckley, 2018). The Euphasmatodea are divided into Aschiphasmatodea and Neophasmatodea as suggested by Engel et al. (2016). Our study thus confirms the idea of Aschiphasmatodea (= Aschiphasmatinae) forming the sister group to all remaining euphasmatodeans, which originally stems from the cladistic analysis of morphological characters by Tilgner (2002). In the past, this was controversially discussed (Bradler et al., 2003), but also recovered most recently by Robertson et al. (2018).

The subdivision of Neophasmatodea gives rise to an Old World and New World clade of stick and leaf insects, which was previously unsuspected. For these well-supported major clades we introduce the new rank-free taxon names Oriophasmata tax. nov. ("Eastern phasmids," Old World) and Occidophasmata tax. nov. ("Western phasmids," New World). There has never been any taxonomic scheme or morphological character presented

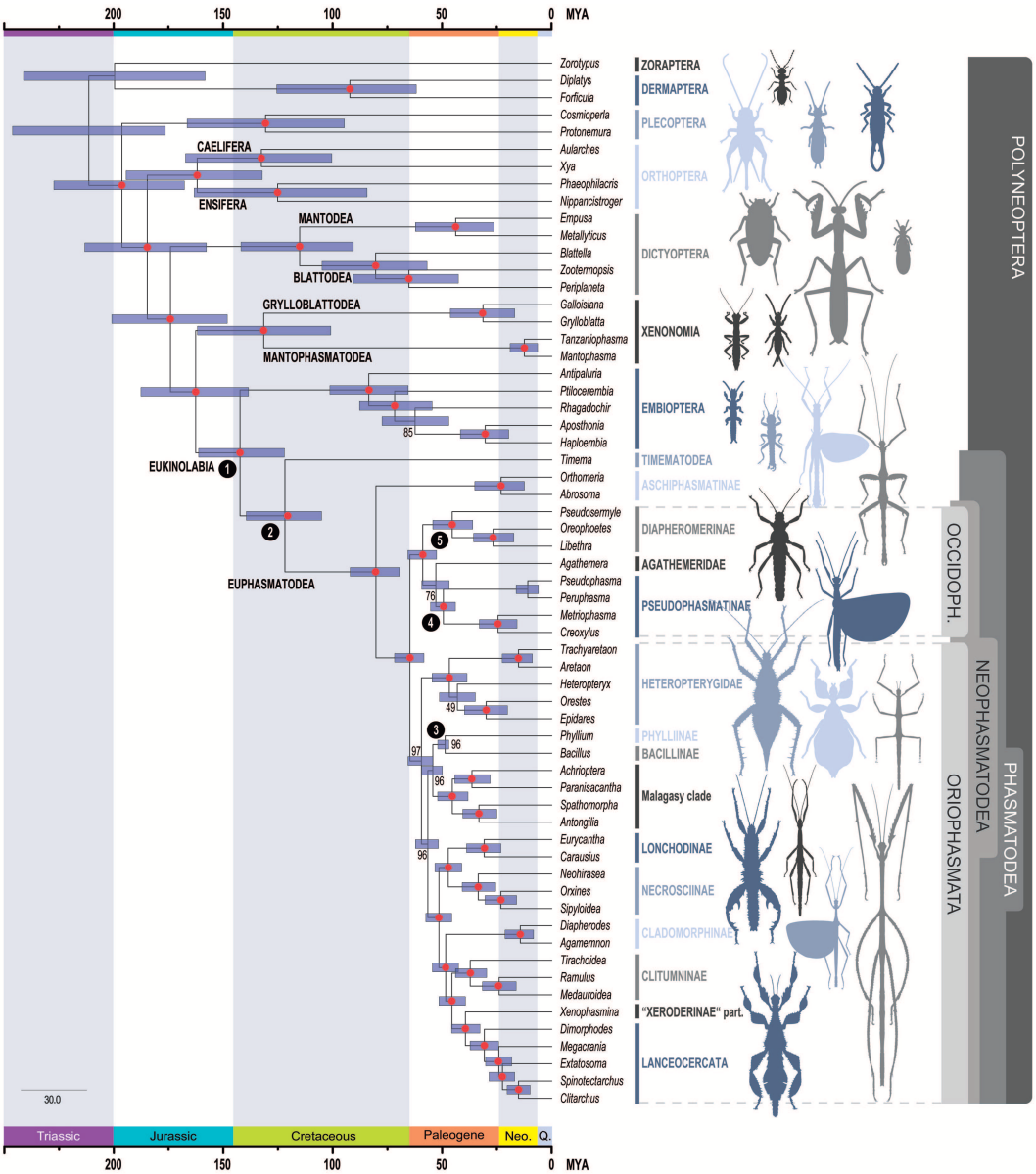

FIGURE 2 | Time-calibrated phylogeny of Phasmatodea. Inferred phylogenetic relationships based on dataset $AA_{decisive}$ (387,987 aa positions, 205 metapartitions). Colored circles represent bootstrap support derived from 100 BS. Node dates (posterior mean) were inferred using the dataset $AA_{decisive}$ reduced to sites containing >95% data completeness, and five fossil calibrations. Error bars represent 95% confidence intervals. Fossils used for calibrations are indicated as numbers in black circles at nodes: 1: Nel and Delfosse (2011), 2: Wedmann et al. (2007), 3: Sellick (1994), 4, 5: Poinar (2011) (see also **Table 1**). OCCIDOPH., Occidophasmata; Neo., Neogene; Q., Quaternary.

that suggested these clades, in consequence, neither have there ever been alternative robust phylogenetic hypotheses postulated for their major subgroups that would question this novel assumptions.

The New World clade Occidophasmata comprises the two species-rich and dominant stick insect groups of South and North America, the Diapheromerinae and Pseudophasmatinae (= Pseudophasmatidae by some authors), which were originally assigned to the two traditional suborders "Areolatae" (Pseudophasmatinae) and "Anareolatae" (Diapheromerinae), based on the presence or absence of a triangular field at the apex of the tibiae (Günther, 1953). While all previous phylogenetic studies already demonstrated that the traditional subdivision of Phasmatodea into "Areolatae" and "Anareolatae" is meaningless, there is not a single morphological character known to support a close relationship of Diapheromerinae and Pseudophasmatinae. Yet, this clade receives support from a biogeographical point of view considering that we have seen in the past that biogeography generally plays a more important role for the evolutionary history of stick insects than morphological

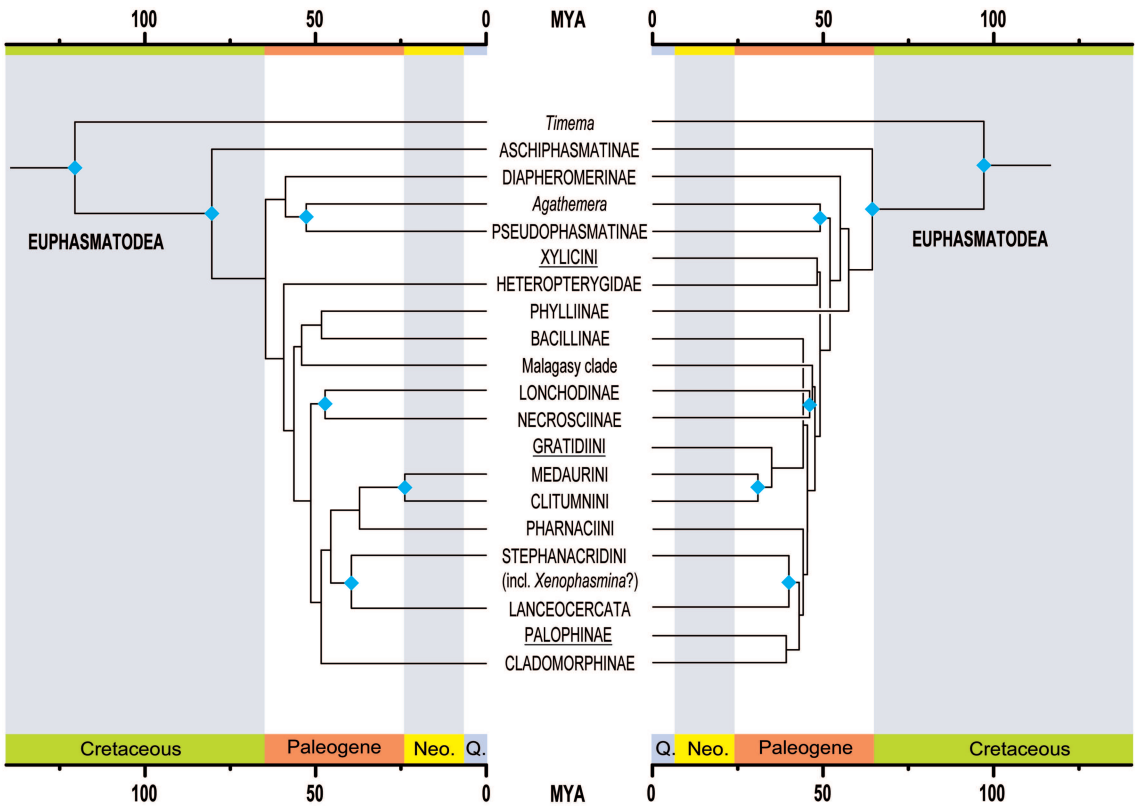

FIGURE 3 | Comparison of topology and divergence time estimations between the herein presented new phylogeny of Phasmatodea (left side) to the most recent and comprehensive phylogeny based on Sanger sequence data by Robertson et al. (2018). The underlined taxa are African lineages included in the study from Robertson et al. (2018) but missing in the present study. The blue rhomb symbols indicate taxa supported in both studies. Neo., Neogene; Q., Quaternary.

similarity (Buckley et al., 2009; Bradler et al., 2015). This New World clade also comprises *Agathemera*, a wingless South American taxon with a stout body form and eight described species from Chile and Argentina (Domínguez et al., 2009, Vera et al., 2012). The phylogenetic position of *Agathemera* has been an evolutionary enigma. Based on morphological evidence, *Agathemera* was repeatedly placed as sister group to all remaining Euphasmatodea (Bradler, 2000, 2009; = Neophasmatidae sensu Bradler, 2003; = Verophasmatodea sensu Zompro, 2004; Klug and Bradler, 2006; Klug, 2008; Friedemann et al., 2012). However, this assumption and consequently the monophyly of Verophasmatodea have never been supported by molecular studies, which place *Agathemera* as a subordinate taxon, albeit with unstable position among stick insects (Whiting et al., 2003; Buckley et al., 2009; Bradler et al., 2014, 2015; Goldberg et al., 2015; Büscher et al., 2018). Most recently, *Agathemera* has been found to be the sister group to Pseudophasmatinae including Heteronemiini and Prisopidini (Robertson et al., 2018), thus basically re-erecting the Pseudophasmatinae that included all these taxa as originally proposed by Günther (1953). Our results partially support this view here by a placement of *Agathemera* as sister to Pseudophasmatinae in the trees inferred from the datasets $AA_{decisive}$ (**Figure 2**) and $NT_{decisive}$ (**Supplementary Figure S4**), yet this is one of the lesser supported clades (BS = 76 and BS = 94, respectively), and our analysis does not include members of Prisopodini and Heteronemiini. In contrast, trees inferred from the dataset AA_{SOS} support *Agathemera* as sister group to a clade comprising Pseudophasmatinae and Diapheromerinae (**Supplementary Figure S5**). However, further FcLM analyses in combination with permutation tests show that the position of *Agathemera* as sister to Pseudophasmatinae in the trees inferred from the datasets $AA_{decisive}$ could not be explained by confounding signal. In contrast, the position of *Agathemera* as sister group to a clade comprising Pseudophasmatinae and Diapheromerinae inferred by the dataset AA_{SOS} may be caused by the presence of confounding signal (e.g., heterogeneous amino-acid site composition, non-stationary substitution processes, or non-random distribution of missing data). For details refer to **Supplementary Material Data Sheet 1**.

Furthermore, we recovered a subdivision of Pseudophasmatinae (or Pseudophasmatidae) into Pseudophasmatinae (*Peruphasma*, *Pseudophasma*) and Xerosomatinae (*Creoxylus*, *Metriophasma*). Within Diapheromerinae, the subdivision into Oreophoetini (*Libethra*, *Oreophoetes*) and Diapheromerini (*Pseudosermyle*) is supported (Robertson et al., 2018).

The Oriophasmata comprise all remaining neophasmatodean taxa with Heteropterygidae as sister group to the rest. Within

Heteropterygidae, the Obriminae (*Aretaon, Trachyaretaon*) and Dataminae (*Epidares, Orestes*) (traditionally referred to as Obrimini and Datamini, see Bradler and Buckley, 2018) were recovered, and *Heteropteryx* (representing the third subgroup Heteropteryginae or, traditionally, Heteropterygini) as sister to Dataminae in the trees inferred from the dataset $AA_{decisive}$ (**Figure 2**). The latter clade, Dataminae + Heteropteryginae, gained extremely low support (BS = 49), but was repeatedly recovered before (Büscher et al., 2018; Robertson et al., 2018). In contrast, Bradler et al. (2015) obtained a topology Dataminae + (Heteropteryginae + Obriminae), which was also favored based on phylogenetic analysis of morphological characters by Bradler (2009) and also in our study supported by the trees inferred from the datasets $NT_{decisive}$ and AA_{SOS} (**Supplementary Figures S4, S5**). The third possible topology Heteropteryginae + (Obriminae + Dataminae), as proposed by Zompro (2004), was favored by one previous molecular phylogeny (Goldberg et al., 2015) but was not recovered by any of our phylogenetic inferences. Additional FcLM analyses in combination with permutation tests revealed that the inferred relationship by the dataset AA_{SOS} (*Heteropteryx* and Obriminae being closest relatives) is strongly biased by confounding signal. The FcLM analyses further supported a sister group relationship of *Heteropteryx* with Dataminae which is less prone to confounding signal in the dataset $AA_{decisive}$ as well as AA_{SOS} (for details, please refer to **Supplementary Material Data Sheet 1**). However, given the low number of possible drawn quartets (88) and the low support observed in the present analysis for a sister group relationship of *Heteropteryx* with Dataminae, the internal phylogeny of Heteropterygidae must still be considered an open question.

Within the remaining Oriophasmata, *Bacillus* + *Phyllium* form an early branch together with the Malagasy clade of stick insects. The subordinate phylogenetic placement of Phylliinae, the true leaf insects (represented here by *Phyllium philippinicum*), within these Old World Euphasmatodea, is in contrast to recent molecular phylogenies that favor Phylliinae to be a rather early diverging lineage among Euphasmatodea (Kômoto et al., 2011; Bradler et al., 2015; Robertson et al., 2018). Again, our finding corroborates the view of Günther (1953) who considered Phylliinae to be just one subordinate subfamily of many within Phasmatodea. A close affinity between Phylliinae and members of Bacillinae has never been postulated before, yet we received moderate support ($AA_{decisive}$: BS = 96; $NT_{decisive}$: BS = 80; AA_{sos}: BS = 100) for a sister group relationship of *Phyllium* and the European *Bacillus*. However, the FcLM analyses and further permutation tests of the two amino-acid datasets ($AA_{decisive}$, AA_{sos}) revealed that the tree reconstructions might be biased by confounding signal (for details refer to **Supplementary Material Data Sheet 1**). Nevertheless, this grouping receives support from a biogeographical point of view: Although the extant Phylliinae have a predominantly Asian distribution, the fossil record provides evidence of a European origin of leaf insects with the 47-million-years-old *Eophyllium*, the extinct sister group of all remaining leaf insects, described from Grube Messel in Germany (Wedmann et al., 2007).

A monophyletic Malagasy clade comprises Anisacanthidae (*Paranisacantha*), Achriopterini (*Achrioptera*), Antongiliinae (*Antongilia*), and Phasmatidae taxa *incertae sedis* (*Spathomorpha*), with the former two and the latter two forming sister taxa in accordance with previous results (Bradler et al., 2015; Goldberg et al., 2015; Büscher et al., 2018; Robertson et al., 2018; Glaw et al., 2019). Closely related Malagasy stick insects were only recently suggested but not recovered as monophyletic when certain African taxa were included that are lacking in the present analysis (Bradler et al., 2015; Robertson et al., 2018).

One major radiation within Oriophasmata comprises Lonchodidae (Lonchodinae + Necrosciinae, Robertson et al., 2018) that contain over 1,000 described species, thus accounting for one third of the described extant phasmatodean diversity. The sister lineage of Lonchodidae contains taxa that have been recovered multiple times before as monophyletic groups including Lanceocercata and its sister taxon Stephanacridini, Cladomorphinae, Medaurini (*Medauroidea*), Clitumnini (*Ramulus*), and Pharnaciini (*Tirachoidea*) (Buckley et al., 2009, 2010; Bradler et al., 2014, 2015; Büscher et al., 2018; Robertson et al., 2018), however, with a slightly different topology in our tree based on transcriptomes.

Monophyly of Lanceocercata with *Dimorphodes* as sister group to all remaining Lanceocercata appears to be undisputed (Buckley et al., 2009, 2010; Bradler et al., 2014, 2015; Büscher et al., 2018; Robertson et al., 2018). In previous studies, Stephanacridini were usually observed as sister taxon to Lanceocercata. Here, we obtain *Xenophasmina* as sister to Lanceocercata, a taxon currently considered to be a member of the Xeroderinae. Since Xeroderinae are an obviously polyphyletic assemblage (Buckley et al., 2009; Bradler et al., 2015), *Xenophasmina* must be considered as a taxon *incertae sedis* that might be a member of Stephanacridini, which needs to be corroborated in subsequent analyses.

Surprisingly, we infer monophyletic Clitumninae as erected by Hennemann and Conle (2008), to be comprised of Clitumnini, Medaurini, and Pharnaciini, as well as to be more closely related to Lanceocercata than the Neotropical Cladomorphinae. This is in sharp contrast to numerous previous results that concordantly inferred polyphyletic Clitumninae and suggested a well-supported lineage of Cladomorphinae + (Stephanacridini + Lanceocercata) (Buckley et al., 2009, 2010; Bradler et al., 2014, 2015; Büscher et al., 2018; Robertson et al., 2018). This disagreement needs to be further addressed in future analyses by adding missing taxa such as Stephanacridini and members of Gratidiini that were demonstrated to be closely related to Medaurini and Clitumnini in the past (Bradler et al., 2014, 2015; Büscher et al., 2018; Robertson et al., 2018).

Divergence Time Estimation

According to our analyses, extant Phasmatodea started to diversify in the Mesozoic with the split between *Timema* and Euphasmatodea lying in the Early Cretaceous (95% confidence interval [CI]: 105.1–139.4 mya; mean: 121.8 mya, **Figure 2**), with the oldest currently known fossils assigned unambiguously to stick insects being from the Mesozoic of China, ∼128 mya (Wang et al., 2014). This estimation is older than previous estimates

(see **Figure 3** for comparison), for instance, ∼103 mya (CI: 85.52–122.12 mya, Bradler et al., 2015) or ∼95 mya (Buckley et al., 2009). The overall divergence time estimates for the early splits of stick and leaf insects are older than in previous studies, for instance, ∼61.26 mya (CI: 51.04–75.43 mya) for the earliest node within Euphasmatodea according to Bradler et al. (2015), and indicate a diversification of Euphasmatodea around 80.3 mya (CI: 69.6–92.0 mya), which constitutes the split between Aschiphasmatodea and Neophasmatodea in our study. Neophasmatodea further radiated into Orio- and Occidophasmata around 64.8 mya (CI: 58.4–71.8 mya). Radiation of Occidophasmata in North and South America began ∼58.9 mya (CI: 52.6–65.7 mya), with *Agathemera* being a separate, old genus since about 52.9 mya (CI for the split from Pseudophasmatinae: 46.8–59.4 mya).

Within Oriophasmata, radiation started approximately at the same time, namely, 59.5 mya (CI: 54.2–65.6 mya), when the ground-dwelling Heteropterygidae split off from the remainder of this clade. The start of Heteropterygidae radiation is estimated at ∼46.8 mya (CI: 38.7–54.6 mya), which largely confirms the date recovered by Robertson et al. (2018) who gave a mean of 46.4 mya (between 53 and 40 mya, see **Figure 3**).

The Malagasy clade radiation started between 38.2 and 52.1 mya (mean: ∼46.8 mya) with the split from its sister group occurring around 56.6 mya (CI: 51.8–62.2 mya), which is most probably much younger than the separation of Madagascar from any significant landmass (65–96 mya; Vences et al., 2009). This corroborates the previous assumption that stick insects colonized this fragmentary island long after it became isolated, between 38 and 51 mya (Bradler et al., 2015).

Further significant radiation dates within Oriophasmata include Lonchodidae at 47.3 mya (CI: 41.1–53.3 mya), constituting the split between Lonchodinae and Necrosciinae, and Clitumninae at 37.3 mya (CI: 29.7–44 mya). The Neotropical Cladomorphinae diverged from the Australasian stick insects between 42.6 and 54.5 mya (mean: 48.4 mya). This lies within the dates for the rifting of Antarctica from Australia and South America, which was implicated as the origin for the split of the New World Cladomorphinae from their Australasian sister taxon (Buckley et al., 2010). However, the biogeographic reconstructions favor an orientally distributed ancestor (see below).

The Lanceocercata radiation is relatively young, starting around 30.6 mya (CI: 24.3–37.3 mya), which is in the range of

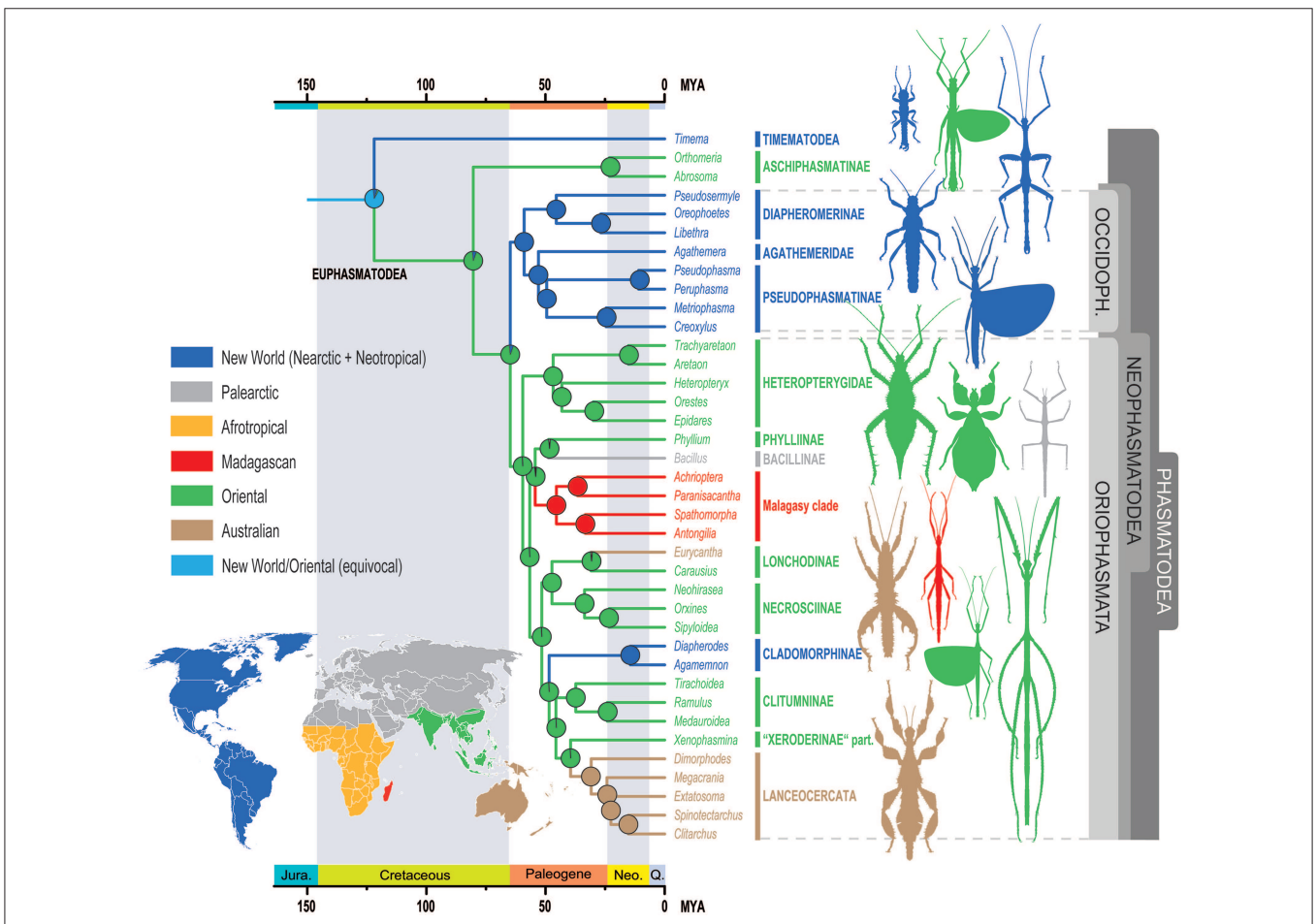

FIGURE 4 | Ancestral range estimates of Phasmatodea for the BioGeoBEARS DIVALIKE+J model. The nodal pie charts show the relative probability of the geographic ranges according to the in-figure color code. OCCIDOPH., Occidophasmata, Jura., Jurassic, Neo., Neogene, Q., Quaternary.

previous estimates (or younger) spanning from 32 mya (CI: 29.4–37.5 mya, Buckley et al., 2009) over ∼40 mya (Bradler et al., 2015) up to 51.76 mya (36.23–69.78 mya, Buckley et al., 2010), the latter based on the arthropod molecular clock rates suggested by Brower (1994), i.e., without fossil calibrations.

In summary, our novel divergence time estimation generally supports the previous molecular clock analyses that suggested the extant radiation of stick and leaf insects to be rather young, having occurred largely after the Cretaceous–Tertiary (K-T) boundary (∼66 mya) (Buckley et al., 2009; Bradler et al., 2015; Robertson et al., 2018), although some early splits and some lower 95% confidence interval boundaries fall into the Late Cretaceous. The reason for the successful, rather recent radiation of Euphasmatodea is not yet fully understood. It has been partly explained by the co-evolution of phasmatodeans with angiosperms (Archibald and Bradler, 2015) although similar ecological associations such as predator-prey interactions encountered by plant-mimicry were already found in Cretaceous stick insects living in gymnosperm forests (Wang et al., 2014). Other studies suggested that horizontal gene transfer of pectinase genes from gut bacteria into the genome of stick insects (Shelomi et al., 2016) or that the development of hard-shelled seed-like eggs (Robertson et al., 2018) were key innovations explaining the recent success of Euphasmatodea. These properties surely enhanced their ability to mimic and feed on angiosperm plants, and most probably a combination of these traits might be accountable for the impressive euphasmatodean diversification.

Historical Biogeography

Our biogeographical model selection analysis under the maximum likelihood optimization criterion in BioGeoBEARS resulted in DIVALIKE +J being the best fitting model and, generally, showed a clear preference for the three models incorporating the J parameter indicating the significance of potential jump dispersal and founder events (see **Supplementary Table S5** for details on the results).

The ancestral geographic range at the root of Phasmatodea was equivocally reconstructed to be New World (Nearctic + Neotropical) and Oriental, and must be considered unresolved (**Figure 4**). The recent report of Burmese amber fossils interpreted as mid-Cretaceous members of Timematodea (Chen et al., 2018) would further support an Oriental origin of Phasmatodea, but a critical re-evaluation of this finding is still pending. Every following node is clearly resolved. However, while the ancestral region of Aschiphasmatinae and Neophasmatodea is depicted as Oriental according to the best-fitting model DIVALIKE +J, the estimations calculated by the models DEC and BAYAREALIKE (with and without parameter J) show the node as unresolved (see **Supplementary Data Sheet 2**). Similarly, the ancestral range of Neophasmatodea is Oriental according to the best-fitting model, but unresolved for some of the other models, whereas the origin of Oriophasmata is unambiguously reconstructed as Oriental and that of Occidophasmata Nearctic/Neotropical.

Beyond this ambiguity at the base of the tree, reconstruction of the historical biogeography appears to be rather straightforward. On account of the young age of the recovered phasmatodean lineages, their geographic distribution must be explained by dispersal events rather than vicariant processes. A few major colonization events out of Southeast Asia can be observed: A single colonization of Madagascar, although this might have occurred via Africa (Bradler et al., 2015) with the African taxa in question lacking in our study. Furthermore, Southern Europe was colonized once (*Bacillus*) by a lineage probably also including the leaf insects (Phylliinae) with a potential European origin (see above). The Cladomorphinae of Central and South America also originated in Southeast Asia and can be interpreted as the result of a transoceanic, most probably trans-Pacific dispersal event, or via Antarctica which was connected to Australia and South America. Ancient long-distance dispersals in eastward direction across the Pacific have been reported for terrestrial arthropods before, for instance in *Amaurobioides* coastal spiders (Araneae; Ceccarelli et al., 2016) and metalmark moths (Lepidoptera: Choreutidae, Rota et al., 2016). Transoceanic crossings repeatedly played a pivotal role for stick and leaf insect distribution (Buckley et al., 2009, 2010), with oceanic distances covered as far as from Australia to the Mascarene Archipelago (Bradler et al., 2015). Above-water dispersal might have occurred via animals rafting on mats of vegetation (King, 1962) or as eggs that are exceptionally robust in phasmatodeans and have been shown to survive extended periods floating in sea water (Kobayashi et al., 2014) and even passing the digestive tract of insectivorous birds (Suetsugu et al., 2018).

CONCLUSION AND OUTLOOK

Our study confirms the power of phylogenomic approaches for inferring evolutionary relationships that have been difficult to assess in the past by yielding a well-supported topology at the base of the tree of life of stick and leaf insects. We provide strong evidence for resolving the deep phylogenetic nodes among all major lineages of Phasmatodea, and were furthermore able to date the individual divergence events and reconstruct their biogeographic history. Our study provides a substantial basis for establishing a natural classification of the stick and leaf insects and for further developing the role of phasmatodeans as emerging model systems in evolutionary research. Future studies need to address minor but crucial taxonomic problems that still await revelation such as the phylogenetic placement of the Southeast Asian Stephanacridini, the African Gratidiini, Bacillinae, and Palophinae, and the Neotropical Heteronemiini, by for instance, applying DNA enrichment methods in order to generate phylogenetically informative data sets that can be combined with those generated in the present study.

DATA AVAILABILITY

The transcriptome data will be made available via NCBI GenBank BioProject ID PRJNA183205 (https://www.ncbi.nlm.nih.gov/bioproject/183205). Supplementary data files are available from

the Dryad Digital Repository: https://doi.org/10.5061/dryad.65492qt (Simon et al., 2019).

AUTHOR CONTRIBUTIONS

SBr, SS, BW, and TB designed the study. SBr, TB, BW, and RM collected or provided samples. AD, SL, LP, XZ, KM, and SS assembled and processed the transcriptomes. AD, BM, LP, KM, and SS developed scripts, datasets, and programs. SS phylogenetically analyzed the transcriptomes and performed topology tests. HL conducted age divergence analysis. SBa performed biogeography reconstruction. SBr generated the figures. SBr, SS, SBa, and TB wrote the manuscript. BW and HL added to manuscript editing. All authors approved the final version of the manuscript.

FUNDING

This study was supported by the German Science Foundation (DFG grants BR 2930/2-1, 2930/3-1, BR 2930/4-1, and BR 2930/5-1 to SBr, and WI 4324/1-1 to BW).

ACKNOWLEDGMENTS

The presented data are the result of the collaborative efforts of the 1KITE consortium and the authors extend their gratitude to all those who assisted with any aspect of this project, from specimen collection, to molecular lab work, to bioinformatics, and all our analyses. Thank you to all who assisted with specimen acquisition, including: Lars Möckel, Hans Pohl, Dieter Schulten, Rene Koehler, Reinhard Predel, Adriana Marvaldi as well as Julia Goldberg and Nicolas Cliquennois who assisted during field work on Madagascar, Ondrej Hlinka for High-Computing Performance assistance, and other colleagues from BGI-Shenzhen who contributed to sample and data curation and management. Thank you to BGI-Shenzhen for supporting and funding this study, through the 1KITE initiative. We thank Christoph Seiler for providing photographs and Bernd Baumgart for technical assistance with the graphics.

SUPPLEMENTARY MATERIAL

The Supplementary Material for this article can be found online at: https://www.frontiersin.org/articles/10.3389/fevo.2019.00345/full#supplementary-material

REFERENCES

Archibald, S. B., and Bradler, S. (2015). Stem-group stick insects (Phasmatodea) in the early Eocene at McAbee, British Columbia, Canada, and Republic, Washington, United States of America. *Can. Entomol.* 147, 744–753. doi: 10.4039/tce.2015.2

Bank, S., Sann, M., Mayer, C. U., Meusemann, K., Donath,. A., Podsiadlowski, L., et al. (2017). Transcriptome and target DNA enrichment sequence data provide new insights into the phylogeny of vespid wasps (Hymenoptera: Aculeata: Vespidae). *Mol. Phyl. Evol.* 116, 213–226. doi: 10.1016/j.ympev.2017.08.020

Beutel, R. G., Friedrich, F., Ge, S.-Q., and Yang, X.-K. (2014). *Insect Morphology and Phylogeny*. Berlin: Walter de Gruyter GmbH.

Bradler, S. (2000). On the systematic position of *Agathemera* Stal 1875 within the Phasmatodea (Insecta). *Zoology* 103(Suppl. III):99.

Bradler, S. (2003). "Phasmatodea, Gespestschrecken," in *Lehrbuch der Speziellen Zoologie, Bd. I, Wirbellose Tiere, 5. Teil Insecta*, ed H. H. Dathe (Heidelberg; Berlin: Spektrum). 251–261.

Bradler, S. (2009). Phylogenie der Stab- und Gespenstschrecken *(Phasmatodea*). *Spec. Phyl. Evol.* 2, 3–139. doi: 10.17875/gup2009-710

Bradler, S. (2015). Der Phasmatodea Tree of Life: Überraschendes und Ungeklärtes in der Stabschrecken-evolution. *Entomologie heute* 27, 1–23.

Bradler, S., and Buckley, T. R. (2018). "Biodiversity of Phasmatodea," in *Insect Biodiversity: Science and Society*, Vol. II, eds R. G. Foottit and P. H. Adler (Hoboken, NJ: Wiley-Blackwell), 281–313.

Bradler, S., Cliquennois, N., and Buckley, T. R. (2015). Single origin of Mascarene stick insects: ancient radiation on sunken islands? *BMC Evol. Biol.* 15:196. doi: 10.1186/s12862-015-0478-y

Bradler, S., Robertson, J. A., and Whiting, M. F. (2014). A molecular phylogeny of Phasmatodea with emphasis on Necrosciinae, the most species-rich subfamily of stick insects. *Sys. Ent.* 39, 205–222. doi: 10.1111/syen.12055

Bradler, S., Whiting, M. F., and Klug, R. (2003). Basal diversification and the evolution of wings in stick insects (Phasmatodea). *Entomol. Abh.* 61, 132–133.

Bradley, J. C., and Galil, B. S. (1977). The taxonomic arrangement of the Phasmatodea with keys to the subfamilies and tribes. *Proc. Entomol. Soc. Wash.* 79, 176–208.

Brand, P., Lin, W., and Johnson, B. R. (2018). The draft genome of the invasive walking stick, *Medauroidea extradendata*, reveals extensive lineage-specific gene family expansions of cell wall degrading enzymes in Phasmatodea. *G3* 8, 1403–1408. doi: 10.1534/g3.118.200204

Breinholt, J. W., Lemmon, A., Lemmon, E., Xiao, L., Earl, C., and Kawahara, A.Y. (2018). Resolving relationships among the megadiverse butterflies and moths with a novel pipeline for Anchored Phylogenomics. *Syst. Biol.* 67, 78–93. doi: 10.1093/sysbio/syx048

Brock, P. D., Büscher, T. H., and Baker, E. (2017). "Phasmida species file online: phasmida species file version 5.0/5.0," in *Species 2000 and ITIS Catalogue of Life*, eds Y. Roskov, G. Ower, T. Orrell, D. Nicolson, N. Bailly, P. M. Kirk, T. Bourgoin, R. E. DeWalt, W. Decock, E. van Nieukerken, J. Zarucchi, and L. Penev (Leiden: Species 2000; Naturalis). Available online at: www.catalogueoflife.org/col (accessed April 20, 2019).

Brock, P. D., and Marshall, J. (2011). Order Phasmida Leach. 1815. In: Zhang, Z.-Q. (Ed.) Animal biodiversity: an outline of higher-level classification and survey of taxonomic richness. *Zootaxa* 3148:198. doi: 10.11646/zootaxa.3148.1.36

Brower, A. V. Z. (1994). Rapid morphological radiation and convergence in geographical races of the butterfly, *Heliconius erato*, inferred from patterns of mitochondrial DNA evolution. *Proc. Nat. Acad. Sci. U.S.A.* 91, 6491–6495. doi: 10.1073/pnas.91.14.6491

Buckley, T. R., Attanayake, D., and Bradler, S. (2009). Extreme convergence in stick insect evolution: phylogenetic placement of the Lord Howe Island tree lobster. *Proc. R. Soc. Lond. B* 276, 1055–1062. doi: 10.1098/rspb.2008.1552

Buckley, T. R., Attanayake, D., Nylander, J. A. A., and Bradler, S. (2010). The phylogenetic placement and biogeographical origins of the New Zealand stick insects (Phasmatodea). *Sys. Ent.* 35, 207–225. doi: 10.1111/j.1365-3113.2009.00505.x

Büscher, T. H., Buckley, T. R., Grohmann, C., Gorb, S. N., and Bradler, S. (2018). The evolution of tarsal adhesive microstructures in stick and leaf insects (Phasmatodea). *Front. Ecol. Evol.* 6:69. doi: 10.3389/fevo.2018.00069

Ceccarelli, F. S., Opell, B. D., Haddad, C. R., Raven, R. J., Soto, E. M., and Ramírez, M. J. (2016). Around the world in eight million years: Historical biogeography and evolution of the spray zone spider *Amaurobioides* (Araneae: Anyphaenidae). *PLoS ONE* 11:e0163740. doi: 10.1371/journal.pone.0163740

Chen, S., Deng, S.-.W., Shih, C., Zhang, W.-W., Zhang, P., Ren, D., et al. (2018). The earliest timematids in Burmese amber reveal diverse tarsal pads of stick insects in the mid-Cretaceous. *Ins. Sci.* 26:945–957. doi: 10.1111/1744-7917.12601

Chernomor, O., von Haeseler, A., and Minh, B. Q. (2016). Terrace aware data structure for phylogenomic inference from supermatrices. *Syst. Biol.* 65, 997–1008. doi: 10.1093/sysbio/syw037

Dell'Ampio, E., Meusemann, K., Szucsich, N. U., Peters, R. S., Meyer, B., Borner, J., et al. (2014). Decisive data sets in phylogenomics: lessons from studies on the phylogenetic relationships of primarily wingless insects. *Mol. Biol. Evol.* 31, 239–249. doi: 10.1093/molbev/mst196

Domínguez, M. C., San-Blas, G., Agrain, F., Roig-Juñent, S. A., Scollo, A. M., and Debandi, G. O. (2009). Cladistic, biogeographic and environmental niche analysis of the species of *Agathemera* Stål (Phasmatida, Agathemeridae). *Zootaxa* 2308, 43–57. doi: 10.11646/zootaxa.2308.1.3

Drummond, A. J., Suchard, M. A., Xie, D., and Rambaut, A. (2012). Bayesian phylogenetics with BEAUti and the BEAST 1.7. *Mol. Biol. Evol.* 29, 1969–1973. doi: 10.1093/molbev/mss075

Eddy, S. R. (2011). Accelerated profile HMM searches. *PLoS Comput. Biol.* 7:e1002195. doi: 10.1371/journal.pcbi.1002195

Engel, M. S., Wang, B., and Alqarni, A. S. (2016). A thorny, 'anareolate' stick-insect (Phasmatidae s.l.) in Upper Cretaceous amber from Myanmar, with remarks on diversification times among Phasmatodea. *Cret. Res.* 63, 45–53. doi: 10.1016/j.cretres.2016.02.015

Evangelista, D. A., Wipfler, B., Béthoux, O., Donath, A., Fujita, M., Kohli, M. K., et al. (2019). An integrative phylogenomic approach illuminates the evolutionary history of cockroaches and termites (Blattodea). *Proc. R. Soc. Lond. B* 286:20182076. doi: 10.1098/rspb.2018.2076

Friedemann, K., Wipfler, B., Bradler, S., and Beutel, R. G. (2012). On the head morphology of *Phyllium* and the phylogenetic relationships of Phasmatodea (Insecta). *Acta Zool.* 93, 184–199. doi: 10.1111/j.1463-6395.2010.00497.x

Glaw, F., Hawlitschek, O., Dunz, A., Goldberg, J., and Bradler, S. (2019). When giant stick insects play with colors: Molecular phylogeny of the Achriopterini and description of two new splendid species (Phasmatodea: *Achrioptera*) from Madagascar. *Front. Ecol. Evol.* 7:105. doi: 10.3389/fevo.2019.00105

Goldberg, J., Bresseel, J., Constant, J., Kneubühler, B., Leubner, F., Michalik, P., et al. (2015). Extreme convergence in egg-laying strategy across insect orders. *Sci. Rep.* 5:7825. doi: 10.1038/srep07825

Grimaldi, D., and Engel, M. (2005). *Evolution of the Insects*. Cambridge: Cambridge University Press.

Gu, X., Fu, Y. X., and Li, W. H. (1995). Maximum likelihood estimation of the heterogeneity of substitution rate among nucleotide sites. *Mol. Biol. Evol.* 12, 546–557.

Gullan, P. J., and Cranston, P. S. (2014). *The Insects: An Outline of Entomology, 4th Edn*. Oxford: Wiley-Blackwell.

Günther, K. (1953). Über die taxonomische Gliederung und geographische Verbreitung der Insektenordnung der Phasmatodea. *Beitr. Entomol.* 3, 541–563.

Hennemann, F. H., and Conle, O. V. (2008). Revision of oriental Phasmatodea: the tribe Pharnaciini, Günther, 1953, including the description of the world's longest insect, and a survey of the family Phasmatidae Gray, 1835 with keys to the subfamilies and tribes (Phasmatodea: "Anareolatae": Phasmatidae). *Zootaxa* 1906, 1–316. doi: 10.11646/zootaxa.1906.1.1

Ho, S. Y., and Jermiin, L. S. (2004). Tracing the decay of the historical signal in biological sequence data. *Syst. Biol.* 53, 623–637. doi: 10.1080/10635150490503035

Holt, B. G., Lessard, J. P., Borregaard, M. K., Fritz, S. A., Araújo, M. B., Dimitrov, D., et al. (2013). An update of Wallace's zoogeographic regions of the world. *Science* 339, 74–78. doi: 10.1126/science.1228282

Johnson, K. P., Dietrich, C. H., Friedrich, F., Beutel, R. G., Wipfler, B., Peters, R. S., et al. (2018). Phylogenomics and the evolution of hemipteroid insects. *Proc. Nat. Acad. Sci. U.S.A.* 115, 12775–12780. doi: 10.1073/pnas.1815820115

Kômoto, N., Yukuhiro, K., and Tomita, S. (2012). Novel gene rearrangements in the mitochondrial genome of a webspinner, *Aposthonia japonica* (Insecta: Embioptera). *Genome* 55, 222–233. doi: 10.1139/g2012-007

Kômoto, N., Yukuhiro, K., Ueda, K., and Tomita, S. (2011). Exploring the molecular phylogeny of phasmids with whole mitochondrial genome sequences. *Mol. Phyl. Evol.* 58, 43–52. doi: 10.1016/j.ympev.2010.10.013

Kalyaanamoorthy, S., Minh, B. Q., Wong, T. K., von Haeseler, A., and Jermiin, L. S. (2017). ModelFinder: fast model selection for accurate phylogenetic estimates. *Nat. Methods* 14, 587–589. doi: 10.1038/nmeth.4285

Katoh, K., and Standley, D. M. (2013). MAFFT multiple sequence alignment software version 7: improvements in performance and usability. *Mol. Biol. Evol.* 30, 772–780. doi: 10.1093/molbev/mst010

King, W. (1962). The occurrence of rafts for dispersal of land animals into the West Indies. *Q. J. Florida. Acad. Sci.* 25, 45–52.

Klug, R. (2008). Anatomie des Pterothorax der Phasmatodea, Mantophasmatodea und Embioptera und seine Bedeutung für die Phylogenie der Polyneoptera (Insecta). *Spec. Phyl. Evol.* 1, 171–217.

Klug, R., and Bradler, S. (2006). The pregenital abdominal musculature in phasmids and its implications for the basal phylogeny of Phasmatodea (Insecta: Polyneoptera). *Org. Div. Evol.* 6, 171–184. doi: 10.1016/j.ode.2005.08.004

Kobayashi, S., Usui, R., Nomoto, K., Ushirokita, M., Denda, T., and Izawa, M. (2014). Does egg dispersal occur via the ocean in the stick insect genus *Megacrania* (Phasmida: Phasmatidae)? *Ecol. Res.* 29, 1025–1032. doi: 10.1007/s11284-014-1188-4

Kosiol, C., and Goldman, N. (2005). Different versions of the Dayhoff rate matrix. *Mol. Biol. Evol.* 22, 193–199. doi: 10.1093/molbev/msi005

Lanfear, R., Calcott, B., Kainer, D., Mayer, C., and Stamatakis, A. (2014). Selecting optimal partitioning schemes for phylogenomic datasets. *BMC Evol. Biol.* 14:82. doi: 10.1186/1471-2148-14-82

Lanfear, R., Frandsen, P. B., Wright, A. M., Senfeld, T., and Calcott, B. (2016). PartitionFinder 2: new methods for selecting partitioned models of evolution for molecular and morphological phylogenetic analyses. *Mol. Biol. Evol.* 34, 772–773. doi: 10.1093/molbev/msw260

Le, S. Q., and Gascuel, O. (2008). An improved general amino acid replacement matrix. *Mol. Biol. Evol.* 25, 1307–1320. doi: 10.1093/molbev/msn067

Matzke, N. J. (2013). Probabilistic historical biogeography: new models for founder-event speciation, imperfect detection, and fossils allow improved accuracy and model-testing. *Front. Biogeogr.* 5, 242–248. doi: 10.21425/F55419694

Matzke, N. J. (2014). Model selection in historical biogeography reveals that founder-event speciation is a crucial process in Island Clades. *Syst. Biol.* 63, 951–970. doi: 10.1093/sysbio/syu056

Matzke, N. J. (2018). BioGeoBEARS*: BioGeography with Bayesian (and likelihood) Evolutionary Analysis with R Scripts. version 1.1.1.* San Francisco, CA: GitHub. Available online at: https://github.com/nmatzke/BioGeoBEARS

Meusemann, K., von Reumont, B. M., Simon, S., Roeding, F., Strauss, S., Kück, P., et al. (2010). A phylogenomic approach to resolve the arthropod tree of life. *Mol. Biol. Evol.* 27, 2451–2464. doi: 10.1093/molbev/msq130

Miller, M. A., Schwartz, T., Pickett, B.E., He, S., Klem, E.B., Scheuermann, R.H., et al. (2015). A RESTful API for access to phylogenetic tools via the CIPRES science gateway. *Evol. Bioinform.* 11, 43–48. doi: 10.4137/EBO.S21501

Misof, B., Liu, S., Meusemann, K., Peters, R. S., Donath, A., Mayer, C., et al. (2014). Phylogenomics resolves the timing and pattern of insect evolution. *Science* 346, 763–767. doi: 10.1126/science.1257570

Misof, B., Meyer, B., von Reumont, B. M., Kück, P., Misof, K., and Meusemann, K. (2013). Selecting informative subsets of sparse supermatrices increases the chance to find correct trees. *BMC Bioinform.* 14:348. doi: 10.1186/1471-2105-14-348

Misof, B., and Misof, K. (2009). A Monte Carlo approach successfully identifies randomness in multiple sequence alignments: a more objective means of data exclusion. *Syst. Biol.* 58, 21–34. doi: 10.1093/sysbio/syp006

Müller, T., and Vingron, M. (2000). Modeling amino acid replacement. *J. Comput. Biol.* 7, 761–776. doi: 10.1089/10665270050514918

Nel, A., and Delfosse, E. (2011). A new Chinese Mesozoic stick insect. *Act. Pal. Pol.* 56, 429–432. doi: 10.4202/app.2009.1108

Nguyen, L.-T., Schmidt, H. A., von Haeseler, A., and Minh, B. Q. (2015). IQ-TREE: a fast and effective stochastic algorithm for estimating maximum likelihood phylogenies. *Mol. Biol. Evol.* 32, 268–274. doi: 10.1093/molbev/msu300

Pattengale, N. D., Alipour, M., Bininda-Emonds, O. R. P., Moret, B. M. E., and Stamatakis, A. (2010). How many bootstrap replicates are necessary? *J. Comput. Biol.* 17, 337–354. doi: 10.1089/cmb.2009.0179

Pauli, T., Burt, T. O., Meusemann, K., Bayless, K., Donath, A., Podsiadlowski, L., et al. (2018). New data, same story: phylogenomics does not support Syrphoidea (Diptera: Syrphidae, Pipunculidae). *Syst. Entomol.* 43, 447–459. doi: 10.1111/syen.12283

Peters, R. S., Krogmann, L., Mayer, C., Donath, A., Gunkel, S., Meusemann, K., et al. (2017). Evolutionary history of the Hymenoptera. *Curr. Biol.* 27, 1–6. doi: 10.1016/j.cub.2017.01.027

Petersen, M., Meusemann, K., Donath, A., Dowling, D., Liu, S., Peters, R. S., et al. (2017). Orthograph: a versatile tool for mapping coding nucleotide sequences to clusters of orthologous genes. *BMC Bioinform.* 18:111. doi: 10.1186/s12859-017-1529-8

Poinar, G. O. (2011). A walking stick, *Clonistria dominicana* n. sp. (Phasmatodea: Diapheromeridae) in *Dominican amber*. *Hist. Biol.* 23, 223–226. doi: 10.1080/08912963.2010.522405

Punta, M., Coggill, P. C., Eberhardt, R. Y., Mistry, J., Tate, J., Boursnell, C., et al. (2012). The Pfam protein families database. *Nucleic Acids Res.* 40, D290–D301. doi: 10.1093/nar/gkr1065

Rambaut, A., Drummond, A. J., Xie, D., Baele, G., and Suchard, M. A. (2018). Posterior summarisation in Bayesian phylogenetics using Tracer 1.7. *Syst. Biol.* 67, 901–904. doi: 10.1093/sysbio/syy032

Robertson, J. A., Bradler, S., and Whiting, M. F. (2018). Evolution of oviposition techniques in stick and leaf insects (Phasmatodea). *Front. Ecol. Evol.* 6:216. doi: 10.3389/fevo.2018.00216

Rota, J., Peña, C., and Miller, S. E. (2016). The importance of long-distance dispersal and establishment events in small insects: historical biogeography of metalmark moths (Lepidoptera, Choreutidae). *J. Biogeogr.* 43, 1254–1265. doi: 10.1111/jbi.12721

Sellick, J. T. C. (1994). Phasmida (stick insects) eggs from the Eocene of Oregon. *Paleaontology* 37, 913–921.

Shelomi, M., Danchin, E. G., Heckel, D., Wipfler, B., Bradler, S., Zhou, X., et al. (2016). Horizontal gene transfer of pectinases from bacteria preceded the diversification of stick and leaf insects. *Sci. Rep.* 6:26388. doi: 10.1038/srep 26388

Simon, S., Blanke, A., and Meusemann, K. (2018). Reanalyzing the Palaeoptera problem–the origin of insect flight remains obscure. *Arthropod Struc. Dev.* 47, 328–338. doi: 10.1016/j.asd.2018.05.002

Simon, S., Letsch, H., Bank, S., Buckley, T. R., Donath, A., Liu, S., et al. (2019). Data from: old world and new world phasmatodea: phylogenomics resolve the evolutionary history of stick and leaf insects. *Dryad Digital Repository*. doi: 10.5061/dryad.65492qt

Soubrier, J., Steel, M., Lee, M. S., Der Sarkissian, C., Guindon, S., Ho, S. Y., et al. (2012). The influence of rate heterogeneity among sites on the time dependence of molecular rates. *Mol. Biol. Evol.* 29, 3345–3358. doi: 10.1093/molbev/mss140

Stamatakis, A. (2014). RAxML version 8: a tool for phylogenetic analysis and post-analysis of large phylogenies. *Bioinformatics* 30, 1312–1313. doi: 10.1093/bioinformatics/btu033

Strimmer, K., and von Haeseler, A. (1997). Likelihood-mapping: a simple method to visualize phylogenetic content of a sequence alignment. *Proc. Natl. Acad. Sci. U.S.A.* 94, 6815–6819. doi: 10.1073/pnas.94.13.6815

Suetsugu, K., Funaki, S., Takahashi, A., Ito, K., and Yokoyama, T. (2018). Potential role of bird predation in the dispersal of otherwise flightless stick insects. *Ecology* 99, 1504–1506. doi: 10.1002/ecy.2230

Suyama, M., Torrents, D., and Bork, P. (2006). PAL2NAL: robust conversion of protein sequence alignments into the corresponding codon alignments. *Nucleic Acids Res.* 34, W609–W612. doi: 10.1093/nar/gkl315

Terrapon, N., Li, C., Robertson, H. M., Ji, L., Meng, W., Booth, W., et al. (2014). Molecular traces of alternative social organization in a termite genome. *Nat. Comm.* 5:3636. doi: 10.1038/ncomms4636

Tilgner, E. H. (2002). *Systematics of Phasmida*, (dissertation), University of Georgia, Athens, GA, United States.

Tilgner, E. H. (2009). "Phasmida (Stick and leaf insects)," in *Encyclopedia of Insects*, 2nd Edn, eds V. H. Resh and R. T. Cardé (Amsterdam; Boston; London; New York; Oxford; Paris; San Diego; San Francisco; Singapore; Sydney; Tokyo: Elsevier), 765–766.

Tomita, S., Yukuhiro, K., and Kômoto, N. (2011). The mitochondrial genome of a stick insect *Extatosoma tiaratum* (Phasmatodea) and the phylogeny of polyneopteran insects. *J. Ins. Biotech. Sericol.* 80, 79–88. doi: 10.11416/jibs.80.3_079

Veerassamy, S., Smith, A., and Tillier, E. R. (2003). A transition probability model for amino acid substitutions from blocks. *J. Comput. Biol.* 10, 997–1010. doi: 10.1089/106652703322756195

Vences, M., Wollenberg, K. C., Vieites, D. R., and Lees, D. C. (2009). Madagascar as a model region of species diversification. *TREE* 24, 456–465. doi: 10.1016/j.tree.2009.03.011

Vera, A., Pastenes, L., Veloso, C., and Méndez, M. A. (2012). Phylogenetic relationships in the genus *Agathemera* (Insecta: Phasmatodea) inferred from the genes 16S, COI and H3. *Zool. J. Linn. Soc.* 165, 63–72. doi: 10.1111/j.1096-3642.2011.00802.x

Wang, M., Béthoux, O., Bradler, S., Jacques, F., Cui, Y., and Ren, D. (2014). Under cover at pre-angiosperm times: a cloaked phasmatodean insect from the Early Cretaceous Jehol biota. *PLoS ONE* 9:e91290. doi: 10.1371/journal.pone.0091290

Wedmann, S., Bradler, S., and Rust, J. (2007). The first fossil leaf insect: 47 million years of specialized cryptic morphology and behavior. *Proc. Nat. Acad. Sci. U.S.A.* 104, 565–569. doi: 10.1073/pnas.0606937104

Whelan, S., and Goldman, N. (2001). A general empirical model of protein evolution derived from multiple protein families using a maximum-likelihood approach. *Mol. Biol. Evol.* 18, 691–699. doi: 10.1093/oxfordjournals.molbev.a003851

Whiting, M. F., Bradler, S., and Maxwell, T. (2003). Loss and recovery of wings in stick insects. *Nature* 421, 264–267. doi: 10.1038/nature01313

Wipfler, B., Letsch, H., Frandsen, P. B., Kaplie, P., Mayer, C., Bartel, D., et al. (2019). Evolutionary history of Polyneoptera and its implications for our understanding of early winged insects. *Proc. Nat. Acad. Sci. U.S.A.* 116, 3024–3029. doi: 10.1073/pnas.1817794116

Wong, T.K., Kalyaanamoorthy, S., Meusemann, K., Yeates, D., Misof, B., and Jermiin, L. (2017). *AliStat Version 1.3*. Canberra, ACT: Commonwealth Scientific and Industrial Research Organisation (CSIRO).

Xie, Y., Wu, G., Tang, J., Luo, R., Patterson, J., Liu, S., et al. (2014). SOAPdenovo-Trans: *de novo* transcriptome assembly with short RNA-Seq reads. *Bioinformatics* 30, 1660–1666. doi: 10.1093/bioinformatics/btu077

Yang, Z. (1994). Maximum likelihood phylogenetic estimation from DNA sequences with variable rates over sites: approximate methods. *J. Mol. Evol.* 39, 306–314. doi: 10.1007/BF00160154

Zhang, S.-Q., Che, L.-H., Li, Y., Liang, D., Pang, H., Slipinski, A., et al. (2018). Evolutionary history of Coleoptera revealed by extensive sampling of genes and species. *Nat. Comm.* 9:205. doi: 10.1038/s41467-017-02644-4

Zhou, Z., Guan, B., Chai, J., and Che, X. (2017). Next-generation sequencing data used to determine the mitochondrial genomes and a preliminary phylogeny of Verophasmatodea insects. *J. Asia-Pacific Ent.* 20, 713–719. doi: 10.1016/j.aspen.2017.04.012

Zompro, O. (2004). Revision of the genera of the Areolatae, including the status of *Timema* and *Agathemera* (Insecta, Phasmatodea). *Verhandl. Naturw. Ver. Hamburg.* 37, 1–327.

Conflict of Interest Statement: The authors declare that the research was conducted in the absence of any commercial or financial relationships that could be construed as a potential conflict of interest.

frontiers in Ecology and Evolution

ORIGINAL RESEARCH
published: 27 May 2020
doi: 10.3389/fevo.2020.00121

A Tale of Winglets: Evolution of Flight Morphology in Stick Insects

Yu Zeng[1,2*], *Connor O'Malley*[1], *Sonal Singhal*[1,3], *Faszly Rahim*[4,5], *Sehoon Park*[1], *Xin Chen*[6,7] *and Robert Dudley*[1,8]

[1] Department of Integrative Biology, University of California, Berkeley, Berkeley, CA, United States, [2] Schmid College of Science and Technology, Chapman University, Orange, CA, United States, [3] Department of Biology, CSU Dominguez Hills, Carson, CA, United States, [4] Islamic Science Institute, Universiti Sains Islam Malaysia, Nilai, Malaysia, [5] Centre for Insect Systematics, Universiti Kebangsaan Malaysia, Bangi, Malaysia, [6] Department of Biology, The College of Staten Island, The City University of New York, New York, NY, United States, [7] Department of Biology, The Graduate School and University Center, The City University of New York, NY, United States, [8] Department of Entomology, Smithsonian Tropical Research Institute, Panama City, Panama

The evolutionary transition between winglessness and a full-winged morphology requires selective advantage for intermediate forms. Conversely, repeated secondary wing reductions among the pterygotes indicates relaxation of such selection. However, evolutionary trajectories of such transitions are not well-characterized. The stick insects (Phasmatodea) exhibit diverse wing sizes at both interspecific and intersexual levels, and thus provide a system for examining how selection on flight capability, along with other selective forces, drives the evolution of flight-related morphology. Here, we examine variation in relevant morphology for stick insects using data from 1,100+ individuals representing 765 species. Although wing size varies along a continuous spectrum, taxa with either long or miniaturized wings are the most common, whereas those with intermediate-sized wings are relatively rare. In a morphological space defined by wing and body size, the aerodynamically relevant parameter termed wing loading (the average pressure exerted on the air by the wings) varies according to sex-specific scaling laws; volant but also flightless forms are the most common outcomes in both sexes. Using phylogenetically-informed analyses, we show that relative wing size and body size are inversely correlated in long-winged insects regardless of sexual differences in morphology and ecology. These results demonstrate the diversity of flight-related morphology in stick insects, and also provide a general framework for addressing evolutionary coupling between wing and body dimensions. We also find indirect evidence for a "fitness valley" associated with intermediate-sized wings, suggesting relatively rapid evolutionary transitions between wingless and volant forms.

Keywords: body size, evolution, flight, phasmid, sexual dimorphism, wing size

OPEN ACCESS

Edited by:
Mariana Mateos,
Texas A&M University, United States

Reviewed by:
Marco Gottardo,
University of Siena, Italy
Sven Bradler,
University of Göttingen, Germany

***Correspondence:**
Yu Zeng
dreavoniz@berkeley.edu

Specialty section:
This article was submitted to Phylogenetics, Phylogenomics, and Systematics, a section of the journal Frontiers in Ecology and Evolution

Received: *16 June 2019*
Accepted: *15 April 2020*
Published: *27 May 2020*

Citation:
Zeng Y, O'Malley C, Singhal S, Rahim F, Park S, Chen X and Dudley R (2020) A Tale of Winglets: Evolution of Flight Morphology in Stick Insects. Front. Ecol. Evol. 8:121. doi: 10.3389/fevo.2020.00121

INTRODUCTION

Flight is fundamental to the ecology and evolutionary diversification of pterygote insects by allowing for three-dimensional mobility and greater access to nutritional resources (Dudley, 2000). Nonetheless, ∼5% of the extant pterygote fauna is flightless (Roff, 1994), and various conditions of reduced wing size (e.g., brachyptery and microptery) are found across the neopteran orders. Given structural costs and high energy expenditure during flight, maintenance of the flight apparatus is not universally favored by selection. Partial reduction or complete loss of wings is associated with

various morphological and ecological factors, such as developmental tradeoffs, enhanced female fecundity, and reduced demand for aerial mobility in certain habitats (Roff, 1990, 1994). In these cases, smaller wings exhibit reduced aerodynamic capability, but may serve secondarily derived non-aerodynamic functions such as use in protection, stridulation, and startle displays (see Dudley, 2000).

Wing evolution can also be influenced indirectly by selection on overall body size. Generally, reduced body mass enables greater maneuverability in flight (e.g., more rapid translational and rotational accelerations), although numerous factors influence insect size evolution (see Blanckenhorn, 2000; Chown and Gaston, 2010). Furthermore, both flight capacity and body size can be subject to sex-specific selection. As a consequence, sexual size dimorphism (SSD) is typically associated with intersexual niche divergence and with sexual selection (see Hedrick and Temeles, 1989; Shine, 1989). Sexual wing dimorphism (SWD) can in some cases be decoupled from SSD, and may be associated with divergence in aerial niche and wing use (e.g., DeVries et al., 2010). Selection for greater locomotor capacity in males can lead to male-biased SWD, and also to female-biased SSD (see Roff, 1986). It is therefore of interest to consider patterns of sexual dimorphism in both wing and body size within a phylogenetic context.

The stick insects (Phasmatodea) exhibit great diversity in both wing and body size (**Figures 1**, **2**), but underlying evolutionary patterns are not well-characterized. Most winged stick insects possess rudimentary and tegmenized forewings. Phasmid hindwings (designated "wings" hereafter) can be of various sizes and exhibit expanded cubital and anal venation with well-developed flight membranes. Fossil evidence suggest that both wing pairs were full-sized in ancestral stick insects (see Shang et al., 2011; Wang et al., 2014; Yang et al., 2019), whereas numerous extant species exhibit wing reduction. Earlier studies have proposed frequent evolutionary transitions between winged and wingless morphologies, although the directionality and the detailed dynamics of phasmid wing evolution remain contested (see Stone and French, 2003; Whiting et al., 2003; Trueman et al., 2004; Whiting and Whiting, 2004; Goldberg and Igić, 2008). Nevertheless, size-reduced wings must lead to degradation in aerodynamic performance, with possibly concurrent changes in body length and mass. Given the unresolved history of wing size evolution of this group, we use the term "reduction" to describe wings that are developmentally truncated relative to a full-sized morphology, without assessing the directionality of wing size evolution within the phylogeny.

Here, we examine the evolution of phasmid flight morphology on a macroevolutionary scale. We first describe variation in wing and body size using data from 1,100+ individuals across 765 species, including intraspecific data from the *Asceles tanarata* species group with three subspecies exhibiting altitudinal variation in both wing and body size (see Brock, 1999; Seow-Choen, 2000; **Figure 2B**). This group represents one of the few well-documented cases of features of insect flight morphology being distinctly correlated with a gradient in environmental parameters. Second, using live specimens, we derive a scaling relationship for wing loading with wing and body size. We then use this empirical model to extrapolate variation in flight capability across all sampled species. Third, we use phylogenetic correlational analyses to quantify the relationship between changes in wing size (reflecting flight ability) and body size through evolutionary time. Throughout these analyses, we also assess overall patterns of sexual dimorphism among phasmid species within phylogenetic and allometric contexts. In particular, we examine the correlation between SWD and SSD to address the role of sex-specific ecology in driving the diversity of flight morphology. For example, if selection on male-biased mobility and on female-biased fecundity were coupled, we might expect an inverse correlation between SWD and SSD.

Abbreviations: A_w, Wing area; p_w, Wing loading; L, Body length; L_w, Wing length; m, Mass; SSD, Sexual size dimorphism; SWD, Sexual wing dimorphism; Q, Relative wing size; ΔL, Sexual size dimorphism index; ΔQ, Sexual wing dimorphism index.

MATERIALS AND METHODS

Morphometrics

Our sampling primarily focused on winged phasmid clades, given available data (see **Figure S1**). Wing length (L_w) and body length (L) data were primarily obtained from literature sources, and were enriched with measurements on both captive-reared and field-collected insects (see section "Scaling of wing loading"). Taxonomic justifications followed Phasmida Species File (Brock et al., 2019), as downloaded and formatted using custom-written scripts in MatLab (**Supplementary Data Sheet 2**). For the *A. tanarata* species group, male and females of three subspecies were collected in the field (see also Brock, 1999). The main dataset includes measurements on 599 males and 533 females from 765 species (∼23% of 3,348 known species), of which 367 species included data on both sexes (**Supplementary Data Sheet 3**). If available, mean measurements were used; otherwise, median values were calculated based on ranges between maximum and minimum values. The relative wing size (Q) was defined as the ratio of wing length to body length:

$$Q = L_w/L \tag{1}$$

To avoid ambiguity, hereafter the term "wing size" primarily refers to the relative wing size. SWD (ΔQ) was calculated as:

$$\Delta Q = (L_{w,M} - L_{w,F})/(L_{w,M} + L_{w,F}) \tag{2}$$

where the subscripts M and F denote male and female, respectively. The sign and magnitude of ΔQ thus represent the type and level of SWD. For example, $\Delta Q < 0$ represents female-biased SWD, $\Delta Q = 0$ represents absence of SWD, and $\Delta Q = 1$ when the female is wingless and the male is winged. Similarly, SSD (ΔL) was calculated as:

$$\Delta L = (L_M - L_F)/(L_M + L_F) \tag{3}$$

Scaling of Wing Loading

The loss of aerodynamic capability was assessed using the parameter wing loading, the ratio of body weight to total wing

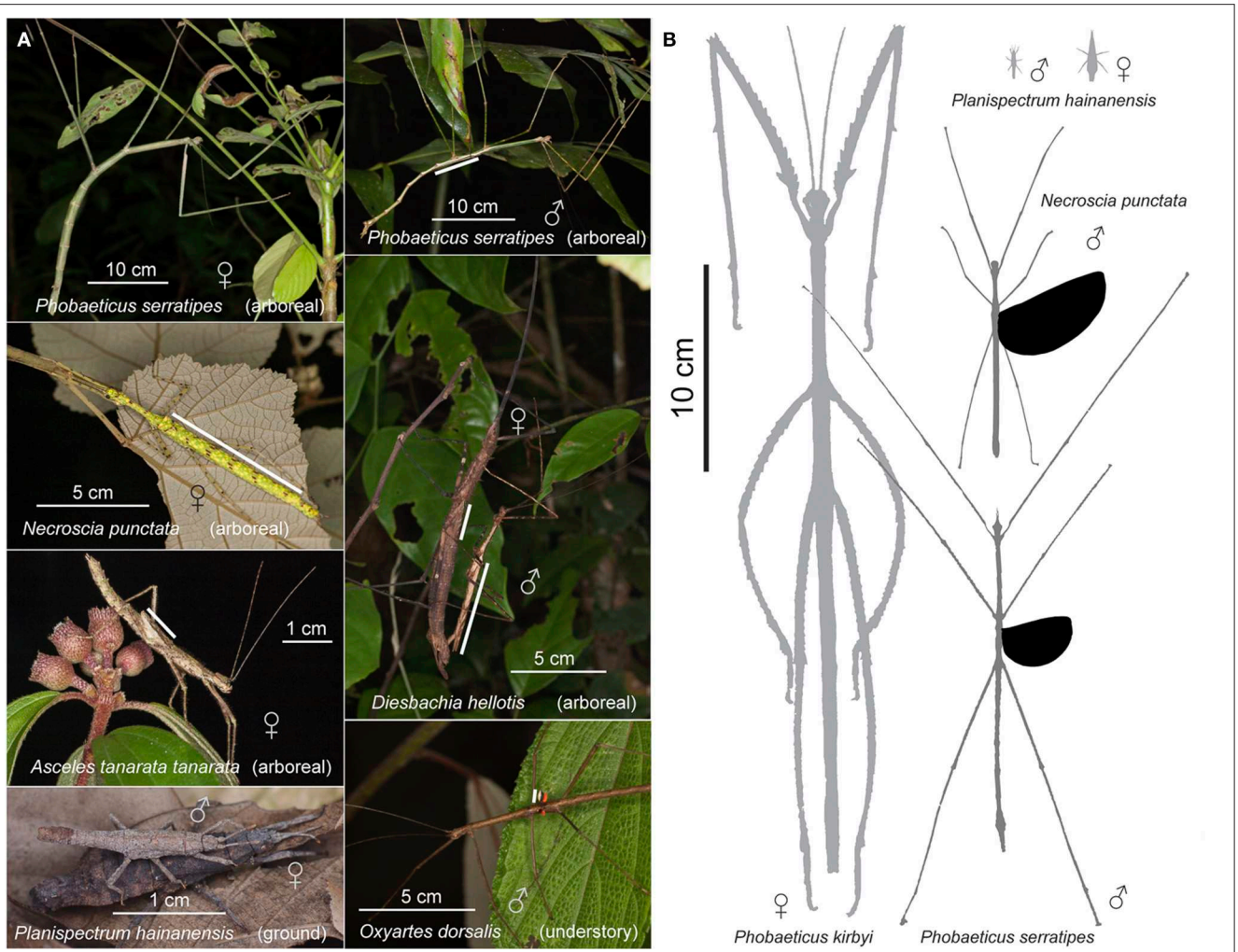

FIGURE 1 | Diversity of flight morphology in stick insects as shown by variation in wing and body size. **(A)** Examples of stick insects with different sized wings; white line segments indicate hindwing length in winged taxa. **(B)** Spectrum of interspecific variation in body and relative wing size for representative species (photo of *Planispectrum hainanensis* courtesy of Chao Wu).

area. First, the scaling of body mass relative to body length can be expressed as:

$$m = C_1 L^a \tag{4}$$

where C_1 is the slope coefficient and a is the scaling exponent. If body mass varies under isometry (i.e., body geometry is conserved across different body sizes), we expect a to equal 3. Similarly, the power-law scaling of total wing area (A_w) with Q can be expressed as:

$$A_w = C_2 L_w^b = C_2 (LQ)^b \tag{5}$$

where C_2 is the slope coefficient and b is the scaling exponent. If wing area varies under isometry, we expect b to equal 2. Combining Equations (4) and (5), we have the power-law scaling of wing loading (p_w) with L and Q:

$$p_w = \frac{mg}{A_w} = C_1 C_2^{-1} g L^{a-b} Q^{-b} \tag{6}$$

We then developed empirical models of the scaling of wing loading for both sexes based on Equations (4)–(6). We sampled total wing area (A_w), body mass (m), and wing length (L_w) from 23 males and 21 females of field-collected and captive-bred insects from 36 phasmid species (**Supplementary Data Sheet 3**). Digital images were obtained dorsally for insects placed on horizontal surfaces with all legs laterally extended; projected areas of fully unfolded wings were manually extracted using Photoshop (CS6, Adobe Systems Inc., San Jose, CA, USA). Values for A_w, L_w, and L were obtained using ImageJ (Schneider et al., 2012).

Bayesian Phylogenetic Reconstruction

We used two mitochondrial genes [cytochrome oxidase subunit I (COI) gene, and cytochrome oxidase subunit II (COII) gene; total length 1,550 bp] and two nuclear genes [histone subunit 3 (H3)

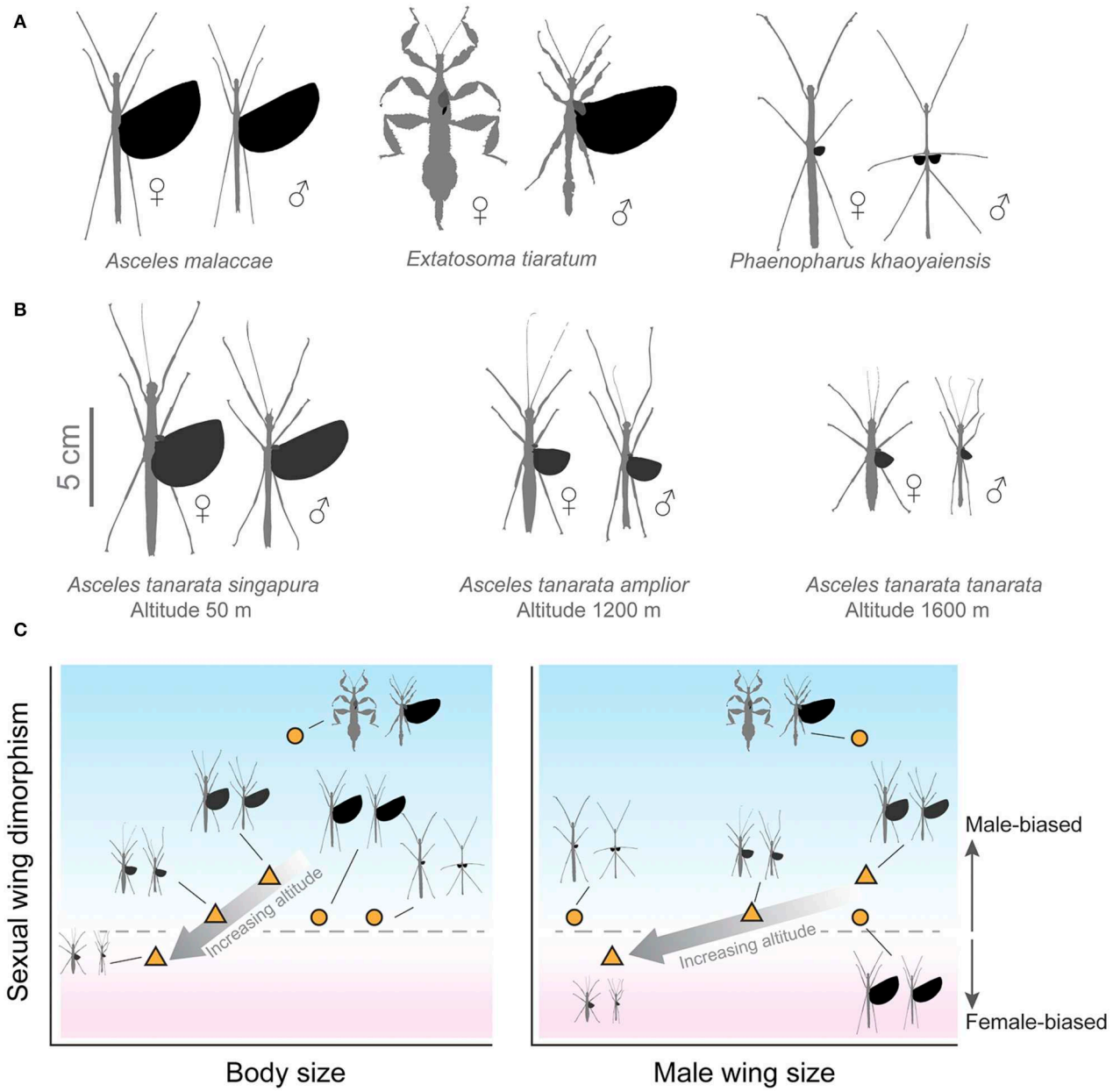

FIGURE 2 | Sexual wing dimorphism (SWD) in stick insects. **(A)** Representative combinations of variable relative wing size and SWD: (1) low SWD with long wings in both sexes, (2) extreme SWD with long wings in males only, and (3) low SWD with short wings in both sexes. **(B)** Variation in wing and body sizes for the *Asceles tanarata* species group, for which SWD transitions from male- to female-biased with increasing altitude. **(C)** Schematic demonstration of variations in SWD with respect to body size and male wing size; numbers denoting taxa depicted in **(A,B)**. The gray arrow indicates elevational changes with increasing altitude in the *A. tanarata* group.

gene and large subunit rRNA (28S) gene; total length 853 bp] (primer details in **Table S1**). Our molecular sequencing covered nine species, including all three taxa from the *A. tanarata* group (**Supplementary Data Sheet 3**). We extracted total genomic DNA from leg tissue using a modified high-salt protocol (Aljanabi and Martinez, 1997) and, subsequently, quantified and diluted the DNA using a Nanodrop spectrometer. We amplified each locus using standard PCR conditions. Amplified products were cleaned with Exosap and sequenced using PCR primers with BigDye v3.1 on an Applied Biosystems 3730 machine. For other species, we downloaded sequence data from the same four genes from GenBank. Our molecular data set covers about 70% of the recognized tribes of Phasmatodea (Brock et al., 2019) and two outgroup species (Embioptera). Given a well-resolved phylogeny is unavailable for most lineages, the use of tribes here is only to organize morphological sampling, without presuming

any phylogenetic relationship among sampled taxa (also, see **Supplementary Text**).

Sequences were assembled in Geneious (v6.1.7, Biomatters) and aligned using the MUSCLE algorithm (Edgar, 2004). Gene alignments were checked manually for accuracy. jModelTest v0.1.1 was used to determine the best fitting substitution model for each gene based on the Akaike Information Criterion (AIC) (Posada, 2008). Next, we estimated a time-calibrated phylogeny in BEAST package (v1.10.4; Drummond et al., 2012). Across genes, we used unlinked substitution models and linked clock and tree models. To date the phylogeny, we used the fossil crown group phasmid *Renphasma sinica* dated 122 Myr ago (Nel and Delfosse, 2011) to set the minimum age of the divergence between Embioptera and Phasmatodea. Also, we included two fossil calibrations, following Buckley et al. (2009). Fossil euphasmatodean eggs from mid-Cretaceous dated to 95–110 Myr ago were used (see Rasnitsyn and Ross, 2000; Grimaldi and Engel, 2005) to determine the age of the most recent ancestor of Euphasmatodea. The sister group relationship between *Timema* and Euphasmatodea has been confirmed by both morphological and molecular evidence (Whiting et al., 2003; Bradler, 2009). Therefore, we assumed the divergence between Euphasmatodea and *Timema* occurred more than 95 Myr ago. Furthermore, we used fossil leaf insect dated 47 Myr ago (Wedmann et al., 2007) and fossil eggs of Anisomorphini dated 44 Myr ago (Sellick, 1994) to set the minimum age of the nodes of the most recent common ancestors of leaf insects and Pseudophasmatinae, respectively. We first optimized the Markov chain Monte Carlo (MCMC) operator by performing short runs (1×10^7 cycles) with a relaxed lognormal model and a Yule model, and adjusted the operators as suggested by the program. Then, we ran 10 analyses for 2×10^8 generations each. We monitored convergence and determined the burn-in using TRACER v1.7 (Rambaut et al., 2018). After discarding burn-in (25%), we used a maximum credibility approach to infer the consensus tree in TreeAnnotator v1.10.4.

Phylogenetic Correlations

A total of five morphological traits was used in phylogenetic analyses (L and Q of both sexes and sex-averaged L, ΔQ, and ΔL). First, we calculated the phylogenetic signals (λ) for all characters using the maximum-likelihood approach implemented in Phytools (Pagel, 1999; Revell, 2012). This model was compared with alternative models where λ was forced to be 1 or 0 in order to find the best-fitting model. The best-fitting model was found using the likelihood ratio (LR) test,

$$LR = -2 \times (Lh_{better\ \ fitting\ model} - Lh_{worse\ \ fitting\ model}) \quad (7)$$

whereby the better fitting model has the highest log-likelihood score, *Lh* (Pagel, 1997, 1999; Freckleton et al., 2002). When $\lambda = 0$, this suggests trait evolution is independent of phylogenetic association, which is equivalent to generalized least square (GLS) model. We also assessed the evolutionary distribution of morphological traits with maximum-likelihood ancestral state reconstruction, using "fastAnc" function in Phytools (Revell, 2012).

For the species that lacked molecular data, we added them as polytomous tips to the node representing the latest common ancestor on the tree. We then generated 100 random trees with randomly resolved polytomous tips. Each new node was added using the function "multi2di" (package "ape;" Paradis et al., 2004), and was given a branch length that was randomly drawn from a normal distribution of branch lengths with a mean of 0.1× mean branch lengths of the original tree, and a standard deviation of 0.01× the standard deviation of branch lengths from the original tree.

We analyzed phylogenetically-justified correlations using phylogenetic generalized least square (PGLS) analyses (package "caper;" Orme et al., 2013). For each correlation, we ran PGLS on all random trees and summarized the results (MLλ and coefficients), which were then compared with those from ordinary generalized least square (GLS) tests conducted without referring to the phylogeny (i.e., $\lambda = 0$). To avoid zero-inflation in correlational analyses due to winglessness (i.e., Q = 0), we used two methods for correlations involving Q: (1) excluding species with Q = 0; and (2) converting Q to a pseudo-continuous ordinal variable as: 1 (Q = 0), 2 (0 < Q < 0.3), 3 (0.3 < Q < 0.6), or 4 (Q > 0.6; see Symonds and Blomberg, 2014). Also, we adopted a similar protocol for all correlations involving ΔQ, whereby ΔQ was converted to: 1 (ΔQ < 0), 2 (ΔQ = 0), 3 (0 < ΔQ < 0.3), 4 (0.3 < ΔQ < 0.6), or 5 (ΔQ > 0.6). In addition, to accommodate the bimodal distribution of Q (see Results), we categorized short-winged and long-winged insect groups as "0" and "1," and applied logistic regression models separately. We defined short- and long-winged characters using the distribution of Q values across all species (see dotted line in **Figure 3B**).

RESULTS

Sex-Specific Variation in Flight-Related Morphology

Among all sampled insects, ∼44% of females and ∼51% of males were winged. Relative wing size (Q) varied continuously from complete winglessness (Q = 0) to fully-sized wings (i.e., Q ≈ 0.85; **Figures 3A,B**). For both sexes, the relative frequency of Q was bimodally distributed with a valley near Q = 0.3, and two peaks near Q = 0.1 and Q = 0.7, respectively. Variation in the bimodal distribution was sex-specific, whereby the majority of males exhibited medium- to fully-sized wings (i.e., Q > 0.4) whereas most females exhibited either medium- to fully-sized wings, or alternatively miniaturized wings (Q < 0.3). The frequency distribution of body length (L) was bell-shaped, with females exhibiting a wider range and greater mean length compared to males (male range: 1.7–19.0 cm, female range: 1.3–28.5 cm; male mean: 6.92 cm, female mean: 8.71 cm; see **Figure 3C**). In both sexes, the median body length of the wingless group was greater than that of the winged group. The GLS regression model suggested a significant inverse correlation between Q and L in long-winged males, but not in other groups (**Figures 3D,E**).

At the species level, extent of SWD varied with relative wing size. Of 183 winged species with data from both sexes, ∼57%

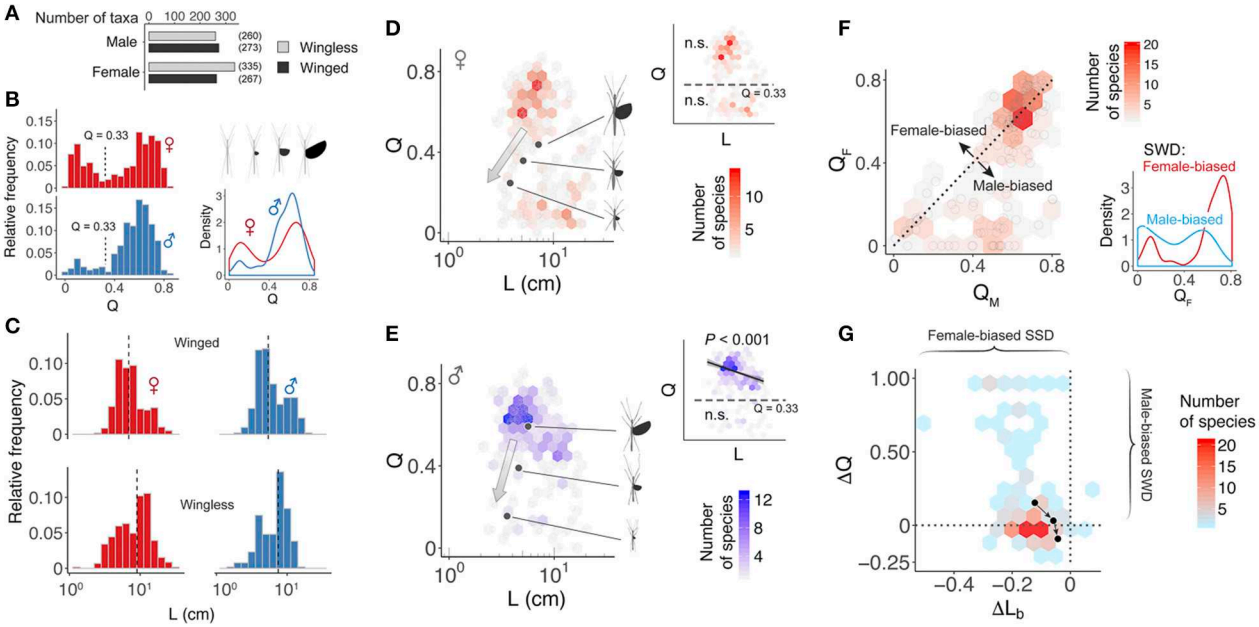

FIGURE 3 | Variation in wing and body size among stick insects. **(A)** Number of winged and wingless species, as grouped by the two sexes. **(B)** Relative frequency distribution and density of relative wing size (Q) for winged taxa. The vertical dashed lines indicate a region of phenotypic space that few species occupy. **(C)** Relative frequency distribution of body size (L). Black dashed lines denote median values. **(D,E)** Scatter plots of Q vs. L for winged stick insects, indicating bimodal distributions. The color of overlaid hexagons represents the number of species, as scaled by the heat map inset. Insets show results of generalized least squares (GLS) regression models (trend line with 95% C.I.) for short- and long-winged insects, as categorized by the cutoff Q defined in **(A)**. An inverse correlation between Q and L is found in long-winged males. **(F)** Scatter plot of female relative wing size vs. male relative wing size ($N = 183$ species). The color of overlaid hexagons represents the number of species for each parameter combination. The majority (80%) of female-biased SWD (i.e., the area above the dashed line) is associated with medium-length to long wings ($Q_F > 0.5$), as indicated by the increasing density of female-biased SWD in long-winged females ($Q > 0.4$) (inset). **(G)** Scatter plot of SWD index vs. SSD index, showing the predominance of female-biased SSD and continuous variation in SWD (57% male-biased and 43% female-biased). For **(D,E,G)**, the three dark dots represent subspecies of the *A. tanarata* group, showing sex-specific trends of wing and body size reduction with increasing altitude (as indicated by arrows).

(88 species) showed various levels of male-biased SWD ($\Delta Q > 0$; **Figure 3F**). Female-biased SWD, however, tended to be found in species for which both sexes possessed long wings. Of the other 42% of species with female-biased SWD ($\Delta Q < 0$), most exhibited long wings ($Q > 0.6$ in both sexes). In general, phasmids showed different combinations of a continuously varying SWD and female-biased SSD (**Figure 3G**). For *A. tanarata* group, the reduction in coefficients of wing and body size toward higher altitudes was sex-specific (**Figures 3D,E**). Males showed a relatively higher extent of wing reduction, leading to a reversal of SWD from male- to female-biased (**Figure 3G**).

Sex-Specific Flight Reduction

Scaling of wing area with wing length was nearly isometric, with an exponent (b) of ∼1.84 in both sexes (**Figure 4A**; **Table 1**). The allometric scaling of insect mass with respect to body length was, however, sex-dependent, with females exhibiting a higher slope coefficient relative to males (**Figure 4B**). Larger female phasmids thus have disproportionally greater mass. Consequentially, the allometric coefficient for wing loading in females (i.e., $C_1 C_2^{-1}$) was ∼1.5 greater than that of males (Equation 6; **Figures 4C–E**). Females generally have much greater wing loading and potentially greater loss of aerodynamic capability when compared to males of the same relative wing size. This may partially underlie the high frequency of female-biased SWD found in long-winged taxa (see Discussion). For males, variation of body size plays little role in the variation of wing loading. With the scaling exponent for body size (i.e., $a - b$; see Equation 6) ∼equal to zero, wing loading in males is exclusively dependent on relative wing size (Q). Notably, the male of *Heteropteryx dilatata*, a morphological outlier with full-sized forewings, exhibits a higher wing loading relative to other males due to its disproportionally greater body mass.

Variation in wing loading can also be presented as a three-dimensional landscape relative to wing and body size. The allometric effect is stronger in females, whereas males exhibit a smaller lower boundary for wing loading without any allometric effect (**Figures 5A,B**). Projecting the species richness distribution onto these landscapes demonstrates a clustering of taxa on the wing loading functional landscape (**Figures 5C,D**). Both sexes showed two major clusters associated with low and high wing loadings, corresponding to long-winged and miniaturized-wing morphologies, respectively. The majority of long-winged females were allometrically constrained to values of wing loading between $1\ \mathrm{Nm}^{-2} < p_w < 10\ \mathrm{Nm}^{-2}$, whereas long-winged males clustered near a value of $1\ \mathrm{Nm}^{-2}$, with a number of taxa characterized by even lower values. The miniaturized-wing taxa in both sexes tended to concentrate within the high wing loading regime (i.e., $p_w > 10^2\ \mathrm{Nm}^{-2}$). Despite sexual differences in the topology of

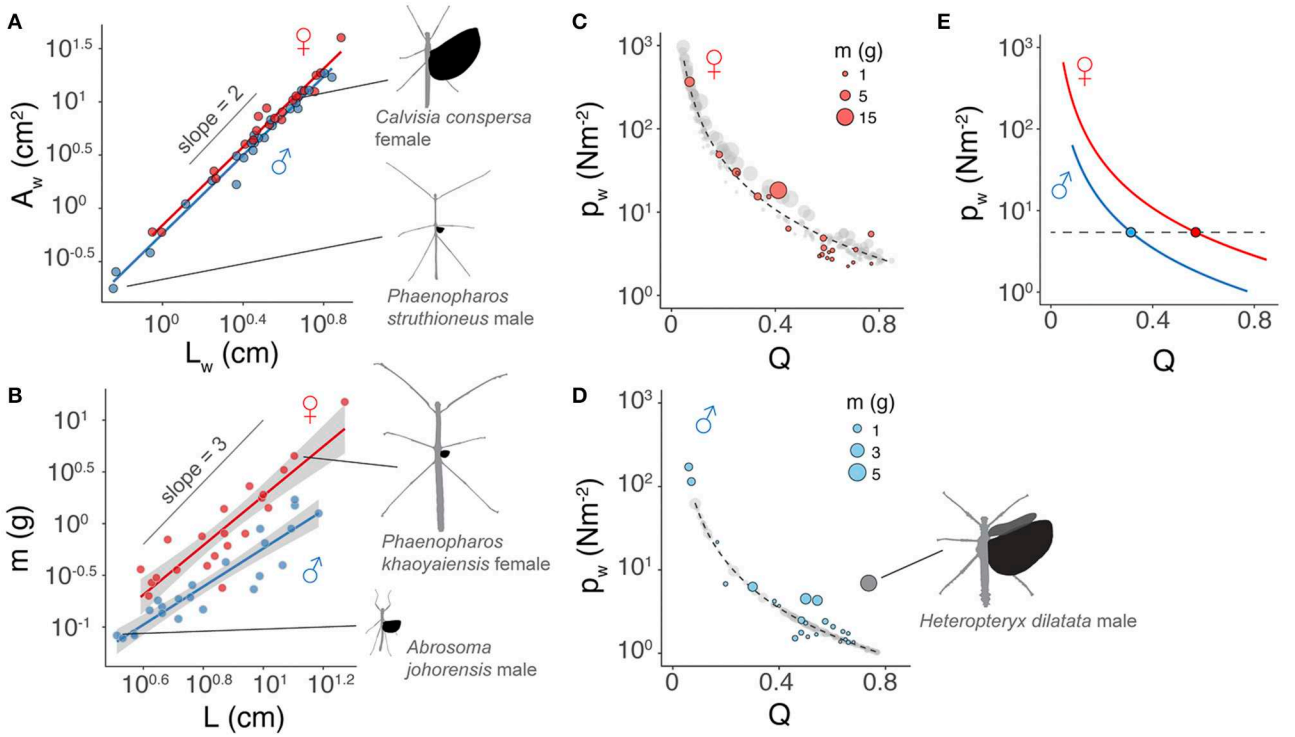

FIGURE 4 | Scaling of flight-related morphology. **(A)** Near-isometric scaling of wing area with relative wing size. Trend lines are based on linear regression models with slopes equal to 1.84 ± 0.05 and 1.84 ± 0.07 (mean ± s.e.m.) for males and females, respectively; $R^2 = 0.98$ and $P < 0.0001$ for both sex groups). **(B)** Allometric scaling of insect body mass with body length. Trend lines are based on linear regression models; Males: slope = 1.84 ± 0.16, $R^2 = 0.86$, $P < 0.0001$, females: slope = 2.39 ± 0.21, $R^2 = 0.86$, $P < 0.0001$. **(C,D)** Allometric scaling of wing loading (p_w) in females and males, respectively. Colored dots represent insects for which body mass and wing area were directly measured. Gray dots are estimates based on wing and body lengths using regression models (see Methods). Trendlines are based on a logistic fit. The regression model for males omitted *Heteropteryx dilatata* (dark gray dot; calculated with the total area of fore- and hindwings), which is a morphological outlier with well-developed forewings. **(E)** Comparison of the scaling of p_w with respect to *Q* between two sexes, showing that disproportionally longer wings in females are required to attain wing loading equivalent to that of males.

TABLE 1 | Comparison of coefficients for the allometric scaling of body mass (m) and the scaling of wing area (A_w) with wing length (L_w) (see Equations 4, 5).

Sex	Models and parameters			
	$m = C_1L^a$		$A_w = C_2L_w^b$	
	C_1	a	C_2	b
F	0.008 (0.004)	2.38 (0.22)	0.69 (0.06)	1.84 (0.07)
M	0.008 (0.003)	1.84 (0.16)	0.57 (0.04)	1.84 (0.06)

Values represent means with 1 s.e. in brackets. Units are consistent with those in text and figures: L, cm; m, g; L_w, cm; A_w, cm^2.

the wing loading landscape, a threshold wing loading near $p_w \approx 10\ Nm^{-2}$ was associated with a largely unoccupied region of phenotypic space (i.e., Q = 0.33; **Figure 3B**).

Wing Size-Dependent Evolutionary Correlations

Our tree topology and estimates of diversification times were largely concordant with those of published phasmid phylogenies (see Whiting et al., 2003; Bradler et al., 2015; Robertson et al., 2018; Simon et al., 2019; **Figure 6**; **Figure S3**). Our tree also showed contradicting results, such as the Phylliinae, instead of Aschiphasmatinae, being the sister taxon of all remaining Euphasmatodea (the Neophasmatodea). These contradictions are mostly the result of poorly resolved deeper nodes of the phasmid phylogeny based on traditional Sanger sequencing markers as used here, which has been seen in other analyses (Bradler et al., 2015). Within the *A. tanarata* group, the divergence time between the lowland subspecies (*A. tanarata singapura*) and two highland subspecies was ∼3 Myr ago, whereas the divergence time between two highland subspecies was ∼1 Myr ago. Significant phylogenetic signal was present in all morphological traits (**Table 2**). Our conservative ancestral state reconstruction showed high evolutionary lability of wing and body size, and suggested that an intermediate relative wing size (Q < 0.4) preceded various levels of gains and losses in both sexes (**Figure S5**). Although deeper nodes in our phylogeny are less confidently resolved, this uncertainty generally does not affect our ancestral state reconstruction because many of the trait transitions occur more recently in evolutionary history.

Based on the PGLS results, there was a significant inverse correlation between Q and L in long-winged insects (Q > 0.33) of both sexes (**Figures 7A,B**; **Table 3**), which supported our initial hypothesis on evolutionary coupling between wing and

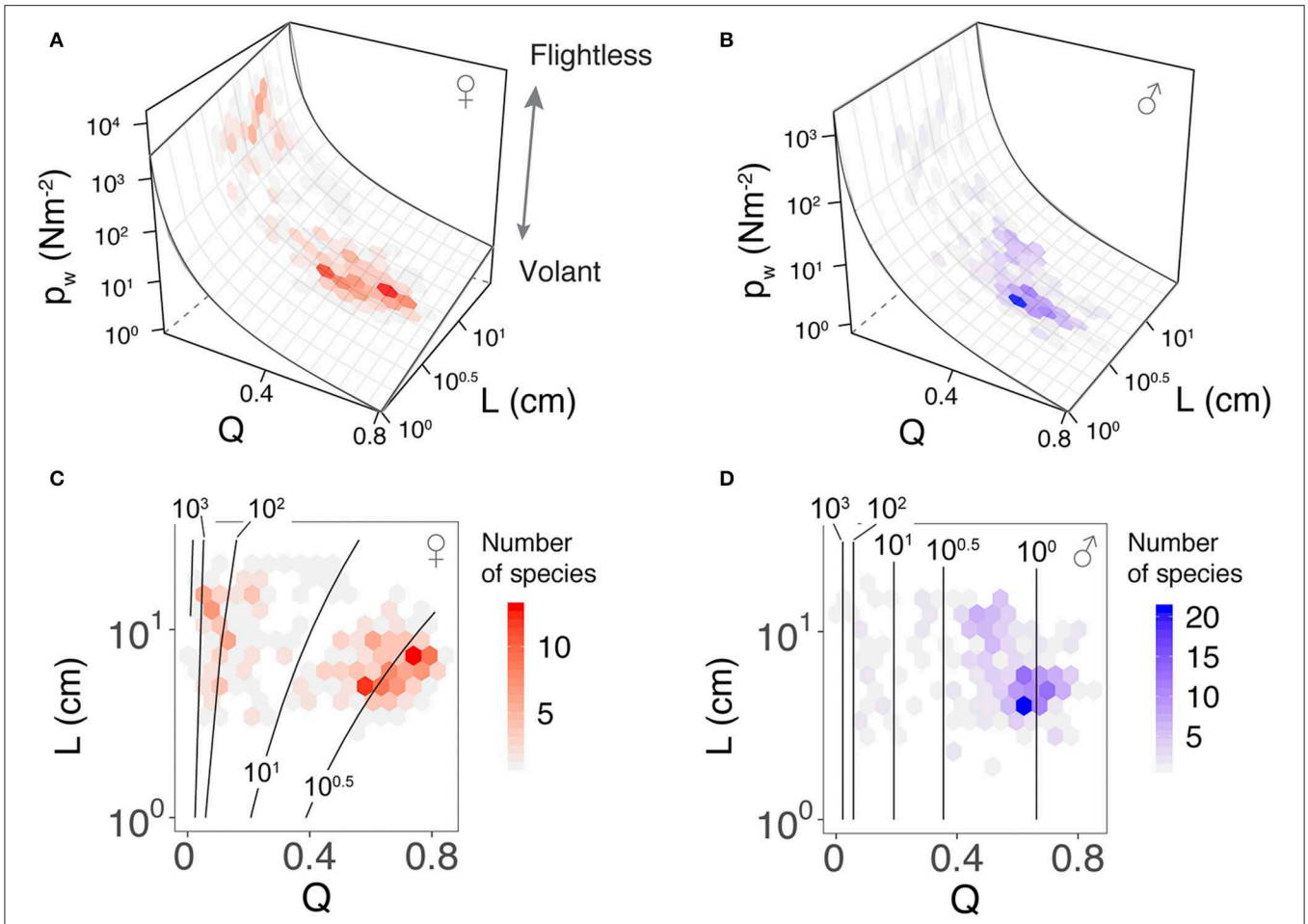

FIGURE 5 | Sex-specific landscapes of wing loading relative to dimorphism and body length among phasmid species. **(A,B)**, wing loading relationships for females and males, respectively, between the two sexes; females typically have higher wing loading than males and stronger allometric effects relative to body length. **(C,D)**, contours of the wing loading landscape for females and males, respectively, as overlaid with hexagonal bins for species counts (**Figures 3D,E**); wing loading distribution differs substantially between the sexes.

body size. In addition, sex-averaged body size was coupled with the extent of both SWD and SSD in long-winged species (Q > 0.33 in both sexes), suggesting opposite trends of variation in SWD and SSD along the gradient of sex-averaged body size (**Figure 7C**). An exemplar of this correlation is demonstrated in **Figures 7D,E**, whereby increases in both SSD and SWD lead to greater sexual differences in wing loading. Short-winged insects generally lacked significant correlations between wing and body size (**Figures 7A,C**). Across all winged species, variation in female traits contributed substantially more to intersexual differences, as shown by the predominant roles of female Q and L values in determining variation in SWD and SSD, respectively (**Figure S4**, **Table S2**).

DISCUSSION

Most winged phasmid species possess either miniaturized or long wings (**Figure 8A**). Few species have intermediate-sized wings, suggesting the presence of a fitness valley defined by two 'adaptive peaks' (see Stroud and Losos, 2016): one peak consists of wingless taxa and those with miniaturized wings (i.e., Q < ~0.3), and another represents volant taxa (i.e., Q > ~0.6). Insects with relative wing size near Q = ~0.3 may be in transition between these two forms, with greater probability of either gaining or losing wing size depending on the interplay between various selective forces (see below). The predominance of wingless phasmid species may, in part, derive from reduced dispersal capacity leading to population isolation and ultimately genetic divergence. Given the possibility that repeated gain and losses of flight are associated with species diversification (Goldberg and Igić, 2008), linkage of evolutionary transitions between winged and wingless forms with diversification rates and overall macroevolutionary patterns should be addressed in future comparative studies. Significant wing size reduction over a relatively short divergence time, as in *A. tanarata* group, further demonstrates that the evolution of flightlessness

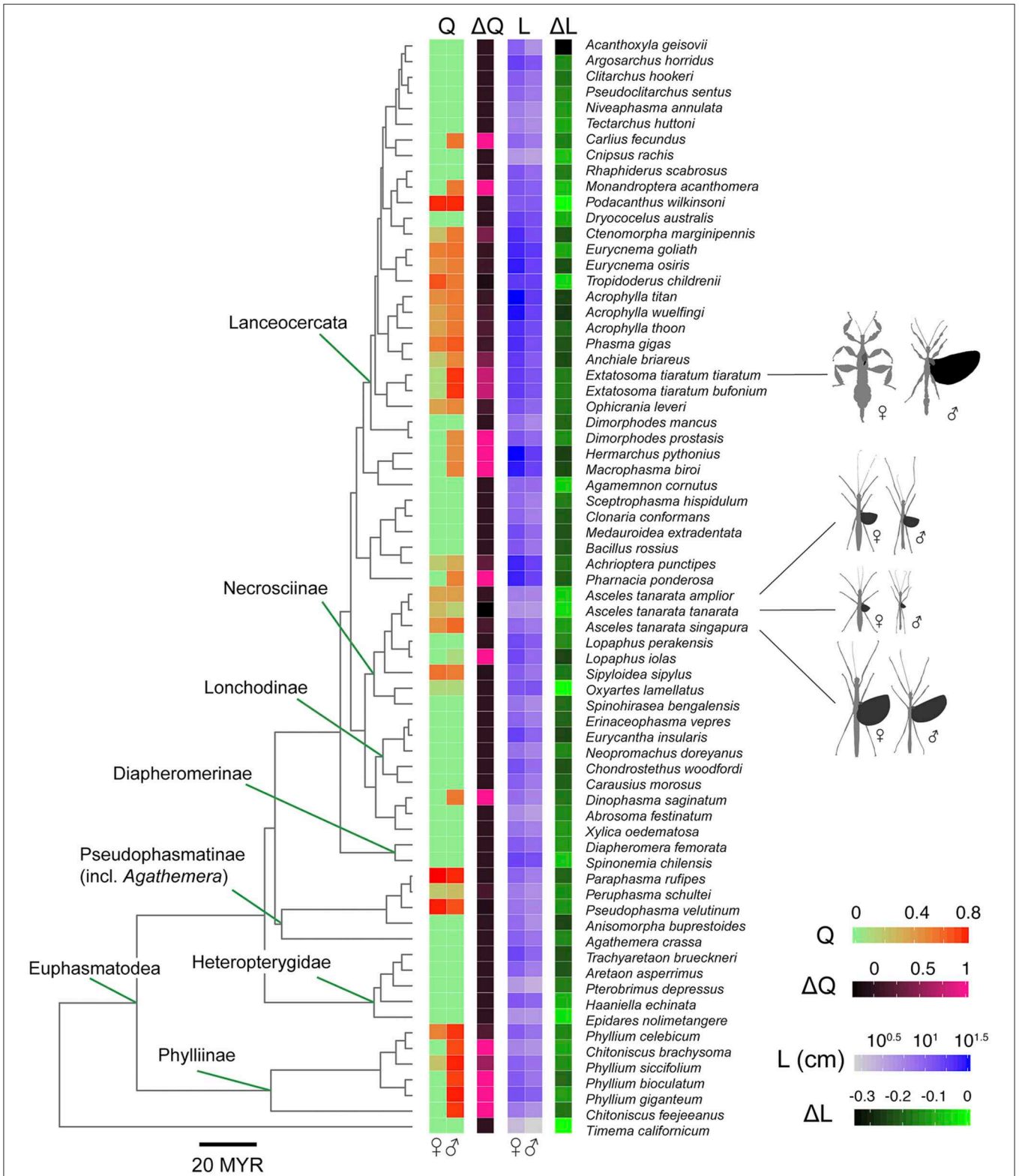

FIGURE 6 | Phylogenetic relationships among sampled taxa, with flight-related morphology annotated on tree tips. Tree topology is based on concatenated COI, COII, H3, and 28S data (see Methods), and branch lengths are proportional to time since divergence (in millions of years). The tree is pruned to show a selection of species with data obtained for both sexes (see **Figure S3** for the complete tree).

TABLE 2 | Summary of statistical results for best model fits, comparing phylogenetic generalized least squares (PGLS) models (λ estimated by maximum likelihood, ML) with generalized least square (GLS) models (λ = 0) for log-transformed body length (i.e., $\log_{10}$ L) and relative wing size (Q).

							PGLS vs. GLS	
	Variable	***N***	**MLλ**	***Lh* (PGLS)**	***Lh* (GLS)**	***Lh* (PIC)**	***LR***	***P***
Male	Q_M	533	1.001	293.3	−111.9	227.5	−810.3	<0.0001
	Log_{10} (L_M)	533	0.922	317.9	108.9	−91.4	−418	<0.0001
Female	Q_F	597	1.001	401.1	−100.4	292.7	−1002.9	<0.0001
	Log_{10} (L_F)	597	0.916	271.8	76.1	−140.1	−391.4	<0.0001
Species-wise comparison	Sex-average L	367	0.967	−1701.9	−1846.7	−1920.5	−289.5	<0.0001
	ΔL	367	0.576	442.9	431.4	88.6	−23	<0.0001
	Sex-average Q	367	0.949	114.5	−59.1	137.2	−347.2	<0.0001
	ΔQ	367	0.926	12.6	−60.2	−3.5	−145.6	<0.0001

Species-wise traits were analyzed for all taxa using available data for both sexes.

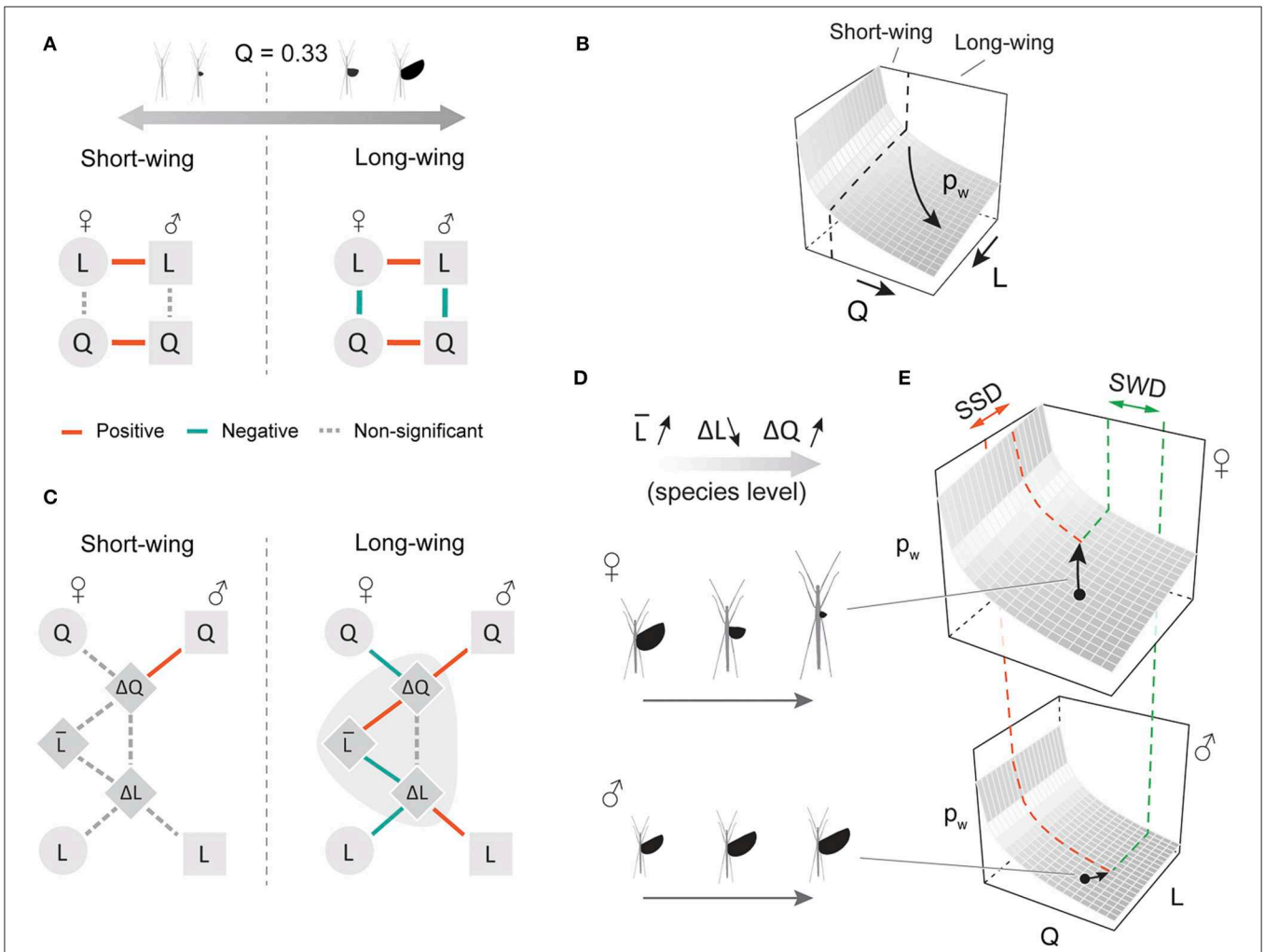

FIGURE 7 | Phylogenetic correlations between wing and body size among stick insect species. **(A)** An inverse correlation between wing and body size was found in both sexes of long-winged species (Q > 0.33 in both sexes), indicated graphically in **(B)** as a coupled transition between different states of wing and body size on the wing loading landscape. **(C)** In long-winged species, sex-averaged L is significantly correlated with ΔL and with ΔQ, demonstrated graphically in **(D)** as an increasing sex-averaged L associated with decreasing ΔL (increasing SSD) and increasing ΔQ (increasing SWD). **(E)** Schematic scenario for consequences of increased sexual dimorphism in flight-related morphology; increases in female-biased SSD and male-biased SWD lead to greater difference in flight capability (i.e., changes in the *z*-position on the wing loading landscape). Details of the PGLS results are provided in **Table 3**.

TABLE 3 | Summary of pairwise correlational analyses using PGLS.

			PGLS			
		Correlations	***N***	**Slope**	**Slope SE**	***P***
Short-wing species	Male	$Q_M \sim Log_{10}(L_M)$	33	0.056 (0.001)	0.064 (0)	0.386 (0.011)
	Female	$Q_F \sim Log_{10}(L_F)$	88	0.015 (0.001)	0.036	0.684 (0.023)
	Wing size, species-wise comparison	$Q_F \sim Q_M$	17	1.368 (0.01)	0.132 (0.003)	<0.001
		$Q_M \sim \Delta Q$	21	0.28 (0.001)	0.066 (0.001)	<0.001
		$Q_F \sim \Delta Q$	21	0.018 (0.001)	0.073 (0)	0.812 (0.012)
		$\Delta Q \sim \Delta L$	21	−1.021 (0.009)	0.705 (0.003)	0.163 (0.003)
		$\Delta Q \sim L_{mean}$	21	0	0.001	0.944 (0.015)
	Body size, species-wise comparison	$L_M \sim L_F$	21	0.724 (0.001)	0.038 (0)	<0.001
		$L_F \sim \Delta L$	21	−339.999 (2.652)	182.43 (0.708)	0.078 (0.003)
		$L_M \sim \Delta L$	21	−130.135 (2.244)	144.314 (0.636)	0.379 (0.009)
		$\Delta L \sim L_{mean}$	21	0	0	0.166 (0.005)
Long-wing species	Male	$Q_M \sim Log_{10}(L_M)$	240	−0.125 (0.005)	0.045 (0)	0.007 (0.002)
	Female	$Q_F \sim Log_{10}(L_F)$	174	−0.192 (0.004)	0.068 (0)	0.005 (0.001)
	Wing size, species-wise comparison	$Q_F \sim Q_M$	114	0.654 (0.017)	0.117 (0.002)	< 0.001
		$Q_M \sim \Delta Q$	114	0.181 (0.006)	0.082 (0.001)	0.029 (0.005)
		$Q_F \sim \Delta Q$	114	−0.964 (0.006)	0.079 (0.001)	< 0.001
		$\Delta Q \sim \Delta L$	114	−0.107 (0.02)	0.117 (0.002)	0.371 (0.097)
		$\Delta Q \sim L_{mean}$	114	0.001	0	0.023 (0.005)
	Body size, species-wise comparison	$L_M \sim L_F$	114	0.59 (0.002)	0.024 (0.001)	< 0.001
		$L_F \sim \Delta L$	114	−81.532 (4.94)	24.047 (0.817)	0.001 (0.001)
		$L_M \sim \Delta L$	114	47.087 (3.46)	17.015 (0.618)	0.008 (0.006)
		$\Delta L \sim L_{mean}$	114	−0.001 (0)	0	0.034 (0.003)

Values represent means from analyses using 100 randomly resolved trees, with 1 s.d. in brackets.

can be recurrent and occur within nominal species. Similar scenarios of wing size reduction have been reported in alpine stoneflies (McCulloch et al., 2016). The evolution of flight-related morphology in phasmids can, in part, be viewed as displacement on the wing loading landscape (**Figure 8B**), reflecting dual effects of variation in wing and body size. This multidimensional view provides a more complete perspective than consideration of wing size alone (as otherwise indicated by the inset arrows of **Figure 8B**).

Flight in general enhances resource acquisition, dispersal, and escape from predators (Dudley, 2000), but wings can readily be lost in evolutionary time, or co-opted for non-aerodynamic purposes. Wing reduction in insects often derives from trade-offs with fecundity in particular contexts (e.g., habitat persistence, colonization of high-altitude environments; see Roff, 1994), whereas miniaturized and aerodynamically irrelevant wings often associate with derived defensive functions (e.g., startle displays and stridulation; Robinson, 1968; **Figure 8C**; **Table S3**). Altitudinal changes in life history strategies likely contribute to both body size miniaturization and wing reduction, as in the *A. tanarata* clade (**Figure 2B**). For high-altitude species more generally, lower plant canopies at high elevations may reduce the functional significance of flight. By contrast, phasmid species with high dietary specificity might experience stronger selection for flight performance (e.g., Blüthgen et al., 2006). No data are presently available on flight abilities and associated aerodynamics among phasmid species.

For long-winged stick insects, aerial mobility may be an important component in sexual selection for enhanced male locomotor performance. Female phasmids tend to be less mobile and inconspicuous, whereas greater mobility in males may allow for greater success in dispersal and mating. The inverse correlation between wing and body size in long-winged stick insects (**Figures 7A,B**) suggests that selection for flight has limited the evolution of larger body size. Similar selection on mobility and an enhanced locomotor apparatus has been documented in other male insects (Kelly et al., 2008). In wingless and short-winged species, larger body size might make a species more competitive in male-male competition (see Sivinski, 1978). A developmental tradeoff may limit the evolution of wing size, as shown by the inverse correlation between mating success and flight capability (as in Orthopteran and Hemipteran insects; Fujisaki, 1992; Crnokrak and Roff, 1995; Fairbairn and Preziosi, 1996). Future studies may compare variation in male body size between winged and wingless clades to test whether the evolution of male body size is constrained by selection for flight performance.

Sexual differences in mass allometry and body size are key factors influencing the evolution of phasmid wing dimorphism. Selection for increased fecundity will favor wing reduction in females, which can then lead to male-biased SWD as well as the evolution of defensive mechanisms that do not rely on flight; strong selection for flight capability may lead to female-biased SWD. Large female wings may be specifically favored in

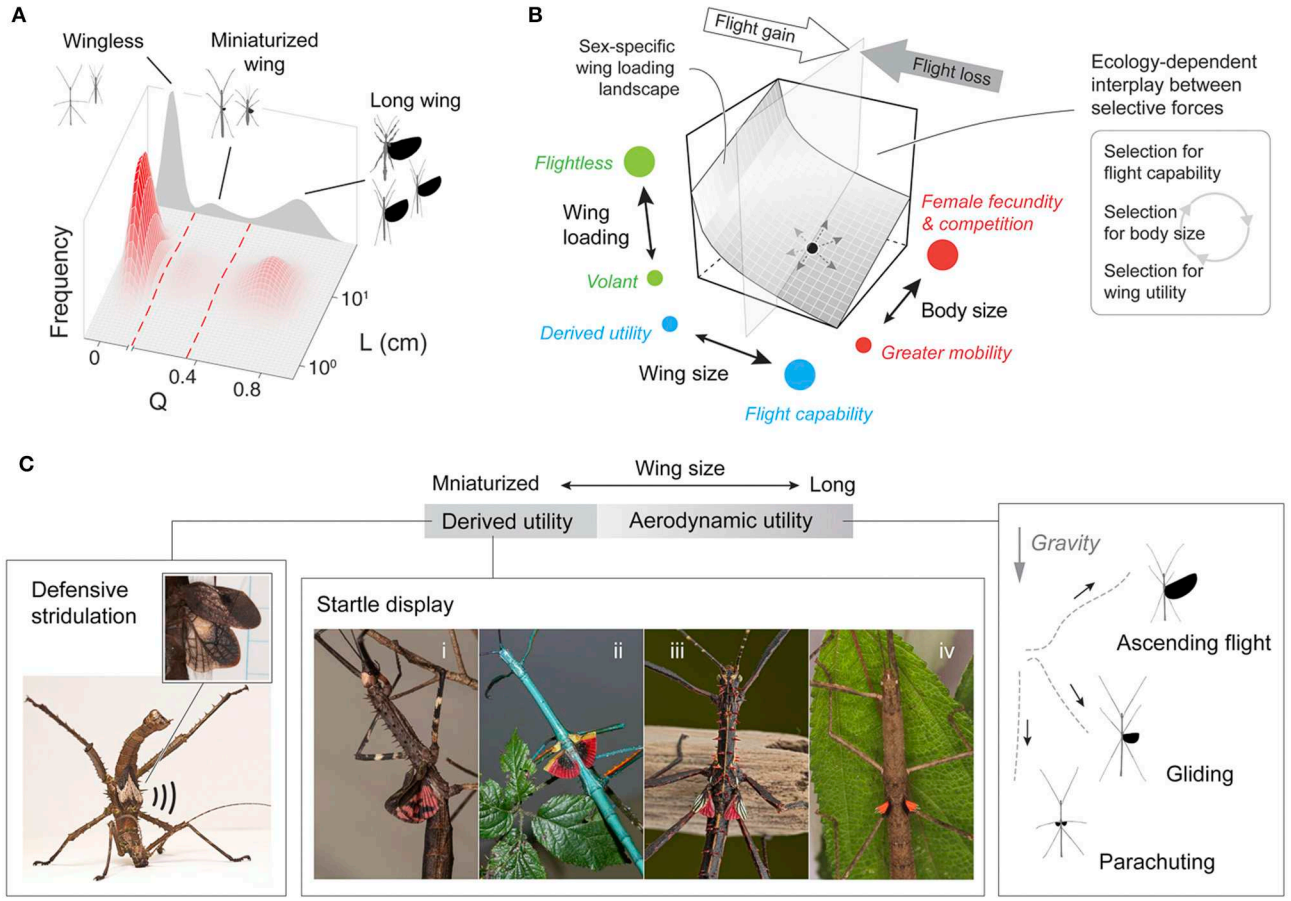

FIGURE 8 | A summary of evolution of flight-related morphology in stick insects. **(A)** Relative occurrence of different flight morphologies with respect to a feature space defined by Q and L (**Figure 3**), indicating three main peaks corresponding to wingless, miniaturized-wing, and long-wing morphologies. **(B)** Schematic demonstration showing that the evolution of flight morphology (for any given position on the wing loading landscape) is driven by the interplay between three major forces and tradeoffs (inset). **(C)** Variation of wing utility with respect to relative wing size. Continuous variation in aerodynamic performance is coupled with the full spectrum of relative wing size variation, whereas derived functions such as use in startle displays or stridulation are frequently found in miniaturized wings. Examples of startle display: (i), *Diesbachia hellotis* female; (ii), *Achrioptera manga* male; (iii), *Parectatosoma* cf. *hystrix* male; (iv) *Oxyartes dorsalis* female [Photos of (i)—(iii) courtesy of Bruno Kneubühler]. Example of defensive stridulation: *Haaniella echinata* male.

winged species with aerial copulation (e.g., *Trachythorax* spp.). Female-biased SSD is likely a canalized feature in orthopteroid insects, more generally (see Bidau et al., 2016). In winged stick insects, the extent of SSD is clearly influenced by selection on fecundity in females, and by selection on flight in males. The allometric variation in SSD (i.e., the inverse correlation between ΔL and sex-averaged L; see **Figures 7C,D**) is consistent with Rensch's Rule (i.e., females are disproportionally larger in large species; Abouheif and Fairbairn, 1997; Fairbairn, 1997; Teder and Tammaru, 2005), instead of the converse outcome (i.e., isometric scaling in both sexes). This result may, however, be biased by allometric changes in body shape. For example, many phasmid species exhibit disproportionately slender bodies that may mimic plant stems, whereas other species have evolved thickened bodies for defense (e.g., the "tree lobster" ecomorph; Buckley et al., 2009). In the scaling of wing loading (**Figure 4D**), the contrast between *H. dilatata* male (family Heteropterygidae) and other phasmids (mostly in the subfamily Necrosciinae) suggests clade-specific allometry scaling. Future comparative assessment of body segment shapes and masses, in addition to body length, would enhance our understanding of allometric variation in SSD among phasmid taxa.

In winged phasmids, SSD and SWD are significantly correlated; this relationship does not pertain for either short- or long-winged species (**Figure 7C**; **Figure S4**), reflecting interaction between multiple selective forces within sex-specific ecological contexts (**Figure 8B**). The evolutionary intercorrelation between SSD and SWD is generally underexplored for most insects. Pterygote insects in general exhibit various types of SWD (e.g., male-biased and female-biased SWD have been reported in at least 11 and 5 orders, respectively; see Thayer, 1992), which can be correlated with sex-specific flight ecology (e.g., flight height and behavior; see DeVries et al., 2010) and with sexual selection for flight capability

(e.g., copulation flight in caddisfly; Gullefors and Petersson, 1993). Future studies may address clade-specific SWD by correlating aforementioned factors within phylogenetic contexts.

These results for stick insects may provide more general insight into evolutionary transitions between wingless and fully winged insects. Given the widespread secondary loss of flight in pterygotes, sex-specific morphological scaling along the wing loading landscape can indicate the possible utility of partially reduced wings. Aerodynamic use of reduced wings during descent may be expected in arboreal pterygotes undergoing wing reduction, whereas non-aerodynamic functions would be predicted to be more likely in non-arboreal taxa (e.g., stridulatory wings in ground-dwelling insects). The eventual loss of aerodynamic utility may be characterized by a threshold wing loading (i.e., $p_w \approx 10\ Nm^{-2}$ shown here), beyond which point selection for aerodynamic utility become insignificant. Similarly, morphological evolution associated with the origin of wings and of insect flight may have been sexually dimorphic, particularly if the earliest winglets served a non-aerodynamic function such as visual display (Alexander and Brown, 1963), with subsequent increases in size and mobility for aerial behaviors (see Dudley, 2000; Dudley and Yanoviak, 2011). Reductions in body size (with concomitantly lower wing loadings) may also favor the evolution of flight, as characterized the lineage leading to birds (Lee et al., 2014; Xu et al., 2014). Allometric variation in body structures can occur on both developmental and macroevolutionary timescales, and likely interacts with selection on aerodynamic performance. For example, if ancestral pterygotes retained winglets across nymphal instars, then selection for lower wing loading would foster allometric increases in wing size as well as a reduction in mass allometry (with less influence of body size increase to wing loading; **Figure 5**). Physical models with wings of different sizes can be used to test biomechanical consequences of such differential allometries, as constrained by relevant morphologies inferred from the fossil record. And for extant phasmids, assessment of flight behaviors and aerial capacity across taxa is now clearly warranted.

DATA AVAILABILITY STATEMENT

The datasets generated for this study can be found in the GenBank (Accession numbers: H3: MT318893 - MT318915; 28s: MT217013 - MT217031; COI: MT318107 - MT318122; COII: MT318915 - MT318926). All other data, input files, and scripts are provided in **Supplementary Materials**.

AUTHOR CONTRIBUTIONS

YZ devised experiments and performed the majority of data collection and analyses. CO'M and SP participated in morphological data collection. SS contributed to molecular data collection. XC contributed to phylogenetic analyses. FR contributed to field data collection of *Asceles tanarata* group. All authors contributed to writing of the manuscript.

FUNDING

This research was supported by National Science Foundation (DDIG 1110855), Essig Museum of Entomology (Margaret C. Walker Fund), Museum of Vertebrate Zoology, the Department of Integrative Biology at UC-Berkeley, the Undergraduate Research Apprentice Program (URAP) of UC-Berkeley, the Society for Integrative and Comparative Biology (SICB Fellowship of Graduate Student Travel), and the Ministry of Higher Education Malaysia Fundamental Research Grant Scheme [FRGS/1/2012/SG03/UKM/03/1(STWN)].

ACKNOWLEDGMENTS

We thank Francis Seow-Choen for providing captive bred insects, helping with field works, and commenting on stick insect natural history. We also thank Lynn Nguyen, Camille Gonzales, Faye Pon, Joan Chen, Nina Gnong, Stephanie Yom, Yuexiang Chen, Chulabush Khatancharoen, Biying Li, Grisanu Naing, Jizel Emralino, Xiaolin Chen, Ho-Yeon Han, Ian Abercrombie, Yamai Shi-Fu Huang, Azuan Aziz, and Juhaida Harun for help with data collection, and David Wake and Sven Bradler for comments on the manuscript. We further thank Paul Brock, Nicholas Matzke, and Emma Goldberg for comments at the early stage of the work, and the Forestry Department of Pahang, Malaysia, for permission of insect collection. Publication made possible in part by support from the Berkeley Research Impact Initiative (BRII) sponsored by the UC Berkeley Library.

SUPPLEMENTARY MATERIAL

The Supplementary Material for this article can be found online at: https://www.frontiersin.org/articles/10.3389/fevo.2020.00121/full#supplementary-material

REFERENCES

Abouheif, E., and Fairbairn, D. J. (1997). A comparative analysis of allometry for sexual size dimorphism: assessing rensch's rule. *Am. Nat.* 149, 540–562. doi: 10.1086/286004

Alexander, R. D., and Brown, W. L. Jr. (1963). Mating behavior and the origin of insect wings. *Occas. Papers Mus. Zool. Univ. Mich.* 628, 1–19.

Aljanabi, S. M., and Martinez, I. (1997). Universal and rapid salt-extraction of high quality genomic DNA for PCR-based techniques. *Nucleic Acids Res.* 25, 4692–4693. doi: 10.1093/nar/25.22.4692

Bidau, C. J., Taffarel, A., and Castillo, E. R. (2016). Breaking the rule: multiple patterns of scaling of sexual size dimorphism with body size in orthopteroid insects. *Rev. Soc. Entomol. Arg.* 75, 11–36.

Blanckenhorn, W. U. (2000). The evolution of body size: what keeps organisms small?. *Q. Rev. Biol.* 75, 385–407. doi: 10.1086/393620

Blüthgen, N., Metzner, A., and Ruf, D. (2006). Food plant selection by stick insects (*Phasmida*) in a bornean rain forest. *J. Trop. Ecol.* 22, 35–40. doi: 10.1017/S0266467405002749

Bradler, S. (2009). Phylogeny of the stick and leaf insects (*Insecta: Phasmatodea*). *Spec. Phyl. Evol.* 2, 3–139. doi: 10.17875/gup2009-710

Bradler, S., Cliquennois, N., and Buckley, T. R. (2015). Single origin of the mascarene stick insects: ancient radiation on sunken islands?. *BMC Evol. Biol.* 15:196. doi: 10.1186/s12862-015-0478-y

Brock, P. D. (1999). *Stick and Leaf Insects of Peninsular Malaysia and Singapore*. Kuala Lumpur: Malaysian Nature Society.

Brock, P. D., Büscher, T., and Baker, E. (2019). *Phasmida Species File Online Version 5.0*. Available online at: http://phasmida.speciesfile.org

Buckley, T. R., Attanayake, D., and Bradler, S. (2009). Extreme convergence in stick insect evolution: phylogenetic placement of the lord howe island tree lobster. *Proc. Royal Soc. B* 276, 1055–1062. doi: 10.1098/rspb.2008.1552

Chown, S. L., and Gaston, K. J. (2010). Body size variation in insects: a macroecological perspective. *Biol. Rev.* 85, 139–169. doi: 10.1111/j.1469-185X.2009.00097.x

Crnokrak, P., and Roff, D. A. (1995). Fitness differences associated with calling behaviour in the two wing morphs of male sand crickets, *Gryllus Firmus*. *Anim. Behav.* 50, 1475–1481. doi: 10.1016/0003-3472(95)80004-2

DeVries, P. J., Penz, C. M., and Hill, R. I. (2010). Vertical distribution, flight behaviour and evolution of wing morphology in *Morpho* butterflies. *J. Anim. Ecol.* 79, 1077–1085. doi: 10.1111/j.1365-2656.2010.01710.x

Drummond, A. J., Suchard, M. A., Xie, D., and Rambaut, A. (2012). Bayesian phylogenetics with BEAUti and the BEAST 1.7. *Mol. Biol. Evol.* 29, 1969–1973. doi: 10.1093/molbev/mss075

Dudley, R. (2000). *The Biomechanics of Insect Flight: Form, Function, Evolution*. Princeton, NJ: Princeton University Press. doi: 10.1515/9780691186344

Dudley, R., and Yanoviak, S. P. (2011). Animal aloft: the origins of aerial behavior and flight. *Integr. Comp. Biol.* 51, 926–936. doi: 10.1093/icb/icr002

Edgar, R. C. (2004). MUSCLE: multiple sequence alignment with high accuracy and high throughput. *Nucleic Acids Res.* 32, 1792–1797. doi: 10.1093/nar/gkh340

Fairbairn, D. J. (1997). Allometry for sexual size dimorphism: pattern and process in the coevolution of body size in males and females. *Annu. Rev. Ecol. Evol. Syst.* 28, 659–687. doi: 10.1146/annurev.ecolsys.28.1.659

Fairbairn, D. J., and Preziosi, R. F. (1996). Sexual selection and the evolution of sexual size dimorphism in the water strider, aquarius remigis. *Evolution* 50, 1549–1559. doi: 10.1111/j.1558-5646.1996.tb03927.x

Freckleton, R. P., Harvey, P. H., and Pagel, M. (2002). Phylogenetic analysis and comparative data: a test and review of evidence. *Am. Nat.* 160, 712–726. doi: 10.1086/343873

Fujisaki, K. (1992). A male fitness advantage to wing reduction in the oriental chinch bug, *Cavelerius Saccharivorus* okajima (*Heteroptera: Lygaeidae*). *Popul Ecol.* 34, 173–183. doi: 10.1007/BF02513529

Goldberg, E. E., and Igić, B. (2008). On phylogenetic tests of irreversible evolution. *Evolution* 62, 2727–2741. doi: 10.1111/j.1558-5646.2008.00505.x

Grimaldi, D., and Engel, M. (2005). *Evolution of the Insects*. Cambridge, UK: Cambridge University Press.

Gullefors, B., and Petersson, E. (1993). Sexual dimorphism in relation to swarming and pair formation patterns in *Leptocerid Caddisflies* (*Trichoptera: Leptoceridae*). *J. Insect Behav.* 6, 563–577. doi: 10.1007/BF01048123

Hedrick, A. V., and Temeles, E. J. (1989). The evolution of sexual dimorphism in animals: hypotheses and tests. *Trends Ecol. Evol.* 4, 136–138. doi: 10.1016/0169-5347(89)90212-7

Kelly, C. D., Bussiere, L. F., and Gwynne, D. T. (2008). Sexual selection for male mobility in a giant insect with female-biased size dimorphism. *Am. Nat.* 172, 417–423. doi: 10.1086/589894

Lee, M. S., Cau, A., Naish, D., and Dyke, G. J. (2014). Dinosaur evolution. Sustained miniaturization and anatomical innovation in the dinosaurian ancestors of birds. *Science* 345, 562–566. doi: 10.1126/science.1252243

McCulloch, G. A., Wallis, G. P., and Waters, J. M. (2016). A time-calibrated phylogeny of southern hemisphere stoneflies: testing for gondwanan origins. *Mol. Phylogenet. Evol.* 96, 150–160. doi: 10.1016/j.ympev.2015.10.028

Nel, A., and Delfosse, E. (2011). A new chinese mesozoic stick insect. *Acta Palaeontol. Pol.* 56, 429–433. doi: 10.4202/app.2009.1108

Orme, D., Freckleton, R., Thomas, G., and Petzoldt, T. (2013). The caper package: comparative analysis of phylogenetics and evolution in R. *R Package Version 5*.

Pagel, M. (1997). Inferring evolutionary processes from phylogenies. *Zool. Scr.* 26, 331–348. doi: 10.1111/j.1463-6409.1997.tb00423.x

Pagel, M. (1999). Inferring the historical patterns of biological evolution. *Nature* 401, 877–884. doi: 10.1038/44766

Paradis, E., Claude, J., and Strimmer, K. (2004). APE: analyses of phylogenetics and evolution in R language. *Bioinformatics* 20, 289–290. doi: 10.1093/bioinformatics/btg412

Posada, D. (2008). jModelTest: phylogenetic model averaging. *Mol. Biol. Evol.* 25, 1253–1256. doi: 10.1093/molbev/msn083

Rambaut, A., Drummond, A. J., Xie, D., Baele, G., and Suchard, M. A. (2018). Posterior summarization in bayesian phylogenetics using tracer 1.7. *Syst. Biol.* 67, 901–904. doi: 10.1093/sysbio/syy032

Rasnitsyn, A. P., and Ross, A. J. (2000). A preliminary list of arthropod families present in the burmese amber collection at the natural history museum, London. *Bull. Mus. Nat. Hist. Geol.* 56, 21–24.

Revell, L. J. (2012). phytools: an R package for phylogenetic comparative biology (and other things). *Methods Ecol. Evol.* 3, 217–223. doi: 10.1111/j.2041-210X.2011.00169.x

Robertson, J. A., Bradler, S., and Whiting, M. F. (2018). Evolution of oviposition techniques in stick and leaf insects (*Phasmatodea*). *Front. Ecol. Evol.* 6:216. doi: 10.3389/fevo.2018.00216

Robinson, M. H. (1968). The defensive behavior of *Pterinoxylus Spinulosus* redtenbacher, a winged stick insect from panama (*Phasmatodea*). *Psyche (Camb. Mass).* 75, 195–207. doi: 10.1155/1968/19150

Roff, D. A. (1986). The evolution of wing dimorphism in insects. *Evolution.* 40, 1009–1020. doi: 10.1111/j.1558-5646.1986.tb00568.x

Roff, D. A. (1990). The evolution of flightlessness in insects. *Ecol. Monogr.* 60, 389–421. doi: 10.2307/1943013

Roff, D. A. (1994). The evolution of flightlessness: is history important?. *Evol. Ecol.* 8, 639–657. doi: 10.1007/BF01237847

Schneider, C. A., Rasband, W. S., and Eliceiri, K. W. (2012). NIH Image to ImageJ: 25 years of image analysis. *Nat. Methods* 9:671. doi: 10.1038/nmeth.2089

Sellick, J. T. C. (1994). Phasmida (stick insect) eggs from the eocene of oregon. *Palaeontology* 37, 913–922.

Seow-Choen, F. (2000). *An Illustrated Guide to the Stick and Leaf Insects of Peninsular Malaysia and Singapore*. Kota Kinabalu: Natural History Publications (Borneo).

Shang, L., Béthoux, O., and Ren, D. (2011). New stem-phasmatodea from the middle jurassic of China. *?Eur. J. Entomol.* 108:677. doi: 10.14411/eje.2011.086

Shine, R. (1989). Ecological causes for the evolution of sexual dimorphism: a review of the evidence. *?Q. Rev. Biol.* 64, 419–461. doi: 10.1086/416458

Simon, S., Letsch, H., Bank, S., Buckley, T., Donath, A., Liu, S., et al. (2019). Old world and new world phasmatodea: phylogenomics resolve the evolutionary history of stick and leaf insects. *Front. Ecol. Evol.* 7:345. doi: 10.3389/fevo.2019.00345

Sivinski, J. (1978). Intrasexual aggression in the stick insects *Diapheromera Veliei* and *D. Covilleae* and sexual dimorphism in the phasmatodea. *Psyche* 85, 395–405. doi: 10.1155/1978/35784

Stone, G., and French, V. (2003). Evolution: have wings come, gone and come again?. *Curr. Biol.* 13, 436–438. doi: 10.1016/S0960-9822(03)00364-6

Stroud, J. T., and Losos, J. B. (2016). Ecological opportunity and adaptive radiation. *Annu. Rev. Ecol. Evol. Syst.* 47, 507–532. doi: 10.1146/annurev-ecolsys-121415-032254

Symonds, M. R., and Blomberg, S. P. (2014). "A primer on phylogenetic generalised least squares," in *Modern Phylogenetic Comparative Methods and Their Application in Evolutionary Biology*, ed L. Z. Garamszegi (Berlin; Heidelberg: Springer), 105–130.

Teder, T., and Tammaru, T. (2005). Sexual size dimorphism within species increases with body size in insects. *Oikos* 108, 321–334. doi: 10.1111/j.0030-1299.2005.13609.x

Thayer, M. K. (1992). Discovery of sexual wing dimorphism in *Staphylinidae* (*Coleoptera*): *"Omalium" Flavidum*, and a discussion of wing dimorphism in insects. *J New York Entomol. Soc.* 100, 540–573.

Trueman, J. W. H., Pfeil, B. E., Kelchner, S. A., and Yeates, D. K. (2004). Did stick insects really regain their wings?. *Syst. Entomol.* 29, 138–139. doi: 10.1111/j.0307-6970.2004.00251.x

Wang, M., Béthoux, O., Bradler, S., Jacques, F. M., Cui, Y., and Ren, D. (2014). Under cover at pre-angiosperm times: a cloaked phasmatodean insect from the early cretaceous jehol biota. *PLoS ONE* 9:e91290. doi: 10.1371/journal.pone.0091290

Wedmann, S., Bradler, S., and Rust, J. (2007). The first fossil leaf insect: 47 million years of specialized cryptic morphology and behavior. *Proc. Natl. Acad. Sci. U.S.A* 104, 565–569. doi: 10.1073/pnas.0606937104

Whiting, M. F., Bradler, S., and Maxwell, T. (2003). Loss and recovery of wings in stick insects. *Nature* 421, 264–267. doi: 10.1038/nature01313

Whiting, M. F., and Whiting, A. S. (2004). Is wing recurrence really impossible?: a reply to Trueman et al. *Syst. Entomol.* 29, 140–141. doi: 10.1111/j.1365-3113.2004.0255.x

Xu, X., Zhou, Z., Dudley, R., Mackem, S., Chuong, C. M., Erickson, G. M., et al. (2014). An integrative approach to understanding bird origins. *Science* 346:1253293. doi: 10.1126/science.1253293

Yang, H., Yin, X., Lin, X., Wang, C., Shih, C., Zhang, W., et al. (2019). Cretaceous winged stick insects clarify the early evolution of phasmatodea. *Proc. Biol. Sci.* 286:20191085. doi: 10.1098/rspb.2019.1085

Conflict of Interest: The authors declare that the research was conducted in the absence of any commercial or financial relationships that could be construed as a potential conflict of interest.

Advantages of publishing in Frontiers

OPEN ACCESS
Articles are free to read for greatest visibility and readership

FAST PUBLICATION
Around 90 days from submission to decision

HIGH QUALITY PEER-REVIEW
Rigorous, collaborative, and constructive peer-review

TRANSPARENT PEER-REVIEW
Editors and reviewers acknowledged by name on published articles

Frontiers
Avenue du Tribunal-Fédéral 34
1005 Lausanne | Switzerland

Visit us: www.frontiersin.org
Contact us: info@frontiersin.org | +41 21 510 17 00

REPRODUCIBILITY OF RESEARCH
Support open data and methods to enhance research reproducibility

DIGITAL PUBLISHING
Articles designed for optimal readership across devices

FOLLOW US
@frontiersin

IMPACT METRICS
Advanced article metrics track visibility across digital media

EXTENSIVE PROMOTION
Marketing and promotion of impactful research

LOOP RESEARCH NETWORK
Our network increases your article's readership